2013

Climate change adaptation in electricity infrastructure with renewable energy resources

Md. Abu Abdullah
University of Wollongong

CLIMATE CHANGE ADAPTATION IN ELECTRICITY INFRASTRUCTURE WITH RENEWABLE ENERGY RESOURCES

A thesis submitted in partial fulfilment of the
requirements for the award of the degree

Doctor of Philosophy

from

University of Wollongong

by

Md. Abu Abdullah

B Sc (Electrical and Electronics Engineering)

School of Electrical Computer and Telecommunications Engineering
Faculty of Engineering and Information Sciences

2013

Certification

I, Md. Abu Abdullah, declare that this thesis, submitted in partial fulfilment of the requirements for the award of Doctor of Philosophy, in the School of Electrical, Computer and Telecommunications Engineering, University of Wollongong, is wholly my own work unless otherwise referenced or acknowledged. The document has not been submitted for qualifications at any other academic institution.

Md. Abu Abdullah

12th May, 2014

This Thesis is Dedicated to

Three Very Special Women in My Life:

My Mother Sultana Mahmuda Akhter,

My Wife Nazma Sultana and My Daughter Arana Abdullah

Table of Contents

Abstract

Climate change mitigation is one of the significant global concerns, and mitigation strategies have been initiated at different sectors including electric power industry. Reduction of Greenhouse Gas (GHG) emissions, less dependency on fossil fuels and increased utilisation of renewable resources are some of the most common climate change mitigation initiatives. Since the conventional electric power generation systems are built based on the fossil fuel based electricity generation technologies, electric power utilities which own these generation systems are responsible for reducing GHG emissions from electricity generation. To achieve this, generation technologies are shifting from conventional to non-conventional, with a gradual increase in the renewable energy penetration. As a result, electricity utilities are required to include the generation mix changes in their electricity network planning practices. The uncertainty and variability in the availability of generation output introduces challenges for electricity utilities to maintain the specified reliability level despite significant increase in the penetration of renewable resources in the grid. The collection of papers in this thesis aims to develop electricity generation planning techniques, which can address the emission reduction in electricity generation, the uncertainty in power availability of renewable resources, and the generation adequacy of both conventional and renewable generation technologies. In order to address these aspects, following approaches have been developed in this thesis

- A novel probabilistic load flow algorithm for distribution network with renewable distributed generations (DGs) has been developed considering the coincidental variations between different demand groups and renewable generation sources to assess the probability distribution of power flow through the distribution feeders. The simulation results show the effectiveness of Pearson's distribution functions

based proposed approach in modelling the probability distribution of the random variables with non-Gaussian distribution.

- New indices and assessment methodologies for distribution network adequacy assessment are proposed. A new approach has been developed considering the joint probability distribution between demand and renewable generation availability to estimate the adequacy of energy supply and service continuation in the distribution network with renewable DG systems. The results demonstrate that proposed analytical methods for distribution network adequacy assessment reduces the computational effort with acceptable accuracy compared to the computationally extensive simulation based methods.

- A novel approach has been proposed for a renewable based hybrid energy system (HES) design in a distribution network thereby achieving sustainability in power generation and distribution. A life cycle assessment process is used to estimate the embodied primary emission of the energy generated from renewable based generation systems. A multi-objective optimisation model is developed to find the optimum solutions for renewable based HES. The potential impact of energy storage systems in the renewable based HES design has been quantified through analysis.

- The performances of different climate change mitigation technologies in emission reduction from an electricity generation system of New South Wales have been studied. A new methodology has been developed to model the embodied emission of the energy supplied through the electricity grid. The results suggest that implementation of climate change mitigation technologies strongly influences the emission reduction capability of renewable generation systems, and coordination between climate change mitigation technologies is also essential to achieve the emission reduction target efficiently.

- A new wind generation planning methodology has been developed using a multi-objective optimisation technique to share the spatially diverse wind generation within multi-area power systems. A trade-off analysis method has been developed to examine the collective effect of multiple objective functions of load carrying capacity of wind farms, emission offset and capacity upgrade of transmission network interconnections for wind resource sharing strategy. The influence of

correlation coefficients between the generation output of wind farms and the system demand on the wind generation capacity allocation has been observed from the simulation results of a case study involving Southeast Australian power systems. It is found that the uncertainty and fluctuation in the output of wind generation systems can be mitigated with the aid of energy storage systems.

- A novel power dispatch strategy has been developed using a stochastic programming model to improve the schedulability and the supply reliability of a battery energy storage system (BESS) integrated wind farm. Moreover, a ranked based dispatch control strategy has been devised by arranging the total BESS integrated with the wind farm into multiple battery units to maintain the wind farm schedulability at a level of expectation. The results emphasises that the proposed strategy can schedule the output of wind farm without the requirement of alteration, and battery lifetime is maximised by avoiding the occurrence of frequent charging and discharging cycles.

- In order to consider the correlation between renewable generation and system demand, a unique non-iterative method has been developed incorporating a joint probability distribution of demand and renewable generation to estimate the effective load carrying capability of the renewable generation plants. The results indicate that the proposed method reduces computational burden while maintaining acceptable accuracy level as compared to the existing methods.

Acknowledgements

This thesis would not have become a realisation without the contributions from many people.

First and foremost I wish to express my utmost gratitude to my principle supervisor Associate Professor Kashem Muttaqi of the University of Wollongong for enabling me to pursue postgraduate studies at the University of Wollongong. I would also like to thank my co-supervisor Dr. Ashish Agalgaonkar of the University of Wollongong for providing valuable suggestions and ideas for timely completion of this project. Thanks also go to my co-supervisor Professor Danny Sutanto for providing guidance and assistance regularly throughout this project. I am grateful to AusAID program for financially supporting my PhD project. Very special thanks go to my friends Md. Jan-e-Alam, Mollah Rezaul Alam and Parvez Mannan, for all the encouragement and support given during good times as well as hard times along the way. I was lucky to have you all around me to share memories over these years in Wollongong. I would also like to especially thank my parents, wife and daughter for being patience in these years, and for being supportive and understanding especially during the final stages of the project.

Declaration on Publications

This thesis includes chapters that have been written as the following journal articles.

Chapter 2 M. A. Abdullah, A. P. Agalgaonkar, K. M. Muttaqi, "Probabilistic load flow for distribution network incorporating correlation between time-varying demand and uncertain renewable generation," Renewable Energy, vol. 55, pp. 532-543, 2013.

Chapter 3 M. A. Abdullah, A. P. Agalgaonkar, K. M., Muttaqi, "Assessment of Energy Supply and Continuity of Service in Distribution Network with Renewable Distributed Generation," Applied Energy, vol. 113, pp. 1015-1026, 2014.

Chapter 4 M. A. Abdullah, K. M. Muttaqi, A. P. Agalgaonkar, "Sustainable Energy System Design with Distributed Renewable Resources Considering Economic, Environmental and Uncertainty Aspects," Submitted to Renewable Energy, (Manuscript number: RENE-D-13-02226).

Chapter 5 M. A. Abdullah, A. P. Agalgaonkar, K. M. Muttaqi, "Climate Change Adaptation with Integration of Renewable Energy Resources in the Electricity Grid of New South Wales, Australia," Renewable Energy, vol. 66, pp. 305-313, June 2014.

Chapter 6 M. A. Abdullah, K. M. Muttaqi, A. P. Agalgaonkar, D. Sutanto, "A New Approach for Sharing Wind Generation Spatial Diversification in Multiarea Power Systems using Trade-off Analysis," In Press for Publication in the Future issue of IET Generation, Transmission and Distribution (Available Online from 14th March 2014).

Chapter 7 M. A. Abdullah, K. M. Muttaqi, A. P. Agalgaonkar, D. Sutanto, "An Effective Power Dispatch Control Strategy to Improve Generation Schedulability and Supply Reliability of a Wind Farm Using a Battery Energy Storage System," under 2nd review by IEEE Transaction on Sustainable Energy, (Manuscript ID: TSTE-00535-2013).

Chapter 8 M. A. Abdullah, K. M. Muttaqi, A. P. Agalgaonkar, D. Sutanto, "A Non-Iterative Method to Estimate Load Carrying Capability of Generating Units Considering Correlation between Demand and Generation in a Renewable Rich Power Grid," In Press for Publication in IEEE Transaction on Sustainable Energy, (Publication date 27th March, 2014).

As the principal supervisor I, A/Prof. Kashem M. Muttaqi, declare that the candidate, Md. Abu Abdullah (appeared as M. A. Abdullah), has contributed greater part of the work in each article listed above. In each of the above listed manuscripts, the

contribution of the candidate is in the development of the main idea/concept, which has been extended, refined and tuned for improvement with advice from myself, and his co-supervisors Dr. Ashish P. Agalgaonkar and Prof. Danny Sutanto, all contributing as co-authors. The candidate has prepared the first draft of each of the manuscripts and revised those according to the suggestions provided by the supervisors. The candidate has been responsible for submitting each of the manuscripts for publication to the relevant journals, and he has been in charge of responding to the reviewers' comments, with assistance from his co-authors.

A/Prof. Kashem M. Muttaqi
Principal Supervisor
12th May, 2014

Nomenclature

ACPT	Available Capacity Probability Table
AEMO	Australian Energy Market Operators
ARMA	Auto Regressive Moving Average
ARMS	Average Root Mean Square
BESS	Battery Energy Storage System
BESU	Battery Energy Storage Unit
BOM	Bureau of Meteorology
CCA	Climate Change Authority
CDF	Cumulative Distribution Function
COPT	Capacity Outage Probability Table
DG	Distributed Generation
DOD	Depth of Discharge
ELCC	Effective Load Carrying Capability
ERED	Expected Renewable Energy Deficiency
ESS	Energy Storage System
ESSP	Energy Served during System Peak
FOR	Forced Outage Rate
GHG	Greenhouse Gas
GRMPT	Generation Reserve Margin Probability Table
GWP	Global Warming Potential
HES	Hybrid Energy System
LCA	Life Cycle Assessment
LCC	Life Cycle Cost
LCE	Life Cycle Emission
LCOE	Levelised Cost of Energy
LDM	Load Duration Method
LOLE	Loss of Load Expectation
LOLP	Loss of Load Probability
MCDM	Multi Criterion Decision Making
MCS	Monte Carlo Simulations
MO	Multi-Objective
NEM	National Electricity Market
NSW	New South Wales
NTNDP	National Transmission Network Development Plan
NWP	Numerical Weather Prediction
OPF	Optimal Power Flow
PDF	Probability Density Function

PLCC	Peak Load Carrying Capability
PLF	Probabilistic Load Flow
PV	Photovoltaic
RBTS	Roy Billinton Test System
RET	Renewable Energy Target
RTS	Reliability Test System
SOC	State of Charge
T&D	Transmission and Distribution
WECS	Wind Energy Conversion System
WF	Wind Farm

List of Tables

List of Figures

Chapter 1

Introduction

1.1 Motivation

The continuous burdens on the environment due to human activities have contributed significantly to the historic change of climate throughout the world. Global warming, draught, flooding, etc are some of the observed climate change events. The climate change events have significant impact on the human civilisation and are affecting the social development, and human welfare and health severely. Increasing number of natural disasters have been observed in the recent days and this lead to raise the governmental and social awareness for mitigating the climate change events.

The energy demand and associated services to meet the social development, and human welfare and health have been increased throughout the world. Greenhouse gas (GHG) emissions resulting from the provision of energy conversion and related services have contributed significantly to the historic increase in atmospheric GHG concentrations [1]. The increased atmospheric GHG concentration is one of the major responsible factors for the global warming and climate change observed in different parts of the world.

The conventional practice in the electricity systems involves a centralised generation of electric energy from large fossil fuel based generation units and the transmission of generated energy through transmission and distribution networks to the consumers. Due to the extensive utilisation of fossil fuel in electricity generation, the limited reserve of fossil fuel is depleting and a substantial amount of GHG is released to the atmosphere. In order to meet the social and environmental welfare requirements and to contribute in climate change mitigation, the electricity utility needs to adjust such conventional practice.

Renewable resource based electricity generation is considered as one of the alternative options for electricity utilities to contribute to the climate change mitigation. However, the deployment of renewable resources in the well-established electricity network is a challenging task for both the utilities and regulators due to the stochastic characteristics of renewable resources. Devising methodologies for robust network planning with renewable generation systems is essential.

Renewable resource based generation systems offer sustainable and emission free electricity generation options to the electricity utilities. Inspired by social awareness of climate change mitigation and sustainable development, the energy regulators and utilities are setting targets of renewable resource penetration to be achieved within a certain timeframe [2]. Carbon footprint reduction of electric energy generation is one of the major objectives of renewable energy target (RET) program.

However, the enhancement of conventional electricity generation planning practices is essential for the successful implementation of the RET program. Hence, an emission reduction performance analysis of renewable based generation systems and the associated climate change mitigation technologies need to be included in the electricity generation planning practices.

Moreover, uncertainty is involved in the generation availability from renewable resources and therefore the consideration of the uncertainty aspect demands significant modification in the electricity generation planning practices. Hence, the development of advanced tools is essential to address the stochastic nature of renewable based generation systems and the time varying demands in electricity generation planning.

Due to the uncertainty in generation availability, renewable based generation systems are considered as the non-dispatchable generation systems and their contribution in the generation adequacy to support system load growth is not as significant as compared to that of the conventional fossil fuel based generation systems. Strategies and control mechanisms to improve the dispatchability and the schedulability of renewable based generation systems need to be devised by incorporating different supporting technologies such as energy storage systems and methodologies that can take advantage of spatial diversities and load-generation correlation.

The importance of the alternative practices in electricity generation planning have been realised by the electricity utilities and regulators by adopting ongoing changes due to climate change mitigation and sustainable generation system development. Although different aspects related to climate change mitigation strategies have been investigated to some extent in the literature, some gaps and challenges still exist in the electricity generation planning practices that take into account the GHG emission assessment, the uncertainty in the generation availability from renewable resources and the generation adequacy analysis to adopt climate change mitigation strategies in the electricity network [3].

Renewable resources are naturally distributed over geographical locations and hence renewable based distributed generation (DG) along with central generation systems can aid in the utilisation of distributed renewable resources efficiently. The presence of active power source in a conventional passive distribution network can cause reverse power flow in the distribution feeders. Most of the existing work uses a computationally extensive Monte Carlo simulation approach to solve probabilistic load flow for the distribution network planning with renewable DG [4, 5]. Load flow constraints play an important role in distribution network planning with optimal renewable DG placement. Monte Carlo simulation based probabilistic load flow solutions requires long computational time to solve the optimisation problems associated with the distribution network planning. However, analytical methods using probabilistic load flow solution can reduce the computational burden and provide better insight in the network operational impacts assessment due to renewable DG integration.

In addition, limited outcomes have been reported in the literature on the uncertainties associated with the available generation from renewable DG systems and utilising the correlation between time-varying load-demand and the wind generation in the distribution feeder. Due to the diurnal and seasonal variations, a correlation may exist between the load demand in distribution feeder and the available generation from renewable DG. The correlation associated with the load demand in a distribution feeder and the available generation from the renewable DG may significantly influence power flows through the distribution feeders. The non-consideration of the correlation between distribution feeder load and the generation from the renewable DG may lead to improper utilisation of distributed resources. This emphasises the requirement to develop new analytical methods for the probabilistic load flow of a distribution network

considering the correlation between the time varying demand and the stochastic power output by renewable DG systems.

Adequacy assessment of energy supply and service continuity are essential in distribution network planning, especially when active power sources such as renewable DG systems are present [6]. The correlation between the load in the distribution feeder and the renewable DG output availability may significantly influence the energy supply adequacy and the continuity of service in the distribution network. The correlation between the load and the available generation from a renewable DG system will help in the continuity of energy supply and may lead to the reduction of excessive installed capacity of distribution network infrastructure and limited utilisation of the renewable DG potential.

The indices to assess the adequacy of energy supply and the continuity of service for the generation systems and transmission networks are well defined. However, limited studies have been reported on the energy supply adequacy and the continuity of service indices for distribution network containing renewable DG. It is essential to develop indices to quantify energy supply and service continuity in a distribution network to ensure the proper utilisation of infrastructure capacity and the renewable DG potential. Accordingly, the development of methodologies considering the correlation between the load and the generation availability of renewable DG is needed.

A sustainable and environmentally supportive distribution network design can help to achieve the climate change mitigation goal through climate change adaptation in the electricity infrastructure. Fossil fuel and renewable based hybrid energy systems (HESs) are commonly used for the electrification of isolated facilities and the design of such systems concerns the economic and the environmental aspects related to energy generation, and the reliability of energy supply [7]. However, a fossil fuel based DG produces GHG emissions and may not be a suitable option for environmentally supportive distribution network design. Hence, renewable based DG systems can be best used for electric energy generation in the sustainable distribution network design. A life cycle assessment is commonly used to estimate the life cycle emission of renewable based generation systems. An embodied emissions index is usually considered as the indicator of life cycle emission of the generation systems. In addition to reduced embodied emission of energy, there may be several other objectives associated with a

sustainable distribution network design. Therefore, a design strategy considering the environmental and the techno-economic aspects needs to be developed for a sustainable and environmentally supportive distribution network as part of climate change mitigation strategies for the electricity network.

The strategies for climate change mitigation for an electricity network need to be implemented in the overall generation systems along with DG systems. The existing work in relation to the renewable generation penetration impacts on the electricity utilities has investigated the economic aspects of different climate change mitigation technologies such as demand side management, energy storage, less emission extensive generation units, flexible generation units [8, 9]. However, the performances of the climate change mitigation technologies in reducing the overall GHG emission from the electricity utilities along with the use of different penetration levels of renewable based generation systems are yet to be investigated, particularly the coordination of the different strategies to mitigate climate change [10]. The aggregated emission model of the generation systems is required for the emission reduction performance analysis of the climate change mitigation technologies and renewable based generation systems. This highlights the need to develop aggregated emission model of the overall generation systems and an emission reduction analysis of the climate change mitigation technologies to achieve a climate change mitigation goal with the coordination among different strategies.

Wind is one of the fastest growing renewable resources in the electricity utility infrastructure to achieve a large portion of the national and international renewable energy target. However, due to the lack of correlation between the available wind generation output and the system load demand, wind generation system is not considered as an option to support system load growth and therefore, the wind resource potentials are unutilised. The Effective load carrying capability (ELCC) is commonly used to quantify the potential of generation units in supporting system load growth and the ELCC of wind generation systems is found to be insufficient when compared to that of the fossil fuel based conventional generation units [11].

A better correlation between system the peak demand and the peak wind generation power output can improve the ELCC of the wind generation systems. Diversity exists between the power outputs from the wind generation systems located at different

geographical locations and there may be a higher correlation between the load demand in an area and the power output of a wind generation system at distant location [12]. Limited work has been reported in relation to the spatial diversity of wind resources and existing work ignores the ELCC improvement potential of the wind generation systems located at different geographical locations. Sharing of wind resources among the interconnected multi-area power systems can aid in achieving the renewable energy target (RET) of individual power system with a higher ELCC value. This emphasises the need to develop a wind resource spatial diversity sharing strategy among interconnected multi-area power systems to improve the ELCC of the combined wind generation systems.

The uncertainty and the frequent fluctuation in the availability of wind generation are some of the major reasons for wind farms to be non-dispatchable energy resources and limit the growth of wind generation in the power generation systems [13]. The lack of schedulability and dispatchability of wind farms makes the market operator's job challenging in dispatching generation units and requires the flexible generation units to adapt to the fluctuation in the wind generation output power.

Most of the existing work considers the use of the mean of the forecasted wind speed time series data for the scheduling of wind farms in the generation unit commitment studies. Moreover, limited outcomes have been reported on considering the forecast error and the uncertainties in the available generation output from wind farms, especially in the generation unit dispatch studies. The uncertainty associated with the forecasted wind speed time series data may significantly affect the dispatching of generation units and the non-consideration of wind generation fluctuation requires frequent re-scheduling of the generation units. Hence, it is essential to develop an algorithm for the wind farm scheduling considering the uncertainty in the wind speed forecasting. Furthermore, advanced technologies such as energy storage, should be integrated along with wind farm to mitigate the wind generation output fluctuation. Accordingly, a control strategy for the energy storage integrated wind farm needs to be developed to ensure the minimum alteration of the scheduled output of the generation units from their dispatch schedule.

The capacity value estimation of generation units is an essential part of generation system planning. ELCC is commonly used for quantifying the capacity value of

renewable based generation systems [14]. A distinct method is required for the ELCC estimation of renewable based generation systems as compared to that of the conventional generation units. The iterative method is commonly used for the ELCC estimation of renewable based generation systems. However, the iterative method for the ELCC estimation is computationally extensive and requires longer computational time. A limited number of non-iterative methods [11] have been reported for ELCC estimation, however, most of the reported work ignores the correlation between the renewable generation output power and the system load demand. The correlation between the renewable generation output power and the system load may have a significant impact on the capacity value of the renewable based generation systems and ignoring the correlation can introduce errors in the result. Accordingly, a non-iterative capacity value estimation method with fast computation time needs to be developed considering the correlation between the wind generation output power and the load of the system for sustainable energy generation system planning with the view of achieving the climate change mitigation target.

1.2 Research Objectives

The prime objectives of the work presented in this thesis are to develop strategies and enhance assessment tools for power system planning with renewable based generation systems to achieve the climate change mitigation target. The aims of this thesis are achieved through:

- The development of a probabilistic load flow solution formulation method for distribution networks which can consider the correlation between the renewable DG power output and the time varying load in a distribution feeder. The developed probabilistic load flow solution tool can be integrated in the distributed resource planning and the reliability assessment of the distribution network with high penetration of distributed renewable resources as part of climate change mitigation strategies.

- The establishment of indices for energy supply and continuity of service adequacy assessment in distribution network and the development of a methodology to estimate and assess the energy supply and continuity of service

adequacy indices. The developed adequacy indices will aid in distribution network planning incorporating climate change mitigation technologies, like distributed renewable resources.

- The modelling of the embodied emissions from renewable based DG systems and the formulation of a renewable based hybrid energy systems design problem for a sustainable distribution network. The design tool will aid in hybrid energy system development maintaining the optimal security and environmental disorder.

- The modelling of aggregated emissions from energy supplied through the grid in a power system and the impact assessment of the climate change mitigation technologies on emission reduction by increasing renewable generation penetration.

- The development of a strategy for sharing the wind generation spatial diversity within interconnected multi-area power systems to improve the capacity value and emission reduction potential of wind generations systems with minimum interconnection expansion. The maximisation of renewable resource utilisation, a key strategy for climate change mitigation, will be supported through this approach.

- The development of dispatch and control strategies for the wind farm output power scheduling in the electricity market to mitigate the fluctuations in the availability of wind generation output power with the aid of a battery energy storage system (BESS). The risk in renewable resource based generation systems dispatch will be reduced and the growth of the renewable based generation system will be encouraged.

- The development of the capacity value estimation method for renewable based generation systems considering the correlation between the system load and the intermittent generation output from renewable resources. The tool can be applied to the electricity network with renewable based generation systems for risk assessment and generation system planning to support climate change mitigation strategies.

1.3 Solution Approaches

The solution approaches to achieve the research objectives in the previous section are briefly presented in the following paragraphs.

An analytical method has been developed for the probabilistic load flow solution of distribution network with renewable DG to reduce the computational time and effort. The dependency between the time varying load demands of different consumer classes and the intermittent generation from different types of renewable resources are modelled by the cross moments and cumulants. A transformation matrix based load flow formulation is developed to solve the probabilistic load flow. The performance of the series estimation methods to estimate the probability distribution of the random variable with a non-Gaussian distribution is generally unacceptable, and therefore Pearson distribution functions are used to estimate the probability distributions of the line flows from their cumulants.

Novel indices have been developed to estimate the energy supply and the continuity of services adequacy which are essential to evaluate the distribution network adequacy and reliability. A joint probability based analytical method is formulated to assess the adequacy in terms of energy supply and the continuity of service in distribution networks embedded with DG systems. A well-being analysis has been applied to assess the energy supply and the continuity of services adequacy of the distribution network with renewable DG systems using the proposed indices.

A multi-objective optimisation technique has been formulated to design a renewable based HES thereby achieving sustainability in power generation and distribution. Life cycle embodied emissions, levelised cost of energy (LCOE) and supply continuity in the distribution network are considered as different attributes for a multi-objective decision making problem of a renewable based HES design. A life cycle assessment method has been applied to estimate the embodied emission and the LCOE of the renewable based HES. Method of moments is used to estimate the supply continuity, related to the uncertainty in renewable resources, from renewable based HES.

To assess the climate change mitigation technology impacts on emission reduction by increasing the renewable generation penetration, the mitigation indices based on the

impacts of the mitigation strategies on the demand and generation mix are developed. The change in the average demand, the variation in the peak and off-peak demand, the generation flexibility and the generation mix index are considered to evaluate the impact of the climate change mitigation strategies to facilitate the renewable generation growth in the electricity network. The marginal emission of the individual generation units is modelled using a thermodynamic model of the unit. The aggregated emission model for the energy supplied through the grid from a number of generation plants is developed based on the fuel mix of the grid.

A multi-objective decision making problem has been formulated to optimally share the installed wind generation capacity in a multi-area power systems. For a multi-objective wind generation capacity sharing strategy, the objectives include the emission reduction, the capacity value of the aggregated wind generation and interconnection expansion. Trade-off analysis has been used to select the best wind resource sharing plans. Computational models for emission reduction, capacity value and interconnection expansion are formulated for the wind generation capacity sharing strategy.

To schedule the BESS integrated wind farm (WF) dispatch level during each dispatch interval a stochastic programming model is developed considering the uncertainty in wind generation output and energy price forecasting. A ranked based dispatch algorithm is developed for BESS with multiple battery energy storage units (BESUs) based on the realised WF generation output and the scheduled dispatch level submitted to the energy market operator in advance. The ranked BESU dispatch algorithm is developed to maintain the equal lifetime of each BESU and to restrain frequent switching between charging and discharging modes which reduces the lifetime of BESS.

A non-iterative analytical technique using the joint probability distribution of the demand and the renewable generations is proposed to estimate the Loss of Load Expected (LOLE) and the peak load carrying capability (PLCC) of the system, and the ELCC of the renewable generation plant. In order to account for the seasonal and diurnal variation and the correlation between the load demand and the available renewable generations, the joint probability distribution of the demand and the renewable generations is used for the estimation of reliability indices. The ELCC of the

renewable generation plant is estimated from the PLCC values of the system before and after adding the renewable generation plant in the generation system.

1.4 Outline of the Thesis

The contents of the remaining chapters are briefly described as follows.

Chapter 2 proposes an analytical methodology to obtain the distribution network probabilistic load flow solution, considering the correlation between the time varying load demands of different consumer classes and the intermittent generation from different types of renewable resources, using a method based on cumulants and Pearson's distribution functions. The use of a transformation matrix based load flow formulation and a Pearson's distribution based parametric estimation method for probability distribution function has been presented. The results obtained using the proposed method has been presented and compared with the results from Monte Carlo simulations. The comparative study indicates that the average root mean square error remains well under 5%.

The content of Chapter 2 was published in **Renewable Energy**, vol. 55, pp. 532-543, 2013.

Chapter 3 proposes novel indices for the distribution network adequacy assessment of energy supply and service continuity considering the correlation between the load of the distribution feeder and the renewable based DG output. A methodology for estimating the proposed indices and the adequacy estimation of distribution network with renewable DG are presented using the joint probability distribution of distribution feeder load and renewable based DG output. The proposed methodology is tested using a standard test distribution network and a practical distribution network, and the results obtained using the proposed method and those from the Monte Carlo simulations are compared. The results suggest that a significant capacity in distribution feeder can be released with the integration of renewable DG and the proposed adequacy assessment method can highlight the distribution capacity release.

The content of Chapter 3 was published in **Applied Energy**, vol. 113, pp. 1015-1026, 2014.

Chapter 4 presents a renewable based hybrid energy system (HES) design strategy for the grid connected distribution network to attain sustainability in energy generation and distribution. The formulation of the objective functions is described and the application of trade-off analysis method to select feasible options for sustainable distribution network design is presented. The simulation results of the proposed design strategy using a practical distribution network are discussed and the sensitivity analysis of the HES design problem is conducted. The results suggest that energy storage system plays a significant role in the HES design for a sustainable distribution network. Energy storage system can potentially improve emission reduction and the system reliability at the cost of capital investment.

The content of Chapter 4 has been submitted for publication in **Renewable Energy** (2013) (Under Review).

Chapter 5 analyses the impacts of different climate change mitigation technologies on the emission reduction performance from renewable energy penetration in the electricity grid of New South Wales, Australia. The formulation of mitigation indices based on the impacts of the mitigation strategies on the demand and generation mix is presented. The developed aggregated emission model for the grid connected generation systems is described. The results from the impact assessment study using the proposed climate change mitigation indices on the emission reduction from a renewable generation penetration in the electricity grid of New South Wales, Australia are discussed and the results suggest that the coordination between different climate change mitigation technologies are required to efficiently achieve the goal of emission reduction from renewable resources.

The content of Chapter 5 is published in **Renewable Energy**, vol. 66, pp. 305-313, June, 2014.

Chapter 6 describes a wind resource sharing strategy, for interconnected power systems, to achieve the national renewable energy target from wind generation systems. A multi-objective decision making problem has been formulated with the objectives of load carrying capability, emission reduction and interconnection expansions. The detailed formulation for estimating the objective functions within the feasible decision variable space is presented with the aid of a three area power system example. The proposed strategy is validated using the interconnected power systems in Southeast

Australian power pool and the results suggest that wind generation capacity is allocated based on the correlation coefficient value between the system load and the wind generation power output.

The content of Chapter 6 is in Press for publication in the future issue of **IET Generation, Transmission and Distribution**.

Chapter 7 addresses the uncertainty aspect in the wind generation availability to schedule the wind farm in energy market. Hence the use of a battery energy storage system (BESS) in the wind generation fluctuation mitigation has been discussed. The formulation of a stochastic programing model for BESS integrated wind farm scheduling is presented considering the uncertainty in the wind generation availability and energy price. The developed BESS control strategy to mitigate wind generation fluctuation is presented. The simulation results for BESS integrated wind farm scheduling and dispatching in the energy market using the proposed methodology are discussed. The simulation results suggest that the proposed scheduling and dispatch control strategy can improve the system reliability and the revenue stream of the wind farm.

The content of Chapter 7 has been submitted for publication in **IEEE Transaction on Sustainable Energy**, (2013) (Reviewers comments have been addressed and the revised manuscript is under review).

Chapter 8 proposes a non-iterative method for the effective load carrying capability (ELCC) of renewable based generation plants considering correlation between the demand and the available generation from renewable resources. The proposed method is illustrated using an example power system and the validation of the proposed method is presented using the IEEE Reliability Test System (RTS) and the New South Wales power system. The simulation results using the proposed method are compared with those from the existing ELCC estimation methods, and the results from comparative study supports the applicability of the proposed method in overcoming the limitations of the existing methods.

The content of Chapter 8 is in Press for publication in **IEEE Transaction on Sustainable Energy**, (2013).

References:

[1] Intergovernmental Panel for Climate Change, “Renewable Energy Sources and Climate Change Mitigation”, Cambridge University Press, 2012.

[2] Climate Change Authority, Australian Government, “Renewable Energy Target Review, Final Report”, December 2012.

[3] Australia Energy Market Commission, “Review of Energy Market Frameworks in Light of Climate Change Policies”, September 2009.

[4] P. Chen, Z. Chen, B. Bak-Jensen, "Probabilistic load flow: A review," *Proc. Of International Conference on Electric Utility Deregulation and Restructuring and Power Technologies, 2008. DRPT 2008. Third* , pp.1586,1591, 6-9 April 2008.

[5] J. A. Martinez, J. Mahseredjian, "Load flow calculations in distribution systems with distributed resources. A review," *IEEE Power and Energy Society General Meeting, 2011*.

[6] Y. M. Atwa, E. F. El-Saadany, M. M. A. Salama, R. Seethapathy, M. Assam, S. Conti, "Adequacy Evaluation of Distribution System Including Wind/Solar DG During Different Modes of Operation,", *IEEE Transaction on Power Systems*, vol. 26, no. 4, pp. 1945-1952, Nov. 2011.

[7] W. Zhou, C. Lou, Z. Li, L. Lu, H. Yang, “Current status of research on optimum sizing of stand-alone hybrid solar-wind power generation systems,” *Applied Energy*, vol. 87, no. 3, pp. 380-389, 2010.

[8] T. B. Nguyen, N. Lu, C. Jin, “Modeling impacts of climate change mitigation technologies on power grids”, *Proc of IEEE Power and Energy Society General Meeting 2011*.

[9] Z. A. Muis, H. Hashim, Z. A. Manan, F. M. Taha, P. L. Douglas, “Optimal planning of renewable energy-integrared electricity generation schemes with CO2 reduction target”. *Renewable Energy*, vol. 35, pp. 2562-2570, 2010.

[10] M. P. McHenry, “Integrating climate change mitigation and adaptation: Refining theory for a mathematical framework to quantify private and public cost-effectiveness and C emissions for energy and development projects”, *Renewable Energy*, vol. 36, pp. 1166-1176, 2011.

[11] A. Keane, M. Milligan, C. J. Dent, , B. Hasche, , C. D'Annunzio, K. Dragoon, H. Holttinen, N. Samaan, , L.Soder, and M.O'Malley, "Capacity Value of Wind Power," *IEEE Transaction on Power Systems*, pp. 564 - 572 vol. 26, no. 2, May 2011.

[12] Australian Energy Market Operator, “Wind Integration in Electricity Grids Work Package 3: Simulation using Historical Wind Data”, *Wind Integration Investment Work Package 3*. http://aemo.com.au/Electricity/Planning/Related-Information/~/media/Files/Other/planning/0400-0056%20pdf.ashx, accessed May 2013

[13] U.S. Department of Energy (2008, July), “20% wind energy by 2030, Increasing wind energy’s contribution to U.S. electricity supply“, Oak Ridge, TN. [Online]. Available: http://www.nrel.gov/docs/fy08osti/41869.pdf.

[14] R. Perez, M. Taylor, T. Hoff, J. P. Ross, “Reaching consensus in the definition of photovoltaics capacity credit in the USA: Apractical application of satellite-derived solar resource data,” *IEEE Journal of Selected Topics in Applied Earth Observations and Remote Sensing*, vol. 1, no. 1, pp. 28-33, Mar, 2008.

Chapter 2

Probabilistic Load Flow for Electricity Infrastructure with Renewable Energy Resources

ABSTRACT

The time-varying demand and stochastic power generation from renewable distributed generating resources necessitate an exhaustive assessment of distribution feeder parameters for the purpose of long-term planning. This chapter proposes a novel formulation of probabilistic load flow for distribution feeders with high penetration of renewable distributed generation. The dependency between the load demand of different consumer classes and generation from different types of renewable resources is addressed in this study. In order to capture the coincidental variations of demand and generation, associated time series data for the same time instances are used. A transformation matrix based probabilistic load flow is formulated using the method of cumulants. Moreover, Pearson distribution functions are used to estimate the probability distribution of the line flows. The proposed load flow method is tested on a practical distribution feeder with high penetration of solar photovoltaic and wind energy conversion systems. The results demonstrate the aptitude of the proposed method for conducting probabilistic load flow studies with dependent non-Gaussian distribution of load and generation.

2.1 Introduction

The increased concerns about clean energy generation and effective utilisation of distributed resources are accelerating the growth of renewable Distributed Generation (DG) into distribution networks. The growing trend of renewable DG requires the consideration of bidirectional power flow in a typical distribution feeder. Uncertainty associated with power injection from renewable resources and time varying load demands introduce abrupt variations in the power flows throughout the feeder. Probabilistic Load Flow (PLF) can be used to determine the amount of certainty in various network parameters obtained using sequential power flow solutions. Despite of uncertainties associated with variations in demand and generation, certain level of dependency exists between these quantities [1]. In order to evaluate the network parameters, both the uncertainty and the dependency among the varying quantities should be considered. A PLF solution, that can address the variations in the network parameters such as line flows, can aid in distribution feeder planning and operation with renewable DG units.

PLF is first proposed by Borkowska in 1974 [2]. In Ref. [3], convolution of the probability density functions (PDFs) of nodal powers is applied in DC load flow to compute the PDF of line flows for the network. Fast Fourier Transformation technique is used for computing the convolution between the density functions. In Ref. [4], point estimation method is used for PLF solution. For this method, *2m* load flow calculations are required to solve the PLF with *m* number of uncertainties of the network components. It has been reported in Ref. [5] that the point estimation method is computationally complex for multivariate distribution of the nodal power injections. PLF solution for a distribution feeder is presented in Ref. [6] using Monte Carlo Simulation (MCS) based technique. Cumulants method is proposed in Ref. [7] to compute the reliability index of the electricity network and Laguerre series is used to estimate the PDF of load and generation. A comparative study on the performance of the series estimation with different numbers of cumulants is also presented in Ref. [7]. In Ref. [8], the method of moments is used for PLF calculation involving transmission network congestion. The Gram-Charlier series expansion is used to estimate the probability distribution of the line flows. In Ref. [5], Cornish-Fisher expansion series is used to estimate the probability distribution of line flows using short term forecasting

data. Combined point estimation and cumulants method are used to evaluate the moments and cumulants of the line flows.

The determination of state variables for an electricity network with renewable resources demands for the consideration of stochastic generation patterns in the PLF formulation. In Ref. [6], the PLF is developed for a distribution feeder with solar photovoltaic (PV) based generation. In Refs. [9, 10], wind generation is considered in the PLF to estimate the line flows of the transmission network.

The dependency between the demand and the renewable power generation must be considered in the PLF solution. In Ref. [11], linear dependency among the demands at different nodes is considered in the PLF. Linear dependency between the active and reactive power is also considered in this MCS based PLF solution. In Ref. [5], the correlation among the generation levels of different wind farms is considered in the PLF formulation. The correlation among the load demands at different nodes is also considered separately in this study. In Ref. [12], the correlation among the power outputs of different photovoltaic DG units in a distribution feeder is considered for PLF solution. It is noted that the correlation between generation and the demand is not considered in the studies reported in Refs. [5], [9] and [12].

Dependent random number generation presented in Refs. [5,12] is developed based on the generation of the multivariate normal random numbers with a given correlation coefficient matrix. Afterwards, the multivariate normal random numbers are transformed into uniformly distributed random numbers and followed by the transformation to the actual distributed random numbers of the desired distribution. As a result, the individual random variables generated using this process show the respective distributions for their marginal distributions. However, the dependency among the multivariate random numbers remains same as the normal multivariate random numbers. An impact of this consequence can be found in the third cross central moments of the random numbers. Since the third order cross central moments of the multivariate normally distributed random numbers are zero, the third order cross central moments of the random variables generated using the procedures described in [5] and [12] are found to be zero. In real case, the dependency among the random variables may not follow the normal distribution [13].

From different studies reported in the literature on the PLF solution using the method of moments, it is observed that the procedures involved in PLF solution can be divided into four steps, as shown in Fig. 2.1, namely uncertainty modelling of the random variables, generation of the moments and cumulants of the random variables, computation of the cumulants of the dependent random variables, and estimation of the probability distribution of the dependent random variables. In many PLF studies, the Taylor series approximation is used for estimating the probability distribution of the dependent random variables. With the series expansion methods such as Gram-Charlier series, Edgeworth series and Cornish-Fisher series, Normal density function is used as the base function. Although these series expansions show satisfactory performance for the Gaussian or near-Gaussian distribution, non-Gaussian distribution cannot be accurately estimated using these series expansions [14]. Since, the load demand typically follows Gaussian distribution; series approximation can be suitable for PLF solution of the electric network with low penetration of renewable energy resources. The probability distributions of the generated power from different types of renewable DG systems are usually non-Gaussian. The non-Gaussian components dominate the probability distributions of the line flows when the renewable DG penetration is high. For this reason, new methodology is required for obtaining PLF solution of a distribution feeder with high penetration of the renewable DG units. The load demand in the distribution feeder and the power from renewable DG systems may be affected by weather conditions, seasonal variations and human activities. It is envisaged that there could be a dependency between the time varying load demand and stochastic generation from renewable DG systems, which needs to be accounted while obtaining a PLF solution.

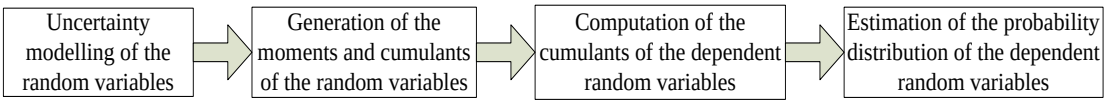

Fig. 2.1. Steps involved in PLF based on method of moments.

Analytical methods for probabilistic analysis of power systems are widely used since those are less computationally intensive with acceptable accuracy and can provide greater insight on the influencing attributes related to the power system operation. On the other hand, Monte Carlo simulations (MCS) techniques are preferred for complex

system analysis where it is difficult to model the large number of variables. Sequential MCS technique uses transition probabilities between the component states to sample the chronological order of random variables. Hence, sequential MCS technique can include the correlation between random variables and considered as a standard methodology for benchmarking results obtained from analytical methods. Non-sequential MCS technique uses random sampling from the probability distributions of the variables and it exhibits fast convergence characteristics and simplicity compared to time sequential MCS technique [15]. However, non-sequential MCS technique requires additional computational efforts to establish correlation between random variables. Also, it is to be noted that the non-sequential MCS technique demands for high computation time and lacks accuracy in estimating PDF and cumulative distribution function (CDF) of the network parameters as compared to the proposed method.

Load duration method (LDM), linear regression method and non-linear regression method are used for non-sequential MCS in Ref. [16] to incorporate the correlation between demand and solar photovoltaic (PV) generation. Latin hypercube sampling technique has been applied for random sampling of non-sequential MCS technique in Ref. [17] to account the correlation between demand and wind generation. In Ref. [18], data clustering technique, aggregated Markov model, LDM and pseudo-chronological method are used in non-sequential MCS technique to incorporate the dependency between demand, generation outage and scheduled maintenance for reliability study of power systems. A detailed comparison between these methods and with sequential MCS technique is also presented in Ref. [18].

This chapter proposes a new methodology to solve PLF for a distribution feeder with high penetration of renewable DG units. The dependency between the load demands of different consumer classes and generation from different types of renewable resources is also addressed in this study. In order to capture the coincidental variations, time series data of the demand and generation for the same time instance are used to evaluate cross moments and cumulants. The sufficiently long length of the time series data has been considered to include the seasonal variations in the demand and generation. A transformation matrix based probabilistic load flow is formulated and used for obtaining a PLF solution. Pearson distribution functions are used to estimate the probability distribution of the line flows. The proposed method is tested on a practical distribution feeder with high penetration of renewable DG units.

The paper is organised as follows. In Section 2.2, the uncertainty modelling of demand and generation, and transformation matrix based load flow formulation are presented. In Section 2.3, applicability of method of cumulants in PLF formulation is presented. Section 2.4 describes the estimation method for the probability distribution of the line flows using Pearson distribution functions. In Section 2.5, the computational procedures for obtaining the PLF solution are presented. The practical distribution feeder details, for testing the proposed PLF solution method, are presented in Section 2.6. The results are elaborated in Section 2.7 while concluding remarks are discussed in Section 2.8.

2.2 Load Flow Formulation for Distribution Feeders with Demand and Generation Fluctuations

The timer varying load demands and stochastic renewable power generation patterns are independent of each other and their peaks may not coincide in most of the cases. In this Section, modelling of time varying load demands and stochastic renewable power generation outputs will be discussed, and a classical load flow approach for estimating power flows in distribution feeders under demand and generation fluctuations will be presented.

2.2.1 Modelling of load demands

The variation of the load demand in distribution feeder contains deterministic and stochastic components. Time and climate are the two factors for deterministic component of the demand variation, whereas stochastic component is an independent random variable. Daily, weekly and seasonal variations can be observed for the load demand in the distribution feeder. The daily and weekly variations in the demand mainly depend on the behavioural patterns of different energy consumers. The consumers in the distribution feeder can be classified based on the variations in their demands at different time intervals of the day. Based on the behaviour of the consumer classes, different daily demand profiles can be found for different days in a week. Moreover, seasonal variations in the daily demand profile can also be observed. Typical daily load profiles of different consumer classes can be acquired from the chronological

demand data of the region [19]. The weekly and seasonal variations can be obtained by statistical analysis of the historical data. Despite of the fact that daily load profiles are different for different energy consumer classes, certain relationship exists between the demand profiles of the different energy consumer classes. The relationships between the demands of the different consumer classes can be obtained from the statistical quantities, such as covariance and cross moments, and can be evaluated from their demand profiles at the same time instances. The seasonal variation and stochastic variation of the demand for the energy consumers in a distribution feeder can be presented with the aid of demand profile of one year.

It is assumed that the demand of the same consumer class varies simultaneously and follows the same normalised daily load profile with weekly and seasonal variations. Based on the average load connected at different nodes of the distribution feeder within the same consumer class, the instantaneous nodal demand can be different. The daily load profile of an energy consumer class can be expressed in vector form as follows.

$$DLP_{Ci,WD} = \left[L_{Ci,WD}(1), L_{Ci,WD}(2), ...L_{Ci,WD}(t)....L_{Ci,WD}(N_d)\right] \tag{2.1}$$

$$DLP_{Ci,WE} = \left[L_{Ci,WE}(1), L_{Ci,WE}(2), ...L_{Ci,WE}(t)....L_{Ci,WE}(N_d)\right] \tag{2.2}$$

$$\Delta t = \frac{24}{N_d} \tag{2.3}$$

where, $DLP_{Ci,WD}$ and $DLP_{Ci,WE}$ are the daily load profiles of consumer class *Ci* for week days and weekends, respectively. $L_{Ci,WD}(t)$ and $L_{Ci,WE}(t)$ are the normalised average demand of the consumer class *Ci* during t^{th} interval of weekdays and weekends, respectively. N_d is the number of intervals of the day and Δt is the duration of each time interval considered for daily load profile. The monthly variations and stochastic variation of the demand can be incorporated with the daily load profile, and annual demand profile can be evaluated using (2.4).

$$L_{Ci,W}(m,d,t) = f_P(m,d) \times L_{Ci,W}(t) + b_L(m,d) \tag{2.4}$$

$$for, \quad w \in [WD, WE] \ \ and \quad t \in [1, 2, ..., N_d]$$

where, $L_{Ci,W}(m,d,t)$ is the normalised average demand of consumer class *Ci* at the d^{th} day of the m^{th} month during t^{th} time interval. Two functions $f_P(m,d)$ and $b_L(m,d)$ are used to

model the deterministic and stochastic component of the demand profile, respectively. These functions can be obtained from the historical data of the demand for the associated consumer class.

2.2.2 Modelling of renewable generating systems

The generation outputs of renewable energy resources depend on the availability of the primary resource, e.g. solar irradiation, wind speed, etc. In general, the modelling of renewable generation outputs involves modelling the availability of the renewable resources and associated energy conversion processes. The resource availability model can be different for different types of renewable resources. Solar PV and wind turbine are two commonly used technologies for renewable DG systems. The modelling of these generating resources will be discussed below.

Generated power of the solar PV cell arrays depends on the solar irradiation incident on the cell surface and the PV cell array parameters, such as cell material and inclination. The variation of the solar irradiation incident on the cell surface has deterministic and stochastic components. The solar irradiation on the horizontal plane of extra-terrestrial surface is the deterministic component. For a particular geographic location, the solar irradiation on the horizontal plane of extra-terrestrial surface has specific pattern throughout the year and can be obtained from astronomical data. The stochastic component of variations in solar irradiation incident on the cell surface is due to the deviations in sky clearness. The sky clearness is characterised by the clearness index. Solar irradiation on the PV cell during time *t* can be evaluated using (2.5).

$$I_g(t) = k_C(t) \times I_0(t) \tag{2.5}$$

where, $I_g(t)$ and $I_0(t)$ are the solar irradiations on the horizontal plane of the earth surface and on the extra-terrestrial surface during time *t*, respectively. The clearness index at time *t* is denoted by $k_C(t)$ and is a random quantity. The probability distribution of $k_C(t)$ can be evaluated from the historical meteorological data. The power output from the solar PV array can be evaluated using (2.6) [6].

$$P_{Spv}(t) = \eta_{Spv} \times A_{ca} \times \left(T_{SPV} \times I_g(t) - T'_{SPV} \times I_g^2(t)\right) \tag{2.6}$$

where, $P_{Spv}(t)$ is the output power generated by the solar PV system during time t. η_{Spv} is the efficiency of solar PV cell array and A_{ca} is the effective surface area of the PV cell array. T_{SPV} and T'_{SPV} are the parameters of the solar PV array installation and depend on inclination, declination, reflectance of the ground, latitude-longitude, hour angle, sunset hour angle, day of the year and ambient temperature.

The power generated from the wind turbine depends on the wind speed at the hub height of the whole installation. The seasonal effect can be observed for wind speed in certain area. The wind speed at the hub height can be estimated using the Autoregressive Moving Average (ARMA) model as shown in (2.7) [20].

$$\begin{aligned} v_W(t) = a_1 v_W(t-1) + a_2 v_W(t-2) + ... + a_n v_W(t-n) \\ + w(t) - b_1 w(t-1) - b_2 w(t-2) - ....b_m w(t-m) \end{aligned} \tag{2.7}$$

where, $v_W(t)$ is the wind speed at hub height during time t and $w(t)$ is the white noise. $a_i(i=1,2,...n)$ and $b_i(i=1,2,....,m)$ are the autoregressive and moving average parameters of the model respectively. The order of the ARMA is n and m for autoregressive and moving average components, respectively. From the time series data of wind speed at hub height of the wind turbine, the power output can be computed using (2.8) [21].

$$P_{Wind}(t) = \begin{cases} 0 & 0 \le v_W(t) < v_{ci} \\ \left(A_W + B_W \times v_W^3(t)\right) \times P_{Wr} & v_{ci} \le v_W(t) < v_r \\ P_{Wr} & v_r \le v_W(t) < v_{co} \\ 0 & v_{co} \le v_W(t) \end{cases} \tag{2.8}$$

where, $P_{Wind}(t)$ is the power generated from the wind turbine at time t. v_{ci}, v_r and v_{co} are the cut in speed, rated speed and cut out speed for the wind turbine respectively. A_W and B_W are the wind turbine parameters, which depend on v_{ci}, v_{co} and v_r respectively. P_{Wr} is the rated power of the wind turbine.

2.2.3 2.2.3 A classical load flow approach

The load connected at the nodes of the distribution feeder can be composed of either with the single energy consumer class or the combination of the energy consumer classes. The net load demand at node k can be expressed using (2.9) and (2.10) in terms of the instantaneous real and reactive power injection, by the individual energy consumer class, respectively.

$$\left[P_{load,k}(t)\right]=\left[A_{c2n}\right]\times\left[P_{Load,Ci}(t)\right] \tag{2.9}$$

$$\left[Q_{load,k}(t)\right]=\left[A_{c2n}\right]\times\left[Q_{Load,Ci}(t)\right] \tag{2.10}$$

$$\textit{where, } \left[P_{load,Ci}(t)\right]=\begin{bmatrix} P_{load,C1}(t) \\ P_{load,C2}(t) \\ \vdots \\ \vdots \\ P_{load,CNc}(t) \end{bmatrix} \left[Q_{load,C}(t)\right]=\begin{bmatrix} Q_{load,C1}(t) \\ Q_{load,C2}(t) \\ \vdots \\ \vdots \\ Q_{load,CNc}(t) \end{bmatrix}$$

$$\textit{and} \quad \left[A_{c2n}\right]=\begin{bmatrix} p_{c,11} & p_{c,12} & \cdots & \cdots & p_{c,1Nc} \\ p_{c,21} & p_{c,22} & \cdots & \cdots & \vdots \\ \vdots & \vdots & \ddots & & \vdots \\ \vdots & \vdots & & \ddots & \vdots \\ p_{c,Nn1} & \cdots & \cdots & \cdots & p_{c,NnNc} \end{bmatrix}$$

where, $P_{load,k}(t)$ and $Q_{load,k}(t)$ are the net real and reactive power demands for node k at time t respectively. Similarly, $P_{load,Ci}(t)$ and $Q_{load,Ci}(t)$ are the normalised real and reactive power demands of the consumer class Ci at time t. Nn and Nc is the total number of nodes and total number of energy consumer classes in the distribution feeder, respectively. A_{c2n} is a transformation matrix of $Nn \times Nc$ order and is used to convert the normalised power demands of individual consumer class to the net demand. $p_{c,ik}$ is the element of A_{c2n} matrix at the i^{th} row and k^{th} column. The value of $p_{c,ik}$ is equal to the peak demand of the consumer class k connected at node i of the distribution feeder. In this analysis the load current is considered as the negative injected current. The current injection at node k can be computed from the real and reactive power injection using (2.11).

$$I_{load,k}(t)=\left(\frac{P_{load,k}(t)+jQ_{load,k}(t)}{V_k(t)}\right)^* \tag{2.11}$$

where, $I_{load,k}(t)$ and $V_k(t)$ are the nodal current injection and node voltage at node k during time t respectively. The notation "*" in (2.11) indicates the conjugate of the complex quantity inside the bracket. The current flowing through every line section of the radial distribution feeder constitutes of the current flowing through the subsequent line sections and the nodal current injection at the receiving end of that line section. The real and reactive components of the line current can be evaluated using (2.12) and (2.13).

$$I_{real,line,i}(t) = \sum_{l} I_{real,line,l}(t) + I_{real,load,k}(t) \tag{2.12}$$

$$I_{reactive,line,i}(t) = \sum_{l} I_{reactive,line,l}(t) + I_{reactive,load,k}(t) \tag{2.13}$$

where, $I_{real,line,i}(t)$ and $I_{reactive,line,i}(t)$ are the real and reactive components of the line current flowing through i^{th} line section at time t, respectively. The set l consists of the line section numbers which are connected to the receiving end of line section i (k^{th} node). $I_{real,load,k}(t)$ and $I_{reactive,load,k}(t)$ are the real and reactive component of the load current injection at node k (the receiving end of the line section i) during time t, respectively. Since the distribution feeders are radial, (2.12) and (2.13) can be written in the matrix form for all the line flows as shown in (2.14) and (2.15), respectively.

$$\left[I_{real,line}(t)\right] = \left[A_{n2l}\right] \times \left[I_{real,load}(t)\right] \tag{2.14}$$

$$\left[I_{reactive,line}(t)\right] = \left[A_{n2l}\right] \times \left[I_{reactive,load}(t)\right] \tag{2.15}$$

$$where,\ \left[I_{real,line}(t)\right] = \begin{bmatrix} I_{real,line,1}(t) \\ I_{real,line,2}(t) \\ \vdots \\ \vdots \\ I_{real,line,Nl}(t) \end{bmatrix} \qquad \left[I_{real,load}(t)\right] = \begin{bmatrix} I_{real,load,1}(t) \\ I_{real,load,2}(t) \\ \vdots \\ \vdots \\ I_{real,load,Nn}(t) \end{bmatrix}$$

$$\left[I_{reactive,line}(t)\right] = \begin{bmatrix} I_{reactive,line,1}(t) \\ I_{reactive,line,2}(t) \\ \vdots \\ \vdots \\ I_{reactive,line,Nl}(t) \end{bmatrix} \qquad \left[I_{reactive,load}(t)\right] = \begin{bmatrix} I_{reactive,load,1}(t) \\ I_{reactive,load,2}(t) \\ \vdots \\ \vdots \\ I_{reactive,load,Nn}(t) \end{bmatrix}$$

$$\left[A_{n2l}\right] = \begin{bmatrix} k_{l,11} & k_{l,12} & \cdots & \cdots & k_{l,1Nn} \\ k_{l,21} & k_{l,22} & \cdots & \cdots & \vdots \\ \vdots & \vdots & \ddots & & \vdots \\ \vdots & \vdots & & \ddots & \vdots \\ k_{l,Nl1} & \cdots & \cdots & \cdots & k_{l,NlNn} \end{bmatrix}$$

where, A_{n2l} is the transformation matrix of $Nl \times Nn$ order and is used to transform the nodal current injection to the line current. Nl is the total number of line sections in the distribution feeder. $k_{l,ik}$ is the element at the i^{th} row and k^{th} column of A_{n2l} matrix. The value of $k_{l,ik}$ is equal to 1 if the k^{th} node is fed through the i^{th} line section of the feeder. If the k^{th} node is not fed through i^{th} line section, the value of $k_{l,ik}$ is equal to 0. Nl and Nn are the total numbers of line sections and nodes in the distribution feeder, respectively. The voltages at the downstream nodes of the radial distribution feeder are calculated by

subtracting the voltage drop of each line section, between the respective node and the substation, from the voltage at the substation. The voltage drop in each line section is equal to the product between the impedance of the line section and the line current. The node voltages of the distribution feeder can be evaluated using (2.16).

$$[V_i(t)] = [V_0] - [Z_{line}] \times \left([I_{real,load}(t)] + \hat{j}[I_{real,load}(t)] \right) \tag{2.16}$$

$$\text{where, } [V_i(t)] = \begin{bmatrix} V_1(t) \\ V_2(t) \\ \vdots \\ \vdots \\ V_{Nl}(t) \end{bmatrix} \quad [V_0] = \begin{bmatrix} V_0 \\ V_0 \\ \vdots \\ \vdots \\ V_0 \end{bmatrix}$$

$$[Z_{line}] = \begin{bmatrix} Z_{l,11} & Z_{l,12} & \cdots & \cdots & Z_{l,1Nn} \\ Z_{l,21} & Z_{l,22} & \cdots & \cdots & \vdots \\ \vdots & \vdots & \ddots & & \vdots \\ \vdots & \vdots & & \ddots & \vdots \\ Z_{l,Nl1} & \cdots & \cdots & \cdots & Z_{l,NlNn} \end{bmatrix}$$

where, $[Z_{line}]$ is the transformation matrix of $Nn \times Nl$ order and is used to transform the line current injection to the voltage drop of the line sections. $Z_{l,ik}$ is the element at the i^{th} row and k^{th} column of Z_{line} matrix. The value of $Z_{l,ik}$ is equal to the impedance of the line section involving k^{th} node being fed by i^{th} line section of the feeder. If the k^{th} node is not fed through i^{th} line section, the value of $Z_{l,ik}$ will be equal to 0. The load flow can be solved by iterative methods using the equations (2.9) to (2.16).

The renewable DG units are modelled as negative load in the load flow formulation for the radial distribution feeder. In this study, solar PV and wind based DG units are considered as an energy consumer class with negative load.

2.3 Probabilistic Load Flow Formulation using Method of Cumulants

Probability of occurrence of an event in a series of events can be defined as the fraction of total number of events in that series for which the event has occurred. PDF of a random variable is a function that represents the probability of occurrence of an event in the complete series of events when the random variable takes the value corresponding to that event. Moments and cumulants of the random event can be used

to define the characteristics of the PDF [22]. Due to the properties of moments, cumulants of the random event can be used in computing the function of random variables.

2.3.1 Moments and cumulants

The v^{th} moments of a single random variable about the origin can be computed using (2.17) and (2.18) for continuous and discrete data series respectively.

$$\mu_v' = E\left[X^v\right] = \int_{-\infty}^{\infty} x^v f(x)dx \tag{2.17}$$

$$\mu_v' = E\left[X^v\right] = \frac{1}{N}\sum_i x_i^v \tag{2.18}$$

where, x_i is the i^{th} data in the given data series, X and N is the total number of data points in the data series. *E[X]* and *f(x)* are the expected value and PDF of the random variable X respectively. μ_v' is the v^{th} order moment of the single random variable X. The 1st order moment (μ_1') is called the mean of the random variable. Mean of the random variable describes the location of the PDF. Mean value is also known as the expected value and is used to compute the central moments of the data series as follows.

$$\mu_v = E\left[(X-\mu_1')^v\right] = \int_{-\infty}^{\infty} (x-\mu_1')^v f(x)dx \tag{2.19}$$

$$\mu_v = E\left[(X-\mu_1')^v\right] = \frac{1}{N}\sum_i (x_i-\mu_1')^v \tag{2.20}$$

where, μ_v is the v^{th} central moment of X. Variance is the second central moment of a probability distribution and describes the span of the PDF. The higher the variance of a distribution, the higher the span of the probability density of the random variables would be.

When the multiple random variables with dependency are involved in the analysis, the cross moments among the random variables need to be considered. Let us consider a vector X with Nrv number of random variables, where $\boldsymbol{X}=[X_1, X_2, \ldots, X_{Nrv}]$. The v^{th} order central moments can be expressed with the aid of (2.21).

$$\mu_{[v]} = E\left[\prod_{i=1}^{v}\left(X_i - {}_{Xi}\mu_1'\right)\right] \tag{2.21}$$

$$where,\ [v] = [\overbrace{i1, i2, ..., in_v}^{v}] \qquad i1, i2, ... \in [1, 2, ...Nrv]$$

where, ${}_{xi}\mu'_1$ is the mean of the random variable X_i and $\mu_{[v]}$ is the v^{th} order cross central moments. Nrv and n_v are the total number of random variables in $\boldsymbol{X}$ and the number of elements in vector v, respectively. The number of elements in the vector v is the order of the central moments. If an element is repeated $n_{i,r}$ times in the vector v, the order for the random variable corresponding to the element is equal to $n_{i,r}$.

The characteristics of the probability distribution of the random variables can be assessed from the cumulants of the random variables. The cumulants of v^{th} order can be evaluated using the central moments of the random variables as shown in (2.22) [23].

$$\left.\begin{aligned}
\kappa_{[i]} &= \mu'_{[i]} \\
\kappa_{[i,j]} &= \mu_{[i,j]} \\
\kappa_{[i,j,k]} &= \mu_{[i,j,k]} \\
\kappa_{[i,j,k,l]} &= \mu_{[i,j,k,l]} - \mu_{[i,j]}\mu_{[k,l]} - \mu_{[i,k]}\mu_{[j,l]} - \mu_{[i,l]}\mu_{[j,k]} \\
\cdots \quad & \cdots \quad \cdots \quad \cdots
\end{aligned}\right\} \tag{2.22}$$

where, $\kappa_{[v]}$ is the v^{th} order cumulant of the random variable. If all the elements of the vector $[v]$ are same, the cumulants $\kappa_{[v]}$ are called as self-cumulants. On the other hand, if more than one element in vector $[v]$ are same, the cumulants $\kappa_{[v]}$ are called as cross-cumulants. For independent random variables, the values of the cross cumulants become equal to zero.

2.3.2 Cumulants of the sum of random variables

The PDF of the random variable, which is the sum of other random variables, can be evaluated by the convolutions of the PDFs of the random variables. There exists a relationship between the cumulants of the resultant random variable and that of the components' random variables. Let a random variable Y be the linear combination of random variables $\boldsymbol{X}$ as follows.

$$Y = A \times X + b \tag{2.23}$$

where, A is a row vector of $(1 \times n_x)$ order and n_x is the number of random variables in X. The term b in (2.23) is a constant. The relationship between the cumulants of X and the cumulants of Y are shown in (2.24) [23].

$$\left.\begin{aligned} \kappa_{y,1} &= b + \sum_{i=1}^{n_x} a_i \times \kappa_{x,[i]} \\ \kappa_{y,n_v} &= \overbrace{\sum_{i1=1}^{n_x}\sum_{i2=1}^{n_x}\cdots\sum_{in_v=1}^{n_x}}^{n_v}\left(\prod_{j=i1}^{in_v} a_j\right)\times\kappa_{x,[v]} \end{aligned}\right\} \tag{2.24}$$

where, n_v is the number of elements in vector v. $\kappa_{y,1}$ and $\kappa_{y,nv}$ are the 1st and n_v^{th} order cumulants of the random variable Y.

2.3.3 Load flow formulation using cumulants

The cumulants of the line flow in (2.14) and (2.15) can be evaluated from the self-cumulants and cross cumulants of the demands of different energy consumer classes using the properties demonstrated in (2.24). The cumulants of the line flows can be expressed as follows.

$$I\kappa_{line,i,\mathrm{Re},n_v} = \overbrace{\sum_{i1=1}^{Nc}\sum_{i2=1}^{Nc}\cdots\sum_{in_v=1}^{Nc}}^{n_v}\left(\prod_{k=i1}^{in_v} A_{n2l,k}(i,k)\right)\times I\kappa_{load,\mathrm{Re},[v]} \tag{2.25}$$

$$I\kappa_{line,i,\mathrm{Im},n_v} = \overbrace{\sum_{i1=1}^{Nn}\sum_{i2=1}^{Nn}\cdots\sum_{in_v=1}^{Nn}}^{n_v}\left(\prod_{k=i1}^{in_v} A_{n2l,k}(i,k)\right)\times I\kappa_{load,\mathrm{Im},[v]} \tag{2.26}$$

$$where,\ [v] = [\overbrace{i1, i2, ..., in_v}^{n_v}] \qquad i1, i2, ... \in [1, 2, ...Nn]$$

where, $I\kappa_{line,i,Re,nv}$ and $I\kappa_{line,i,Im,nv}$ are the n_v^{th} order cumulant of the real and imaginary component of the current through i^{th} line section, respectively. $I\kappa_{load,Re,[v]}$ and $I\kappa_{load,Im,[v]}$ are the n_v^{th} order cumulant of the real and imaginary component of the current injection from the consumer classes in [v], respectively. $A_{n2l,j}(i,k)$ is element from i^{th} row and k^{th} column of matrix A_{n2l}.

2.4 Estimation of Probability Distribution

To estimate probability distribution of power flows for different line segments in a distribution feeder, it is necessary to understand the behaviour of probability distribution parameters so that a suitable density function can be adopted. In this section, the characteristics of parameters of probability distributions are discussed and different types of density functions under Pearson distribution family are presented.

2.4.1 Characteristic parameters of probability distributions

Shape and location of the PDF of a quantity can be described by the parameter mean, median, mode, variance, skewness and kurtosis of the sample. Mean, median and modes of the random variable are used to describe the location of the PDF. Median is the value of the random variable that divides the total probability into two parts. Mode is the value of random variable that occurs most frequently in the data series. For some distribution, there may be more than one mode value and is known as multi modal distribution. For certain distribution, such as normal distribution, mean coincides with the mode of the random variable. Skewness of the random variable illustrates the property of symmetry with respect to the mean value in its probability distribution. The skewness, λ_1 of the random variable can be expressed using the 2nd and 3rd order moments and cumulants as shown in (2.27).

$$\lambda_1 = \frac{\mu_3}{\mu_2^{3/2}} = \frac{\kappa_3}{\kappa_2^{3/2}} \tag{2.27}$$

The value of the skewness of a random variable indicates that the PDF is symmetric with respect to the mean. The probability distribution of a random variable with zero skewness indicates that the mean, mode and median are at the same location. The positive skewness indicates that the upper tail of the distribution is heavier than the lower tail (i.e. mean > median > mode). The negative skewness indicates that the upper tail of the distribution is heavier than the lower tail (i.e. mode > median > mean). Kurtosis of a random variable indicates the sharpness of the distribution at and near the mean value. Moreover, the tail behaviour of the probability distribution can be estimated from the value of the kurtosis of the random variable. The kurtosis, λ_2 of a

data series can be expressed using the 2nd and 3rd order moments and cumulants of the random variable as shown in (2.28).

$$\lambda_2 = \frac{\mu_4}{\mu_2^2} - 3 = \frac{\kappa_4}{\kappa_2^2} \tag{2.28}$$

Therefore, the cumulants of the data series can be used to estimate the PDF of the data series.

2.4.2 Pearson's distribution family

Let *X* be a random variable with PDF of *f(x)*. The differential equation depicted in (2.29) defines the probability distributions of random variables based on their skewness and kurtosis [22, 24].

$$\frac{df(x)}{dx} = \frac{(x-a)\times f(x)}{b_0 + b_1 x + b_2 x^2} \tag{2.29}$$

The family of density functions that follows (2.29) are known as the Pearson distributions [22, 25]. There are total 12 types of Pearson distributions including seven main types of distributions [25, 26]. The main distribution types of Pearson distributions are presented in Table 2.1. The boundaries of each type of distributions can be defined by two parameters: β_1 and β_2. The values of β_1 and β_2 can be evaluated from the skewness and kurtosis of the random variable as detailed in (2.30).

$$\left.\begin{aligned} \beta_1 &= \lambda_1^2 = \frac{\kappa_3^2}{\kappa_2^3} \\ \beta_2 &= \lambda_2 + 3 = \frac{\kappa_4}{\kappa_2^2} \end{aligned}\right\} \tag{2.30}$$

Table 2.1. PDF of Pearson Distribution Family

Distribution Type	Name of the Distribution	Probability Density Function, f(x)
I	Beta Distribution	$\frac{1}{\beta(a,b)} x^{a-1}(1-x)^{b-1}$

II	Symmetric Beta Distribution	$\frac{1}{a\times\beta(b,b)}\left(1-\frac{x^2}{a^2}\right)^{b-1}$
III	Gamma Distribution	$\frac{a^{\lambda}}{\gamma(\lambda)}x^{\lambda-1}e^{-ax}$
IV	Pearson's Type IV Distribution	$k\left(1+\frac{x^2}{a^2}\right)^{-m}e^{-\nu\tan^{-1}\left(x/a\right)}$
V	Inverse Gamma Distribution	$\frac{\lambda^{p-1}}{\gamma(p-1)}x^{-p}e^{-\lambda/x}$
VI	Beta Prime Distribution	$\frac{1}{\beta(a,b)}\frac{x^{a-1}}{(1+x)^{a+b}}$
VII	Student-t Distribution	$\frac{1}{a\times\beta(1/2,b-1/2)}\left(1+\frac{x^2}{a^2}\right)^{-b}$
Normal	Normal Distribution	$\frac{1}{a\sqrt{2\pi}}e^{-\frac{(x-b)^2}{2a^2}}$

The equations of the boundaries of the main Pearson distributions are shown in equations (2.31)-(2.34) [25]. Equation (2.31) is the boundary between the upper limit of all distributions and Type I(U) distribution. Type I(U) is the multimodal beta distribution with U-shaped PDF. The curves corresponding to (2.32) are the boundaries for Type I(J) distribution. Type I(U) is the multimodal beta distribution with U-shaped PDF. Equation (2.33) is the relation between β_1 and β_2 for Type III distribution. Type III distribution curve and upper boundary of Type I(J) are the boundaries for Type I(M) distribution known as unimodal beta distribution. Equation (2.34) represents the values of β_1 and β_2 for Type V distribution and lower limits for Type IV distribution. The equations (2.33) and (2.34) are the boundaries for Type VI distribution. Type II distribution, Normal distribution and Type VII distribution are located on the β_2 axis since these are the symmetric distributions with respect to mean. The boundaries of different types of Pearson distributions on the β_1 and β_2 plane are shown in Fig. 2.2.

$$\beta_2-\beta_1-1=0 \tag{2.31}$$

$$4(4\beta_2-3\beta_1)(5\beta_2-6\beta_1-9)^2=\beta_1(\beta_2+3)^2(8\beta_2-9\beta_1-12) \tag{2.32}$$

$$2\beta_2 - 3\beta_1 - 6 = 0 \tag{2.33}$$

$$\beta_1(\beta_2 + 3)^2 = 4(4\beta_2 - 3\beta_1)(2\beta_2 - 3\beta_1 - 6) \tag{2.34}$$

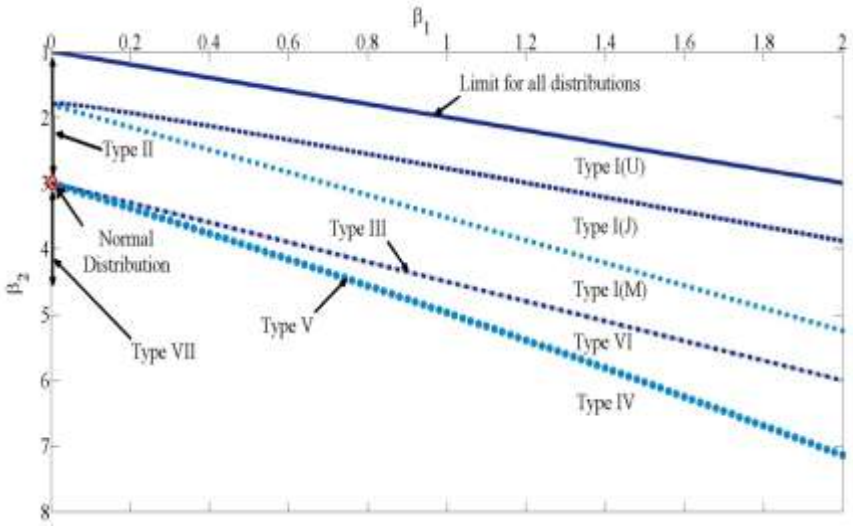

Fig. 2.2. Boundaries of Pearson distribution family in the β_1 and β_2 plane.

2.5 Computational Procedure

The PLF solution method proposed in this chapter estimates the PDF of the current and power, flowing through the line sections of a distribution feeder, from the data series of coincidental power injections at different nodes. The inputs are the load profile of different energy consumer classes, availability of renewable energy resources and energy conversion processes. The flow chart of the PLF computation procedures is shown in Fig. 2.3. The steps involved in PLF computation are discussed below.

Step 1: Time series data are generated for the availability of the renewable energy resources using the historical data and statistical analysis. The power outputs of the renewable DG systems are evaluated using the energy conversion processes and the time series data associated with the availability of these generating resources. The coincidental time series demand data of each energy consumer class are generated with the aid of historical data analysis. The demand data and the generation data are then normalised.

Step 2: The self moments and cross moments of 1^{st} to 4^{th} order for the renewable DG output and the demand of different consumer classes are computed from the time series data. The self cumulants and cross cumulants of 1^{st} to 4^{th} order for the renewable DG output and the demands of different consumer classes are computed.

Step 3: The transformation matrix A_{n2l} and A_{c2n} are evaluated from the line data and the consumer class data of the distribution feeder. The transformation matrix Z_{line} is computed from the line data of the feeder.

Step 4: The mean value of the line currents and node voltages is computed using the equations (2.9)-(2.13) iteratively. The cumulants of the power flows are computed from the self cumulants and cross cumulants of the power injections. The cumulants of the line flows are computed using the mean value of the nodal voltages and the cumulants of the power flows.

Step 5: β_1 and β_2 are computed for each line current and power flows from their respective cumulants. From the location of the (β_1, β_2) in the β_1-β_2 plane, the distribution type for each line current and power flows is determined.

Step 6: The parameters of the distribution function corresponding to each line current and power flows are evaluated from the moments of the corresponding quantities [27, 28]. Probability density function and cumulative distribution function (CDF) of each line current and power flows can be evaluated using the corresponding parameters. Normalisation and scaling of the random variable may have to be conducted for certain distributions, if required.

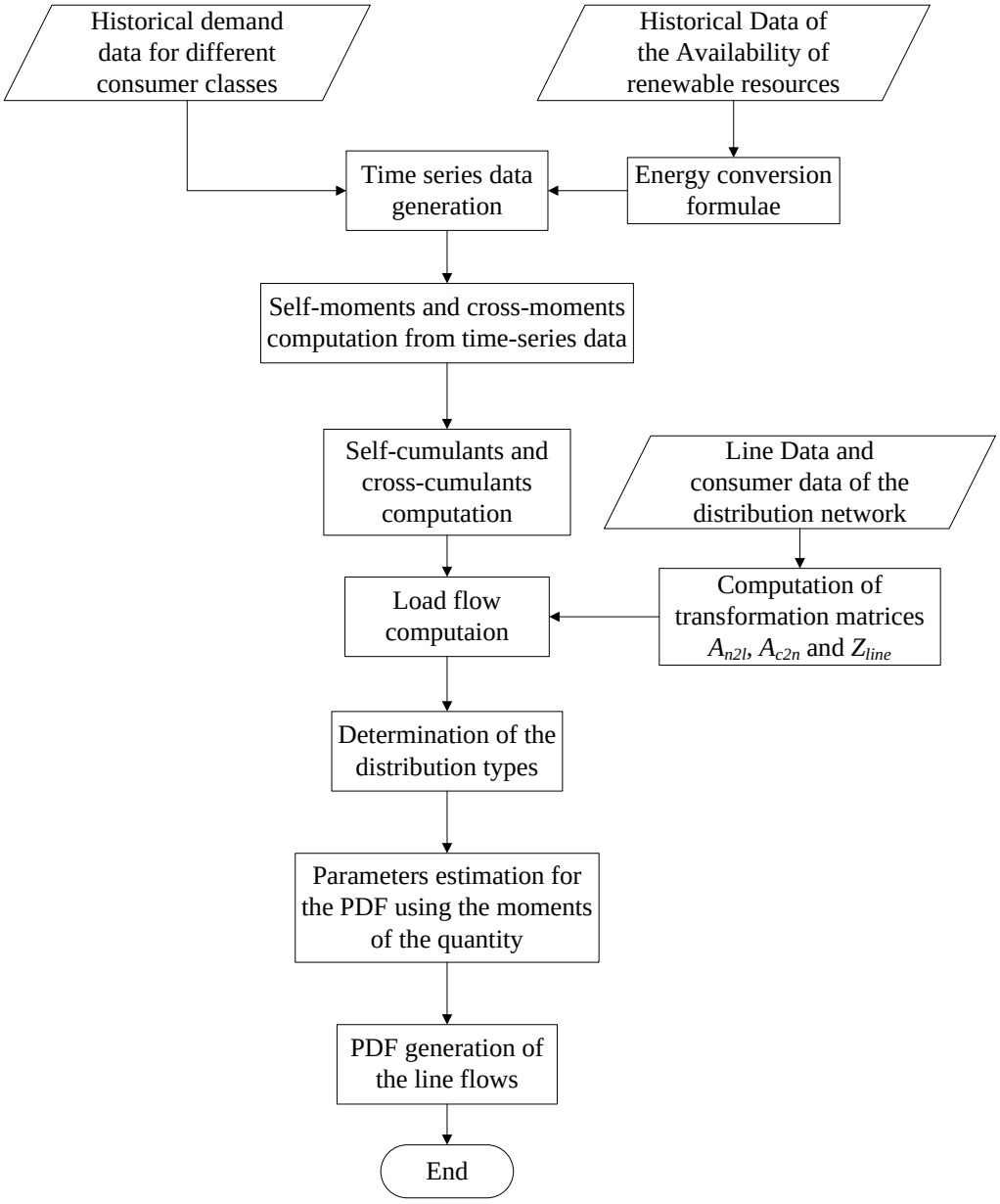

Fig. 2.3. Flow chart of the PLF computation.

2.6 A Case Study

The proposed PLF method is applied to a practical distribution feeder for evaluating the PDFs of the currents and power flows through different line sections. The time series data of hourly demand and hourly generation for a period of one year are considered in this chapter. MATLAB is used to implement the proposed algorithm for obtaining a PLF solution.

2.6.1 Description of the distribution feeder under study

An 11 kV radial distribution feeder used in this study is extracted from the electricity distribution system in New South Wales (NSW), Australia. The topology of the feeder with 87 nodes is shown in Fig. 2.4. There are 60 load points in this distribution feeder with an annual peak demand of 2.8 MW. The average power factor of the load is around 0.95. The base values for the per unit quantities are 11kV and 2.8MVA for this analysis. The energy consumers of the distribution feeder are divided into residential, industrial and commercial consumer classes. The annual peak demand of each consumer class and its nodal connectivity are shown in Table 2.2. In this study, it is considered that five solar photovoltaic (PV) units and five wind turbine generator units are connected to the 10 different nodes of the test feeder. The installed capacity of each DG unit is considered to be 500 kVA that constitutes to the total renewable DG installed capacity of 5 MVA. Hence, the total installed capacity of the renewable DG units is 170% of the annual peak of the distribution feeder. It is considered that the distribution substation transformers and protection systems will allow the upstream injection of the excess power generated in the distribution feeder. Since the geographical area served by the distribution feeder is not very large, the availability of each type of renewable resources (i.e. solar PV and wind) is considered to be same throughout the feeder.

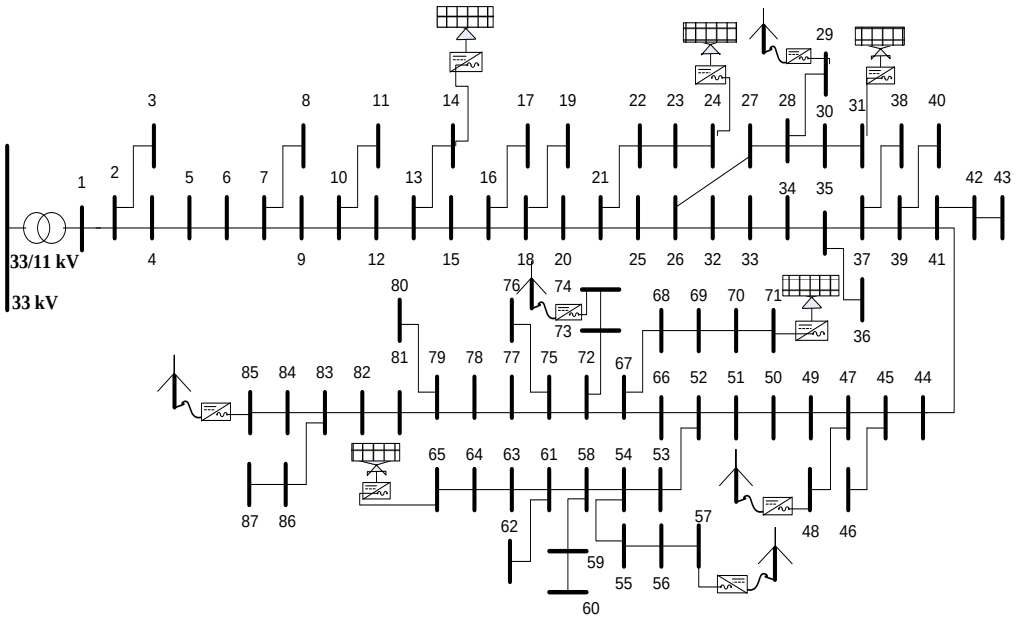

Fig. 2.4. Network topology of the distribution feeder under study.

2.6.2 Demand and generation data

The normalised daily load profile of each consumer class is shown in Fig. 2.5 in terms of average of load demands for typical weekdays (WD) and weekend (WE) of a week. The normal distribution function with unit mean and σ^2 variance is considered as the function $f_p(m,d)$ and normally independently distributed ($NID\{0, 1\}$) is considered for $b_L(m,d)$ in (2.4). The variance σ^2 of the $f_P(m,d)$ at different seasons of a year for different consumer classes is shown in Fig. 2.6. The time series data of the demand for different consumer classes are generated using (2.4).

Table 2.2. Energy consumer types and annual peak demand at the different nodes of the distribution feeder

Node No.	Consumer Class	Annual Peak Demand (kVA)	Node No.	Consumer Class	Annual Peak Demand (kVA)	Node No.	Consumer Class	Annual Peak Demand (kVA)
3	RES	64	**32**	RES	92.5	**62**	RES	35.4
4	RES	25.4	**33**	COM	28.5	**63**	RES	48.5
5	RES	12.3	**34**	RES	7.7	**64**	COM	48.5
6	RES	23.1	**36**	RES	53.9	**65**	RES	48.5
8	COM	223.5	**38**	RES	19.3	**66**	RES	27
9	RES	8.5	**40**	RES	37	**68**	RES	23.1
11	RES	37	**42**	RES	48.5	**69**	RES	23.1
12	RES	34.7	**43**	RES	48.5	**70**	RES	53.9
15	RES	34.7	**44**	RES	44.7	**71**	RES	64
17	IND	57.8	**46**	RES	7.7	**73**	RES	46.2
19	RES	28.5	**48**	RES	19.3	**74**	RES	19.3
20	RES	23.1	**49**	RES	73.2	**76**	RES	19.3
22	IND	404.6	**50**	RES	18.5	**77**	RES	46.2
23	COM	231.2	**51**	RES	62.4	**78**	RES	23.1
24	RES	11.6	**53**	RES	53.2	**80**	RES	28.5
25	RES	20	**55**	RES	16.2	**81**	RES	7.7
27	RES	28.5	**56**	RES	38.5	**82**	RES	25.4
29	RES	28.5	**57**	RES	51.6	**84**	RES	35.4
30	IND	67	**59**	RES	48.5	**85**	RES	17
31	RES	19.3	**60**	RES	48.5	**86**	RES	39.3

RES: Residential; COM: Commercial; IND: Industrial

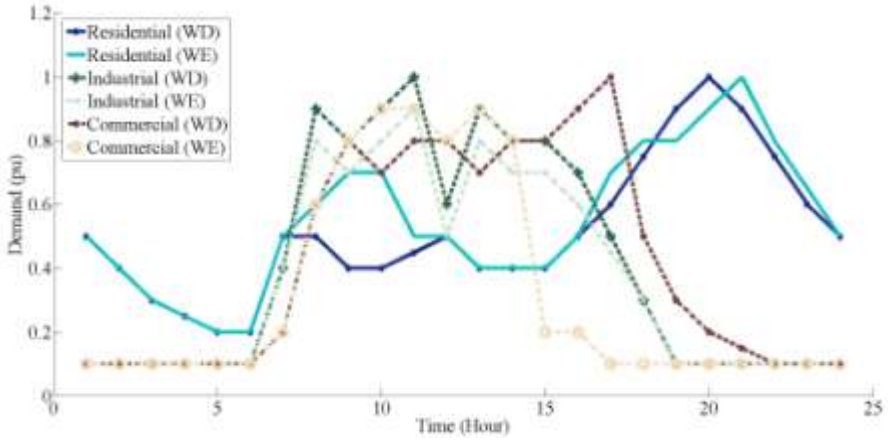

Fig. 2.5. Normalised daily load profile for different consumer classes in the distribution feeder.

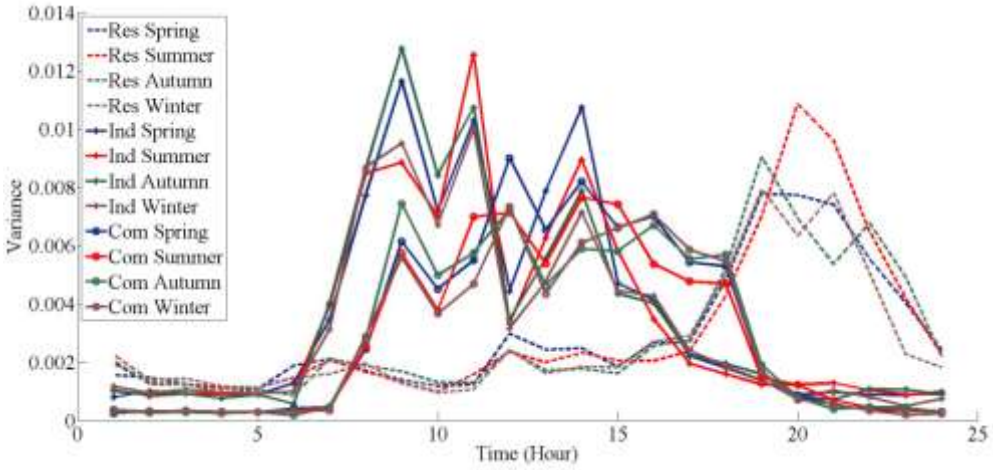

Fig. 2.6. Variance of the daily load profile for different consumer classes during different seasons.

The normalised daily irradiation profile at the extra-terrestrial surface and the sky clearness index is collected from the Bureau of Meteorology (BOM), Australia for the whole year. The sky clearness index is modelled by the random numbers of beta distribution to generate the time series data of the solar irradiation at the earth surface in the area where the distribution feeder is located. It is noted that the sky clearness index can be represented using beta distribution for the region wherein the test feeder is located. The α and β parameters of the beta distribution function for the sky clearness are found to be 4.23 and 1.18 respectively. The time series data for the power output of the solar PV type DG is generated using (2.6).

The wind speed at the hub height is modelled using the ARMA model with an order of (3, 0). The ARMA model for wind speed at hub height of 20 m in the area of distribution feeder is shown below.

$$v_W(t) = 1.751 \times v_W(t-1) - 0.5721 \times v_W(t-2) - 0.1788 \times v_W(t-3) + w(t) \quad (2.35)$$

The cut in speed, rated speed and cut out speed of the wind turbine are considered to be 3 m/s, 15 m/s and 25 m/s respectively. The hourly time series data of the wind turbine output are generated from the wind speed data and the associated energy conversion processes.

2.7 Results and Discussions

The PDFs and CDFs of the line currents and power flows are evaluated for the distribution feeder with and without renewable DG units using the proposed method of cumulants. In order to evaluate the performance of the proposed method, the results obtained using the proposed method of cumulants are compared with the results obtained from time sequential MCS technique. Moreover, the proposed transformation matrix based load flow solution method, used in time sequential MCS technique, is compared with the conventional Newton-Raphson based load flow solution method for accuracy.

The mean values of the voltages at different nodes of the distribution feeder with and without renewable DG are shown in Fig. 2.7. The PDF and CDF of the line flow through line 1 (node-1 to node-2) using the proposed method of cumulants and time sequential MCS technique for the distribution feeder with and without renewable DG are presented in Fig. 2.8. It can be seen that the accuracy of the proposed transformation matrix based load flow solution method is very close to the conventional load flow solution method. Moreover, the proposed PLF method can represent the PDF and CDF of the line flows, which is in agreement with results obtained from the time sequential MCS technique. It can be observed that the probability distribution of the line flow with the renewable DG units doesn't follow normal distribution. Hence, the proposed method of cumulants is best suited for the distribution feeder with high penetration of renewable DG units.

The simulations were conducted in MATLAB-R2012a environment on a PC with 2.93GHz Intel Core i7 CPU, 8GB RAM and 64 bit operating system. The computation times to estimate the PDF and CDF of the line current, through line section 1 of the test distribution feeder with renewable DG, using the proposed method of moments, non-sequential MCS technique with load duration method and time sequential MCS technique are found to be 15.968s, 37.573s and 61.482s, respectively. It is noted that the proposed method requires minimal computation time as compared to time sequential and non-sequential MCS techniques.

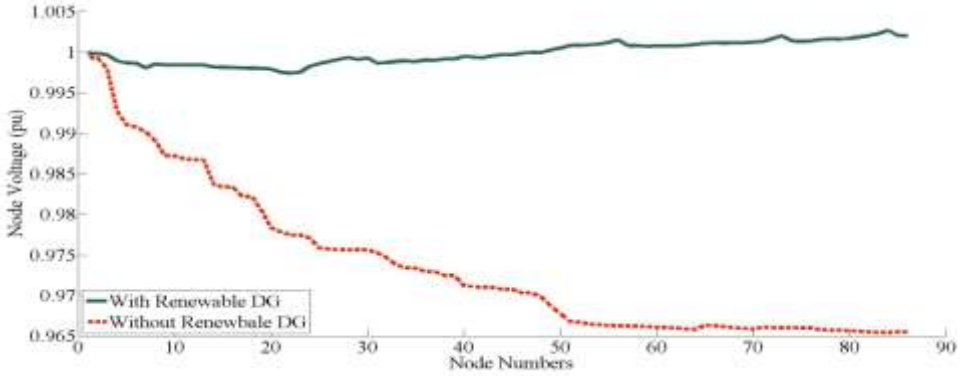

Fig. 2.7. Mean values of the nodal voltages of the distribution feeder.

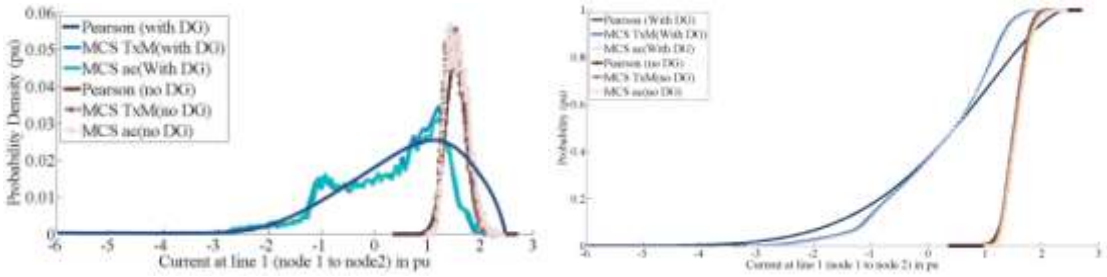

(a) **(b)**

Fig. 2.8. (a) PDF and (b) CDF of the line flow through line section 1 (node-1 to node-2).

Analysis has been carried out in order to estimate the beta distribution parameters for proposed method, and time sequential and non-sequential MCS techniques. As an example, the beta distribution parameters for current through line section 1 are found to be *(5.6866, 1.8117), (4.8084, 1.3006)* and *(5.5823, 1.8469)* for the proposed method, non-sequential MCS with load duration method and time sequential MCS techniques respectively. It is noted that the beta distribution parameters for the proposed method are comparable with that of time sequential MCS technique.

In order to demonstrate the accuracy of the PDF approximation using Pearson's distributions, average root mean square (ARMS) error of the PDF given in (2.36) is evaluated using time sequential MCS results [8].

$$ARMS = \frac{\sqrt{\sum_{i=1}^{Nx}\left(f_{PD}(x_i) - f_{MC}(x_i)\right)^2}}{Nx} \tag{2.36}$$

where, $f_{PD}(x_i)$ and $f_{MC}(x_i)$ are the PDF for x_i evaluated using the proposed method of cumulants and time sequential MCS technique, respectively. Nx is the number of random variables in X. The ARMS error for the different line flows of the distribution feeder is shown in Fig. 2.9. It is noted that the ARMS error for most of the line flows remains well under 5%.

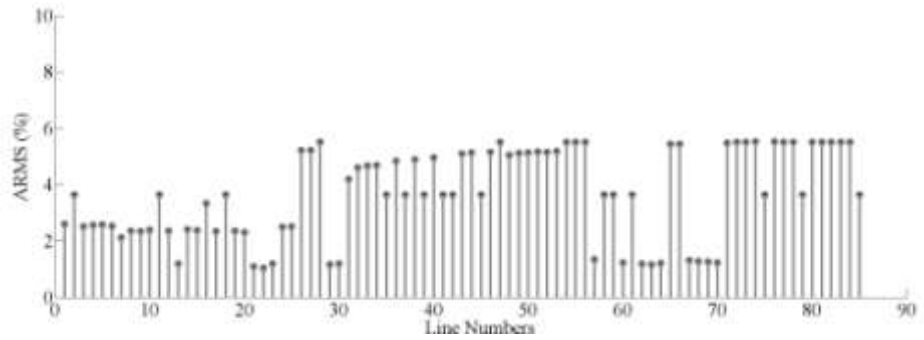

Fig. 2.9. ARMS for different line flows.

The PDF of the real power flow through the line section between node-13 and node-14 are shown in Fig. 2.10. The negative value of the real power flow indicates the upstream power flow, from solar PV type DG unit (node-14) to the substation. In certain cases, the thermal limit of the feeder section can be violated due to the high penetration of the renewable DG units in the distribution feeder. The probability and duration of the line loading, that causes the violation of thermal limit, can be evaluated from the CDF of the line loading with respect to the normal current rating of the line section. The CDFs of the line loading for the line section between node 2 and 4 are shown in Fig. 2.11. It can be seen that the probability of line section being overloaded is 0.0114. This highlights the fact that the line section will be over-loaded for 100 hours in a year. Hence, the proposed PLF methodology can be applied to evaluate the probability of the line section in a distribution feeder that may be overloaded due to high penetration of renewable DG units.

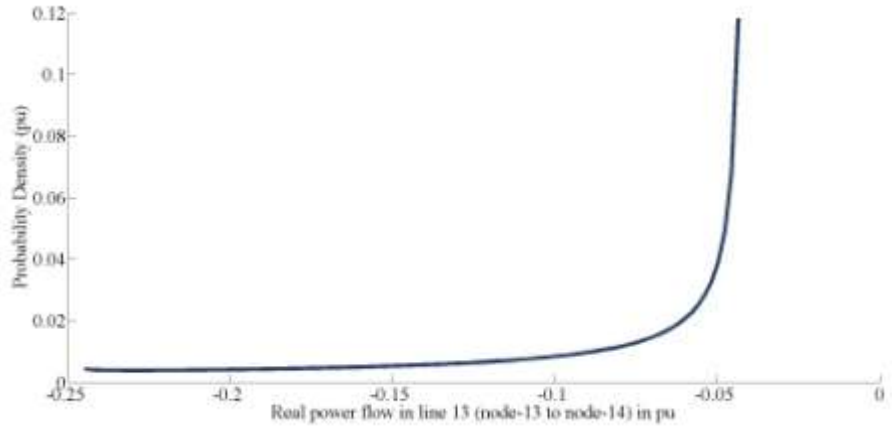

Fig. 2.10. PDF of the real power flow through the line section between node-13 and node-14.

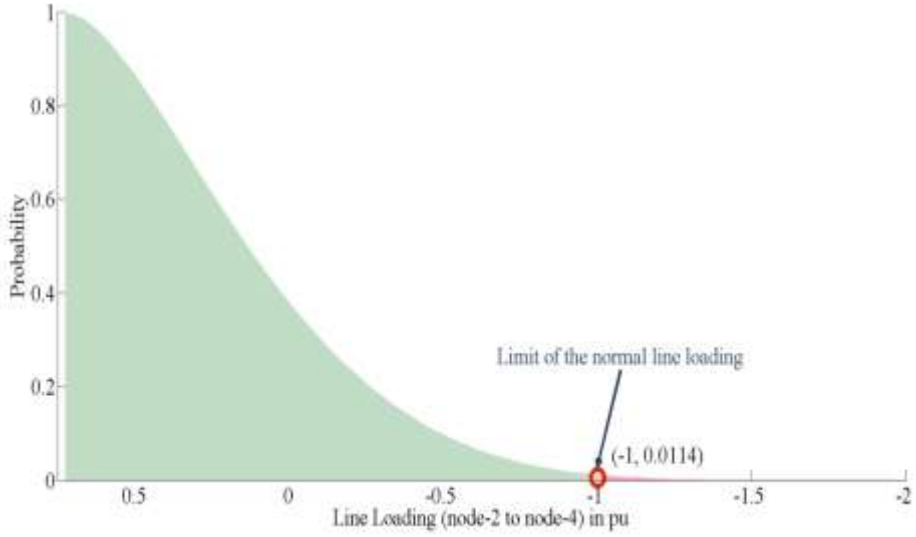

Fig. 2.11. CDF of line loading for the line section between node-2 and node-4.

The real and reactive power flows through the line section connected to the substation transformer can be used to examine the line flow between the grid and the distribution feeder. The PDF and CDF of the real and reactive power flows through the line section connected to the substation are shown in Fig. 2.12. The negative values indicate export of the real and reactive power from distribution feeder to the grid. It can be seen that for about 37.44% of the time, the distribution feeder can export energy to the grid. From the PDF of the line flows of the adjacent lines closed to the distribution substation, it can be found that the distribution feeder can be operated in an islanded mode for about 195 hours in a year to ensure self sufficiency.

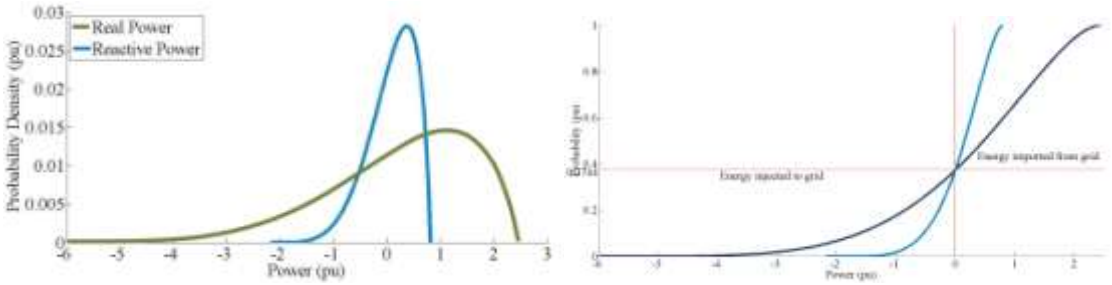

(a) **(b)**

Fig. 2.12. (a) PDF and (b) CDF of the real and reactive power transfer between the distribution feeder and grid.

2.8 Conclusion

This chapter proposes a novel methodology for solving probabilistic load flow (PLF) with non-Gaussian probability distributions of the multivariate random variables. A distribution feeder embedded with high penetration of renewable DG units is a typical example of this type. The coincidental variations among the time-varying load demands of the different consumer classes and stochastic power generation from different types of renewable energy resources are considered. Time series data of load demands and generations for the same time instance are used in cross central moments and cumulants evaluation. The sufficiently long length of the time series data is considered to include the seasonal variations in demand and generation. A transformation matrix based load flow is formulated and applied to evaluate the cumulants of the line flows. The skewness and kurtosis of the line flows are considered to estimate the probability density function (PDF) using Pearson's distribution functions. The proposed method is tested on a practical distribution feeder with high penetration of renewable DG units, and various network parameters are evaluated to assess the impacts of renewable DG integration. The proposed PLF method can be applied to evaluate the probability of a line section in a distribution feeder that may be overloaded due to high penetration of renewable DG units. It is noted that the results obtained using the proposed method of moments are comparable with the time sequential Monte Carlo simulation technique. Furthermore, the proposed method requires minimal computation time and effort as compared to time sequential and non-sequential MCS techniques.

References:

[1] H. Valizadeh Haghi, M. Tavakoli Bina, M. A. Golkar, S. M. Moghaddas-Tafreshi, "Using Copulas for analysis of large datasets in renewable distributed generation: PV and wind power integration in Iran", *Renewable Energy*, vol. 35, pp. 1991-2000, 2010.

[2] B. Borkowska, "Probabilistic Load Flow:, *IEEE Transaction on Power Apparatus and Systems*, vol. PAS-93 pp. 752-759, 1974.

[3] R. N. Allan, A. M. L. Da Silva, R. C. Burchett, "Evaluation methods and accuracy in probabilistic load flow solutions", *IEEE Transaction on Power Apparatus and Systems*, vol. PAS-100, pp. 2539-2546, 1981.

[4] C. -L. Su, "Probabilistic load-flow computation using point estimate method", *IEEE Transaction Power Systems*, vol. 19, pp. 676-682, 2004.

[5] J. Usaola, "Probabilistic load flow with correlated wind power injections", *Electric Power Systems Research*, vol. 80, pp. 528-536, 2010.

[6] S. Conti, S. Raiti, "Probabilistic load flow using Monte Carlo techniques for distribution networks with photovoltaic generators", *Solar Energy*, vol. 81, pp. 1473-1481, 2007.

[7] W. D. Tian, D. Sutanto, Y. B. Lee, H. R. Outhred, "Cumulant based probabilistic power system simulation using Laguerre polynomials", *IEEE Transaction on Energy Conversion*, vol. 4, pp. 567-574, 1989.

[8] P. Zhang, S. T. Lee, "Probabilistic load flow computation using the method of combined cumulants and Gram-Charlier expansion", *IEEE Transaction on Power Systems*. Vol. 19, pp. 676-682, 2004.

[9] J. Usaola, "Probabilistic load flow in systems with wind generation", *IET Generation, Transmission and Distribution*, vol. 3, pp. 1031-1041, 2009.

[10] D. Villanueva, J. L. Pazos, A. Feijoo, "Probabilistic load flow including wind power generation", *IEEE Transaction on Power Systems*, vol. 26, pp. 1659-1667, 2011.

[11] A. M. L. da Silva, V. L. Arienti, R. N. Allan, "Probabilistic load flow considering dependence between input nodal powers", *IEEE Transaction on Power Apparatus and Systems*, vol. 103, 1524-1530, 1984.

[12] F. J. Ruiz-Rodriguez, J. C. Hernandez, F. Jurado, "Probabilistic load flow for photovoltaic distributed generation using the Cornish-Fisher expansion", *Electric Power Systems Research*, vol. 89, pp. 129-138, 2012.

[13] B. Klockl, G. Papaefthymiou, "Multivariate time series models for studies on stochastic generators in power systems", *Electric Power Systems Research*, vol. 80, pp. 265-276, 2010.

[14] M. B. De Kock, Gaussian and non-Gaussian-based Gram-Charlier and Edgeworth expansions for correlations of identical particles in HBT interferometry, *Masters thesis*, Department of physics, University of Stellenbosch, South Africa, (2009).

[15] F. Vallee, C. Versele, J. Lobry, F. Moiny, "Non-sequential Monte Carlo simulation tool in order to minimize gaseous pollutants emissions in presence of fluctuating wind power", *Renewable Energy*, vol. 50, pp. 317-324, 2013.

[16] Z. Shu, P. Jirutitijaroen, "Non-sequential simulation method for reliability analysis of power systems with photovoltaic generation", *Proc. Of IEEE 11th International Conference on Probabilistic Methods Applied to Power Systems (PMAPS)*, vol. 11, pp. 703-709, 2010.

[17] Z. Shu, P. Jirutitijaroen, "Latin hypercube sampling techniques for power systems reliability analysis with renewable energy sources", *IEEE transaction on Power Systems*, vol. 20, pp. 2066-2073, 2011.

[18] F. F. C. Veliz, C. L. T. Borges, A. M. Rei, "A comparison of load models for composite reliability evaluation by nonsequential Monte Carlo simulation", *IEEE transaction on Power Systems*, vol. 25 pp. 649-656, 2010.

[19] J. A. Jardini, C. M. V. Tahan, M. R. Gouvea, S. U. Ahn, F. M. Figueiredo, "Daily load profiles for residential, commercial and industrial low voltage consumers", *IEEE Transaction on Power Systems*, vol. 15, pp. 375-380, 2000.

[20] R. Billinton, H. Chen, R. Ghajar, "Time-series models for reliability evaluation of power systems including wind energy", *Microelectronics Reliability*, vol. 36, pp. 1253-1261, 1996.

[21] V. Thapar, G. Agnihotri, V. K. Sethi, "Critical analysis of methods for mathematical modelling of wind turbines", *Renewable Energy*, vol. 36, pp. 3166-3177, 2011.

[22] A. Stuart, K. Ord, Kendall's Advanced Theory of Statistics, Volume 1, Distribution Theory, 6th Edition, Wiley, NY, 1994.

[23] P. McCullagh, Tensor methods in statistics, Chapman and Hall, London, 1987.

[24] K. Pearson, "Contributions to the mathematical theory of evolution. II. Skew variation in homogeneous material", *Philosophical Transaction of the Royal Society of London A*, vol. 186, pp. 343-414, 1895.

[25] K. Pearson, "Mathematical contributions to the theory of evolution. XIX. Second supplement to a memoir on skew variation", *Philosophical Transaction of the Royal Society of London A*, vol. 216, pp. 429-457, 1916.

[26] Y. Nagahara, "A method of simulating multivariate nonnormal distributions by the Pearson distribution system and estimation", *Computational Statistics & Data Analysis*, vol. 47, pp. 1-29, 2004.

[27] K. O. Bowman, L. R. Shenton, "The beta distribution, moment method, Karl Pearson and R.A. Fisher", *Far East Journal of Theoretical Statistics*, vol. 23, pp. 133-164, 2007.

[28] H. K. Solvang, Y. Nagahara, S. Araki, H. Sawada, S. Makino, "Frequency-domain Pearson distribution approach for independent component analysis (FD-Pearson-ICA) in blind source separation", *IEEE Transaction on Audio, Speech and Language Processing*. Vol. 17, pp. 639-649, 2009.

Chapter 3

Adequacy Assessment of Electricity Network Infrastructure with Renewables

ABSTRACT

Continuity of electricity supply with renewable distributed generation (DG) is a topical issue for distribution system planning and operation, especially due to the stochastic nature of power generation and time varying load demand. The conventional adequacy and reliability analysis methods related to bulk generation systems cannot be applied directly for the evaluation of adequacy criteria such as 'energy supply' and 'continuity of service' for distribution networks embedded with renewable DG. In this chapter, new indices highlighting 'available supply capacity' and 'continuity of service' are proposed for 'energy supply' and 'continuation of service' evaluation of generation-rich distribution networks, and analytical techniques are developed for their quantification. A probability based analytical method has been developed using the joint probability of the demand and generation, and probability distributions of the proposed indices have been used to evaluate the network adequacy in energy supply and service continuation. A data clustering technique has been used to evaluate the joint probability between coincidental demand and renewable generation. Time sequential Monte Carlo simulation has been used to compare the results obtained using the proposed analytical method. A standard distribution network derived from Roy Billinton test system and a practical radial distribution network have been used to test the proposed method and demonstrate the estimation of the well-being of a system for hosting renewable DG units. It is found that renewable DG systems improve the 'energy supply' and 'continuity of service' in the distribution networks. The results suggest that the consideration of the time varying demand and stochastic renewable generation output

has significant impact on the ‘energy supply’ and ‘continuity of service’ in the distribution networks.

3.1 Introduction

Adequacy of the electricity network can be defined as the existence of the facility within the system to satisfy the customer demand [1]. Distribution network service providers are primarily responsible for designing the network to ensure the continuity and quality of the electric supply. The capacity of the distribution feeder to supply demand of the feeder is to be assessed for distribution network expansion planning [2]. Integration of renewable distributed generation (DG) has impacts on the energy supply and service continuation of the distribution networks. The time varying demand and the uncertainty in power generation from renewable DG introduces difficulties in the conventional distribution network adequacy estimation methods. Load based reliability indices and customer oriented reliability indices are estimated in the conventional distribution network adequacy analysis using either analytical approach or Monte Carlo simulation (MCS) techniques [3-15].

In [3], both analytical and MCS techniques have been applied to evaluate the probability distributions of the customer oriented reliability indices for a distribution network. In [4], MCS technique has been applied for the adequacy assessment of a distribution network with distribution generation (DG) systems. It uses state duration sampling approach and evaluates adequacy index from the negative marginal load of the network. In [5], distribution network adequacy evaluation methodology is developed with the aid of loss of load and system well-being indices for grid connected and islanded operation of distributed and renewable generation systems. In [6], capacity outage table is used to evaluate adequacy of the distribution network with intermittent DG supply, and new reliability indices are proposed. In [7], energy based adequacy indices are proposed and a comparative study is presented for assessing the impact of load growth and different types of generating units on the indices. In [8], the impacts of generating units, operated as peak load and base load power plants, the generation system adequacy is analysed using the sequential MCS technique. In [9], an analytical approach using probability distribution of demand and renewable generation is proposed for the well-being assessment of an isolated power system with renewable

generation units. An energy based system well-being analysis of power system is presented in [10]. In [11], well-being analysis of various generation systems involving wind generators is carried out using capacity outage table; and impact of the load and generation forecasting on reliability has been also investigated. In [12], the capacity credit of wind generation system is evaluated for isolated distribution network using the analytical method. In [13], a new reliability index composed of customer side reliability indices has been proposed to assess the contribution of the DG in improving the risk of energy supply in a distribution network. The load point reliability parameters and average load have been considered in [13, 14] for evaluating the customer oriented reliability indices of the distribution networks.

The existing distribution network adequacy indices and estimation technique may not be able to provide sufficient information for assessing distribution system adequacy due to the time varying nature of load demand and stochastic power generation by renewable DG systems that exhibit in practical systems. The network aspects such as nodal voltages, power losses and power transfer capacity may also affect the hosting capacity of renewable DG units [15]. Moreover, the above mentioned network aspects are also dependent on the size, location, mode of operation, type and number of renewable DG units, and the uncertainty in generation and demand. Evaluation of the adequacy in terms of energy supply and continuity of service of the distribution networks can aid in the plan and design of distribution networks to avoid loss of continuity of the services and redundancy in the networks. Conventional adequacy indices are developed based on the system risk concept which provides the quantitative indication of load interruption due to the failure of equipment. In most of the practical distribution feeders, the total or partial load can be transferred to the neighbouring distribution feeder through closing the generally opened tie connection to ensure supply security. It is important to estimate the ability of the distribution feeder to transfer and receive load to and from the feeder connected with tie line, respectively.

It has been noted that the reported methods for adequacy analysis of distribution network can be classified into two major groups: adequacy estimation from the source of energy supply and adequacy estimation from potential contingency of the feeder equipment. The existing methods, related to estimation of the supply adequacy and continuity of service adequacy, consider constant load demand and generation. As indicated earlier, the existing methods assume the successful load transfer capacity of

the distribution feeder to be constant and estimate it from the peak demand level of both the distribution feeders [1, 16]. However, the peak demands of the two neighbouring distribution feeders may not coincide with each other. Moreover, the transferrable load of the distribution feeder with outage could be less and the available capacity of the neighbouring distribution feeder may become higher during the off-peak hours.

In the reported analytical methods for adequacy evaluation of the distribution network, the demand and output from renewable generation systems are considered to be independent. The coincidental occurrence of the demand and renewable generation has significant impacts on the adequacy of the distribution network. It has been observed that the reliability of the distribution network does not improve greatly after installation of DG system unless islanding operation is allowed [5, 6]. However, islanding operation is not permissible by the existing standards and utilities do not allow islanding in most of the electricity networks [17-19]. As a result, new indices and methodology are required to assess the energy supply and service continuity adequacy for distribution network that can facilitate he integration of DG systems.

In this chapter, issues related to the energy supply and service continuation assessment of a distribution network embedded with renewable DG units are addressed. New indices have been developed to estimate the energy supply adequacy and continuity of services adequacy which are essential to evaluate the distribution network adequacy and reliability. The adequacy assessment indices and methods of bulk generation systems are well established. Hence, it is required to develop new indices for distribution network so that existing generation adequacy assessment methodologies for bulk generation systems can be applied to the distribution network adequacy assessment incorporating renewable DG. Energy supply indices enable the distribution network planner to estimate the energy supply adequacy using the capacity credit of renewable DG and well-being analysis of the distribution network with renewable DG. The continuity of service indices proposed in this chapter can incorporate the time varying demand and variable generation from renewable DG systems whereas in the conventional distribution network adequacy assessment methods peak demand and installed generation capacity of the renewable DG are considered for the purpose. A joint probability based analytical method is developed for the assessment of network adequacy in terms of energy supply and continuity of service in distribution networks embedded with DG systems. Well-being analysis has been applied to assess the energy

supply and continuity of services adequacy of the distribution network with renewable DG systems using the proposed indices. Probabilities of different operating states have been evaluated and reported.

3.2 Indices for distribution network energy supply and service continuation evaluation

The adequacy and reliability analysis of distribution network with renewable distributed generation (DG) requires installed DG capacities, available capacity in the distribution substation and load transfer capacity of the distribution feeder on the occurrence of outage of the distribution feeder. Hence maximum renewable DG hosting capacity of the distribution feeder, energy supplied during system peak, distribution substation capacity release, transferrable load, additional available capacity to accommodate the transferrable load and successfully transferrable load are to be estimated in the adequacy and reliability analysis of distribution network with renewable DG. Distribution substation and DG are the sources of the energy for satisfying the consumer demands in a distribution network [5, 6]. Supply adequacy of the distribution network depends on the feeder capacity of the line connecting the load points to the distribution substation transformers and capacity of the DG systems. On the other hand, to maintain the continuity of the supply, the distribution network should be capable of meeting load demand under all the system conditions. In this chapter, the indices to evaluate the adequacy of distribution network are categorised into two groups: supply adequacy indices and continuity of service adequacy indices. These are explained in the following sub-sections. Also, steps involved in distribution network adequacy and reliability analysis are shown in Fig. 3.1.

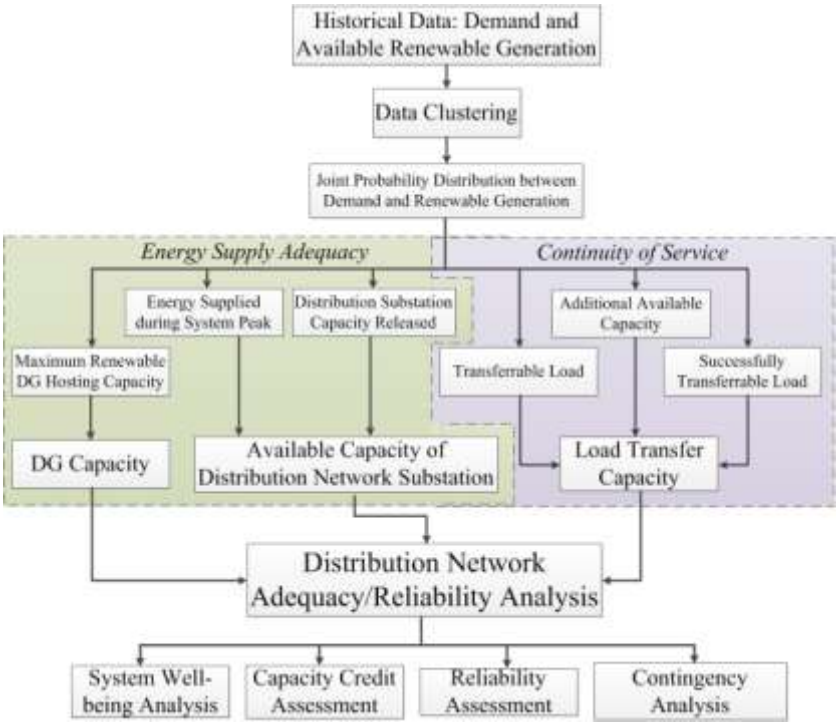

Fig. 3.1. Steps involved in distribution network adequacy and reliability analysis.

3.2.1 Supply adequacy indices

In recent practice associated with distribution network operation, total or partial consumer load can be supplied by locally generated energy resources. In the adequacy estimation of the distribution feeder with renewable DG, the capacity of renewable DG systems are selected arbitrarily [16]. Considering renewable DG with higher capacity than the maximum renewable DG hosting capacity in a distribution feeder can cause the violation of the operational constraints of the distribution feeder. Therefore, estimating the maximum renewable DG hosting capacity can provide the distribution network planner with a limit of renewable DG capacity in capacity credit estimation. The capacity of the renewable DG system is limited by the availability of the renewable resources, existing network configuration, network constraints and operation strategies of the DG and the network [20-23]. The maximum renewable DG hosting capacity (C_{DGmax}) index is proposed as an indicator of the supply adequacy from local generation embedded in a distribution network. The C_{DGmax} is the maximum capacity of the renewable DG that can be connected to the distribution network without violating the network constraints [24]. The C_{DGmax} can be expressed as follows:

$$C_{DG\max} = \max(\Sigma_i C_{DG,i}) \tag{3.1}$$

where, $\Sigma_i Cap_i$ is the sum of the optimal DG capacities connected to the i^{th} node in the distribution network. The capacity of the DG unit and hence, the C_{DGmax} of the distribution network for renewable DG technologies will be affected by distribution network configuration, DG technology and demand-generation coincidence [20].

Distribution network with higher C_{DGmax} is able to supply more energy through local power generation of DG units, which essentially leads to higher penetration of the renewable energy resources. As a consequence of the condition mentioned above, the distribution network becomes less dependent on the central generation and transmission systems for supplying the local demands. In addition, the potentiality of the renewable DG units to supply energy during the peak demand time of the system will reduce the stress and improve the generation adequacy of the system. Therefore, the capability of the distribution network with renewable DG units to meet the load demand during the system peak can be an indicator of the distribution network supply adequacy. The contribution from renewable generation during the system peak is often used as the capacity credit of the renewable generation units in the buck generation systems. Energy Served during System Peak (ESSP) is proposed to evaluate the capability of the distribution network with renewable DG units to supply energy during system peak. ESSP is defined as the fraction of the distribution network demand supplied by the renewable DG units during the system peak. Hence, ESSP represents the contribution of the renewable DG during the system peak hours and hence the ESSP index can be directly used in capacity credit estimation of the renewable DG. ESSP of the distribution network can be expressed as follows:

$$ESSP = \frac{\sum_{h_{SystemPeak}} G_{DG}(h_{SystemPeak})}{\sum_{h_{SystemPeak}} D_{DNW}(h_{SystemPeak})} \tag{3.2}$$

where, $D_{DNW}(h_{SystemPeak})$ and $G_{DG}(h_{SystemPeak})$ are the load demand of the distribution network and the available generation from renewable DG units during $h_{SystemPeak}^{th}$ time instance, respectively. $h_{SystemPeak}$ is the time instance when the load of system is at its peak.

In the generation or supply adequacy analysis of the bulk generation system, well-being analysis is used to indicate the adequacy level of the generation system. The generation system well-being states (healthy, marginal and at risk) are estimated from the difference between the demand and the available generation capacity. Energy from transmission system is delivered to the distribution network through the distribution substation transformers to serve the load points; and rate of energy flow is limited by the capacity of these transformers. Hence the capacity-release of the distribution substation transformer due to renewable DG integration is required to be estimated in the supply adequacy analysis of distribution feeder. It is to be noted that more than one feeder can be connected to the distribution substation transformer and the capacity of the transformer can be shared by all the feeders connected to the substation. Capacity-release of the distribution substation transformer can raise the peak load carrying capacity of the distribution network and support load growth. The capacity-release of the substation transformer due to renewable DG integration in a distribution feeder can be expressed using the following equation:

$$C_{release,k}(h) = C_{Xformer} - \sum_{i} L_{i,k}(h) + \sum_{j} G_{j,k}(h) \tag{3.3}$$

where, $C_{release,k}(h)$ is the released capacity of the distribution substation transformer due to the renewable DG integration at k^{th} feeder, and $C_{Xformer}$ is the total capacity of the distribution substation transformers. $L_{i,k}(h)$ is the demand of i^{th} load point in k^{th} feeder and $G_{j,k}(h)$ is the generation of the j^{th} DG unit in k^{th} feeder during h^{th} time instance. Since the demand of the distribution network is time varying in nature, the capacity margin of the distribution substation transformer will also be time varying. To model this, probabilistic considerations need to be accounted for evaluating capacity release of the substation transformer. Integration of the DG units into the distribution feeders can increase the capacity-release of the transformer and hence can support the load growth of the feeders. Effective load carrying capacity (ELCC) of the renewable generation system is used as the index to represent the contribution from the renewable generation system in the generation system adequacy. ELCC of the renewable DG is the amount of incremental demand of the distribution feeder that can be supported by the renewable DG without altering the risk level of the distribution feeder. Hence the released capacity of the distribution substation transformer due to renewable DG integration can be used as the upper limit of the incremental demand without violating the capacity constraints

in the estimation of ELCC of the renewable DG in a distribution feeder. Well-being analysis of distribution substation capacity can be useful to quantify the adequacy of energy supply to the distribution feeders, especially with the aid of local generation.

3.2.2 Continuity of service adequacy indices

The continuity of energy supply to the load points in distribution network can be interrupted due to the outage of electrical components in the generation and transmission systems or the component outages within the distribution feeders. Discontinuity of supply due to upstream outages is accounted in the adequacy analysis of upstream generation and transmission systems. The discontinuity of energy supply within the distribution network due to the local outage is analysed differently in this chapter. On the occurrence of an outage in the distribution feeder, part or total load of the distribution network can be transferred to the neighbouring feeder, usually connected with the normally opened line. In the existing literature of reliability analysis, for distribution feeder, the load transfer capacity of the distribution feeder to the neighbouring distribution feeder is assumed to be constant. Since the time varying demand and stochastic generation from renewable resources are present in the distribution feeder, the load transfer capacity of the distribution feeder to the neighbouring feeder is time dependent. The transfer of the load depends on the location of the outage as well as the capacity of the neighbouring feeder to deliver the supply to the load to be transferred [1]. Unsuccessful transfer of the load on the occurrence of a load transfer results in insufficient supply of energy at load points and subsequently the loss of load may occur in the distribution network. Therefore, the load transfer capacity can be considered as an adequacy criterion for the distribution feeder.

Unscheduled outage of the components in a distribution network is a random event and can occur at any instance of time. Since the network load varies with respect to time, outages at different time instances may result in variation in load to be transferred. On the other hand, the capacity of the neighbouring feeder to accommodate the additional load also varies with the time due to inherent time varying characteristics of load in a distribution network. The amount of load transfer, on the occurrence of an outage at a distribution feeder, can be computed using the following equation:

$$L_{Xfer,j,k}(t) = \sum_{i} L_{i,j,k}(t), \qquad for\, t = h, h+1, ..h+r \tag{3.4}$$

where, $L_{Xfer,j,k}(t)$ is the transferrable load at time t after the occurrence of an outage on node j of distribution feeder k and r is the repair time for the outage. $L_{i,j,k}(t)$ is the load of i^{th} load point at t^{th} time instance after the occurrence of outage- at node j of the distribution feeder k, and i is a component of a subset consists of the load points which are affected due to the occurrence of outage at node j. The capacity of the distribution feeder to accommodate additional load depends on the capacities of the different line sections that will carry the additional load. The additional available capacity of distribution feeder to accommodate additional load from the neighbouring feeder can be expressed using the following equation:

$$P_{avail,k}(h) = \min\left\{C_{line,i,k} - \max\left\{I_{line,i,k}(h \mid h : h+r)\right\}\right\} \tag{3.5}$$

where, $P_{avail,k}(h)$ is the additional available capacity of the distribution feeder k at h^{th} time instance, r is the repair time for the outage and $C_{line,i,k}$ is the capacity of i^{th} line in the distribution feeder k. $I_{line,i,k}(h)$ is the load served via i^{th} line section of distribution feeder k at h^{th} time instance and i is a component of a subset consisting of the lines sections between the distribution substation and tie interconnection with the neighbouring distribution feeder. Well-being analysis of the additional available capacity can provide information about the adequacy level of the different state of the distribution network. For successful transfer of load points to the neighbouring feeder, the capacity of the neighbouring feeder should be sufficient to supply its own demand and also the additional demand transferred due to outage. The maximum load that can be transferred successfully can be evaluated using the following equation:

$$L_{XferSuc,j,k}(h) = \begin{cases} \max\left\{L_{Xfer,j,k}(h)\right\}, & if\ C_{avail,k}(h) \geq L_{Xfer,j,k}(h) \\ C_{avail,k}(h), & otherwise \end{cases} \tag{3.6}$$

$$for \qquad for\ h, h+1, .., h+r$$

where, $L_{XferSuc,j,k}(h)$ is the successfully transferrable load of distribution feeder k at h^{th} time instance for an outage at node j, and r is the repair time. Renewable DG systems integrated in the distribution feeder can increase the additional available capacity and also reduce the amount of load that needs to be transferred without DG in the feeder.

3.3 Proposed technique for distribution network energy supply and continuity of service evaluation

Probabilistic evaluation of the energy supply and continuity of service indices are required due to the time varying demand of the distribution network and uncertainty in power generation from renewable DG systems. Though the demands at different load points and generation from renewable resources are stochastic in nature and independent of each other, some correlation exists between these quantities. Therefore, joint probability of the demands and the generation is to be applied in the analysis as shown in Fig. 3.1. Joint probability of the coincidental quantities can be evaluated from the chronological data of the demand and power generation availability of the renewable resources for the same time interval. A data clustering technique presented in [25] will be applied to evaluate the joint probability distributions of the demand and generation.

3.3.1 Joint probability evaluation using data clustering technique

Data associated with different quantities, varying with respect to time, and within the same time interval needs to be considered for evaluating the joint probability distribution. Data with different resolution should be processed to satisfy this requirement. The coincident data among the quantities will be normalised and thereafter the data within the range of a data bin, will be put in the same cluster or data bin. Data bin is a bounded data set where the boundaries are the ranges of the steps of all the quantities considered for data clustering. A representative data set composed of two different quantities represented in x and y axis is shown in Fig. 3.2. Number of data points in each data bin indicates the frequency of simultaneous occurrences of the events within the time span and the ranges of the data bin considered. Joint probability density of the quantities in each data bin can be evaluated from the number of occurrences of each data bin divided by the total number of the events as shown below:

$$P\{x_i, y_j\} = \frac{B_{ij}}{\sum_{i=1}^{N_x}\sum_{j=1}^{N_y} B_{ij}} \tag{3.7}$$

where, $P\{x_i,y_j\}$ is the joint probability density of the data set (x_i,y_j) and B_{ij} is the frequency of simultaneous occurrence of the event. N_x and N_y are the number of data bins along x axes and y axes, respectively. Each quantity in the data bin is then converted to the corresponding actual quantity using inverse transformation. The marginal probability density of the x_i can be evaluated using the following equation:

$$P\{x_i \mid y\} = \sum_{j=1}^{N_y} P\{x_i, y_j\} \tag{3.8}$$

The demand data with higher resolution (e.g. quarter hourly) can be averaged to compute the desired resolution (e.g. hourly) of data. Chronological data of each type of customer demand and load points can be aggregated to evaluate the total demand of the distribution feeder. The data associated with the renewable resources such as solar irradiance, cloud clearness index and wind speed can be collected from the meteorological department and can be used to compute the generated output from the energy conversion model of the respective DG technology. The outputs of the wind energy conversion system (WECS) and solar photovoltaic (PV) can be derived from the power curve of the wind turbine and PV module, respectively.

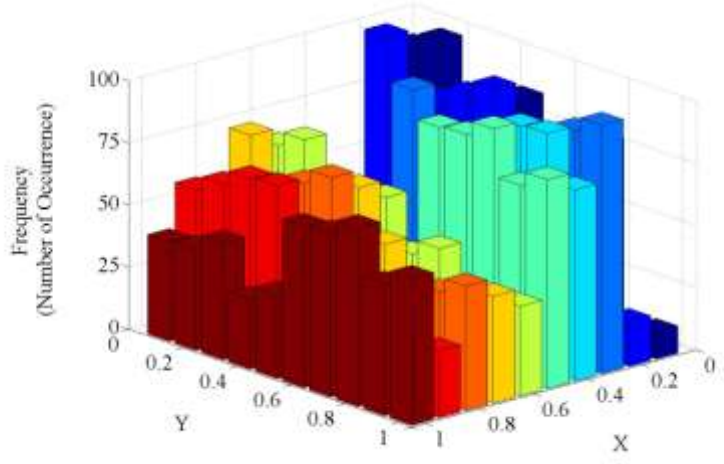

Fig. 3.2. Joint probability distribution of two sets of data.

3.3.2 Maximum renewable DG hosting capacity

Maximum renewable DG hosting capacity (C_{DGmax}) can be evaluated using the probabilistic optimal power flow (OPF) solution [26]. For OPF, joint probability of the

loads and normalised generation output are to be computed using data clustering as discussed earlier. The optimisation problem can be formulated for the C_{DGmax} as follows:

Objective function: $$\text{Maximise}\left(\sum_i C_{DG,i}\right) \tag{3.9}$$

Constraints:

$$T_{P,i,b} + G_{P,i,b} - \sum_j V_{i,b} V_{j,b} Y_{i,j} \cos(\theta_{i,j} - \delta_{i,b} + \delta_{j,b}) = 0 \tag{3.10}$$

$$T_{Q,i,b} - \sum_j V_{i,b} V_{j,b} Y_{i,j} \sin(\theta_{i,j} - \delta_{i,b} + \delta_{j,b}) = 0 \tag{3.11}$$

$$\textit{Where,}\quad G_{P,i,b} = A_{i,b} \times C_{DG,i} \tag{3.12}$$

Boundary conditions:

$$V_{\min} \le V_{i,b} \le V_{\max} \tag{3.13}$$

$$L_{line,\min,i} \le L_{line,i,b} \le L_{line,\max,i} \tag{3.14}$$

$$T_{P,1,b} \ge 0 \tag{3.15}$$

where, $C_{DG,i}$ is the capacity of the DG at node i and $A_{i,b}$ is the normalised generation output of data bin b from DG at node i. $T_{P,i,b}$ and $T_{Q,i,b}$ are the real and reactive power taken from the distribution substation at node i for the b^{th} data bin, respectively. $G_{P,i,b}$ is the real power generation from the renewable DG at node i and for the b^{th} data bin. Data clustering method has been applied to identify the unique coincidental demand and available renewable generation levels. The joint probability density for each set of non-unique coincidental demand and available renewable generation level, known as data bin, has been estimated from the frequency of occurrence. The constraints of the optimisation problem shown in Eqs. (3.10) to (3.15) are formulated for each demand and generation levels in a data bin. In order to ensure the constraints for each time period are maintained, the solution of the optimisation should satisfy all the constraints for every data bin. The total number of constraints in the optimisation problem is 6 times the number of data bins with non-zero frequency. A set of the optimal capacity of the DG can be evaluated using the OPF for all possible options of DG connections at

the distribution network. The maximum capacity value in the set will be C_{DGmax} for the distribution network under investigation.

Modern DGs may be capable of providing reactive power support based on their reactive capability. This may have an impact on the overall reliability/adequacy analysis, which can be easily incorporated in the proposed formulation. However, traditionally the adequacy analysis of the electricity network is associated with real power output of the DG [4-6,15,16]. Accordingly, the proposed research focuses on the best case scenario wherein real power output from the DG is at its maximum (unity power factor operation) thereby providing maximum hosting capacity for improving the overall system reliability. If the DG starts injecting the reactive power, the real power output drops (based on the reactive capability curve of the machine) thereby providing additional margin for hosting real power sources in the system. In the current context, the DG units at the medium voltage level are expected to operate at unity power factor (as adopted in the paper) without any active control [17,18].

3.3.3 Energy served during system peak

Joint probability between the total demand of the system and total generation from the renewable DG units is required for evaluation of energy served during the system peak (ESSP). Level of the system demand is to be defined so that the load above this level can be considered as the system peak demand. Using joint probability of generation and demand, the ESSP of the distribution network with renewable DG systems can be evaluated as follows:

$$ESSP = \frac{\sum_{b} G(b|_{Ls>Lsp\lim}) \times P\{b|_{Ls>Lsp\lim}\}}{\sum_{b} G(b) \times P\{b\}} \tag{3.16}$$

where, *Ls* is the total system demand and *Lsplim* is the level of system demand above which the total system demand will be considered as the peak demand. *G(b*) is the total generation from the renewable DG units at data bin *b* and *P*{*b*} is the probability of the occurrence of b^{th} data bin. $b|_{Ls>Lslim}$ is the index of the data bin when total system demand is at peak.

3.3.4 Capacity release

Capacity release of the distribution substation transformer can be computed from the joint probability distribution between the sum of the demand at all the load points and the sum of the generated output of all the renewable DG units attached to the distribution feeder. The capacity release of the distribution substation transformer for each combination of total feeder load and total generation in the same feeder can be computed as follows:

$$C_{release,k}(b) = C_{Xformer} - L_k(b) + G_k(b) \tag{3.17}$$

The probability of each $C_{release,k}(b)$ level will be equal to the probability of the b^{th} data bin. In order to apply well-being analysis, the capacity level for healthy, marginal and risk state are to be defined for capacity release of the distribution substation transformer. The distribution substation transformer capacity will be at healthy state if released capacity is higher than or equal to the sum of the peak demands of the neighbouring feeders connected to the same distribution transformer plus the capacity of the largest transformer. In the marginal state, the distribution substation transformer will have capacity-release lower than the healthy state but equal or greater than the sum of the peak demands of the individual feeders. The distribution substation transformer will be at risk state if the transformer capacity-release is less than the sum of the peak demands of individual neighbouring feeders. The probability of each state can be evaluated by multiplying the cumulative probability of the corresponding capacity release and outage probability of the distribution substation transformers.

3.3.5 Continuity of service adequacy

Evaluation of the distribution network continuity of service adequacy indices requires the information about the demand of the distribution feeder, neighbouring feeder and generation output during repair time after occurrence of the outage. The joint probability of the demand and generation for the outage time instances are required for the evaluation of the continuity of service adequacy. Let us assume that there are 3 load levels and 2 available renewable generation levels in the joint probability distribution between demand and available renewable generation of a distribution feeder section which is isolated after an outage at node *j* of distribution feeder *k*. The transition rate

between two states is the normalised number of transitions from the initial state (x) of the next state (y). The transition rate between two sets of demand and available renewable generation level is represented by $\lambda_{x,y}$. The matrix showing the transition rate between two sets of demand and available renewable generation level is shown in Table 3.1. Let us assume that repair time on the occurrence of an outage in the distribution feeder is 3 h and the demand and available renewable generation level at the moment of outage (h = 1) is (l_1,g_1). Hence, 36 combinations of demand and available renewable generation sequences are possible for outage of 3 h as shown in Fig. 3.3. There are five more sets of these combinations for the six states of unique demand and available renewable generation sequences, each started with different demand and available renewable generation level.

Table 3.1. Transition rate matrix

	(l_1,g_1)	**(l_2,g_1)**	**(l_3,g_1)**	**(l_1,g_2)**	**(l_2,g_2)**	**(l_3,g_2)**
(l_1,g_1)	$\lambda_{1,1}$	$\lambda_{1,2}$	$\lambda_{1,3}$	$\lambda_{1,4}$	$\lambda_{1,5}$	$\lambda_{1,6}$
(l_2,g_1)	$\lambda_{2,1}$	$\lambda_{2,2}$	$\lambda_{2,3}$	$\lambda_{2,4}$	$\lambda_{2,5}$	$\lambda_{2,6}$
(l_3,g_1)	$\lambda_{3,1}$	$\lambda_{3,2}$	$\lambda_{3,3}$	$\lambda_{3,4}$	$\lambda_{3,5}$	$\lambda_{3,6}$
(l_1,g_2)	$\lambda_{4,1}$	$\lambda_{4,2}$	$\lambda_{4,3}$	$\lambda_{4,4}$	$\lambda_{4,5}$	$\lambda_{4,6}$
(l_2,g_2)	$\lambda_{5,1}$	$\lambda_{5,2}$	$\lambda_{5,3}$	$\lambda_{5,4}$	$\lambda_{5,5}$	$\lambda_{5,6}$
(l_3,g_2)	$\lambda_{6,1}$	$\lambda_{6,2}$	$\lambda_{6,3}$	$\lambda_{6,4}$	$\lambda_{6,5}$	$\lambda_{6,6}$

For each sequence, the continuity of service adequacy indices and their associated probability can be estimated. For example let us consider the sequence of demand and available renewable generation levels of (l_1,g_1), (l_2,g_1) and (l_3,g_2) during 1st, 2nd and 3rd hour of outage, respectively. The transferrable load from the isolated distribution feeder section to the neighbouring distribution feeder during the repairing time is the maximum value of the net load of the isolate feeder section during this time for the combination of demand and available renewable generation sequence. The probability of the transferrable load level is the products of probability of the net load level at hour 1, transition rate between net load levels from hour 1 to 2 and from hour 2 to hour 3. The transferrable load, $L_{Xfer,j,k,m}$ and associated probability, $P\{ L_{Xfer,j,k,m} \}$ of the transferrable load for this sequence are estimated using the following equations respectively:

$$L_{Xfer,j,k,m} = \max\left(l_1 - g_1, l_2 - g_1, l_3 - g_2\right) \tag{3.18}$$

$$P\left\{L_{Xfer,j,k,m}\right\} = P\left\{(l_1, g_1)\right\} \times \lambda_{1,2} \times \lambda_{2,6} \tag{3.19}$$

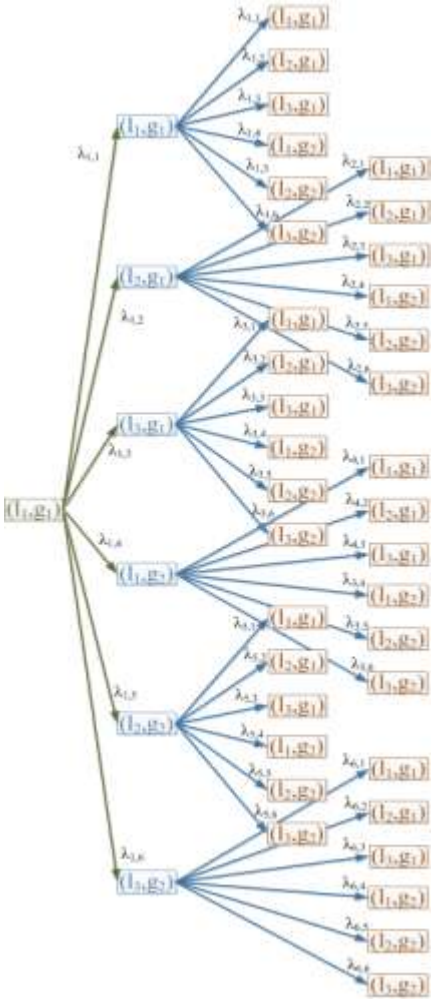

Fig. 3.3. Combinations of possible load-generation transition.

A set of transferrable load and associated probability can be estimated for the all possible combinations of demand and available renewable generation sequence. However, there is only six unique levels of transferrable load can be found from all possible combinations of demand and available renewable generation sequence. Hence the probability of each unique transferrable load level is the sum of the probability of the combinations with the corresponding transferrable load sequence.

In general for a repair time of *r*, the demand and generation pairs for the time sequences can be generated and the joint probability of the sequences can be evaluated.

The probability of each unique transferrable load level on the occurrence of an outage at the distribution feeder can be evaluated using the following equations:

$$L_{Xfer,j,k,m} = \max\left(l_{h+1,m} - g_{h+1,m}, l_{h+2,m} - g_{h+2,m}, \ldots l_{h+r,m} - g_{h+r,m}\right) \quad (3.20)$$

$$P\{L_{Xfer,j,k,m}\} = P\{(l_{h+1,m}, g_{h+1,m})\} \times \lambda_{h+1,h+2,m} \times \lambda_{h+2,h+3,m} \times \ldots \times \lambda_{h+r-1,h+r,m} \quad (3.21)$$

$$P\{L_{Xfer,j,k}\} = \sum_m P\{L_{Xfer,j,k,m} = L_{Xfer,j,k}\} \quad (3.22)$$

where, $P\{(l_{h+1,m},g_{h+1,m})\}$ is the joint probability of the occurrences of the demand and generation pairs $(l_{h+1,m},g_{h+1,m})$ during the time instance $h+1$ of outage duration in the m^{th} combination of the demand and generation. $P\{L_{Xfer,j,k}\}$ is the probability of the unique transferrable load level $L_{Xfer,j,k}$.

The available capacity in a distribution to supply the demand of the isolated feeder section in the neighbouring distribution feeder is the spare capacity of the distribution feeder after serving its own load demand. The available capacity of the distribution feeder to receive the transferrable load of the neighbouring feeder section is the minimum spare capacity during the outage time known as repair time of the outage in the neighbouring feeder. The spare capacity, $P_{avail,j,k,m}$ in a distribution feeder section j for the m^{th} load-generation sequence during the repair time of the neighbouring feeder is the capacity, $I_{cap,j,k}$ of the feeder section j less the maximum power $I_{j,k,m,l(h+1),g(h+1)}$ flowing through the feeder section to supply its own demand of the distribution feeder k during the repair time as shown in Eq. (3.23). The available capacity of the whole distribution feeder, $P_{avail,k,m}$ to accommodate the transferrable load of the neighbouring feeder during repair time is the minimum among the spare capacities of the feeder sections those lies between the distribution substation node and the tie line connecting the neighbouring feeder as shown in Eq. (3.24). Since several combinations of demand and available renewable generation sequence are possible in a distribution feeder during the repair time of the neighbouring feeder outage, the available capacity, $P_{avail,k,m}$ to accommodate transferrable load of the neighbouring distribution feeder can be estimated for each combination of demand and available renewable generation level of the distribution feeder. The probability of available capacity $P\{P_{avail,k,m}\}$ of the distribution feeder k for m^{th} demand generation sequence is the products of probability

of the net load level $P\{(l_{h+1,m},g_{h+1,m})\}$ at hour 1 and transition rates between net load levels between consecutive hours during repair time of the neighbouring distribution feeder as shown in Eq. (3.25). A set of available capacity and associated probability can be estimated for the all possible combinations of demand and available renewable generation level of the distribution feeder. However, only a few unique levels of available capacity levels can be found from all possible combinations of demand and available renewable generation sequence. Hence the probability of each unique available capacity level $P\{P_{avail,k}\}$ is the sum of the probability of the combinations with the corresponding available capacity level as shown in Eq. (3.26).

$$P_{avail,j,k,m} = C_{line,j,k} - \max\left(I_{j,k,m,l(h+1),g(h+1)}, I_{j,k,m,l(h+2),g(h+2)},\cdots I_{j,k,m,l(h+r),g(h+r)}\right) \tag{3.23}$$

$$P_{avail,k,m} = \min\left(P_{avail,1,k,m}, P_{avail,2,k,m},\ldots P_{avail,Nd,k,m}\right) \tag{3.24}$$

$$P\{P_{avail,k,m}\} = P\{(l_{h+1,m},g_{h+1,m})\}\times\lambda_{h+1,h+2,m}\times\lambda_{h+2,h+3,m}\times\cdots\times\lambda_{h+r-1,h+r,m} \tag{3.25}$$

$$P\{P_{avail,k}\} = \sum_m P\{P_{avail,k,m} = P_{avail,k}\} \tag{3.26}$$

The success in transferring load of the isolated feeder sections on the outage in the distribution feeder depends on the available capacity to receive the transferrable load of the neighbouring feeder during the repair time. If the available capacity in the neighbouring distribution feeder is equal to or greater than the transferrable load of the distribution feeder with outage, all the load points in the isolated feeder sections can be transferred to the neighbouring feeder during repair time. Otherwise, load points in the isolated feeder section for which the sum of the demand is equal to or less than the available capacity of the neighbouring feeder can be transferred to the neighbouring distribution feeder. The successfully transferrable load $L_{XferSuc,j,k,m}$ for each combination of load and available renewable generation sequence can be estimated using Eq. (3.27). Since several combinations of demand and available renewable generation level are possible in both the distribution feeder and neighbouring distribution feeder during the repair time, the transferrable load and available capacity can be estimated for each combination of demand and available renewable generation level of both the distribution feeders which result to a successful transfer of a single load. A set of unique

successfully transferrable load $L_{XferSuc,j,k}$ can be found from all possible combination of demand and available renewable generation sequence and the probability of each unique successfully transferrable load $P\{L_{XferSuc,j,k}\}$ can be estimated by adding the probabilities of same successfully transferrable load levels as shown in (3.28). The first summation in the right hand side of Eq. (3.28) is the probability of successfully transferrable load when the available capacity in the neighbouring distribution feeder is equal to or greater than the transferrable load in the distribution feeder with a outage. The second summation in the right hand side of Eq. (3.28) expresses the probability of successfully transferrable load for the case when available capacity in the neighbouring distribution feeder is less than the transferrable load of the distribution feeder with outage.

$$L_{XferSuc,j,k,m} = \begin{cases} L_{Xfer,j,k,m} & \text{if } P_{avail,k,m} \geq L_{Xfer,j,k,m} \\ P_{avail,k,m} & \text{Otherwise} \end{cases} \tag{3.27}$$

$$\begin{aligned} P\{P_{XferSuc,j,k}\} = & \sum_m P\{P_{Xfer,j,k,m} = P_{XferSuc,j,k}\} \times P\{P_{avail,k,m} \geq P_{XferSuc,j,k}\} \\ & + \sum_m P\{P_{Xfer,j,k,m} > P_{XferSuc,j,k}\} \times P\{P_{avail,k,m} = P_{XferSuc,j,k}\} \end{aligned} \tag{3.28}$$

Well-being analysis can be applied on the additional available capacity of the distribution feeder. The distribution feeder is at healthy state if the additional available capacity is equal to or higher than the annual peak demand of the transferrable load of the neighbouring feeder. In the marginal state of the distribution feeder, the additional available capacity is less than the annual peak demand of the transferrable load but greater than the annual minimum demand of the transferred load during the repairing time. The distribution feeder is at risk state if the additional available capacity is less than the annual minimum demand of the transferred load during the repairing time.

3.4 Case study

Case studies are carried out on a standard distribution network derived from Roy Billinton test system and a practical radial distribution network to test the proposed method and demonstrate its effectiveness for assessing the energy supply and continuity of service in distribution networks with renewable distributed generation.

3.4.1 Energy supply and continuity of service adequacy evaluation of RBTS distribution network

The proposed methodology is applied on the distribution network connected at bus 5 of Roy Billinton Test System (RBTS) [27] to evaluate the proposed adequacy indices. Four distribution feeders are connected to the bus 5 of RBTS with 26 load points. The topology of the distribution network is shown in Fig. 3.4. A time varying load demand for the distribution network is generated using HOMER software tool with the aid of the typical hourly demand patterns outlined in Ref. [28]. The power factor is assumed to be 0.90 (lagging) and annual peak demand of the distribution network is 16.5 MW. Solar irradiance and cloud clearness index, and wind speed of 10 years are extracted from the Bureau of Meteorology Australia [29] for the Cattai region at the state of New South Wales (NSW) in Australia, and time varying power outputs of solar PV and wind power are used. The hourly system demand, demand of the distribution feeder, generation outputs from solar PV and wind turbine systems as the percentage of peak for a week are given in Fig. 3.5. It is noted that the distribution feeders are connected to bus 5 of transmission network at the voltage level of 132 kV through two parallel transformers each rated at 16 MVA. The main distribution feeder impedance is $0.265+j0.13$ ohm/km and the impedance of the lines between main distribution feeder and 11/0.415 kV distribution transformers is $1.28+j0.413$ ohm/km. The current carrying capacities of the main distribution feeder and the secondary distribution feeder are 370 A and 110 A, respectively. Simulations on the test network have been carried out using MATLAB.

The maximum renewable DG hosting capacity (C_{DGmax}) of the test distribution network is evaluated for DG technology of solar PV type only, wind turbine type only and combination of solar PV and wind turbine with equal capacity ratio. A number of options are generated for renewable DG connection in different nodes of each distribution feeder. For each option of each distribution feeder, the optimisation program formulated in Section 3.3.2 is run and maximum capacity of the renewable DG is estimate for the option. Hence the option with maximum renewable DG hosting capacity of the distribution feeder is estimated using equation (3.1). The maximum renewable DG hosting capacity, C_{DGmax} of the test network is estimated and presented in Table 3.2. It is observed that for all four feeders, solar PV has higher hosting capacity than that of the wind turbine. Moreover, distribution feeder F1 has the highest C_{DGmax} since the total demand of the F1 feeder is the highest among all the four feeders. For the

combination of solar PV and wind turbine with equal capacity ratio, the C_{DGmax} is higher than that of the Solar PV only and also it is higher than that of wind turbine only for feeder F1 and F4.

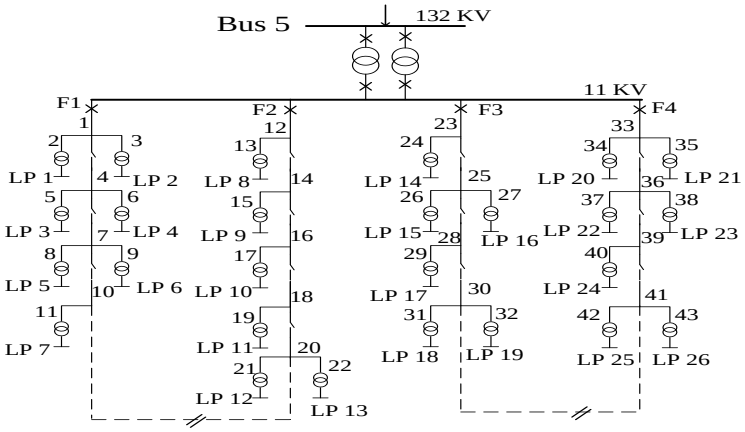

Fig. 3.4. Topology of the distribution network at bus 5 of RBTS.

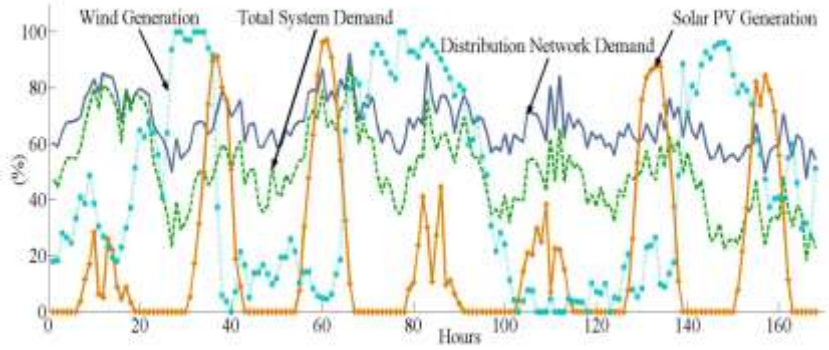

Fig. 3.5. Hourly system demand, distribution Feeder demand, solar PV and wind generation in a week.

Energy Served during System Peak (ESSP) is evaluated for each types of generation technologies used to evaluate C_{DGmax} using both, the proposed analytical method and time sequential MCS technique. The distribution substation hourly capacity-release from the F1 feeder of the test network is evaluated using both analytical and time sequential MCS technique for the system without DG integration and the system with the above mentioned DG technologies. The maximum hosting capacity of each type of renewable DG technology is used as its installed capacity in the analysis. Well-being analysis of the distribution substation capacity release is performed for cases with and without DG integration. The resulting ESSP and probability of the different well-being

states of the distribution substation transformer due to DG integration at feeder F1 are presented in Table 3.3. Comparing the results of the analytical evaluation method and time sequential MCS for the proposed supply adequacy indices, it is found that the results do not vary significantly. It is observed that among the observed renewable DG technologies solar PV technology has the lowest coincidence with the peak of the total system demand. The probability of the healthy state of the distribution substation capacity-release increases significantly and the probability of state at risk reduces with the integration of the renewable DG unit. This indicates that the renewable DG system can support load growth of the distribution feeder.

Table 3.2. Maximum Renewable DG Hosting Capacity of the Test Distribution Network

Feeder Number	**Solar PV**	**Wind Turbine**	**Combined Solar PV and Wind Turbine**	**Connected Load Points**
Units	MVA	MVA	MVA	MVA
F1	3.1444	3.0049	3.2372	2, 6
F2	2.2301	2.1359	2.1018	9, 13
F3	2.5870	2.3160	2.5453	15, 17
F4	2.8682	2.7765	2.9793	21, 25
Total	10.8297	10.2333	10.8636	

The sequential Monte Carlo simulation (MCS) technique is used to generate time sequential data of the proposed indices and the probability distribution estimate from the time sequential data is compared with the results obtained from proposed analytical method in Section 3.3.4. The time series data of demand and renewable generation is generated from the statistical data of the demand and available renewable generation transition rates between states and joint probability distribution respectively. Transition rate between two states is the normalised number of transitions from the initial state to the next state. The ‘energy supply’ and ‘continuity of service’ adequacy indices are estimated from each time step data of demand and available renewable generation. Hence, the probability distribution of the supply adequacy index and the ‘continuity of service’ adequacy indices are estimated from the time series data of the corresponding quantity.

The additional available capacity and average successfully transferrable load of the F1 feeder on the occurrence of the outage at different hours of the year is estimated using proposed analytical and time sequential MCS for no DG connection, solar PV only, wind turbine only and combination of solar PV and wind turbine of equal share. The installed DG capacity is considered equal to maximum renewable DG hosting capacity and repair time is considered to be 4 h. The well-being analysis of load carrying capacity is applied to the F1 feeder and the results are presented in Table 3.3.

Table 3.3. Proposed Indices to Estimate Energy Supply and Service Continuation for The RBTS Distribution Network at Bus 5

	Proposed Analytical Method				**Time Sequential MCS Method**			
	No DG	**Solar PV**	**Wind Turbine**	**Combined Solar PV and Wind**	**No DG**	**Solar PV**	**Wind Turbine**	**Combined Solar PV and Wind**
ESSP	-	10.21%	12.82%	12.24%	-	10.21%	12.82%	12.24%
Probability of the States of Distribution Substation Capacity Release								
Healthy	0.0318	0.2805	0.5166	0.4862	0.0347	0.2660	0.5380	0.5318
Marginal	0.9682	0.7195	0.4824	0.5138	0.9653	0.7340	0.4620	0.4682
Probability of the States of Additional Available Capacity (pu)								
Healthy	0.4100	0.6300	0.6920	0.8000	0.4256	0.5662	0.6752	0.8073
Marginal	0.5400	0.3500	0.2880	0.2000	0.4352	0.4338	0.3248	0.1927

The probability distributions of the additional available capacity and average successfully transferrable load due to the outage at line 1 of the feeder F1 for no DG, solar PV only, wind turbine only and combination of solar PV and wind turbine with equal capacity are shown in Fig. 3.6. It can be observed that the additional available capacity and successfully transferrable load of the distribution feeder are not constant even without renewable DG. Hence consideration of peak demand condition for additional available capacity and successfully transferrable load of the distribution feeder in the adequacy and reliability analysis of distribution feeder cannot be justified. Moreover, it is observed that the probability of the additional available capacity greater than and equal to 4.5 MW load increases significantly with the integration of renewable DG in the distribution feeder. This is due to the reduced demand and reduced power flow through the lines of the distribution feeder during peak demand period when renewable DG is operated in the distribution feeder. Hence the renewable DG can

improve the additional available capacity of the distribution feeder to receive the transferred load from the neighbouring distribution feeder. Similarly, it is found that the probability of 4 MW successfully transferrable load increases substantially with the integration of renewable DG in the distribution feeder. The increased probability of 4 MW successfully transferrable load indicates that the transferrable load of the distribution feeder with outage is reduced by the renewable DG. Hence, the probability of successful load points restoration on the occurrence of an outage in the distribution feeder can be increased with the integration of renewable DG.

3.4.2 Energy supply and continuity of service adequacy evaluation of a practical distribution network

The proposed distribution network adequacy indices are evaluated for a practical distribution feeder in the Cattai region of New South Wales (NSW), Australia [30]. The topology of the feeder is shown in Fig. 3.7, wherein three feeders have emerged out of a distribution substation of 30 MVA (2 × 15 MVA transformers) capacity. The test feeder under examination has 87 nodes with 60 load points. The peak load of the test feeder is recorded as 3.9 MVA during the operation period from July 2007 to June 2008. The annual peak demand of the other two neighbouring feeders is 13 MVA. The current carrying capacity of the test feeder is 300 A. The laterals of the test feeder are composed of several sub-feeders with current ratings from 110 A to 300 A. The total system demand of the NSW grid obtained from Australian Energy Market Operator (AEMO) is used for calculating ESSP of the test feeder embedded with renewable DG systems. The hourly system demand, distribution feeder demand, solar generation and wind generation as percentage of the peak for a typical week are shown in Fig. 3.8. The distribution feeder can accommodate maximum three renewable DG systems due to the stability and power quality issues of the feeder. The proposed distribution network adequacy indices are evaluated for the test feeder by conducting simulation studies in MATLAB.

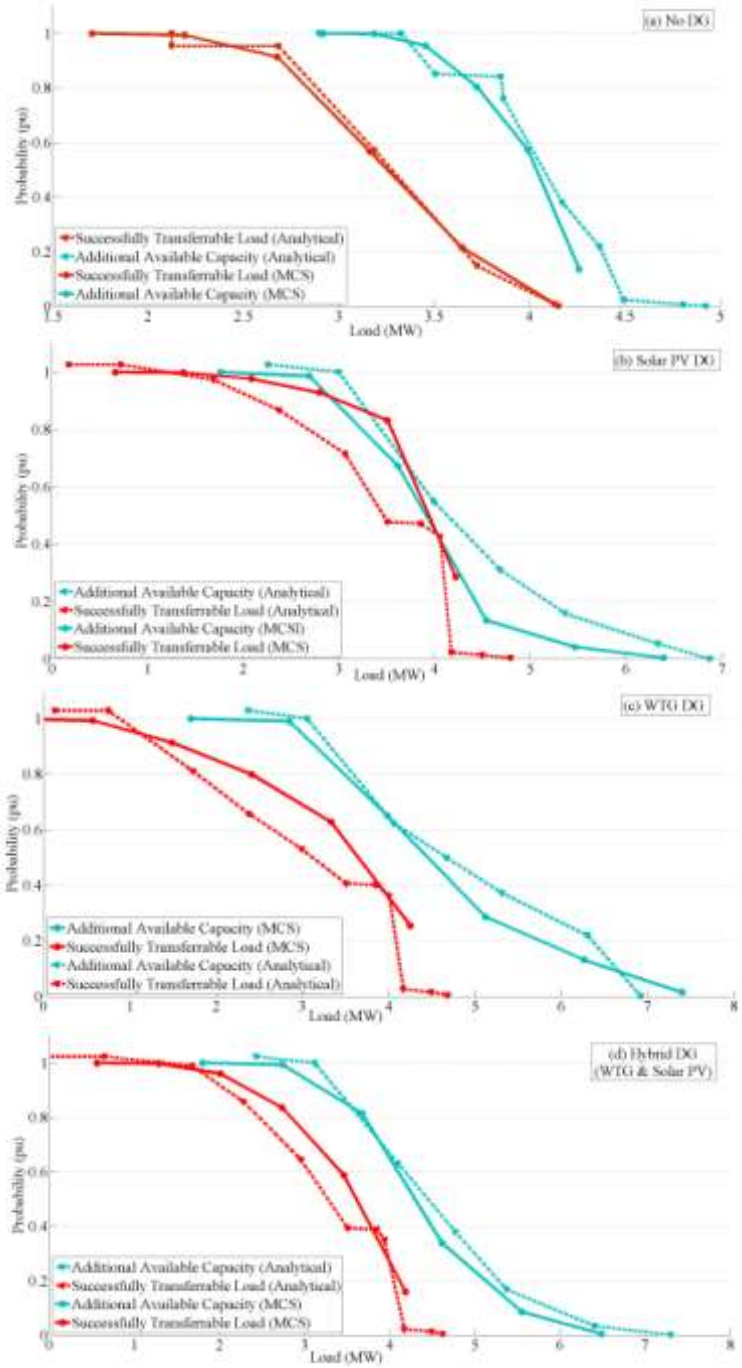

Fig. 3.6. Probability distribution of the additional available capacity and successfully transferrable load of the feeder F1 of the test distribution network for various DG types.

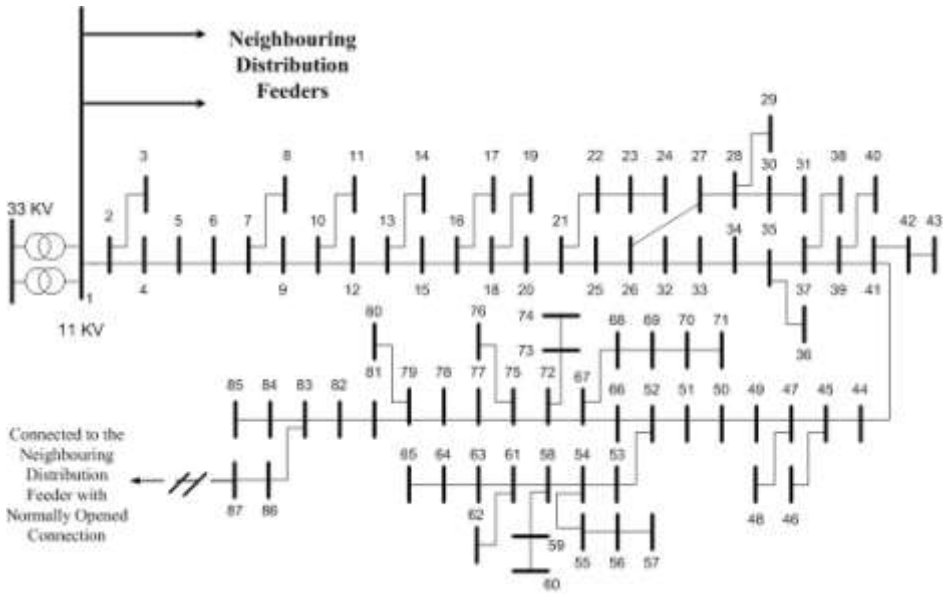

Fig. 3.7. Topology of practical distribution feeder.

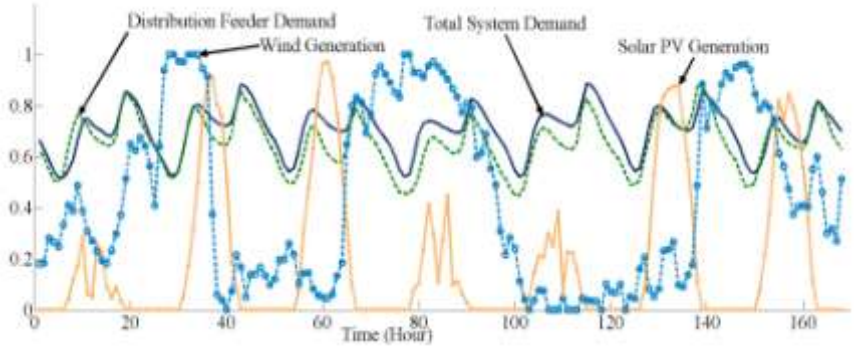

Fig. 3.8. Hourly system demand, test distribution feeder demand, solar PV generation and wind generation for a typical week.

For the renewable DG connected in different nodes of the distribution feeder, a number of options are generated through simulations. For each renewable DG connection option, the optimisation program as presented in Section 3.3.2 is executed, and the maximum capacity of the renewable DG is estimate. Then the option with maximum renewable DG hosting capacity of the distribution feeder is calculated using Eq. (3.1). The energy supply adequacy indices and service continuity adequacy indices for the test feeder are presented in Table 3.4 and Table 3.5. It can be seen that for the practical distribution network combined solar PV and wind turbine DG units showed better performance in improving the ESSP, and probability of the healthy state of distribution substation capacity-release than those of the solar PV only and wind turbine

only. The probability distributions of the additional available capacity and average successfully transferrable load on the occurrence of an outage on the line section between nodes 1 and 2 of the test feeder for different DG technologies are shown in Fig. 3.9. It can be seen that the probabilities of the higher additional available capacity increases with the integration of the renewable DG units. In addition to that the additional available capacity of the distribution feeder increases by more than 1 MW. It indicates that the probability of accommodating the peak-time load of the neighbour feeders increases with the integration of renewable DG units into the test feeder. It can be also observed that renewable DG reduces the probability of the successfully transferrable load between 2.5 MW and 3.5 MW, and increases the probability of the successfully transferrable load between 0.5 MW and 2.5 MW. Since the demand of the distribution feeder with outage is reduced by the renewable DG, transferrable load to the neighbouring feeder reduces. Hence integration of the renewable DG improves the successful load points restoration probability of the distribution on the occurrence of an outage.

Table 3.4. Maximum Renewable DG Hosting Capacity for the Test Feeder

	No DG	**Solar PV**	**Wind Turbine**	**Combined Solar PV and Wind Turbine**
C_{DGmax}	-	2.2086 MVA	1.6317 MVA	2.3012 MVA

Table 3.5. Proposed Indices to Estimate Energy Supply and Service Continuation for the Test Feeder

	Proposed Analytical Method				**Time Sequential MCS Method**			
	No DG	**Solar PV**	**Wind Turbine**	**Combined Solar PV and Wind Turbine**	**No DG**	**Solar PV**	**Wind Turbine**	**Combined Solar PV and Wind Turbine**
ESSP	-	12.14	12.5 %	15.53 %	-	12.14	12.5 %	15.53 %
Probability of the States of Distribution Substation Capacity Release								
Healthy	0.1599	0.4287	0.5285	0.8193	0.2409	0.5102	0.6287	0.7058
Marginal	0.8401	0.5713	0.4715	0.1807	0.7591	0.4898	0.3713	0.2942
Probability of the States of Additional Available Capacity (pu)								
Healthy	0.0870	0.6750	0.7530	0.8190	0.1085	0.6735	0.7339	0.8537
Marginal	0.9130	0.3250	0.2470	0.1810	0.8915	0.2265	0.2661	0.1463

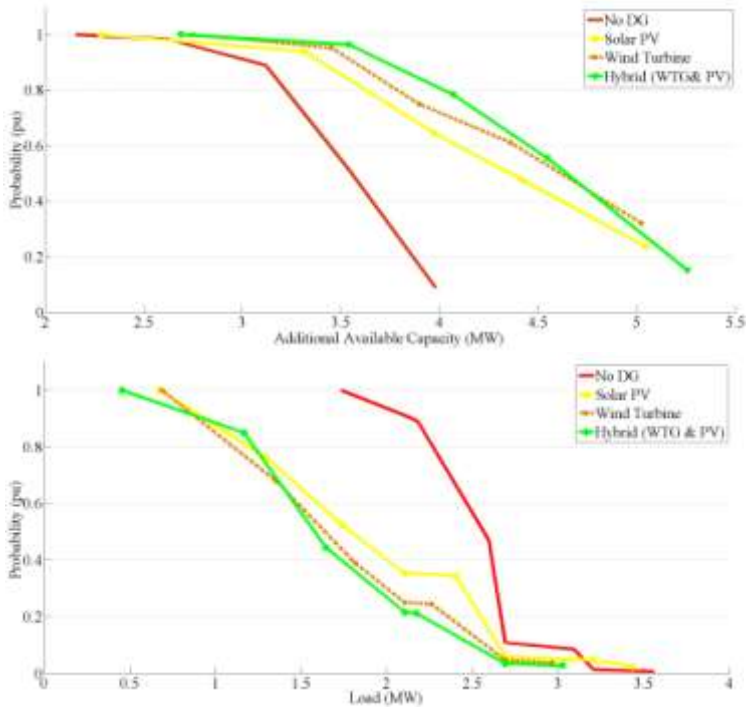

Fig. 3.9. Probability distribution of the additional available capacity and successfully transferrable load of the test feeder for various DG types.

3.5 Conclusion

This chapter has addressed the issues related to the 'energy supply' and **'**continuity of service**'** assessment for distribution networks embedded with renewable DG units. New indices for 'energy supply' and 'continuity of service' assessment have been developed and tested. A joint probability based analytical technique has been developed using data clustering approach for the assessment of network adequacy in terms of 'energy supply' and 'continuity of service' with incorporating both, uncertainty and coincidental occurrence in power availability and time varying demand. The results obtained using proposed analytical approach are compared with the results of the time sequential MCS and the performance of the proposed analytical method is found to be very close and promising. The proposed adequacy indices can be used to rank different renewable DG technologies in terms of their suitability for integration in distribution networks. The proposed method has been tested on a standard distribution network derived from Roy Billinton test system and also on a practical distribution network. The probability distributions of the proposed indices are presented and analysed for different renewable DG systems to compare the performance of each DG type. The results

suggest that the ‘energy supply’ and ‘continuity of service’ in the distribution networks great depends on the consideration of the time varying demand and stochastic renewable generation output. Moreover, improvement of the ‘energy supply’ and ‘continuity of service’ in the distribution networks is found due to integration of renewable DG systems.

References:

[1] R. Billinton, R. N. Allan, Reliability Evaluation of Power Systems. 2nd ed. New York: Plenum; 1996.

[2] R. Dashti, S. Afsharnia, H, Ghasemi, "A new long term load management model for asset governance of electrical distribution systems", *Applied Energy*, vol. 87, pp. 3661-3667, 2010.

[3] O. Shavuka, K. O. Awodele, S. P. Chowdhury, S. Chowdhury, "Reliability analysis of distribution networks", *Proc. Of International Conference on Power System Technology (POWERCON)*, pp. 1-6, October 2010.

[4] Y. G. Hegazy, M. M. A. Salama, A. Y. Chikhani, "Adequacy assessment of distributed generation systems using Monte Carlo Simulation", *IEEE Transactions on Power Systems*, vol. 18, no.1, pp.48- 52, 2003.

[5] Y. M. Atwa, E. F. El-Saadany, M. M. A. Salama, R. Seethapathy, M. Assam, S. Conti, "Adequacy Evaluation of Distribution System Including Wind/Solar DG During Different Modes of Operation", *IEEE Transactions on Power Systems*, vol. 26, no.4, pp. 1945-1952, 2011.

[6] L. D. Arya, L. S. Titare, D. P. Kothari, "Distribution system adequacy assessment accounting customer controlled generator sets", *International Journal on Electrical Power & Energy Systems*, vol. 33, no. 5, pp. 1161-1164, 2011.

[7] S. Fockens, A. J. M. van Wijk, W. C. Turkenburg, C. Singh, "Application of energy based indices in generating system reliability analysis", *International Journal on Electrical Power & Energy Systems*, vol. 16, no. 5, pp. 311-319, 1994.

[8] R. Billinton, D. Huang, "Sensitivity of system operating considerations in generating capacity adequacy evaluation", *International Journal on Electrical Power & Energy Systems*, vol. 32, no. 3, pp. 178-186, 2010.

[9] D. K. Khatod, V. Pant, J. Sharma, "Analytical Approach for Well-Being Assessment of Small Autonomous Power Systems With Solar and Wind Energy Sources", *IEEE Transactions on Energy Conversion*, vol. 25, no. 2, pp. 535-545, 2010.

[10] G. Taljan, M. Maksic, A. F. Gubina, "Energy Based System Well-Being Analysis", *Proc. IEEE Power Engineering Society General Meeting 2007*, Florida, USA 2007.

[11] R. Billinton, B. Karki, "Well-Being Analysis of Wind Integrated Power Systems", *IEEE Transactions on Power Systems*, vol. 26, no. 4, pp. 2101-2108, 2011.

[12] G. Caralis, A. Zervos, "Value of wind energy on the reliability of autonomous power systems", *IET Renewable Power Generation*, vol. 4, no. 2, pp. 186-197, 2010.

[13] R. M. Ciric, N. L. J. Rajakovic, "A new composite index of reliability of supply in the industrial systems with distributed generation", *International Journal on Electrical Power & Energy Systems*, vol. 44, no. 1, pp. 824-831, 2013.

[14] R. Billinton, "Distribution system reliability performance and evaluation", *International Journal on Electrical Power & Energy Systems*, vol. 10, no. 3, pp. 190-200, 1988.

[15] A. Moreno-Munoz, J. J. Gonzalez de la Rosa, J. M. Flories-Arias, F. J. Bellido-Outerino, A. Gil-de-Castro, "Energy efficiency criteria in uninterruptible power supply selection", *Applied Energy*, vol. 88, no. 4, pp. 1312-1321, 2011.

[16] A. A. Chowdhury, S. K. Agarwal, D. O. Koval, "Reliability modelling of distributed generation in conventional distribution systems planning and analysis", *IEEE Transactions on Industry Applications*, vol. 39, no. 5, pp. 1493-1498, 2003.

[17] Photovoltaic (PV) Systems-Characteristics of the Utility Interface, *IEC Standard 61727*, December 2004.

[18] IEEE Standard for Interconnecting Distributed Resources with Electric Power Systems, *IEEE Standard 1547*, July 2003.

[19] Grid Connection of Energy Systems via Inverters, *Australian Standard 4777*, April 2005.

[20] M. H. Bollen, F. Hassan, Integration of Distributed Generation in the Power System. 1st ed. Wiley: New Jersey, 2011.

[21] A. G. Madureira, J. A. P. Lopes, "Coordinated voltage support in distribution networks with distributed generation and microgrids", *IET Renewable Power Generation*, vol. 3, no. 4, pp. 439-454, 2009.

[22] O. Ekren, B. Y. Ekren, "Size optimization of a PV/wind hybrid energy conversion system with battery storage using response surface methodology", *Applied Energy*, vol. 85, no. 11, pp. 1086-1101, 2008.

[23] A. Roy, S. B. Kedare, S. Bandyopadhyay, "Optimum sizing of wind-battery systems incorporating resource uncertainty", *Applied Energy*, vol. 87, no. 8, pp. 2712-2727, 2010.

[24] R. Niemi, P. D. Lund, "Decentralized electricity system sizing and placement in distribution networks", *Applied Energy*, vol. 87, no. 6, pp. 1865-1869, 2010.

[25] L. Baringo, A. J. Conejo, "Corrlated wind-power production and electric load scenarios for investment decisions", *Applied Energy*, vol. 101, no. 1, pp. 475-482, 2012.

[26] Y. M. Atwa, E. F. El-Saadany, "Probabilistic approach for optimal allocation of wind-based distributed generation in distribution systems", *IET Renewable Power Geneneratin*, vol. 5, no. 1, pp. 79-88, 2011.

[27] R. Billinton, S. Jonnavithula, "A test system for teaching overall power system reliability assessment", *IEEE Transactions on Power Systems*, vol. 11, no. 4, pp. 1670-1676, 1996.

[28] J. A. Jardini, C. M. V. Tahan, M. R. Gouvea, S. U. Ahn, F. M. Figueiredo, "Daily load profiles for residential, commercial and industrial low voltage consumers", *IEEE Transactions on Power Delivery*, vol. 15, no. 1, pp. 375-380, 2000.

[29] Bureau of Meteorology, Australian Govenrment. Online. Available : http://www.bom.gov.au/climate/data-services/, access on Jan 2012.

[30] Endeavour Energy, New South Wales, Australia. Online. Available: http://www.endeavourenergy.com.au/wps/wcm/connect/EE/NSW/NSW+Homepage/

Chapter 4

Sustainable Energy System Design with Distributed Renewable Resources

ABSTRACT

Electricity generation using renewable energy generation technologies is one of the most practical alternatives for network planners in order to achieve national and international Greenhouse Gas (GHG) emission reduction targets. Renewable Distributed Generation (DG) based Hybrid Energy System (HES) is a sustainable solution for serving electricity demand with reduced GHG emissions. A multi-objective optimisation technique for minimising cost, GHG emissions and generation uncertainty has been proposed in this chapter to design HES for sustainable power generation and distribution system planning while considering economic and environmental issues and uncertainty in power availability of renewable resources. Life cycle assessment has been carried out to estimate the global warming potential of the embodied GHG emissions from the electricity generation technologies. The uncertainty in the availability of renewable resources is modelled using the method of moments. A design procedure for building sustainable HES has been presented and the sensitivity analysis is conducted for determining the optimal solution set.

4.1 Introduction

The conventional electricity generation systems have been established based on the fossil fuel fired generation technologies. As a result, the electricity generation and consumption are contributing to significant portion of the global Greenhouse Gas (GHG) emissions. In the recent years, various initiatives have been taken globally to reduce the GHG emission levels by adapting climate change mitigation strategies. Being one of the major sources of global GHG emissions, electricity utilities have also set targets to reduce GHG emissions from electricity generation as part of climate change mitigation strategy.

The increasing concern for implementing climate change mitigation strategies in electricity utilities is driving utilities to develop and implement alternative practices involving non-conventional electricity generation systems. As a result, decentralised power generation, distributed generation (DG), micro-grid, smart grid, stand-alone power systems with renewable generation systems are becoming some of the attractive options for the utilities. Among the distributed energy resources, hybrid energy system (HES) is found to be more reliable option than the systems with single source of energy [1]. For this reason, hybrid Solar-Wind and Solar-Wind-Diesel are broadly studied for distributed energy resource planning as revealed in the literature.

Studies on small stand-alone HES design methods have been reported in [2]. In [3], solar photovoltaic (PV) and integrated battery have been studied for remote electricity supply to an isolated stand-alone facility. Stand-alone off grid HESs are designed using different configurations of solar PV system, wind turbine generation system, battery energy storage and diesel generator as detailed in [4]-[6]. Isolated stand-alone power systems designed using solar PV, wind turbine and battery storage have been reported in [7]-[9]. Though diesel generator is considered in some HES design process, significant GHG emissions are involved in the operation of diesel generator due to diesel consumption.

Electricity regulators in many countries are conducting feasibility studies for 100% renewable electricity generation [10]-[11]. Renewable DG in the distribution network can be one of the options to achieve 100% renewable electricity generation target. Apart from the distribution network support, renewable DG units can offer benefits like

deferral in building transmission and distribution infrastructure. Hence, net zero energy distribution network can be a part of future sustainable electricity generation and supply systems. Since the availability of the renewable power generation is stochastic in nature, combined usage of different renewable resources to generate electricity along with energy storage systems (ESSs) can mitigate intermittency and uncertainty in power availability. Hence, generation planning technique for HES is to be developed for sustainable distribution network design with the consideration of 100% renewable energy based electricity generation systems.

In this chapter, a multi-objective optimisation technique has been formulated for designing renewable based HES thereby achieving sustainability in power generation and distribution. In this study, solar PV, wind turbine and battery energy storage technologies have been considered as a part of renewable based HES. Life cycle embodied emissions, levelised cost of energy (LCOE) and supply continuity in the distribution network are considered as different attributes for multi-objective studies associated with renewable based HES design. Life cycle assessment method has been applied to estimate embodied emission and the LCOE of the renewable based HES. Method of moments is used for estimating the supply continuity, related to the uncertainty in renewable resources, from renewable based HES. Trade-off analysis has been used to resolve conflicting objective functions and select feasible optimal HES design options for ensuring sustainability in distribution networks. Also, the sensitivity of life cycle cost and emissions, associated with the ESS, on the optimal solution set of the HES design problem has been investigated.

Renewable based HES design problem is discussed in Section 4.2 of this chapter followed by the mathematical formulation of the proposed objective functions in Section 4.3. The proposed multi-objective optimisation problem formulations and solution method for renewable based HES design is presented in Section 4.4. A case study of the renewable based HES design for a practical distribution network has been illustrated in Section 4.5 followed by the conclusion in Section 4.6.

4.2 Renewable based Hybrid Energy System Design

Solar radiation and wind are the two most commonly available renewable energy resources in most of the geographical locations on the earth. Since availability of these resources is not guaranteed, there could be issues such as generation deficiency when it comes to satisfying the load demand, solely by means of these resources, all the time in a day. Combining two or more of these resources to operate in tandem, whenever needed, may reduce the variability in generation availability; however, the availability of electricity generation on a continuous basis cannot be assured. Hence, energy storage systems (ESSs) need to be deployed for ensuring continuity of supply in the distribution network. Battery storage is one of the favourable technologies for ESS due to its easy installation and other operational benefits. Therefore, solar PV system and wind turbine generation system along with battery energy storage system (BESS) are the preferred combination for renewable based HES to achieve sustainability in distribution networks. A typical arrangement of such a system is shown in Fig. 4.1.

Fig. 4.1. A typical renewable based HES configuration for achieving sustainability in distribution networks.

The design criteria for small standalone (or off-grid) HES as reported in literature include considerations of economic and environmental aspects, and risk in supply

adequacy [2]-[9]. Total investment cost, life cycle cost (LCC), fuel cost and LCOE are used as economic attributes of the decision making process in renewable based HES design. Operational emissions, embodied energy, life cycle emissions (LCE), primary energy saving ratio and wasted renewable energy are considered to be the environment related objectives associated with renewable based HES design.

Economical and environmental impacts and uncertainty in renewable power availability are to be included as different attributes in the design of renewable based HES which is one of the sustainable solutions for electricity networks. LCOE includes annualised capital investment and operational cost for every unit of electric energy consumption. Hence, minimisation of LCOE minimises both the capital investment cost and operational cost associated with electricity generation. In the proposed study, LCOE is considered as an indicator of economic aspects associated with the design of HES.

Air pollution can be considered as one of the major impacts on environment, resulted from the conventional electricity generation systems. Embodied emissions of energy are the life cycle pollutant emissions to the air associated with a unit energy generation. Life cycle emissions include the primary emissions associated with the processing of raw material, manufacturing and transportation of the equipment used in the infrastructure construction and disposal stages, and secondary emission related to operational stage of life cycle of the generation facilities. Since renewable DG facilities do not use fossil fuel for electric energy generation, the operational emissions of these technologies can be considered to be zero. On the other hand, fossil fuel based generation facilities, such as diesel generator and gas generator, does exhibit operational emissions associated with fuel consumption. The total life cycle emissions of the generation facility are then divided by the total energy generated during the life cycle of the facility to estimate the embodied emissions of the energy. In the proposed study, the environmental impact of renewable based HES is modelled in terms of embodied emissions related to the electric energy generation.

The generation output from HES depends on the availability of renewable resources (such as solar radiation and wind speed) and the state of charge (SOC) of the BESS. Since the availability of the renewable resources is uncertain and the BESS is used to store the excess energy generated by the renewable energy generation technologies (in the off-peak periods), the combined output of the HES is also uncertain. Energy is

imported from the grid when the available energy output from HES is insufficient to meet the load demand of the distribution network. In order to be less dependent on the grid, the HES is to be designed to meet the time varying load demand of the distribution network for most of the time in a day. The dependency on the grid for importing energy can be modelled by the deficiency of energy supply from the HES due to the uncertainty in the availability of the renewable resources and time varying load demand of distribution network. In the proposed study, expected renewable energy deficiency (ERED) of renewable based HES is considered to represent the uncertainty in the demand and renewable generation.

The design procedure of the HES, which is an integral part of the sustainable distribution network involves sizing of each type of generation technology and development of control strategy for deriving dispatch schedules of the generation units. The installed capacity of individual generation technology type is one of the control variables for the HES designer. Since multiple attributes are to be considered in the renewable based HES design problem, multi-objective (MO) optimisation techniques are employed in this chapter. A trade-off technique has been used to obtain a set of feasible design options. The mathematical models of the objective functions and MO optimisation formulation are detailed in the next section.

4.3 Mathematical Formulation

The design technique of renewable based HES for ensuring sustainability in distribution networks is developed to minimise the LCOE, embodied emissions of the electric energy and probability of expected energy deficiency. The higher installed capacity of the HES will reduce dependency on the grid. However, the higher installed capacity will impose higher life cycle cost and result into higher levels of unused energy from the renewable resources. As a consequence, the LCOE and embodied emissions of the energy will be increased to meet the requisite load demand. In addition, different combinations of solar PV, wind turbine generation system and BESS will result into different LCOE and embodied emissions. Since different renewable generation technologies have different embodied primary emissions and different capital costs, minimum LCOE option may not result into minimum embodied emissions of the

energy. Therefore, the objective functions associated with determining the optimal design of the renewable based HES for securing sustainability in distribution network are conflicting in nature. The associated mathematical formulation is detailed in the following subsections.

4.3.1 Levelised Cost of Energy (LCOE)

The life cycle cost of the renewable based HES includes the cost of the equipment, commissioning cost, site acquisition cost, replacement cost less the end of life inventory cost. The operation and maintenance (O&M) cost of the HES includes fixed and variable costs associated with each unit. The annualised capital cost, $C_{A,Cap}$, and O&M cost, $C_{AO\&M}$, are estimated using equations (4.1) and (4.2), respectively.

$$C_{A,Cap} = \sum_i \left\{ \left(C_{Equip,i}(S_i) + C_{Acq,i}(S_i) + C_{Com,i}(S_i) - C_{Inv,i}(S_i) \right) \times \frac{d(1+d)^{n_i}}{(1+d)^{n_i} - 1} + C_{rep,i}(S_i) \times \frac{d}{(1+d)^{r_i} - 1} \right\} \tag{4.1}$$

$$C_{A,O\&M} = \sum_i \left\{ C_{FO\&M,i} + C_{VO\&M,i} \times (S_i) \right\} \tag{4.2}$$

where, S_i is the installed capacity of i^{th} generation technology in the HES. $C_{Equip,i}(S_i)$, $C_{Acq,i}(S_i)$, $C_{Com,i}(S_i)$, $C_{Inv,i}(S_i)$ and $C_{rep,i}(S_i)$ are the capital cost of the equipment, site acquisition cost, commissioning cost, end of life inventory cost and equipment replacement cost for i^{th} energy generation and storage technology, for an installed capacity of S_i, respectively. The annual interest rate and, life time of the equipment in i^{th} energy generation and storage technology is denoted by d and n_i, respectively. The life time of the equipment requiring replacement of the i^{th} energy generation and storage technology is denoted by r_i. $C_{FO\&M,i}$ and $C_{VO\&M,i}(S_i)$ are the annual fixed O&M cost and, variable O&M cost, depending upon the installed capacity of S_i, of i^{th} energy generation and storage technology respectively. The objective function f_1, which is the LCOE of the HES is then estimated using the annualised capital and O&M costs of the energy generation and storage technology and the annual energy demand in the distribution network as shown in equation (4.3).

$$f_1 = LCOE = \frac{C_{A,Cap} + C_{A,O\&M} + C_{GE}}{\sum_t D_t} \tag{4.3}$$

where, D_t is the total load demand of the distribution network at the time instance t. C_{GE} is the cost of energy purchased from the grid due to the deficiency of energy supply from the renewable based HES.

4.3.2 Embodied Emissions of Energy

Embodied emission of energy is estimated using the life cycle air pollutants' emissions caused by the energy generation and storage technologies. Life cycle air pollutants' emissions of the energy generation and storage technologies are estimated using life cycle assessment (LCA) technique. LCA is a tool to estimate the environmental impacts of a product or process throughout the life time of the product or service. Life cycle air pollutants' emissions of the product or service, which is one of the outcomes from LCA, are the sum of air pollutants' emissions involved at different phases during the life cycle of the unity amount of the product or service. For energy generation and storage technologies, life cycle emissions of the air pollutants can be quantified in terms of air pollutants from per unit rated generation and energy storage capacity, respectively. Several different pollutants are released to the air in the life cycle of the energy generation and storage technologies and different air pollutants have different levels of impact on the environment. Hence, it is required to express the emissions by different air pollutants using a common metric which can estimate aggregate emissions of the pollutants to the air from life cycle of the energy generation and storage technologies.

The global warming potential (GWP) represents how much a given mass of an air pollutant contributes to global warming over a given time period compared to the same mass of carbon dioxide and is estimated from the ratio of the warming caused by the air pollutant to the warming caused by a similar mass of carbon dioxide. Hence, the life cycle GWP of each air pollutant from per unit rated generation and energy storage capacity can be estimated from the products of the GWP of the air pollutant and the life cycle emission of the air pollutant from the per unit rated generation and energy storage capacity. The total life cycle GWP emissions from per unit rated generation and energy storage capacity is the sum of life cycle GWP of each air pollutant. The total life cycle GWP emissions from per unit rated generation and energy storage capacity is then divided by the life time of the energy generation and storage technology to estimate the

annualised GWP emissions of per unit rated generation and energy storage capacity. The annualised GWP emissions of per unit rated capacity, $GWP_{A,i}$ of the i^{th} technology, can be estimated using equation (4.4) as shown below.

$$GWP_{A,i} = \frac{\left[G_{AP1,i}, G_{AP2,i}, \cdots\cdots, G_{APns,i}\right] \times \left[M_{AP1,i}, M_{AP2,i}, \cdots\cdots M_{APns.i}\right]^T}{n_i} \tag{4.4}$$

where, $G_{APj,i}$ and $M_{APj,i}$ are the GWP and life cycle emission of the air pollutant AP_j (where j varies from 1 to ns) by per unit rated capacity of the i^{th} technology respectively. The total annualised emissions from an energy generation or storage technology expressed in term of GWP can be estimated by multiplying the installed capacity of the technology, S_i, and annualised GWP emissions from per unit rated capacity of the technology, $GWP_{A,i}$. Hence, the second objective function of the renewable based HES design problem is formulated as the embodied emission of the energy in term of GWP and can be estimated using equation (4.5) as shown below.

$$f_2 = EE_{GWP} = \frac{\sum_i (GWP_{A,i} \times S_i) + \sum_t (GWP_{GE,t} \times E_{GE,t})}{\sum_t D_t} \tag{4.5}$$

where, $GWP_{GE,t}$ and $E_{GE,t}$ are the GWP emissions of grid energy embodied emissions and energy imported from the grid at time instance t. The GWP of grid energy embodied emissions can be either estimated using the methodology presented in [12] or achieved from the emission reporting of individual generating system [13].

4.3.3 Expected Renewable Energy Deficiency (ERED)

Due to the time varying nature of load demand in the distribution network and intermittent nature of the renewable resource availability, the net generation from the HES may not be sufficient to meet the demand of the distribution network at all times. Hence, it may be required to import energy from the grid. Currently, fossil fuel based generating plants are dominating and generating most of the grid power. Hence, the grid energy contains higher embodied emissions, and distribution network with the HES can be designed to import energy from the grid only during emergency situations. Accordingly, the renewable based HES may be designed based on the forecasted solar radiation and wind speed availability to satisfy the consumer demand in distribution

network. However, due to uncertainty in the availability of renewable resources, the forecasted renewable generation output may vary over a period of time posing risk in meeting the demand. Since the demand in the distribution network and energy generation availability from the HES are uncertain in nature, the probability of energy generation shortfall to meet the demand can be used as the indicator of the HES reliability and grid energy supply independency. The probability of energy generation shortfall from the DG unit of the HES is a time dependent quantity. Single valued index designated as expected renewable energy deficiency (ERED) can be represented in terms of objective function as defined in equation (4.6).

$$f_3 = ERED = \frac{1}{N_t} \times \sum_t \Pr(E_{HES,t} - D_t) \tag{4.6}$$

where *Pr(.)* stands for probability and $E_{HES,t}$ is energy generation available from the HES at t^{th} time instance. $E_{HES,t}$ is the sum of the available power generation from renewable generation systems and available energy stored in the BESS for discharge purposes whenever needed. The probability of energy generation shortfall from the DG unit of the HES can be estimated using the method of moments. The uncertainty in the availability of stored energy in the BESS depends on the uncertainty in the availability of energy for storage and SOC of the BESS in the previous time instance. Hence, the moments of the energy available in the BESS for discharging can be estimated using equation (4.7) as shown below.

$$\mu_m(E_{ESS,t}) = \mu_m(E_{ESS,t-1}) + \mu_m(E_{SPV,t-1}) + \mu_m(E_{W,t-1}) + (-1)^m \times \mu_m(D_{t-1}) \tag{4.7}$$

where, $\mu_m(.)$ indicates the m^{th} order moments of the quantities within the parenthesis. $E_{ESS,t}$ is the energy available in the BESS for discharging at t^{th} time instance. $E_{SPV,t}$ and $E_{W,t}$ are the energy generation from solar PV and wind turbine generation system at t^{th} time instance, respectively. The moments of available energy generation from the renewable based HES at t^{th} time instance can be estimated using equation (4.8). Using the moments of available energy generation from the HES and the moments of distribution network demand, the moments of surplus energy generation from the HES at t^{th} time instance can be estimated using equation (4.9).

$$\mu_m(E_{HES,t}) = \mu_m(E_{ESS,t}) + \mu_m(E_{SPV,t}) + \mu_m(E_{W,t}) \tag{4.8}$$

$$\mu_m(E_{HES,t} - D_t) = \mu_m(E_{ESS,t}) + (-1)^m \times \mu_m(D_t) \tag{4.9}$$

The moments of the demand and available renewable generation output can be estimated from the historical data or the recorded probability distribution of the respective quantities. Once the moments of the available energy generation from the HES are found, the probability distribution of surplus energy generation from the HES can be estimated using either series expansion or parametric estimation methods [14, 15]. Hence, the objective function, ERED of the HES can be estimated using the probability distribution of surplus energy generation at t^{th} time instance as shown in (4.6).

4.4 Proposed Renewable based HES Design Technique

4.4.1 Objective Functions

The main objective of the renewable based HES design for ensuring sustainability in distribution networks is to obtain a set of optimal generation capacity of each technology which can generate energy at lower cost and environmental pollution with reduced dependency on the grid for energy supply. Hence, the optimal HES design for distribution networks can be achieved by minimising the objective functions formulated in Section 4.3 and applying multi-objective optimisation presented in (4.10).

$$\min\ f = \min([\, f_1, f_2, f_3 \,]) \tag{4.10}$$

For higher installed capacity of the energy generation and storage technologies, the objective function f_3 i.e., dependency on the grid for energy supply will be minimised. However, it may not guarantee the minimisation of other objective functions. Similarly, lower installed capacity of the energy generation and storage technologies will reduce the objective function f_1 i.e., the LCOE at the cost of other objective functions. It is noted that the objective functions of the multi-objective minimisation problem formulated in (4.10) are conflicting in nature. Therefore, a trade-off analysis is to be applied for decision making in selecting the optimum installed capacities of different energy generation and storage technologies in the renewable based HES.

4.4.2 Constraints

The solution set of the multi-objective optimisation problem is required to satisfy the constraints of the distribution network. The constraints of the multi-objective optimisation problem are presented as follows.

$$\sum_{k}(S_k \times CF_k) \geq mean[D_t] \tag{4.11}$$

$$0 \leq S_i \leq S_{\max} \tag{4.12}$$

The constraint in (4.11) ensures that the energy generated by the renewable generation technologies is sufficient to meet the energy demand of the distribution network with the support of BESS. The set of renewable generation technologies, *k*, is a subset of the set *i* which constitutes energy generation and storage technologies. CF_k is the capacity factor of the k^{th} generation technology of renewable based HES. The upper and lower limits of the installed capacity of the energy generation and storage technologies are regulated by the constraints in equation (4.12).

4.4.3 Trade-off Analysis for Optimal Set of Solutions

Trade-off analysis is used in this chapter to solve the multi-objective optimisation problem with conflicting objective functions. The constraints of the decision variables define the feasible solution set in the decision variable space. The combinations of the decision variables from the feasible solution set are known as the plans. Objective space is then mapped for each feasible solution set of decision variables or plans. Lastly, trade-off analysis is applied to the feasible objective space to select the set of optimal values of objective functions.

The optimal values of objective functions are estimated from the feasible objective space by applying two conditional decision criteria. The first criterion is called strictly dominance criterion and application of strictly dominance criterion results in a set of optimal solutions known as Pareto Frontier. Pareto Frontier is the boundary between the sets of possible and the sets of unachievable solutions in the objective space. Pareto Frontier consists of plans that are not strictly dominated by any other plans in the objective space. For example, a plan P_A strictly dominates plan P_B if all the objective

functions associated with plan P_A demonstrate better performance in comparison with plan P_B.

The second criterion to estimate the particular conditional decision set is called significantly dominance criterion and a set of feasible plans known as Knee Set is determined by applying this criterion in the objective space. As an example, a plan P_A significantly dominates plan P_B if at least one of the objective functions of plan P_B is much worse than the corresponding objective function of plan P_A and if none of the objective functions of plan P_B are significantly better than objective functions of plan P_A. Hence, the selection of Knee Set is governed by two parameters namely: 'much worse' and 'significantly better'. Selection of the values of these two parameters determines the number of plans in the Knee Set. Knee Set contains the plans on and near the knee region of the Pareto Frontier.

The steps involved in the renewable based HES design algorithm using trade-off analysis are summarised as follows.

Step 1: The plans from the combinations of decision variables within the feasible decision variable space are determined by the constraints in equations (4.11) and (4.12).

Step 2: Map the plans in the objective space using the objective functions formulated in equations (4.3), (4.5) and (4.6).

Step 3: Apply strictly dominance criterion in the objective space to estimate the Pareto Frontier set of plans.

Step 4: Select 'much worse' and 'significantly better' parameters and apply significantly dominance criterion to determine the Knee Set of the associated plans.

4.5 Case Study

4.5.1 Data

4.5.1.1 Demand

The renewable based HES is designed for an 11 kV rural distribution network which is extracted from the electricity distribution system in New South Wales, Australia. The

peak demand of the distribution network is found to be 1.8 MW during an evening time summer and annual average of hourly demand in the distribution network is found to be 1.05 MW. Hourly load profile of the distribution network is used in this study. The time varying embodied emission data of the energy supplied through the grid, extracted from [13], is used in this study.

4.5.1.2 Solar PV

Life cycle assessment of multi-crystalline solar PV panel, with rated capacity of 33 kW, and the associated equipment such as mountings structure and inverter has been conducted. The life cycle emission of the PV panel is found to be 65.718 ton CO_2 equivalent. Therefore, the annualised embodied GWP associated with unit installed capacity of solar PV panel is estimated as 99.57 kg CO_2 eqv./kW-yr. The lifetime of the solar PV generation system is assumed to be 20 years. The total life cycle cost of equipment, site acquisition cost, and commissioning cost less the end of life cycle inventory cost for multi-crystalline solar PV generation system is found to be $1600 per kW. The fixed and variable O&M cost of the solar PV generation system used for this study are $200 per year and $0.5 per kW-yr, respectively. The information about the solar irradiation and sky clearness index within the proximity of the test distribution network is collected from [16]. The capacity factor of the solar PV generation output in area of the network is found to be 15.7%.

4.5.1.3 Wind Turbine

A wind turbine with 600 kW rated capacity has been considered for life cycle assessment. The GWP of the life cycle air pollutant emissions from the construction, material extraction, manufacturing of the equipment, transportation and end of life dismantle stages of the wind turbine is found as 780 ton CO_2 eqv. for each wind turbine generation system structure. The lifetime of the wind turbine is assumed to be 20 years. Accordingly, the annualised embodied emissions associated with unit installed capacity of wind turbine generation system in terms of GWP is estimated as 65 kg CO_2 eqv./kW-yr. The total life cycle cost of the wind turbine generation system used for this study is $2000 per kW which includes cost of equipment, site acquisition cost, commissioning cost less the end of life cycle inventory cost. The fixed and variable O&M costs of the wind turbine generation systems are used as $600 per year and $0.2 per kW-yr

respectively in this study. The wind speed data at 20m height is collected from the Bureau of Meteorology, Australia [17] for the area of the distribution network. Two different wind turbines with 100 kW and 600 kW rated capacities are considered for the renewable based HES design. The 100 kW wind turbine has a hub height of 20m and wind turbine rated at 600 kW capacity has a hub height of 75m. The wind speed at 75m is estimated from the wind speed data at 20m height using the equation (4.13) [18].

$$\frac{v(h_2)}{v(h_1)} = \left(\frac{h_2}{h_1}\right)^{\alpha} \tag{4.13}$$

where, $v(h_1)$ is the wind speed at height h_1 and α is the friction coefficient derived from the experiment. The power output from wind generation system is estimated from the power curve of the respective wind turbine. The capacity factors of 100 kW and 600 kW wind turbine generation systems are found to be 34% and 36% respectively for the wind speed profile in the close vicinity of the area covering the distribution network.

4.5.1.4 BESS

Lead acid battery units each rated with 12 V and 504 Ah are considered in this study. The round trip efficiency, full cycles in life time and minimum State of Charge allowed for the battery are 80%, 1460 cycles and 20%, respectively. From the life cycle assessment of the BESS, the embodied emissions are found 26.5 kg CO_2 eqv./kVAh-yr. The annualised capital cost of unit BESS capacity used for this study is $203 per kVAh. The fixed and variable O&M cost of the BESS is estimated as $200 per year and $0.1 per kVAh-yr in this study.

4.5.2 Results

The proposed renewable based HES design technique for the distribution network is simulated in MATLAB using the code developed by the authors. The maximum installed capacity limits for solar PV and wind turbine generation systems are set to be 8 MW, 4.8 MW, 4 MW and 12 MWh for the BESS. Applying the constraints presented in equations (4.11) and (4.12), the feasible decision variable space is formed as shown in Fig. 4.2 (a). The feasible HES plans are generated from the combinations of the decision variables of the feasible space. The objective space for the renewable based HES design problem has been mapped from the feasible plans using the objective functions

presented in equations (4.3), (4.5) and (4.6). The objective space for the HES design problem in the distribution network is presented in Fig. 4.2 (b). It can be observed that bounded feasible decision variables form a bounded objective space indicating the convex form of the multi-objective minimisation problem.

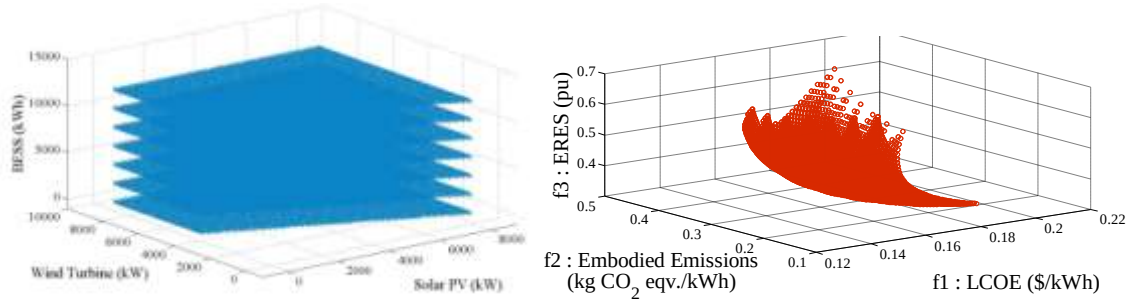

(a) **(b)**

Fig. 4.2. (a) Decision variable space (b) Objective space of the HES DG design problem for the distribution network.

The strict dominance criterion is applied to the feasible plans in the objective space and the Pareto Frontier is estimated for the renewable based HES design problem for the distribution network. The Pareto Frontier of the HES design problem for the distribution network is presented in Fig. 4.3 by the red circles. Comparing Fig. 4.2(b) and Fig. 4.3, it is apparent that the plans in the Pareto Frontier set are on the boundary surface between the sets of possible and unachievable plans in the objective space. Hence, the significance dominance criterion is applied to the feasible plans in the objective space and Knee Set for the HES design problem is found as shown by the blue dots in Fig. 4.3. The 'much worse' and 'significantly better' parameters applied to individual objective functions are expressed as the per-cent value of the difference between the maximum and minimum values of the respective objective function. The values of 'much worse' parameters applied to objective functions f_1, f_2 and f_3 for estimating the Knee Set are selected as 10%, 10% and 8% respectively. The values of 'significantly better' parameters applied to objective functions f_1, f_2 and f_3 for estimating the Knee Set are 6%, 5% and 3% respectively. The Knee Set contains the optimal solutions obtained by relaxing the selection criterion using 'significantly better' parameters and by restricting the selection criterion using 'much worse' criterion.

Hence, the solutions in the Knee Set are also optimal solutions with the designer's relative preferences for objective functions.

Four extreme points from the set of optimal solutions (Pareto Frontier and Knee Set) are selected as shown by the A, B, C and D marked in Fig. 4.3. The values of the decision variables and objective functions for the four points are presented in Table 4.1. Comparing the selected extreme plans from the optimal solutions, it is found that none of solutions are better than each other considering all the three objective functions.

The plan at point A contains all the energy generation and storage technologies at their maximum limit. In such case, the reliability of the renewable based HES is very high at the cost of high LCOE and high embodied emissions of the energy due to redundant generation and storage capacity. On the other hand, the plan at point C is the least cost option and does not contain any energy storage. As a result, the values of embodied emissions and ERED of the energy are high. Hence, the distribution network is dependent on the grid for satisfying the energy demand resulting into higher values of ERED and embodied emission of energy. The plan indicated by point B is an extreme point on the Pareto Frontier which lies between points A and C. Since the plan at point B is at the knee region of the Pareto Front, it demonstrates moderate performance with the consideration of all the objective functions. It can be noted that the embodied emissions of energy in the renewable based HES is lower than the plans at points A and C. This is due to the particular combination of energy generation and storage technologies. The plan pointed by D is a Knee Set solution and is not located on the Pareto Frontier. Set. Though the plan at D is strictly dominated by some plans of the Pareto Frontier, the value of the objective functions are within close proximity of associated plans. Hence, the designers have option to apply some selection criteria through the significance dominance parameters to avoid the extreme solutions and extending the solution space without strong deterioration of the associated objective function values. It is to be noted that the embodied emissions of the energy generated by renewable based HES is significantly reduced with compared to NSW grid energy average emission factor of 0.9034 kg CO_2 eqv./kWh [13].

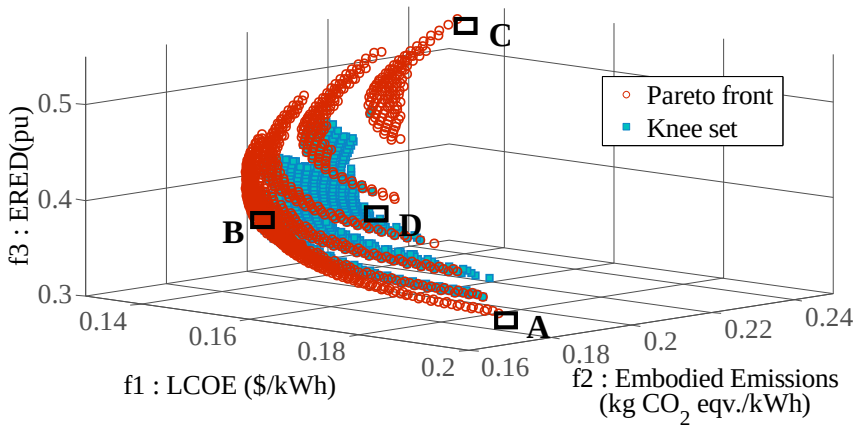

Fig 4.3. Pareto Frontier and Knee Set of the HES DG system design problem.

Table 4.1. Results of the extreme points from solution space.

Plans	Decision Variables				Objective Functions		
	Solar PV	600 kW Wind Turbine	100 kW Wind Turbine	BESS	LCOE	Embodied Emissions	ERED
	kW	kW	kW	kWh	$/kWh	kg CO_2	pu
A	5800	1800	0000	12000	0.1931	0.1766	0.322
B	2600	2400	2000	6000	0.1399	0.1958	0.4525
C	1600	3600	300	2000	0.1309	0.2508	0.5308
D	3400	3000	1800	6000	0.1409	0.1916	0.4049

The sensitivity of the plans within the purview of Pareto Front on the BESS technologies is studied using the Nickel-metal hybrid (NiMh) and Sodium-Sulphide (NaS) based BESS. The embodied emissions of NiMh and NaS based BESS is found to be 1.43 and 0.157 times of the embodied emissions associated with lead acid (Pb acid) based BESS, respectively. The cost associated with NiMh and NaS based BESS is 10.4 and 0.737 times of the cost associated with Pb acid based BESS, respectively. The Pareto Fronts obtained for the NiMh, Pb acid and NaS based BESS in the renewable based HES design problem are plotted in Fig. 4.4. It is observed that the knee region in Pareto Frontier solution set of renewable based HES with cheaper and lower embodied emissions containing NaS is closer to the axes origin. This indicates that the HES with NaS based BESS can provide energy with lower cost, lower GHG emissions and minimal dependency on the grid. Comparing the Pareto Frontier of the HES with Pb acid and NiMh based BESS, it can be observed that the least cost plan of the two cases coincides and do not contain any BESS. On the other hand, the HES with NaS based

BESS has the least cost plan which contains 2000 kWh of storage and the LCOE, embodied emissions and ERED of this plan are recorded as $0.1456 per kWh, 0.2045 kg CO_2 eqv./kWh and 0.4991, respectively. Hence, the BESS with lower cost and less embodied emission in the renewable based HES design can offer energy generation with lower LCOE, embodied emission and risk of energy import from the grid.

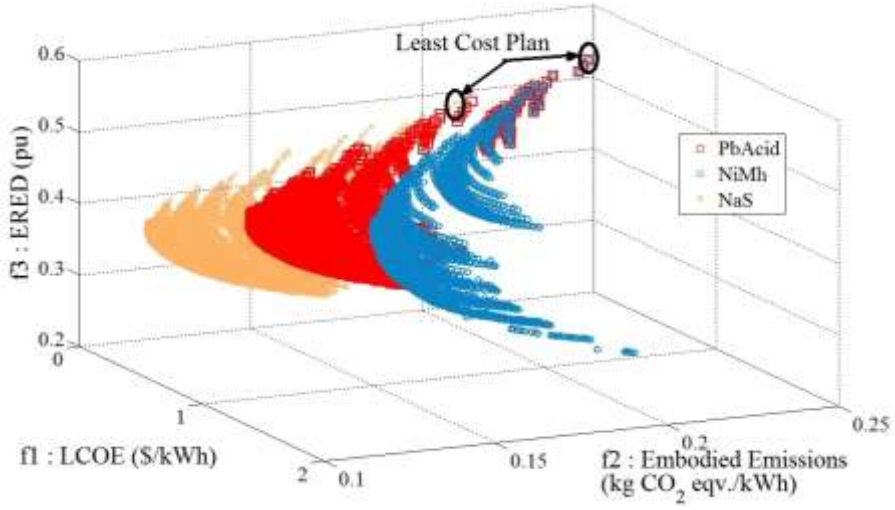

Fig 4.4. Pareto Frontier of the HES system with Pb acid, NiMh and NaS based BESS.

4.6 Conclusion

Renewable based hybrid energy system (HES) is a promising option for reducing emissions from electricity generation and utilising distributed renewable resources in a best possible manner. The generation planning for cost effective, environmental friendly and reliable renewable based HES in the distribution network is a challenging task for network planners. This chapter develops a planning technique using multi-objective optimisation formulation for sustainable HES design in the distribution network. Solar photovoltaic, wind turbine and battery energy storage systems are considered as the energy generation and storage technologies for the HES. A multi-objective optimisation problem is formulated for designing renewable based HES in the distribution network by ensuring minimisation of levelised cost of energy (LCOE) and embodied emissions of energy, and maximisation of reliability of energy generation from the HES. Mathematical models of the objective functions are presented. Life cycle assessment technique is used to estimate the embodied emissions of energy consumed in the

distribution network and global warming potential index is used to quantify the impact on air pollution from different Greenhouse Gas (GHG) emissions. The uncertainty in the availability of the generation output from the HES is modelled in terms of the expected renewable energy deficiency (ERED) and method of moments is used to estimate ERED in the distribution network with HES. Consequently, trade-off analysis technique is applied to solve the multi-objective optimisation problem, involving conflicting objectives, for sustainable HES design. The application of the developed technique is presented with the aid of a practical distribution network from the State of New South Wales, Australia. The sensitivity of the battery energy storage technologies on the optimal solution set is studied and reported. The results indicate that the renewable based HES has the potential to reduce GHG emissions from electric energy generation with competitive energy price and generation reliability.

References

[1] M. Muselli, G. Notton, A. Louche, "Design of hybrid-photovoltaic power generator with optimization of energy management," *Solar Energy*, vol. 65, no. 3, pp. 143-157, 1999.

[2] W. Zhou, C. Lou, Z. Li, L. Lu, H. Yang, "Current status of research on optimum sizing of stand-alone hybrid solar-wind power generation systems," *Applied Energy*, vol. 87, no. 2, pp. 380-389, 2010.

[3] G. B. Shrestha, L. Goel, "A study on optimal sizing of stand-alone photovoltaic stations," *IEEE Transaction on Energy Conversion*, vol. 13, no. 4, PP. 373-379, 1998.

[4] R. Dufo-Lopez, J. L. Bernal-Agustin, "Multi-objective design of PV-wind-diesel-hydrogen-battery systems," *Renewable Energy*, vol. 32, no. 15, pp. 2559-2572, 2008.

[5] R. Dufo-Lopez, J. L. Bernal-Agustin, J. M. Yusta-Loyo, J. A. Dominguez-Navarro, I. J. Ramirez-Rosado, J. Lujano, I. Asoo, "Multi-objective optimization minimizing cost and life cycle emissions of stand-alone PV-wind-diesel systems with batteries storage," *Applied Energy*, vol. 88, no. 11, pp. 4033-4041, 2011.

[6] A. T. D. Perera, R. A. Attalage, K. K. C. K. Perera, V. P. C. Dassanayake, "Designing standalone hybrid energy systems minimizing initial investment, life cycle cos and pollutant emission," *Energy*, vol. 54, pp. 220-230, 2013.

[7] H. Yang, Z. Wei, L. Chengzhi, "Optimal design and techno-economic analysis of a hybrid solar–wind power generation system," *Applied Energy*, Volume 86, Issue 2, Pages 163-169, February 2009.

[8] S. Diaf, G. Notton, M. Belhamel, M. Haddadi, A. Louche, "Design and techno-economical optimization for hybrid PV/wind system under various meteorological conditions," *Applied Energy*, Volume 85, Issue 10, Pages 968-987, October 2008.

[9] D. Abbes, A. Martinez, G. Champenois, "Life cycle cost, embodied energy and loss of power supplyprobability for the optimal design of hybrid power systems," *Mathematics and Computers in Simulation*, Article in Press, Available online 1 June 2013.

[10] PwC, "Moving towards 100% renewable electricity in Europe and North Africa by 2050," Technical report, 2011.

[11] Australian Energy Market Operators, "100 per cent renewables study – modelling outcomes," Technical report, 2013.

[12] M. A. Abdullah, A. P. Agalgaonkar, K. M. Muttaqi, "Climate Change Adaptation with Integration of Renewable Energy Resources in the Electricity Grid of New South Wales, Australia," *Renewable Energy*, Article in Press for publication in 2014.

[13] Australian Energy Market Operators (AEMO), "Carbon Dioxide Equivalent Intensity Index, Notice July 2012". Technical Report. Online. Available: http://aemo.com.au/Electricity/Settlements/Carbon-Dioxide-Equivalent-Intensity-Index

[14] M. A. Abdullah, A. P. Agalgaonkar, K. M. Muttaqi, "Probabilistic load flow for distribution network incorporating correlation between time-varying demand and uncertain renewable generation," *Renewable Energy*, vol. 55, pp. 532-543, 2013.

[15] K. Ord. Stuart, *Kendall's Advanced Theory of Statistics*, Volume 1, Distribution Theory, 6th Edition, Wiley, NY, 1994.

[16] Australian Solar Energy Information System (ASEIS), Online. Available : http://www.ga.gov.au/solarmapping/?accept_agreement=on

[17] Bureau of Meteorology Australia. Online. Available : http://www.bom.gov.au/

[18] L. Wang, T. H. Yeh, W. J. Lee, Z. Chen, "Benefit Evaluation of Wind Turbine Generators in Wind Farms Using Capacity-Factor Analysis and Economic-Cost Methods", *IEEE Transactions on Power Systems*, vol. 24, no. 2, pp. 692-704, May 2009.

Chapter 5

Climate Change Adaptation in the Electricity Infrastructure

ABSTRACT

The implementation of climate change mitigation strategies may significantly affect the current practices for electricity network operation. Increasing penetration of renewable energy generation technologies into electricity networks is one of the key mitigation strategies to achieve greenhouse gas emission reduction targets. Additional climate change mitigation strategies can also contribute to emission reduction thereby supplementing the renewable energy generation participation, which may be limited due to technical constraints of the network. In this chapter, the penetration requirements for different renewable energy generation resources are assessed while concurrently examining other mitigation strategies to reduce overall emissions from electricity networks and meet requisite targets. The impacts of climate change mitigation strategies on the demand and generation mix are considered for facilitating the penetration of renewable generation. New climate change mitigation indices namely change in average demand, change in peak demand, generation flexibility and generation mix have been proposed to measure the level of emission reduction by incorporating different mitigation strategies. The marginal emissions associated with the individual generation technologies in the state of New South Wales (NSW) are modelled and the total emissions associated with the electricity grid of NSW are evaluated.

5.1 Introduction

Fossil fuel based conventional power plants produce a large amount of greenhouse gas (GHG) emissions. To mitigate climate change disorder in electricity generation, deployment of mitigation technologies for reduction of GHG emissions is essential [1-4]. Climate change mitigation techniques such as use of renewable energy resources in power generation including change in fuel mix, energy efficient appliances, demand side management strategies, and smart appliances can be applied to reduce emissions from electricity infrastructure [1-2]. Mitigation strategies are required to be developed for introducing such a transition in the well-established power sector. Assessment and quantification of the emission reduction ability for an electricity system with varying penetration of renewable power generation are required to achieve the national and international emission targets [5].

Several economic theories, such as integration of renewable energy resources in the grid, have been reported in the literature to assess the impact of climate change mitigation strategies on the electricity infrastructure. In [3], the author has presented a comparative analysis of the costs associated with and without implementation of GHG emission reduction policies for the Australian electricity sector. The authors in [4] have presented the simulated results detailing impacts of climate change mitigation technologies on power system. In [4], electricity generation cost, energy price, emission rate and transmission congestion are used as the performance indicators for the different technologies. However, cost may not be a suitable indicator of the mitigation ability of an electricity network, especially in the presence of different government incentive schemes and consumer willingness to pay for enacting climate change mitigation.

A composite GHG emission reduction model has been developed in [6] considering emission savings from renewable energy resources, and transmission and distribution efficiency improvements. The integration of renewable generation systems and adoption of carbon price are considered as the climate change mitigation strategies; and marginal emission is used as the performance indicator. In [7], marginal emission of the conventional generation system is used to compute the emission offset from the installation of wind generation systems. Variation in annual emissions is shown as the mitigation indicator for different installed capacities of wind generation systems. In [8], linear programming model is developed to assess the optimal generation mix for the

electricity network with high penetration of wind power generation. The different options of generation mix are evaluated with the aid of different ramp rates of the associated generation technologies, transmission interconnection flexibility and energy storage flexibility in the network. In [9], the emission rate of coal and gas power plants is modelled and impact of system flexibility constraints on the penetration of intermittent generation systems in the electricity network is assessed. The authors of [10] have assessed the impact of system flexibility factor on the penetration of solar photovoltaic (PV) generation systems. It considers surplus energy, capacity factor and energy cost as the mitigation indices of the system. In [11], the effects of climate change mitigation technologies on the penetration of the solar PV system are investigated. System flexibility, energy storage systems and peak load shaving schemes are considered as the mitigation techniques, and the unit cost of energy is used as an indicator for the mitigating of the electricity system.

The emissions from different generation technologies are modelled in [12] considering the variations in the loading levels of the generating units. Emission factor, which is the average GHG emission associated with the per unit energy generation from the plant, is used to estimate the emission from the generation plant corresponding to the net energy generation [13-15]. In [14], emission factor of the input fuel is used to calculate the CO_2 emission from combined heat and power plants. In [15], emission factor is used to evaluate the emissions of the pollutant gases from the distributed cogeneration power plants. However, the GHG emissions from generation plants depend on the output of the generators and emission factor of the plant cannot incorporate the fluctuations in GHG emissions due to the varying output of the generators [16-17]. The dependency of CO_2 emissions of the coal fired power plant on the efficiency of the plant is considered in [16] in order to estimate the CO_2 emissions. In [17], an empirical function of generated power from the generators is used to estimate the emissions from the thermal power generation plants. A number of unit commitment algorithms can be found in the literature [18-22] to determine economic dispatch of generating units for emission reduction. In the emission constrained unit commitment presented in [18-22], empirical models of emissions have been formulated to estimate the total emission from electricity generation. In [21-24], constant emission factor and nonlinear functions of power output have been used to model the emission from generation plants.

The New South Wales (NSW) state government in Australia has set targets to contain emissions to the 2000 levels by 2025 and reduce emissions by 60% by 2050 [25]. In order to achieve the emission reduction target, mitigation strategies are set for different sectors such as energy generation, agriculture, transportation and industrial production. In order to reduce emission from electricity generation, renewable energy generation targets (RET) are set and additional schemes such as carbon tax, incentives on renewable generation systems, energy storage integration, introducing electric vehicles, use of energy efficient appliances are planned to be introduced [25]. These mitigation schemes have impacts on the NSW electricity network such as change in load demand, generation mix, generation flexibility, etc. Depending upon the changes in NSW electricity network, the emissions from electricity generation would be altered, and required renewable generation penetration to achieve NSW emission reduction target from electricity generation would be different. Hence, it is necessary to assess the impacts of climate change mitigation strategies on NSW electricity network and possible emission reduction from electricity generation systems with the increased penetration of renewable generation systems need to be investigated [26].

In this chapter, the impacts of climate change mitigation strategies are assessed to achieve emission reduction targets with the increasing penetration of renewable energy generation in the electricity network. The mitigation indices based on the impacts of the mitigation strategies on the demand and generation mix are developed. Change in average demand, variation in peak and off-peak demand, generation flexibility and generation mix index are considered to evaluate the impact of climate change mitigation strategies on facilitating the renewable generation growth in the electricity network. The marginal emission of the individual generation plant is modelled using thermodynamic model of the plant. The emission model for the energy supplied in the grid from different generation plants is developed based on the fuel mix of the grid. The penetration levels of different renewable energy resources have been evaluated to achieve the set emission reduction target for NSW electricity grid.

5.2 Impacts of Climate Change Mitigation Strategies on Electricity Networks

The extensive usage of renewable energy resources within technical constraints can be one of the attractive options to reduce GHG emissions in the electricity networks. The penetration level of renewable energy generation and the emission offset from conventional i.e. non-renewable generation systems can be considered as indicators to examine climate change mitigation performance of the electricity infrastructure. It is noted that the relationship between emission reduction and penetration of the renewable energy generation is nonlinear [27]. For higher penetration, the emission reduction per unit installed capacity becomes lower due to the curtailment of excess energy. The penetration of the renewable resources can be expressed in terms of their installed capacity with respect to the peak load demand of the network. The emission offset due to the integration of renewable generation systems can be expressed by the fraction of emission reduced from the base case emission.

The conventional strategies and practices in electricity networks may not be significantly beneficial for achieving the emission curtailment target [1]. The uncertainties associated with the power availability from renewable resources, such as solar PV and wind generation, could be one of the major barriers for accommodating renewable generation systems in the electricity infrastructure. In order to accommodate high penetration of renewable energy resources in the electricity infrastructure, novel climate change mitigation strategies need to be developed. The implementation of energy efficient equipment, electric vehicles, demand side management schemes and fuel efficient generation plants can be considered as some of efficient strategies of climate change mitigation. The mitigation strategies can affect the load demand of the network and the operation of conventional, non-renewable generating resources. The effects of various mitigation strategies on the relationship between emission reduction and penetration level of renewable generation are required to be quantified for assessing the effectiveness of their applicability.

5.2.1 Impacts on electricity demand

Implementation of the energy efficient appliances, electric vehicles and demand side management can influence the average daily load demand in the network [28, 29]. These mitigation strategies can change the daily energy consumption and hence the average daily load demand as shown in Fig. 5.1. The changes in daily load pattern of the network due to 10% increase and 10% decrease in average daily load are shown in Fig. 5.1. The average load demand shift can be expressed using (5.1).

$$\Delta\mu_L = \frac{\mu'_L - \mu_{L,Base}}{\mu_{L,Base}} \tag{5.1}$$

where, $\Delta\mu_L$ is the average demand shift. μ'_L and $\mu_{L,Base}$ are the average daily demand with and without implementation of mitigation strategies, respectively. Negative value of $\Delta\mu_L$ means that the average daily load demand of the network has been reduced. On the other hand, positive value of $\Delta\mu_L$ indicates that the average daily load of the network has been increased. If the daily load pattern of the system remains unchanged and only the average demand is shifted, the estimated shifted demand *L'(h)* at time *h* of the day can be computed using (5.2).

$$L'(h) = L(h) \times (1 + \Delta\mu_L) \tag{5.2}$$

where, *L(h)* is the estimated demand of the system at time *h* of the day for the base case.

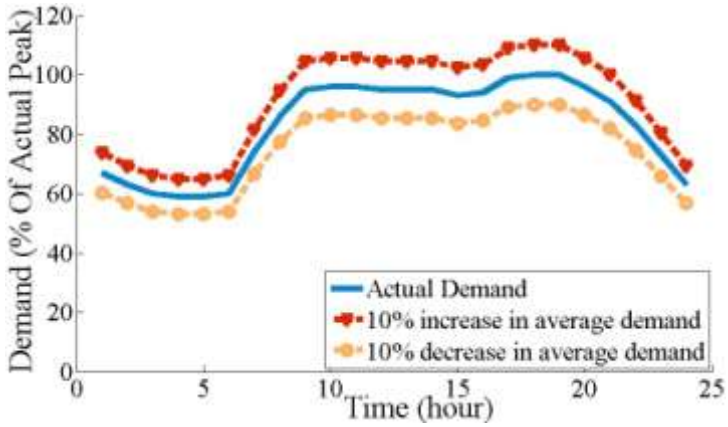

Fig. 5.1. Daily load pattern for 10% change in average demand of NSW network in a typical day of January.

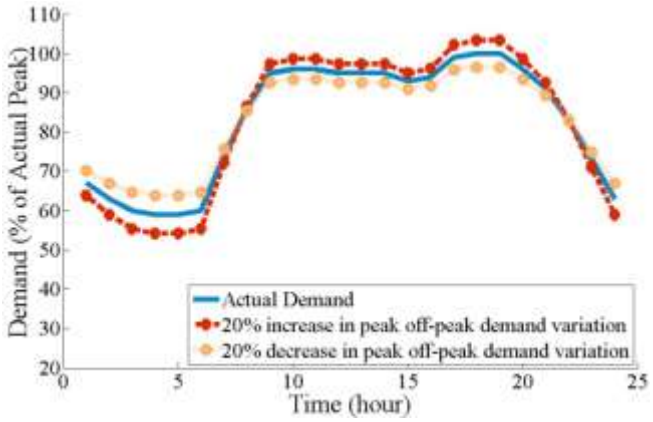

Fig. 5.2. Daily load pattern for 20% change in peak and off-peak demand variation of NSW network in a typical day of January.

Application of the demand side management schemes such as time varying rate, smart appliances, schedulable load and use of energy storage systems can affect the peak and off-peak load demand of the network [11]. Due to the application of such mitigation strategies, the daily average load demand of the system remains unchanged while the load is shifted from peak hours to the off-peak hours changing the shape of the daily load pattern as shown in Fig. 5.2. There may be more than one way to shift the load pattern based on the strategies applied for load shifting. In this chapter, it is assumed that the shifted load demand from the peak hours is evenly distributed among the off-peak hours and the quantity of the shifted load at each hour is proportional to the demand at that hour. The change in the variation of peak demand and off-peak demand of the system can be presented using (5.3)

$$\Delta L_{\text{var}} = \frac{L'_{\max} - L'_{\min}}{L_{\max} - L_{\min}} \tag{5.3}$$

where, ΔL_{var} is the change in the variation between peak demand and off-peak demand. L_{max} and L_{min} are the maximum and minimum load demand of the system in a day without mitigation strategies, respectively. L'_{max} and L'_{min} are the maximum and minimum load demand of the system in a day with the application of mitigation strategies, respectively. The value of ΔL_{var} less than 1 indicates that difference between peak demand and off-peak demand of the system is decreased with the application of demand side management strategies, and vice versa. In addition, negative value of ΔL_{var} indicates that the peak load is shifted from peak demand time to the off-peak demand

time of the day. The estimated demand *L''(h)* at time *h* of the day can be computed using (5.4).

$$L''(h) = (L(h) - \mu_L) \times \Delta L_{\text{var}} + \mu_L \tag{5.4}$$

where, *L(h)* is the estimated demand of the system at time *h* of the day for the base case. μ_L is the daily average load of the system.

5.2.2 Impacts on electricity generation systems

Improved accuracy of the load demand and generation forecasting can reduce the minimum generation level of the conventional, i.e. non-renewable generating resources [10, 11]. This will increase the generation flexibility of the system and aid in accommodating higher penetration of the intermittent renewable energy generation systems. The generation flexibility of the system can be defined as given in (5.5).

$$f_{Flex} = \frac{L_{\max} - G_{\min}}{L_{\max}} \tag{5.5}$$

where, f_{Flex} is the generation flexibility of the conventional, i.e. non-renewable generation system. L_{max} is the maximum demand of the system, and G_{min} is the minimum total generation level that can be reduced by all the conventional generation plants in the system. f_{Flex} can be between 0 to 1. Higher value of the flexibility of the system with conventional resources indicates that the system can accommodate higher penetration of intermittent generation systems by reducing the minimum generation level of the conventional resources.

With the increase in generation flexibility of the system, the minimum generation level of conventional resources decreases. The energy difference between minimum generation level of the conventional resources and the load demand can be supplied by the intermittent generation systems. The contribution of the renewable energy can be increased in meeting the energy demand thereby reducing the minimum generation level for which the conventional resources need to be operated. The minimum generation level of the conventional generating resources can be computed using (5.6).

$$G_{\min} = L_{\max} \times (1 - f_{FLex}) \tag{5.6}$$

Reducing the share of generating stations with higher emission rate and increasing the share of generating stations with lower emission rate in the generation system can reduce the overall emissions from the generation system. Changing the shares of generation mixes will change the operational emission of the grid energy mix. Change in generation mix of the system can be presented in (5.7).

$$f_{Fuel} = \frac{\sum_{i} P_{Fuel,i}}{\sum_{j} P_{Fuel,j}} \tag{5.7}$$

where, f_{Fuel} is the index for the generation mix of the system. $P_{Fuel,i}$ is the normalised share of fuel, that is, changed in the fuel mix of the conventional generating resources. Higher value of f_{Fuel} indicates the increased share of generation plants with fuel group *i* (e.g. natural gas and bio-fuel) and reduced share of generation plants with fuel group *j* (e.g. Coal).

The fuels used in the conventional generating systems can be divided into three groups namely increased share, reduced share and unchanged share. The sum of the normalised share of all the fuel groups is equal to one as given in (5.8).

$$\sum_{i} P_{Fuel,i} + \sum_{j} P_{Fuel,j} + \sum_{k} P_{Fuel,k} = 1 \tag{5.8}$$

where, *i* and *j* are the fuel groups that needs to be shifted and *k* is the fuel group which remains unchanged. Hence, the change in share of one group of fuel can be computed from the information of the share of the other fuel group and generation mix index as given by (5.9) and (5.10), respectively.

$$\sum_{j} P_{Fuel,j} = \frac{1 - \sum_{k} P_{Fuel,k}}{1 + f_{Fuel}} \tag{5.9}$$

$$\sum_{i} P_{Fuel,i} = \frac{f_{Fuel} \times \left(1 - \sum_{k} P_{Fuel,k}\right)}{1 + f_{Fuel}} \tag{5.10}$$

For example, let us assume that fuel group *i* represents natural gas fired power plants and fuel group *j* represents coal fired power plants. The normalised share of the coal and natural gas fired power plants in the total generation capacity is assumed to be 60% and

30%, respectively. Hence, the generation mix index has a value of 0.5. If some of the coal fired power plants are replaced by natural gas fired power plants as a climate change mitigation strategy and the generation mix index is set to 0.6, the normalised share of coal and natural gas fired power plant in the total generation capacity can be found 56.25% and 33.75% using (5.9) and (5.10), respectively.

5.3 Modelling of the Aggregated Marginal Emissions of the Electricity Grid

The assessment of the impact of climate change mitigation strategies on the emission mitigation performances requires the modelling of the emissions from conventional generating resources. The emission rates for the different generating plants are different. In addition, emission rate of the individual plant may also be different depending upon their loading levels. The load demand in an electricity network is time varying and hence, the emissions associated with unit energy generation will also be time dependent.

Emission factor is an average quantity of the marginal emission of the corresponding generation plants and is readily available from the generator manufacturers. In order to model each type of pollutant gas emission as a nonlinear function of output power, the operational data of that pollutant gas emission from the generation plants are required. In this chapter, the marginal emission from different generation plants has been modelled from the thermal properties of the corresponding fuel and generation plant. Also, equivalent global warming potential of each pollutant gas emission has been considered in estimating the total emission reduction from climate change mitigation strategies.

Coal, oil and natural gas are some of the commonly used fossil-fuels for running the conventional power plants worldwide. Beside these fossil fuel based power plants, some renewable energy based power plants have a significant share in the grid mix. Since, hydro, wind and solar PV based power plants release minimal emissions in their operational phase, the operational emissions of these power plants can be considered to be equal to zero. For fossil fuel based power plants, discharge of different gasses from unit energy generation can be expressed using (5.11) and (5.12).

$$ME_{G,i,Cal} = f_{sif,m,fuel} \times \frac{1 - E_{control,G}}{f_{sim,m,G} \times UHV_{fuel}} \tag{5.11}$$

$$ME_{G,i,Elec}(fL_i) = \frac{3.6 \times 10^3 \times ME_{G,i,Cal}}{\eta_i(fL_i)} \tag{5.12}$$

where, fL_i is the ratio of operating load to the rated load of the i^{th} power plant. G is the type of gas discharge and i indicates the power plant type. $ME_{G,i,Cal}$ is the rate of G gas discharge (kg/MJ) from the i^{th} power plant and m is the substances in the polluting gas G contained in the fuel. $f_{sim,m,G}$ and $f_{sif,m,f}$ are the fractional mass content of substance m in the gas G and fractional mass content of substance m in the fuel f, respectively. $E_{control,G}$ is the rate of G gas discharge control in the power plant during the operation cycle and UHV_{fuel} is the higher heating value (MJ/kg) of the fossil fuel used in the power plant. $ME_{G,i,Elec}(f_{L,i})$ is the rate of G gas discharge (kg/MWh) from i^{th} power plant to produce 1 MWh electricity while running at fL_i fraction of rated load. $\eta_i(fL_i)$ is the efficiency of i^{th} power plant while generating power at fL_i of rated condition. CO_x, NO_x, N_2O and SO_x are some of the common emitted gases from the fossil fuel based power plants. The fractional mass content of substance from fuel in some of the common pollutant gases emitted from power plants are given in Table 5.1. Since Oxygen is the common element in the pollutant gases, the fractional mass content of Oxygen can be calculated by subtracting the fractional mass content of the element m in gas X from 1, i.e. $f_{sim,O2,X} = (1 - f_{sim,m,X})$.

Table 5.1. Fractional mass content of element, m in gas G

Gas, G	Element, m	Fraction, $f_{sim,m,G}$
CO_2	Carbon	0.27
CO	Carbon	0.43
SO_2	Sulphur	0.5
N_2O	Nitrogen	0.636
NO	Nitrogen	0.467
NO_2	Nitrogen	0.304

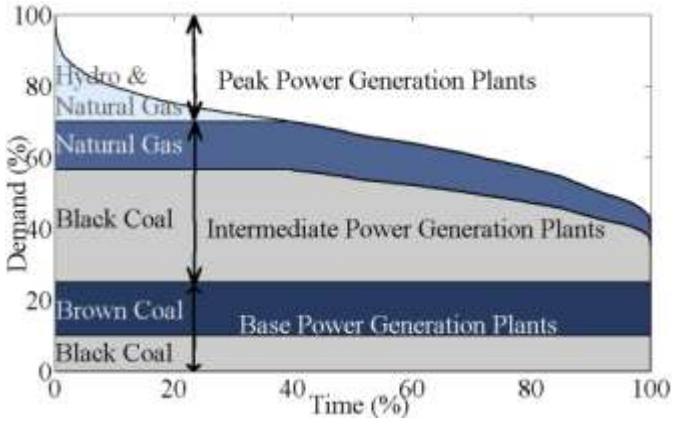

Fig. 5.3. Example load duration curve and fuel mix.

The energy conversion efficiency of generating units and hence power plants varies for various loading levels. The efficiency of the power plant at different loading conditions can be modelled using the rated efficiency and the efficiency de-rating factor as shown in (5.13).

$$\eta_i(fL_i) = \eta_{i,Rated} \times fP_i(fL_i) \tag{5.13}$$

where, $\eta_{i,\,rated}$ is the rated efficiency of the i^{th} power plant. $fP_i(f_{L,i})$ is the efficiency de-rating factor of the i^{th} power plant for operating at $f_{L,i}$ fraction of rated loading condition. Assuming the efficiency de-rating factor of the generating units follows a linear relationship with the fraction of rated load, it can be expressed as shown in (5.14),

$$fP_i(fL_i) = \alpha + \beta \times fL_i \tag{5.14}$$

where, α and β are two coefficients, which depend on the plant type, size, operating temperature, etc. Moreover, energy supplied through the utility system is composed of energy generated by different power plants using different fuels. The generating plants are dispatched economically to generate power at different levels depending upon the net load demand of the electricity network. Some power plants can be classified as base load power stations, some other can be classified as intermediate power plants and others can be classified as peak power plants based on the characteristics of the power plants. Fig. 5.3 shows an example of a load duration curve of a power system composed as the shares of different fuel based generators in meeting the demand of the system. From the information about the type of fuels, number of power plants, plant capacity

and unit operation schedule of the system, rate of discharge of the polluting gases for the base, intermediate and peak demand can be formulated as below.

$$TE_{G,Base} = \left\{ \sum_i ME_{G,i,Elec}(1) \times w_i \right\} \times g_B \tag{5.15}$$

$$TE_{G,Int}(f_D) = \begin{cases} \left[\sum_i ME_{G,i,Elec}\left(\frac{(f_D - g_B) \times w_i}{(g_I - g_B) \times x_i} \right) \times w_i \right] \times (f_D - g_B), & for, g_B \le f_D \le g_I \\ \left[\sum_i ME_{G,i,Elec}(1) \times w_i \right] \times (g_I - g_B), & for, g_I < f_D \end{cases} \tag{5.16}$$

$$TE_{G,Peak}(f_D) = \begin{cases} 0 & for, f_D \le g_I \\ \left[\sum_i ME_{G,i,Elec}\left(\frac{(f_D - g_I) \times w_i}{(g_P - g_I) \times x_i} \right) \times w_i \right] \times (f_D - g_I) & for, g_I < f_D \end{cases} \tag{5.17}$$

where, f_D is the demand level of the grid. $TE_{G,Base}$, $TE_{G,Int}$ and $TE_{G,Peak}$ are the aggregated emission of G gas associated with base, intermediate and peak demand, respectively. $ME_{G,i,Elec}$, w_i and x_i are the rate of G gas discharge, normalised dispatched power and fraction of installed generation capacity supplied by the i^{th} type power plant, respectively. g_B, g_I and g_P are the maximum demand level for base, intermediate and peak demand for generation plant classification, respectively. The derivation of equations (5.15)-(5.17) is presented in Appendix A with example of equation (5.16). The aggregated rate of GHG discharge of the grid mix, $TE_{G,Grid}(f_D)$ can be computed using (5.18).

$$TE_{G,Grid}(f_D) = TE_{G,Base} + TE_{G,Int}(f_D) + TE_{G,Peak}(f_D) \tag{5.18}$$

The discharge rate of the grid mix for different gases during different demand level can be expressed in terms of global warming potential. The marginal CO_2 equivalent emission of the grid mix for the normalised demand level f_D can be computed using (5.19).

$$TE_{Grid}(f_D) = \sum_G \alpha_G \times TE_{G,Grid}(f_D) \tag{5.19}$$

where, α_G is the equivalent global warming potential of G type gas in kg CO_2-eq/kg and $TE_{Grid}(f_D)$ is the total equivalent global warming potential emission of the grid mix in kg CO_2-eq/MWh. The chronological emission of the grid mix can be computed using the unit commitment and the information about the marginal emission rates associated

with each generation plant. Unit commitment has been used as a tool to estimate the output of each power plant during each dispatch interval. From the output level of each power plant during each dispatch interval, the marginal and total emission from that power plant is estimated using the presented emission model for that dispatch interval. Mixed integer linear programming algorithm is used to solve the unit commitment in this study.

5.4 Climate Change Mitigation in NSW Electricity Grid

The proposed emission assessment methodology for various climate change mitigation strategies is assessed for the electricity network in New South Wales (NSW), Australia. The impacts of climate change mitigation strategies on the electricity network in achieving the mitigation target are assessed. Based on the National Transmission Network Development Plan 2011 (NTNDP) prepared by Australian energy market operator [30], the total planning period of 10 years is considered with an overall load growth of 1% every year. Hourly average load demand and generation are used in the proposed study. The existing operational strategy is considered as the base case scenario. The share of existing installed capacity for the generating resources in the state of NSW [30] is shown in Fig. 5.4 using a pie chart. It can be noted that the natural gas to coal fuel ratio in NSW electricity generation system is 0.1667 in the current time. In this analysis, hydroelectric generation system is considered as the conventional generating resource with zero operational emission. It is assumed that the base case generation mix remains the same even with the prospective load growth. The higher heating value, particle contents of the coal and natural gas used in the Australian power plants are given in Table 5.2 [31, 32].

Table 5.2. Thermal property and composition of fuels used in NSW electricity generation plants

Fuel Type	Higher Heating Value (MJ/kg)	Carbon Content (%)	Nitrogen Content (%)	Sulphur Content
Coal	22.9 - 26.27	57.1 – 64.5	1.15 – 1.5	0.34 – 0.55
Natural	51.39	68.5	0	0.025

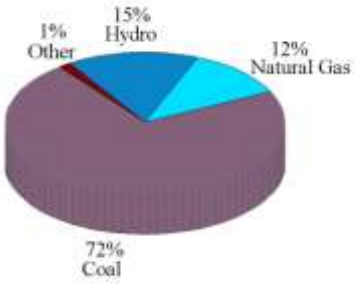

Fig. 5.4. Share of fuels in the grid mix of NSW, Australia.

Solar PV and wind energy conversion system (WECS) are considered as the renewable generation systems in the analysis. Three hypothetical scenarios are considered for maximising the renewable energy generation for climate change mitigation. In scenario 1, WECS is considered as the only available renewable generation technology while in scenario 2, solar PV generating system is the only renewable generation system. In scenario 3, hybrid combination of solar PV and WECS with equal capacities is considered as renewable generation system. In order to operate the network within technical constraints, it is assumed that excessive renewable generation can be curtailed using the curtailment strategy [33]. The impacts of different mitigation strategies on the penetration level of renewable resources are simulated using MATLAB and emission reduction capability corresponding to the penetration level is estimated for the state of NSW, Australia.

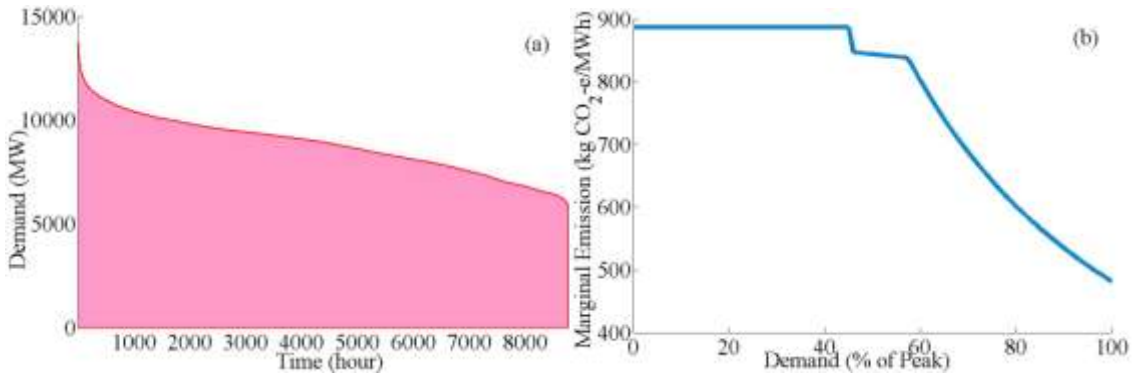

Fig. 5.5. (a) Load duration curve and (b) Marginal emissions of the NSW grid energy.

The load duration curve of NSW electricity network is shown in Fig. 5.5 (a). The marginal emissions associated with the electrical energy disseminated in the NSW grid

are evaluated using the proposed marginal emission computation method and depicted in Fig. 5.5(b). The coal power plants are supplying the base load. The intermediate demand is served by the mix of coal and natural gas power plants and the peak demand is served by the hydro and natural gas power plants. Since the share of the gas turbine power plants increases with the increase in demand and most of the power plants are operated near their rated capacities with maximum efficiencies, the marginal emissions decrease with the increase in intermediate load demand. The GHG emission associated with the peak demand reduced significantly since hydro power plants are operated with zero emission during peak demand periods.

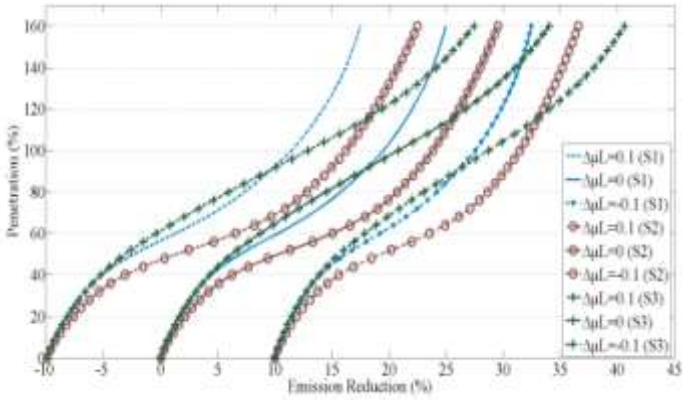

Fig. 5.6. Emission reduction for varying penetration of renewable generation with different average load demands.

5.4.1 Average Demand Shifting

The impact of variation in average demand shift on the emission reduction and renewable generation system penetration for the three scenarios discussed above is shown in Fig. 5.6. Each scenario is simulated with -10%, 0% and 10% increase in the average load of the NSW network. It is found that higher emission reduction is achievable with lower penetration of the renewable energy generation by reducing the average demand of the network. Moreover, it is noted that the marginal emission reduction with the inclusion of renewable generation is lowered for higher penetration levels of the renewable resources. This is due to the high spilling rate of the energy generated from renewable resources. Since, the minimum generation level of the conventional generation plants is fixed, high penetration of the renewable resources

causes the total generation greater than the demand during certain hours. Excess generation is subsequently curtailed to minimise the demand and generation mismatch.

5.4.2 Variation of Peak and Off-Peak Demand

The above mentioned scenarios are simulated for the peak and off-peak demand variation in the base case demand data, and also with 5% and 10% reduction in the variation between daily peak and off-peak demand. The emission reduction and penetration levels of the renewable resources in the electricity network for different values of peak load shifting index are presented in Fig. 5.7. It is seen that reducing the variation between the peak and off-peak load, higher emission reduction can be achieved with lower penetration of the renewable resources. It is remarkable that near the penetration level of 50%, for scenario 1 (S1) and scenario 2 (S2), the change in the peak load shift index is not very effective for overall emission reduction. Similar effect has been found for penetration level near 40% in the case of scenario 3 (S3). This is because the spilling of the renewable energy starts after the penetration level of 40%.

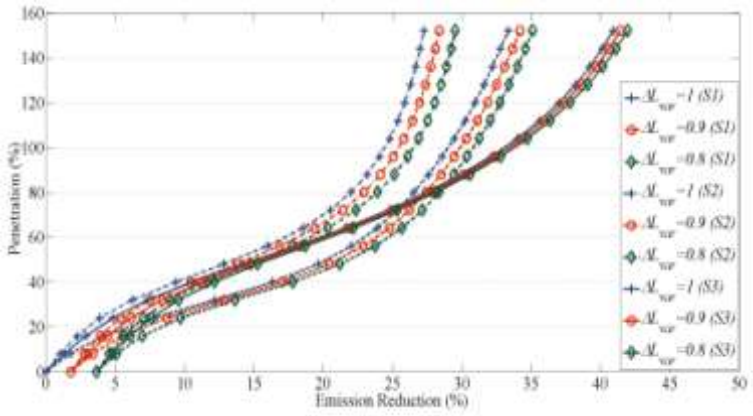

Fig. 5.7. Emission reduction for varying penetration of renewable generation with different peak and off-peak load demand variations.

5.4.3 Changing Generation Flexibility

By increasing the generation flexibility of the system, it is possible to accommodate more intermittent generation systems such as renewables. The impact of changing the flexibility factor of the system is simulated for the above-listed three scenarios. Unit commitment is used to estimate the energy curtailment from renewable energy

generation sources due to the ramp rate limitations and minimum up/down time constraints of the conventional generation plants. For each set of generation flexibility index and penetration level of renewable energy generation sources in each scenario, unit commitment program is run to estimate the absorbable renewable generation in each dispatch interval. Emission reduction performance with the different penetration levels of renewable resources for the generation flexibility of 0.75, 0.8 and 0.85 of the conventional generating systems are shown in Fig. 5.8. It is found that the flexibility index of the system contributes to the emission reduction at higher penetration level of the renewable energy. This is because for higher penetration levels with high flexibility of the conventional generation systems, the spilling of the renewable energy is less.

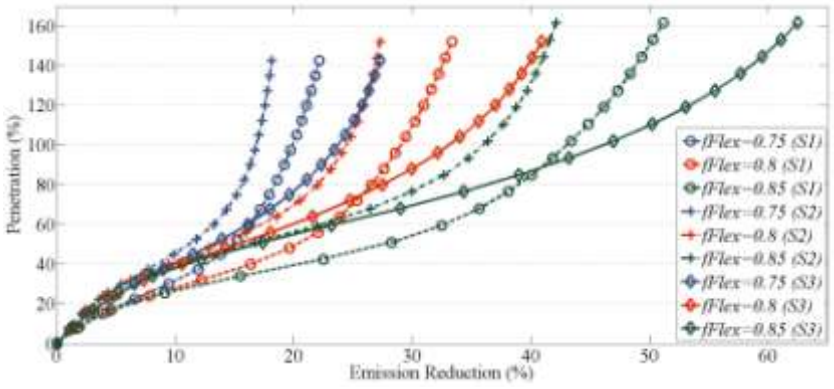

Fig. 5.8. Emission reduction for varying penetration of renewable generation with different generation flexibility.

5.4.4 Changing Generation Mix

Coal is the predominantly used as a primary fuel source in the conventional generation systems of the NSW. Natural gas is at the second position as the fossil fuel used for electricity generation in NSW. Emission rate of the coal fired plants is higher than that of the gas fired power plants. By reducing the capacity of coal based power plants and increasing the capacity of natural gas based power plants, emission reduction can be achieved. For each value of generation mix index and penetration level of renewable energy generation sources in each scenario, the absorbable renewable generation is estimated for each dispatch interval. The marginal emission of the NSW grid for the fuel mix index of 0.1667, 0.2667 and 0.3667 are estimated using the proposed marginal emission evaluation technique.

The impact of the changing fuel mix of the electricity generation system on the emission reduction and renewable resources penetration level is simulated for the above three scenarios and the results are presented in Fig. 5.9. From the results it is found that for all penetration levels of the renewable resources, the emission reduction performance is found to be similar.

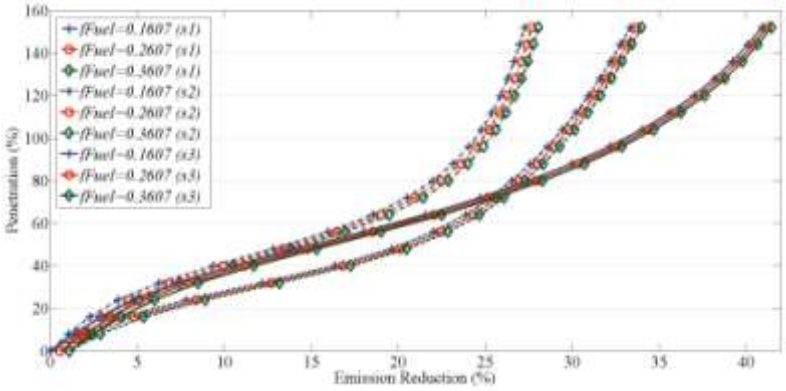

Fig. 5.9. Emission reduction for varying penetration of renewable generation with different generation mix index.

Thus far, in the above analyses, unit commitment is used to estimate the output of each power plant during each dispatch interval and the emission costs are not taken into account in the formulation. In order to investigate the sensitivity of renewable generation penetration requirement on emission costs to achieve different emission reduction level, a unit commitment program has been implemented with the due consideration of emission costs. In the unit commitment accounting emission costs, the equivalent CO_2 emission price is considered as $23/tonne which is the carbon price for year 2011-2012 in Australia [34]. The marginal emissions are estimated using the proposed method for every iterative step of the unit commitment problem and included in the objective function as the cost of emission.

The impact of the average demand shifting on the renewable generation penetration requirement to achieve different emission reduction level is estimated assuming $23/tonne carbon price throughout the planning horizon and the results are shown in Fig. 5.10. Comparing the results with and without considering carbon price in unit commitment formulation (Figs. 5.10 and 5.6 respectively), it is observed that the trends of variation of renewable generation penetration requirement for emission reduction

target level for different scenario are similar. For example, to achieve 20% emission reduction from electricity generation system of NSW using hybrid combination of solar PV and WECS with equal capacities, 120%, 95% and 70% renewable penetrations are required for the 10%, 0% and -10% average demand shifting when carbon price is not considered in the unit commitment, respectively. With the consideration of carbon price in the unit commitment formulation, the renewable penetration drops down to 100%, 75% and 50% for achieving the same average demand shiftings. Hence, the impacts of demand shifting, generation flexibility and fuel mix on the renewable generation penetration requirement to achieve emission reduction are estimated which can reflect the climate change mitigation strategies in electricity system under 'Carbon Pricing Mechanism'.

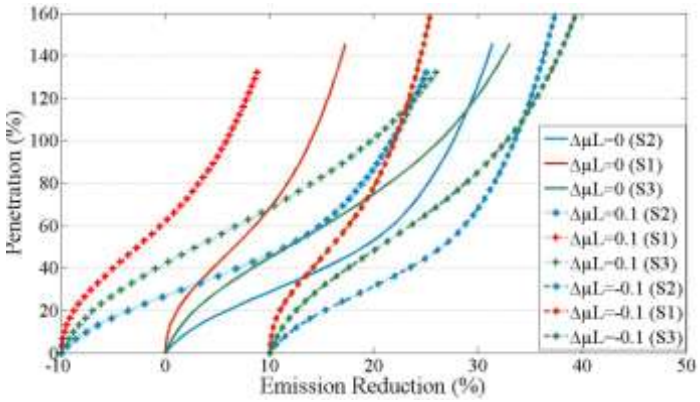

Fig. 5.10. Emission reduction for varying penetration of renewable generation with different average load demands (estimated accounting carbon price).

Based on the performance analysis with the applicability of all climate change mitigation indices proposed, it is found that only increasing the conventional, i.e. non-renewable generation system flexibility up to 0.85 in scenario 3 (S3) can achieve the 60% emission reduction target with a renewable generation penetration level of 160%. It is noted that the emission reduction target of 60% by year 2050, set by the NSW state government, can be achieved through the combinatorial solution incorporating climate change mitigation strategies along with the integration of renewable power generation. In order to achieve the emission reduction target, impacts of the climate change mitigation technologies on the electricity network should be assessed and deployment of the prospective strategies should be selected accordingly. It is found that the scenario 3, where hybrid combination of solar PV and WECS are used as the renewable generation

systems, has the highest emission reduction capability with high penetration levels of these resources. The assessment of optimal renewable generation mix can be one of the possible future trends to achieve the emission reduction targets.

5.5 Conclusion

The impacts of climate change mitigation strategies on the emission reduction in electricity networks embedded with renewable energy generation resources are assessed in this chapter. A mathematical formulation has been developed for examining the effects of different mitigation strategies on the demand and generation in the electricity networks and new mitigation indices are proposed. The overall emission associated with the energy in the grid mix is modelled to account for the time varying load demand in the electricity networks. The proposed model developed based on marginal emissions can be used to assess the performance of the individual generating resources. Penetration levels of advanced renewable generation systems in the state of NSW are assessed for different mitigation indices resulting from the climate change mitigation strategies. The proposed mitigation indices can be used as a measure to select the appropriate climate change mitigation strategies with optimal penetration of renewable generation mix to achieve the emission reduction target. The proposed model has been applied to the electricity network of the state of NSW and results are reported. The results have revealed that with the aid of the proposed climate change mitigation strategies, the overall emission reduction with the integration of different renewable energy generation systems can be maximised. The future research activities are aimed at modelling the impact of individual climate change mitigation technologies on the electricity network and selection of the optimal generation mix for the state of NSW.

Appendix : Derivation of Total Emissions from Intermediate Demand Power Plants

Let's assume that the installed capacity of i^{th} type intermediate demand supplying power plant be C_i and dispatched power of the power plant be g_i during the system demand level f_D. Hence the expression for x_i and w_i can be represented by (5.A1) and (5.A2), respectively.

$$x_i = \frac{C_i}{g_I - g_B} \tag{5.A1}$$

$$w_i = \frac{g_i}{f_D - g_B} \tag{5.A2}$$

The sum of w_i for all the generation plant of same demand type (intermediate demand generation plants) will be equal to one. Now the ratio of operating load to the rated load of the i^{th} generation plant used to estimate marginal emission from the generation plant in equation (5.12) of the paper can be estimated from equation (5.A3) as follows.

$$\frac{g_i}{C_i} = \frac{w_i \times (f_D - g_B)}{x_i \times (g_I - g_B)} \tag{5.A3}$$

Now for the demand level of f_D, the marginal emission due to different generation plant dispatched can be estimated from weighted average of the marginal emission from each generation plant. The weighting factor is the ration of dispatched generation power to the total generations from intermediate demand generation plants which is the normalised generated power as shown in equation (5.A2). Hence the marginal emission from intermediate demand generation plant due to a demand level f_D can be estimated using (5.A4) as shown below.

$$ME_{G,Int}(f_D) = \sum_i ME_{G,i,Elec}\left(\frac{w_i \times (f_D - g_B)}{x_i \times (g_I - g_B)}\right) \times w_i \tag{5.A4}$$

Hence the total emission from intermediate generation plant due to load level of f_D can be estimated using the following equation.

$$TE_{G,Int}(f_D) = \left[\sum_i ME_{G,i,Elec} \left(\frac{w_i \times (f_D - g_B)}{x_i \times (g_I - g_B)} \right) \times w_i \right] \times (f_D - g_B) \quad (5.A5)$$

From equation (5.A1), it is apparent that fraction of installed generation capacity supplied by the i^{th} type power plant, x_i is independent of generation plant dispatch level and demand level of the grid. However, normalised dispatched power i^{th} type power plant, w_i is the generation plant dependent and estimated from the unit commitment problem for system demand level f_D.

References

[1] E. K. Hart, M. Z. Jacobson, "A Monte Carlo approach to generator portfolio planning and carbon emissions assessments of systems with large penetrations of variable renewables", *Renewable Energy*, vol. 36, pp. 2278-2286, 2011.

[2] L. M. Beard, J. B.Cardell, I. Dobson, F. Galvan, D. Hawkins, W. Jewell, M. Kezunovic, T. J. Overbye, P. K. Sen, D. J. Tylavsky, "Key Technical Challenges for the Electric Power Industry and Climate Change", *IEEE Transaction on Energy Conversion*, vol. 25, no. 2, pp. 465-473, 2010.

[3] D. Chattopadhyay, "Modeling Greenhouse Gas Reduction from the Australian Electricity Sector", *IEEE Transaction on Power Systems*, vol. 25, no. 2, pp. 729-740, 2010.

[4] T. B. Nguyen, N. Lu, C. Jin, "Modeling impacts of climate change mitigation technologies on power grids", *Proc. of IEEE Power and Energy Society General Meeting*, MI USA, July 2011.

[5] G. Tsilingiridis, C. Sidiropoulos, A. Penaliotis, "Reduction of air pollutant emissions using renewable energy sources for power generation in Cyprus", *Renewable Energy*, vol. 36, pp. 3292-3296, 2011.

[6] D. Rosso, C. Clark, "Methods and tools to estimate carbon emission savings from integration of renewable and T&D efficiency improvement", *Proc. of IEEE Power and Energy Society General Meeting*, MI USA, July 2011.

[7] E. Denny, M. O'Malley, "Wind generation, power system operation, and emissions reduction", *IEEE Transaction on Power Systems*, vol. 21, no. 1, pp. 341-347, 2006.

[8] C. D. Jonghe, E. Delarue, R. Belmans, W. D'haeseleer, "Determining optimal electricity technology mix with high level of wind power penetration", *Applied Energy*, vol. 88, pp. 2231-2238, 2011.

[9] S. Lu, Y. V. Makarov, Y. Zhu, N. Lu, N. P. Kumar, B. B. Chakrabarti, "Unit commitment considering generation flexibility and environmental constraints", *Proc. of IEEE Power and Energy Society General Meeting*, July 2010.

[10] P. Denholm, R. M. Margolis, "Evaluating the limits of solar photovoltaics (PV) in traditional electric power systems", *Energy Policy*, vol. 35, no. 5, pp. 2852-2861, 2007.

[11] P. Denholm, R. M. Margolis, "Evaluating the limits of solar photovoltaics (PV) in electric power systems utilizing energy storage and other enabling technologies", *Energy Policy*, vol. 35, no. 7, pp. 4424-4433, 2007.

[12] C. L. Weber, P. Jaramillo, J. Marriott, C. Samaras, "Uncertainty and variability in accounting for grid electricity in life cycle assessment", *Proc. of IEEE International Symposium on Sustainable System and Technology*, 2009.

[13] Z. A. Muis, H. Hashim, Z. A. Manan, F. M. Taha, P. L. Douglas, "Optimal planning of renewable energy-integrared electricity generation schemes with CO_2 reduction target", *Renewable Energy*, vol. 35, no. 11, pp. 2562-2570, 2010.

[14] M. Bianchi, A. D. Pascale, "Emission calculation methodologies for CHP plants", *Energy procedia*, vol. 14, pp. 1323-1330, 2012.

[15] P. Mancarella, G. Chicco, "Global and local emission impact assessment of distributed cogeneration systems with partial load models", *Applied Energy*, vol. 86, pp. 2096-2106, 2009.

[16] J. Cristobal, G. Guillen-Gosalbez, L. Jimenez, A. Irabien, "Optimization of global and local pollutant control in electricity production from coal burning", *Applied Energy*, vol. 92, pp. 369-378, 2012.

[17] F. Vallee, C. Versele, J. Lobry, F. Moiny, "Non-sequential Monte Carlo simulation tool to minimize gaseous pollutants emissions in presence of fluctuating wind power", *Renewable Energy*, vol. 50, pp. 317-324, 2013.

[18] T. Gjengedal, "Emission constrained unit-commitment (ECUC)", *IEEE Transaction On Energy Conversion*, vol. 11, no. 1, pp. 132-138, 1996.

[19] N. P. Padhy, "Unit commitment- A bibliographical survey", *IEEE Transactions On Power Systems*, vol. 19, no. 2, pp. 1196-1205, 2004.

[20] J. H. Talaq, F. El-Hawary, M. E. El-Hawary, "A summary of environmental/economic dispatch algorithms", *IEEE Transaction on Power Systems*, vol. 9, no. 3, pp. 1508-1516, 1994.

[21] E. K. Hart, M. Z. Jacobson, "A Monte Carlo approach to generator portfolio planning and carbon emissions assessments of systems with large penetrations of variable renewables", *Renewable Energy*, vol. 36, pp. 2278-2286, 2011.

[22] F. Vallee, C. Versele, J. Lobry, F. Moiny, "Non-sequential Monte Carlo simulation tool in order to minimize gaseous pollutants emissions in presence of fluctuating wind power", *Renewable Energy*, vol. 50, pp. 317-324, 2013.

[23] R. Ramanathan, "Emission constrained economic dispatch", *IEEE Transaction on Power Systems*, vol. 9, no. 4, pp. 1994-2000, 1994.

[24] C. Palanichamy, N. S. Babu, "Analytical solution for combined economic and emissions dispatch", *Electric Power Systems Research*, vol. 78, no. 7, pp. 1129-1137, 2008.

[25] The Office of Environment and Heritage (OEH), "The Carbon Pollution Reduction Scheme: Green Paper - NSW Government Submission 2011". Online. Available: http://www.environment.nsw.gov.au/publications/cprsgp.htm

[26] Bureau of Resources and Energy Economics, "The Australian energy technology assessment (AETA) 2012: Report", Online. Available: http://bree.gov.au/publications/aeta.html

[27] M. A. Abdullah, A. P. Agalgaonkar, K. M. Muttaqi, "Quantification of emission reduction from electricity network with the integration of renewable resources", *Proc. of IEEE Power and Energy Society General Meeting*, MI USA, July 2011.

[28] N. Lu, T. Taylor, W. Jiang, C. Jin, J. Correia, L. R. Leung, P. C. Wong, "Climate Change Impacts on Residential and Commercial Loads in the Western U.S. Grid", *IEEE Transaction on Power Systems*, vol. 25, no. 1, pp. 480-488, 2010.

[29] Z. Darabi, M. Ferdowsi, "Aggregated Impact of Plug-in Hybrid Electric Vehicles on Electricity Demand Profile", *IEEE Transaction on Sustainable* Energy, vol. 2, no. 4, pp. 501-508, 2011.

[30] Australian Energy Market Operator, "National Transmission Network Development Plan 2010", access via internet on May 2011, Available: http://wwww.aemo.com.au/planning/2010ntndp_cd/home.htm.

[31] Australian Government, "National pollutant inventory: Emission estimation technique manual for fossil fuel electric power generation", Version 2.4, 2005.

[32] Environment Australian, "National pollutant inventory: Emission estimation technique manual for Gas supply", 1999.

[33] H. Lund, E. Munster, "Management of surplus electricity production from a fluctuating renewable energy source", *Applied Energy*, vol. 76, no. 11, pp. 65-74, 2003.

[34] Australian Government Clean Energy Regulator, "Carbon Pricing Mechanism", Online. Available : http://www.cleanenergyregulator.gov.au/Carbon-Pricing-Mechanism/Pages/default.aspx

Chapter 6

Sharing Spatially Diverse Wind Generation in Electricity Infrastructure using Trade-off Analysis

ABSTRACT

Wind is one of the fast growing renewable resources that can significantly contribute in achieving emission-free electricity generation system. Since wind resources are distributed across geographical locations, wind resource sharing among different geographical locations is essential to facilitate wind energy penetration and its full utilisation. A wind resource sharing strategy, for interconnected electricity networks, to achieve the national and regional renewable energy target is presented in this chapter. A multi-objective decision making problem has been formulated to optimally share the installed wind generation capacity in a multi-area power systems. Computational models have been developed for wind generation adequacy, emission reduction from wind energy and capacity upgrade requirements for tie-line interconnections. Trade-off analysis has been used to select the best wind resource sharing options. The proposed wind resource sharing strategy has been applied to the interconnected power systems operated within the National Electricity Market (NEM) framework of Southeast Australia to share the available wind resources within the geographical areas of the participating States in the NEM.

6.1 Introduction

The renewable energy targets set by the international energy policies are driving electricity utilities to install large renewable generation plants. Wind is one of the most popular renewable generation options for electricity generation. Emission free energy generation, energy sustainability and reduced dependency on the limited fossil fuels are some of the benefits offered by wind generation systems. However, uncertainties in the availability of wind generation, low capacity factors and large distances between load centres and wind farm locations make the realisation of a significant penetration of wind generation in electricity networks difficult. Wind generation systems are considered as energy resources rather than capacity resources due to their variable and unpredictable characteristics. Unlike traditional capacity resources, intermittent wind energy resources cannot be dispatched to meet the demand of a power system at any particular time. Since traditional generation planning methods focus on reliability and capacity planning, increasing the penetration of energy resources in power systems imposes challenges to balance the overall system demand and the available generation. The capacity credit metric quantifies the contribution of intermittent generation plants in the generation adequacy of interconnected power systems.

The authors in [1] have used frequency domain and time series analysis in order to investigate the wind generation fluctuation mitigation ability of geographically distributed wind farms and reported that the combined available generation outputs from spatially separated wind plants can reduce the variability of the total wind generation output. The time series wind data of U.S. East Coast has been analysed in [2] and the combined output power of the wind farms of different sites shows less fluctuation compared to the power output of individual wind farm at different sites. In [3], an analytical methodology has been presented to select the wind farm locations in the U.S. East Coast to reduce the wind generation fluctuation by interconnecting the wind farms. Hence, the diversity in the wind generation availability from spatially separated wind plants can enhance the generation adequacy advantages offered by individual wind generation plant.

Electric power utilities in many countries are operated as members of a largely interconnected power pool mainly due to the associated benefits, such as the reliability

of supply, offered by the interconnections [4-6]. On the top of the existing transmission and distribution (T&D) network, a new grid namely ‘Supergrid’ which will facilitate the connected utilities to share renewable energy resources has been elaborated in [7-9]. Utilities can take advantages of the diversity in the load and generation mix, shared reserve capacity, differences in unit forced outage rates and maintenance schedules. Deregulated market policies permit the generators in the interconnected systems to participate in the competitive energy market environment allowing the utilities to take advantage of the wind generation diversity in spatially separated wind farms [10]. Jointly owned generation plants among the interconnected systems enable the utilities to share the generation resources of certain geographical locations [11-14]. In this way, abundant wind resources in spatially diverse locations can be shared through joint ownership among the utilities, which are part of an interconnected network, to achieve the renewable energy target (RET).

The objectives for sharing the wind resources among a large interconnected power pool include meeting the targets of renewable energy and greenhouse gas (GHG) emission reduction, and enriching generation adequacy. However, the sharing of the wind resources among the utilities requires the installation of new T&D infrastructures and/or substantial upgrading of the tie-line interconnection capacities. Hence, a strategy needs to be developed for wind resource sharing among the utilities which are part of an interconnected network. With that, a maximum advantage can be achieved with a minimum expansion of the T&D infrastructure. Since multiple objectives are to be achieved from the wind resource sharing strategy, a multi criterion decision making (MCDM) approach needs to be applied. Given that conflicting attributes are involved in the MCDM approach; a trade-off analysis can be applied to devise the wind resource sharing strategy. Trade-off analysis is an effective tool used in the electricity generation planning and energy portfolio design [15-19]. It is applied in this chapter to determine the wind resource sharing strategy among the utilities to select the best options with regards to various attributes such as capacity value, emission reduction capability of wind generation and interconnection expansion.

In this chapter, a wind resource sharing strategy for interconnected power systems is presented to achieve the national and regional renewable energy target. A multi-objective optimisation problem is formulated to share the installed wind generation capacity in each State in NEM and trade-off analysis is used to select the best wind

resource sharing plans. The wind resource sharing strategy is developed based on a mechanism to capitalise on the renewable resources within different geographical areas of the interconnected network. The interconnected power systems operated within the National Electricity Market (NEM) framework of Southeast Australia has been utilised to test the applicability of the proposed wind resource sharing strategy. The result suggests that the States with a high wind potential within the NEM framework can play an important role in achieving the RET of the individual power system through the wind resource sharing strategy. Additionally, it has been found that in order to utilise the available wind resources of all the States in the NEM to achieve the individual RET from wind generation systems, the objective for maximum emission reduction has to be compromised.

6.2 Interconnected Systems and Wind Resource Sharing

Fossil fuel based electricity generation systems are the major contributors for GHG emissions. Due to the recent global concern for GHG emission reduction, a quest for alternative emission free electricity generation systems has become one of the main challenges facing the electric power industries. Energy regulators have set a RET for power utilities to be achieved within a stipulated time frame. Accordingly, the power utilities have been readjusting their long term generation and transmission plans in order to include a considerably higher penetration of renewable generation systems. Hence, substantial changes are required in the conventional reliability and capacity based generation planning strategies.

As indicated earlier, wind generation system is one of the most promising options among all the available renewable generation systems for meeting the RETs. The wind generation power output depends on the availability of wind (and wind speed) in the area where the wind farm is located. Due to the stochastic nature of the wind availability, the wind generation power output is uncertain during generation dispatch intervals. The uncertain wind generation availability during peak demand periods and low capacity factor are the two important reasons for the wind generation system to be a less reliable generation source compared to conventional generation plants. As a result, the wind generation systems are not receiving adequate capacity credit and hence the

penetration of wind generation in the bulk generation system is not increasing significantly.

Moreover, the incremental reliability benefit provided by the wind generation in a power system reduces as the penetration of the wind generation goes higher. This is due to the negative or poor correlation between the peak energy demand and the associated wind generation pattern [20]. Another barrier for the growth of wind generation in power systems is the insufficient wind resources within the geographical area encompassed by the electricity network. The load demand in the electricity network may not be highly correlated with the high wind resource potential in close vicinity [21].

Since diversity exists between the wind farms located at different geographical locations, it may be possible to observe a positive and better correlation between system peak demand and output power of a wind farm at a distant location. The power outputs of wind farms may show statistical independence for short term forecasted data. However, strong seasonal correlations between wind farm power outputs are observed for the cases where distances between the wind farms and load centres are large [1], [20], [22-27]. The wind generation diversity may impact generation system adequacy [18], [20], [21], [24-27]. Hence, the diversity and the correlation between the electricity demand of the network and the power outputs of distantly located wind farms should be considered in generation system planning.

The geographical diversities among wind generation plants can be utilised to enhance the penetration of wind generation systems. The interconnection between utility owned network and supergrid can facilitate the utilisation of the wind generation diversity assisted by the deregulated electricity market environment. Hence, the reliability benefit and the capacity credit contribution from the wind generation systems can be improved through the transmission of electricity generated from the area with potential wind resources to the network with highly correlated demand.

Jointly owned conventional generation plants are shared by the utilities in many interconnected power systems [11-14]. Hence, wind farms can be shared by the interconnected utilities and this strategy can facilitate the utilities to achieve the RET from the wind generation systems. The concept of jointly owned generation plants is to assign the share of the total installed generation capacity to each utility, and each utility

receives available generated power/energy proportional to the respective share [13]. Hence in a wind generation sharing strategy it is essential to assign the installed capacity shares of the wind farms located at different geographical areas within the interconnected power systems to ensure that optimal benefits are incurred by the utilities.

It is the responsibility of the energy regulator to evaluate means of energy generation in meeting the load demand of the utilities. Due to the increasing concern regarding climate change and global warming situations, the energy regulators are setting target for electricity utilities to generate a certain percentage of electric energy by utilising renewable resources to reduce GHG emissions. Further, the energy regulator needs to ensure the service reliability and the cost of service to be within reasonable limits. Energy utilities are responsible to provide energy services to the customers with the least cost and they have to implement the RET and maintain service reliability set by the energy regulator. On the other hand, the customers in the energy market demand for a reliable energy service with the least price and the least environmental aberrations. In such a multiple stakeholder based energy market, the energy market operator is responsible for maintaining the interests of all the stakeholders as shown by the hierarchical diagram in Fig. 6.1. To meet the interests of all the stakeholders, the energy market operators usually conduct feasibility studies as part of the integrated resource planning.

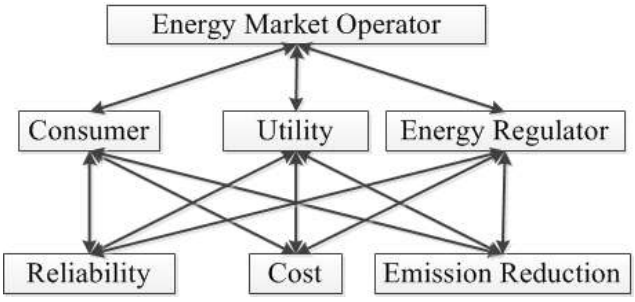

Fig. 6.1. Hierarchical of the stakeholders.

The wind generation sharing strategy should be developed by taking into account the respective RET to be achieved by each utility with the aid of the wind generation, the emission reduction from electric energy generation, the capacity contribution of wind generation in the generation system adequacy and the investment requirement for

infrastructure development and upgrade. Moreover, the allocation of the installed capacity share of wind farms among the utilities depends on the allowable wind farm installation capacity within each geographical area of a power system and the individual RET from wind generation plants. Hence, a simultaneous wind resource sharing plan should be developed for all power systems participating in the wind resource sharing in order to ensure the optimal use of the spatial diversification of wind resources. This chapter aims to address the technical issues associated with the primary stage of generation capacity expansion planning in interconnected large power systems containing spatial diversity of wind power resources, and therefore the objectives are the maximisation of generation adequacy, emission reduction and the minimisation of transmission network expansion to support the growth of wind power penetration. However, operational aspects such as ramp rate control and transmission losses are not considered, as they are usually taken care during design considerations in the next stage of generation expansion planning. In particular, it is assumed that the ramp rate variations due to fluctuations of wind generation can be controlled with the aid of a short term energy storage dispatch and a coordination of flexible generation units as presented in [28-29]. Therefore, the curtailment of wind generation can be avoided with the aid of demand response management. Similar to [30], the chronological simulation of the load and wind generation is used in this study to model spatial and temporal correlation between wind generations and demand of different power systems.

6.3 The Objective Functions of Wind Resource Sharing Strategy

The wind resource sharing strategy is developed with the objectives to gain a maximum capacity value of the wind generation plants, attain a maximum GHG emission reduction from electricity systems and achieve the RET. A higher capacity value and GHG emission reduction can be achieved with the aid of the installation of a large wind farm. However, a large wind farm requires higher interconnection capacities and capital investment [30]. Moreover, there exists a limit for the wind farm installation in each power system due to the operational constraints and limitations associated with land availability. Hence, the wind resource sharing strategy should minimise the installed wind farm capacity per unit generation adequacy increment, the wind

generated energy requirement for per unit GHG emission (MWh/ton CO_2 equivalent emission) reduction and the interconnection capacity upgrade required to support the wind resource sharing. The objective functions of the proposed sharing strategy are detailed in the following subsections.

6.3.1 Installed wind capacity for per unit generation adequacy

The effective load carrying capability (ELCC) of a generation unit is used to measure the contribution of the unit in power system generation adequacy. The ELCC of an additional generator is the maximum amount by which the system demand can be increased after adding the generator without altering the risk level of a system. The ELCC of an additional generation unit can be estimated using (6.1), where, C_t and L_t represent the available generation capacity and the load demand in period t, respectively. G_t is the available capacity during period t for the generator of interest and $Pr\{.\}$ indicates the probability of the quantity within parenthesis. The capacity credit of the wind generation is defined as the ELCC of the wind generation per unit installed capacity as shown in (6.2).

$$\sum_{t=1}^{N} \Pr\{C_t < L_t\} = \sum_{t=1}^{N} \Pr\{C_t + G_t < L_t + ELCC\} \tag{6.1}$$

$$Capacity Credit = \frac{ELCC of\ wind\ generation}{Installed\ wind\ capacity} \tag{6.2}$$

The capacity credit of the wind generation should be higher when there is a correlation between the wind generation output and the system peak demand. It is therefore desirable to allocate most of the installed capacity of a wind farm to a power system when there is a greater correlation between the power output of the wind farm and the peak demand of the system. Besides, a higher capacity credit results from a higher installed capacity of the wind generation systems. Hence, the first objective function (f_1) is to minimise the installed capacity of the wind generation required for per unit ELCC value of the wind generation which is the inverse of the capacity credit of the total wind generation as shown in (6.3).

$$f_1 = \frac{\sum_i \sum_j Wcap_{i,j}}{\sum_i \sum_j ELCC_{i,j}} \tag{6.3}$$

where, $Wcap_{i,j}$ and $ELCC_{i,j}$ are the MW capacity share and ELCC of j^{th} power system in the installed wind farms in i^{th} power system, respectively. The minimisation of (6.3) will maximise the total ELCC from per unit wind installed capacity.

6.3.2 Wind generated energy requirement for per unit emission reduction

Energy generated from the wind farms can reduce the energy generation requirement from fossil fuel based generation plants to balance the system demand. Hence, the GHG emission produced from the conventional fossil fuel based generation systems can be offset by the wind generation. Since conventional generation units are dispatched based on the net system demand level, the GHG emission rate from a conventional generation system depends on the level of system demand. Similar to the system demand, the GHG emission rate is therefore a time varying quantity, and the emission offset by the wind generation depends on the coincidence among different wind generation output levels and emission rates. For a certain capacity factor of the wind generation, the energy production is proportional to the installed capacity. Hence, the share of the installed wind farm capacity is to be allocated to a power system where the correlation between the power output of the wind farm and peak emission rate of the system is greater in order to receive a higher emission offset credit with minimum installed wind generation capacity.

For the reasons stated above, the wind based energy requirement for per unit emission reduction is formulated as the second objective function (f_2) in the proposed method which is presented in (6.4).

$$f_2 = \frac{\sum_j \left(\sum_i Wcap_{i,j} \times CF_i \right)}{\sum_j EmissionOffset_j} \tag{6.4}$$

where, CF_i is the capacity factor of the wind generation in power system i and $EmissionOffset_j$ is the emission reduction by the total wind generation in power system j.

6.3.3 Minimisation of interconnection capacity upgrade

The wind generation imported from different power systems with greater correlation between wind generation and peak demand maximises the capacity credit. Similarly, wind generation imported from different power systems with greater correlation between wind generation and peak emission rate maximises emission reduction potentiality. However, this may require T&D infrastructure upgrades and hence increased capital investment. The wind resource sharing strategy should include the third objective function (f_3) to minimise the normalised total interconnection capacity installation or the upgrade requirements as formulated in (6.5).

$$f_3 = \frac{\sum_l ICreq_l}{\sum_l ICex_l} \tag{6.5}$$

where, $ICreq_l$ and $ICex_l$ are the required and the existing interconnection capacities of the interconnection l, respectively.

6.4 Wind Resource Sharing Algorithm

The objectives of the wind resource sharing strategy are to select the optimum wind resources allocation options among a group of interconnected power systems so that the reliability and environmental benefits from the wind generation systems can be maximised with minimum infrastructure upgrades. The optimal wind resource sharing strategy can be achieved by minimising the objective functions formulated in Section 6.3 and applying multi-objective optimisation as presented in (6.6).

$$\min f = \min([f_1, f_2, f_3]) \tag{6.6}$$

For a higher wind installation capacity throughout the power system, the capacity credit of the wind generation and the emission reduction from the wind generation will be higher; however the interconnecting lines with higher capacities are required. The objective functions related to the capacity value and emission reduction (i.e. f_1 and f_2, respectively) will be minimised for higher wind generation installation capacities, however this will result in a higher value of the interconnection expansion objective

function (i.e. f_3). The GHG emissions per unit electric energy are less when the conventional generation plants are operated near their rated capacity. Since most of the conventional generation plants are operated near rated capacity during the system peak, the emission reduction from per unit energy of wind farms will be less at that time. However, the capacity credit of a wind farm will be higher for injecting energy from wind farms during the system peak. Therefore, injecting energy generated from wind farms during system peak will minimise the capacity value objective function (f_1) resulting in an increase of emission reduction objective function (f_2). As a result, the objective functions of the multi-objective minimisation problem in (6.6) are in conflict with each other. Therefore, a trade-off analysis needs to be applied for decision making in selecting the most suitable wind resource sharing strategy. The formulation of the wind resource sharing strategy using the trade-off analysis is discussed in the following subsections.

6.4.1 Constraints

The constraints to be satisfied for the multi-objective minimisation problem are presented as follows.

$$RET_j \times L_{Avg,j} \le \sum_j Wcap_{i,j} \times CF_i \le RE_{\max} \tag{6.7}$$

$$0 \le Wcap_{i,j} \le Rw_i \times RE_{add,Tot} \div CF_{\min} \tag{6.8}$$

$$\sum_i Rw_i = 1 \tag{6.9}$$

$$RE_{add,Tot} = \sum_j (RET_j \times L_{Avg,j} - Wcap_{Exst,j} \times CF_j) \tag{6.10}$$

where, RET_j and $L_{Avg,j}$ are the renewable energy target to be achieved from the wind generation and the average demand of power system j, respectively. RE_{max} is the maximum limit of renewable energy from the wind resource and is introduced to ensure the convergence of the problem. CF_i is the capacity factor of the wind generation in power system i. Rw_i is the share of the wind generation installed in power system i to achieve the combined renewable energy target of the interconnected power systems. CF_{min} is the minimum value among the capacity factors of all the wind farms. $RE_{add,Tot}$ is the additional wind generation required to achieve the RET with the aid of wind

generation. $Wcap_{Exst,j}$ is the existing wind generation installed capacity in power system j.

The constraint presented in (6.7) imposes upper and lower limit for the wind generation installed capacity to ensure that the renewable energy target from the wind generation for the individual power system is achieved and the objective space is converging. The upper and lower limits for the capacity allocations of the wind resources in a power system are estimated from the constraint given in (6.8). The constraint given in (6.9) maintains the wind resource share balance. The additional renewable energy required from the wind generation to achieve the combined renewable energy target from the wind resources is estimated using (6.10).

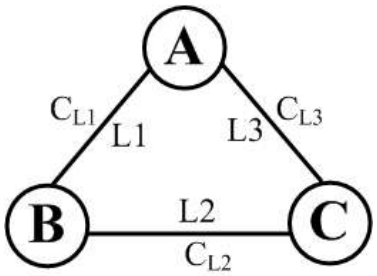

Fig. 6.2. Example 3-area power systems.

6.4.2 Estimation of Interconnection Capacity Upgrade

The interconnection capacity upgrade between different power systems depends on the network configurations, the existing interconnection capacity and the capacity share of each power system in each wind generation system. Fig. 6.2 presents an example of a model of a 3-area power system, which depicts the interconnection of System-A, System-B and System-C through lines L1, L2 and L3 with the power transfer capacity of C_{L1}, C_{L2} and C_{L3} respectively. The wind generation in System-A can be transmitted to System-B through lines L1 and, L3 and L2. The sum of the power transmitted through each path will be equal to the share of System-B in System-A wind generation installed capacity, $Wcap_{A,B}$ as shown in (6.11).

$$P^{A,B}{}_{A-B} + P^{A,B}{}_{A-C-B} = Wcap_{A,B} \tag{6.11}$$

Where, $P^{A,B}{}_{A\text{-}B}$ and $P^{A,B}{}_{A\text{-}C\text{-}B}$ are the maximum power flowing through the line L1 and, lines L3 and L2 to transmit power from system-A to system-B, respectively. It is to be

noted that ‘P’ parameters represent the wind generation capacities, not the temporally varying line flows.

Six capacity shares are possible among the 3 power systems, and hence a total of six power transmission equations can be formed. The power flowing through line L1 ($P^{L1}{}_{A\text{-}B}$ and $P^{L1}{}_{B\text{-}A}$) can be estimated using (6.12) and (6.13) as shown below.

$$P^{L1}{}_{A-B} = P^{A,B}{}_{A-B} + P^{A,C}{}_{A-B-C} + P^{C,B}{}_{C-A-B} \tag{6.12}$$

$$P^{L1}{}_{B-A} = P^{B,A}{}_{B-A} + P^{C,A}{}_{C-B-A} + P^{B,C}{}_{B-A-C} \tag{6.13}$$

Similar to (6.12) and (6.13), four more power flow equations can be formulated for lines L2 and L3 of the 3-area power system shown in Fig. 6.2. The required capacity of the interconnection line between the two power systems to support wind generation sharing is equal to the maximum power transferred through the line. Hence, the required capacity of L1, $C^{req}{}_{L1}$ can be estimated using (6.14) as follows.

$$C^{req}{}_{L1} = \max(P^{L1}{}_{A-B}, P^{L1}{}_{B-A}) \tag{6.14}$$

The interconnection capacity upgrade required to support the wind generation sharing strategy is the difference between the required interconnection capacity and the existing interconnection capacity. The interconnection capacity upgrade depends on the power transmitted through each possible path for the wind generation sharing between the two power systems. Hence, the power transmitted through each path for a minimum total interconnection capacity upgrade can be estimated using a linear programming (LP) based optimisation. The objective function for the 3-area power system in Fig. 6.2 is presented in (6.15) as follows.

$$\text{minimise} : \sum_i C^{req}{}_{Li} - \sum_i C_{Li} \tag{6.15}$$

The objective function of the LP based optimisation problem is subject to the constraints of the six power transmission equations and the three sets of power flow equations through the interconnection lines. For a radial configuration of the power systems, there is only one possible power transmission path between the two power systems. Hence, the difference between the sum of the required interconnection capacities and the sum of the existing interconnection capacities is the minimum

interconnection capacity upgrade required to support the wind generation sharing strategy.

6.4.3 Wind Power Adequacy Modelling

In the traditional multi-area adequacy analysis, the interconnections are modelled as a support from the neighbouring power systems during the generation deficiency in the generation system of the concerned power systems [4-6]. In [11] and [13], the interconnections are modelled to transmit the shared capacity of jointly owned generators among the multi-area power systems and the interconnections are assumed to be adequate for the study. Since the focus of this study is to estimate the capacity credit of the wind generation due to the spatial diversity of the demand and the wind energy generations, the interconnections are modelled as lines connected between the power systems with the wind generation and the load centre of the targeted State owned power system where the wind power is transmitted. Hence the interconnections introduce capacity constraints for the wind generation transfer and additional states in the availability model of the wind generation.

The time series data of the load demand and the wind generation are used to capture the seasonal and diurnal coincidental variations between the load demand and the wind generations in the adequacy estimation process. The inter-ties of each interconnection are modelled using the multi-state availability model of the lines as explained below using the 3-area power system shown in Fig 6.2.

Consider the wind generation transmission from System-A to System-B where there are two paths for wind generation transmission from System-A to System-B. The wind generation transmission from System-A to System-B through interconnection L1 uses only one interconnection line. The available transmission capacity for the wind generation transmission from System-A to System-B through L1 is (PA,BA-B/PL1A-B)×CL1,s when the available transmission capacity of L1 at state s is CL1,s. The probability of (PA,BA-B/PL1A-B)×CL1,s transmission capacity availability for the wind generation transmission from System-A to System-B through L1 is equal to the probability of the available capacity of L1 at state *s*, $Pr\{C_{L1,s}\}$. The available transmission capacity ($C_{L2\text{-}L3,s}$) of wind generation from System-A to System-B through

interconnections L2 and L3, and associate probability Pr{ $C_{L2\text{-}L3,s}$ } can be estimated using (6.16) and (6.17), respectively.

$$C_{L3-L2,s} = \min\left(\frac{P^{A,B}{}_{A-C-B}}{P^{L2}{}_{C-B}} \times C_{L2,s}\,, \frac{P^{A,B}{}_{A-C-B}}{P^{L3}{}_{A-C}} \times C_{L3,s}\right) \tag{6.16}$$

$$\begin{aligned}
&\Pr\{C_{L2-L3,s}\} = \Pr\left\{\frac{P^{A,B}{}_{A-C-B}}{P^{L2}{}_{C-B}} \times C_{L2,s} = C_{L3-L2,s}\right\} \times \\
&\sum_j \Pr\left\{\frac{P^{A,B}{}_{A-C-B}}{P^{L3}{}_{A-C}} \times C_{L3,j} \geq C_{L3-L2,s}\right\} + \\
&\Pr\left\{\frac{P^{A,B}{}_{A-C-B}}{P^{L3}{}_{A-C}} \times C_{L3,s} = C_{L3-L2,s}\right\} \times \\
&\sum_j \Pr\left\{\frac{P^{A,B}{}_{A-C-B}}{P^{L2}{}_{C-B}} \times C_{L2,j} \geq C_{L3-L2,s}\right\}
\end{aligned} \tag{6.17}$$

The available transmission capacity ($C_{L2\text{-}L3,s}$) of the wind generation from System-A to System-B through the interconnections L2 and L3 is the minimum of the available capacity of the interconnection L2 and L3 since the smallest interconnection capacity imposes a transmission constraint. Accordingly, the probability of available transmission capacity ($C_{L2\text{-}L3,s}$) of the wind generation from System-A to System-B through the interconnections L2 and L3 is the sum of the probability of each smallest interconnection capacity as shown in equation (6.17). If the available interconnection L2 has the smallest transmission capacity among the two interconnection L2 and L3 for state *s*, the possible scenario will include all the states of L3 with the available capacity equals to or greater than $C_{L2\text{-}L3,s}$. The total probability of the scenario is represented by the first product term in the right hand side of (6.17). Similarly, the total probability of the scenario when the available interconnection L2 has the smallest transmission capacity among the two interconnection L2 and L3 for state *s*, is represented by the second product term in the right hand side of (6.17).

The total available interconnection capacities, $C_{T,A,B,s}$ and the associated probabilities, $Pr\{C_{T,A,B,s}\}$ of the available interconnection capacities for wind generation transmission from System-A to System-B are then estimated using the convolution of the available capacities and the associated probabilities of each path. The available wind generation capacity $C_{W,A,B,s}(t)$ and the probability $Pr\{C_{W,A,B,s}(t)\}$ of the transferred wind generation from System-A to System-B during t^{th} time instance can be evaluated using the following equations.

$$C_{W,A,B,S}(t) = \min(C_{G,A}(t), C_{T,A,B,S}) \tag{6.18}$$

$$\Pr\{C_{W,A,B,S}(t)\} = \Pr\{C_{T,A,B,S}\} \tag{6.19}$$

where, $C_{G,A}(t)$ is the available wind generation in system A dedicated for system B. The total capacity outage probability table (COPT) of the target power system (System-B) for t^{th} time instance is formed using the convolution between the interconnection capacities at t^{th} instance and the COPT of the conventional generation plants in the target power system. Hence the loss of load expectation (LOLE) of the target power system can be estimated and a decrease in the system LOLE can be observed due to the increase in the generation capacity. The load of the target system is then increased uniformly for the entire time period until the system LOLE becomes equal to the previous LOLE level. The ELCC of the wind generation in the target power system is then estimated as the additional load that returns the system LOLE to the previous LOLE level.

The ELCC of a wind generation in a power system depends on the correlation between the system demand and the available wind generation, and the existing reliability (e.g. LOLE) level of the power system. The wind generation will have a greater ELCC value in a power system with a lower reliability level than a power system with a higher reliability level. Since the objective of this chapter is to allocate the wind generation installed capacity share between the power systems based on the wind generation diversity and the correlation between system demand and the wind generation, the reliability levels of all the interconnected systems should be of the same level. Otherwise the optimisation algorithm will allocate most of the wind generation share to a power system with lower reliability level so that the value of wind generation ELCC becomes higher. The system demands are multiplied by scaling factors in order to maintain a reference reliability level for all the power systems. The scaling factor for each power system is estimated using an iterative process. In each iteration, the system is multiplied by a constant and the system LOLE is estimated. If the system LOLE reaches to the reference LOLE level, the iteration stops. Otherwise the multiplying constant is adjusted to reach the reference LOLE and next iteration is started.

6.4.4 Estimation of Emission Reduction

The emissions from electricity generation systems depend on the emission rate and the dispatched level of each generating unit to balance demand and generation outputs. Fossil fuel based generation units run at their maximum efficiency near the rated power output capacity and generate energy at a minimum emission rate. These fossil fuel based generation units are usually operated at the capacities other than the capacity with maximum efficiency and will produce energy with higher emission rates than those operated at a capacity with maximum efficiency. The generation systems in a power system consist of different generation units which have different emission rates depending on the heat rate, the fuel type and the fuel quality. As mentioned earlier, since the dispatch levels of the generation units depend on the levels of time varying system demand, the emission rates from the generation systems in a power system are also different at different time.

The scheduling of generators is conducted for the entire planning period. From the results, the dispatch levels of each generation unit during different system load conditions are estimated. Hence, the total emissions during each dispatch interval from the power generation systems can be estimated using the dispatched levels, the heat rate of the generation unit, the higher heating value and the component content of the fuel. The total emissions produced by the generation systems over the entire planning period is estimated for the base case which is the case before integrating the wind resource sharing strategy. Energy generated from the wind generation systems is considered as a negative load and the net system demand is estimated by subtracting the total available wind generation from the actual system demand during each dispatch interval. The total emission produced by the generation systems after including the wind resource sharing plan over the entire planning period is estimated from the unit commitment with the net system demand. Therefore, the emission reduction after implementing the wind resource sharing plan is estimated from the difference between the total emission in the base case system and the emission in the system after adopting the wind resource sharing plan.

6.4.5 Option Generation and Application of Trade-off Analysis

The constraint given in (6.8) of the multi-objective optimisation problem imposes limits for the capacity allocations of wind resources in a power system. The wind resource potential at different power systems is not the same. Hence, the share of the wind energy from each power system to achieve the renewable energy target of the interconnected power systems can be assigned based on the potential of the wind resources in that power system. A number of feasible combinations which satisfy the constraint given in (6.9) are determined in the allocation of the share of the wind energy in each power system. Depending on the wind energy share for each power system, the optimum installed wind generation capacity shares among the interconnected power systems can be found. The alternate options for the use in the trade-off analysis are generated by allocating different shares of the wind energy in different power systems.

Trade-off analysis is used in this chapter to solve the multi-objective optimisation problem with conflicting objective functions. The constraints of the decision variables define the feasible solution set in the decision variable space. The combinations of the decision variables from the feasible solution set are known as the plans. Objective space is then mapped for each feasible solution set of decision variables or plans. For each option, an optimisation problem with the interconnection expansion objective function in (6.5) and the constraints presented in (6.7)-(6.9) are solved and each power system's share in the installed wind generation capacity of the other power system is found. Then the other two objective functions given by (6.3) and (6.4) are estimated using the optimum installed wind generation capacity shares for that option. Lastly, trade-off analysis is applied to the feasible objective space to select the set of optimal values of objective functions.

The optimal values of the objective functions are estimated from the feasible objective space by applying the two conditional decision criteria [14, 18]. The first criterion is called the strictly dominance criterion and the application of the strictly dominance criterion results in a set of optimal solutions known as Pareto Frontier. Pareto Frontier is the boundary between the sets of possible and the sets of unachievable solutions in the objective space. Pareto Frontier consists of plans that are not strictly dominated by any other plans in the objective space. For example, a plan P_A strictly

dominates plan P_B if all the objective functions associated with plan P_A demonstrate better performance in comparison with plan P_B.

A second decision set of feasible options called the knee set, can be extracted by applying the 'significantly dominance criterion' on the objective functions of the options. The knee set contains the plans on and near the knee region of the Pareto Frontier. The options in the knee set are not significantly dominated by any other options. The options in the knee set are composed of some or all options in the Pareto Frontier and some options which are not on the Pareto Frontier. The significantly dominant options are determined by applying the "much worse" and "significantly better" indices to all the options. As an example, a plan P_A significantly dominates plan P_B if at least one of the objective functions of plan P_B is much worse than the corresponding objective function of plan P_A and if none of the objective functions of plan P_B are significantly better than objective functions of plan P_A. Hence the selection of higher "much worse" indices value for each objective function relaxes the selection criterion of options in the knee set and options outside from the Pareto Frontier set are included in the knee set. Conversely, the selection of higher "significantly better" indices value for each objective function stretches the selection criterion of options in the knee set and less number of options is included within the knee set. Hence the number of options in the knee set depends on the selection of the "much worse" and "significantly better" indices for each objective function.

Trade-off analysis is proposed for the multi-objective decision making process of the wind generation sharing approach among the interconnected power systems. One of the distinct features of trade-off analysis among other multi-objective decision making processes is the user selectivity option on the objective functions through 'significantly dominance criterion' in filtering the knee set from other alternative options. The "much worse" and "significantly better" indices for individual objective function can be selected by the decision maker and hence relative importance can be assigned to different objective functions using these two indices. At high wind penetration, relaxing and stretching the 'significantly dominance criterion' for objective functions consisting of emission reduction and ELCC, respectively, more relative importance can be assigned to ELCC maximisation objective.

6.4.6 Wind Generation Sharing Algorithm

The wind generation sharing algorithm proposed in the paper is developed based on the following assumptions and limitations:

a) The ramp rate variations of the generation system due to the fluctuations of the wind generation can be controlled with the aid of a short term energy storage dispatch and a coordination of flexible generation units as presented in [28-29].

b) The curtailment of the wind generation can be avoided with the aid of demand response management.

c) The financial aspects of the wind resource sharing approach are not considered in this chapter.

d) The transmission line capacity is considered as a variable of the wind generation sharing strategy. The transmission system capacity is estimated based on the total maximum power to be transmitted through the transmission lines.

e) The thermal loss in the transmission line is not considered in this analysis.

f) The correlation between the wind generations and the load demands of different power systems remains the same in the future.

g) The method developed for the emission reduction analysis is valid only if the system is composed of both conventional fossil fuel based and emission-free generation units.

The steps involved in the proposed algorithm for sharing the wind generation spatial diversification within the interconnected multi-area power systems with the aid of trade-off analysis are summarised as follows.

1. **Option Generation**: The options are generated from the combinations of decision variables within the feasible decision variable space as described in Section 6.4.5. For each combination of feasible decision variables (allocated wind generation capacity for each power system), the interconnection expansion objective function is solved using LP constrained by (6.7)-(6.10). The method for the interconnection expansion capacity requirement for each option is illustrated in Section 6.4.2.

2. **Estimation of Objective Attributes**: The interconnection expansion objective attribute is estimated in the previous step. The capacity value and the emission reduction objective attributes are estimated for each option and the objective space is formed. The estimation method for the capacity value and the emission reduction objective attribute is presented in Section 6.4.3 and 6.4.4, respectively.

3. **Trade-off Analysis**: Trade-off analysis is to be conducted in the objective space of the generated options to determine the Pareto Frontier and the knee set of feasible options. The 'strictly dominance criterion' in the objective space is applied to estimate the Pareto Frontier set of plans. The 'significantly dominance criterion', 'much worse' and 'significantly better' for each objective attribute are selected and the knee set of options is determined as presented in Section 6.4.5.

6.5 A Case Study on Southeast Australian Power Grid

6.5.1 System Description

The National Electricity Market (NEM) operations in Southeast Australia are associated with the interconnected power systems of five states namely Queensland (QLD), New South Wales (NSW), Tasmania (TAS), Victoria (VIC) and South Australia (SA) as shown in Fig 6.3. The power transfer capacities through the interconnections between neighbouring power systems are indicated by the numbers above the directional arrows. The peak demand, the conventional generation capacity and the installed capacity of the wind generation systems in each power system are presented in Table 6.1. The electricity markets are operated independently and the neighbouring power systems actively take part in the electricity market of each other according to the NEM policy. This accessibility of one power system to a nearby electricity market enables the sharing of the inter-state renewable generation.

Hourly demand and wind generation data are used for the case study. The demand and wind generation data are extracted from the National Transmission Network Development Plan 2012 (NTNDP 2012) Database [31]. Forecasted hourly demand and generation output of all existing and planned wind farms for 35 years starting from 2011-2012 can be found in NTNDP 2012 Database. In this analysis forecasted demand

and wind generation data of year 2012-2014 are used for case study to demonstrate the applicability of the proposed wind generation sharing approach. Since data of all hours are available without any dropout, no correction measure is required for this data.

Fig. 6.3. Interconnected power systems in Australian National Electricity Market (NEM).

A RET of 20% of electric energy to be generated from the renewable sources by 2020 has been set by the Australian government and the wind generation system is expected to serve the major share of the RET [32]. The wind resource distribution within the geographical location of NEM power systems is shown in Fig 6.4. Fig. 6.4 shows that SA, VIC and TAS possess most of the high wind potential locations whereas NSW and QLD have only a few high wind potential locations [32]. Hence the states having high wind resources can achieve their RET through wind generation system and the states with less wind resources will face difficulties to meet their RET through their own wind generation. However, it is apparent from Table 6.1 that the energy demands of the states with less wind resources are greater than the energy demands of the states with better wind resources. Moreover, the poor correlation between the energy demand of the power system and the wind generation within the state limits the penetration of the wind generation [20]. Since the wind generation cannot be made available to meet the demand when required, the wind generation systems are considered as energy resources. Hence the RET of the states within Southeast Australian NEM may not be

able to be achieved in the traditional reliability and capacity based generation planning strategies.

Table 6.1. NEM demand and generation data for each State

	SA	TAS	VIC	NSW	QLD
Peak Demand (MVA)	3321	1670	10366	14074	8782
Conventional Generation Capacity (MVA)	3799	3078	10675	18325	13637
Wind Generation Capacity (MVA)	1344.1	140	860	265.8	0

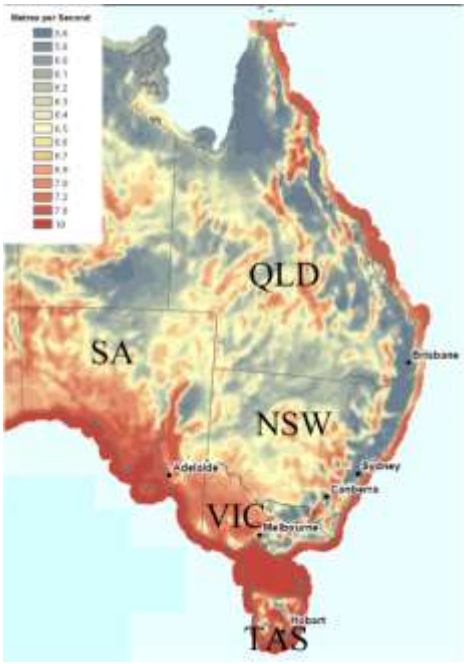

Fig. 6.4. Wind resource distribution in Southeast Australia [32].

There exists diversity between the wind generations at different geographical locations and a higher correlation between the wind generation in one power system and the energy demand of different power systems are observed. The statistical correlation coefficients between the wind generation and the load demands of different power systems are shown in Table 6.2. The correlation coefficient values between the wind generation and the load demand of different power systems are indicators of average relative variation between the wind generation and the load demand. A positive value of correlation coefficient between a pair of wind generation and load demand signifies that on an average the maximum wind generation hours coincide with the system peak

demand hours. Similarly, a negative value of correlation coefficients indicates the lack of coincidence between the peak wind generation and the peak system demand hours. Since the ELCC of the wind farm depends on the coincidence between the peaks of wind generation and the system demand, the wind generation and the system demand pair with greater value of correlation coefficient will have greater ELCC. It can be observed from Table 6.2 that excluding TAS, the wind generation in each power system has a higher correlation with the demand of other power systems.

Table 6.2. Demand and wind generation correlation coefficients between different power systems for data of year 2012-2014

		Wind Generation			
Demand		*SA*	*TAS*	*VIC*	*NSW*
	SA	-0.016	-0.0546	-0.0261	0
	TAS	0.1109	0.0384	0.1508	0.1237
	VIC	0.0222	-0.0463	0.0315	0.0468
	NSW	0.0249	-0.0765	0.0148	0.0429
	QLD	-0.0505	-0.1708	-0.1008	-0.0286

Table 6.3. Correlation coefficients between the demands of different power systems

	SA	TAS	VIC	NSW	QLD
SA	1	0.4797	0.8657	0.7376	0.6082
TAS	0.4797	1	0.6723	0.6905	0.5405
VIC	0.8657	0.6723	1	0.8578	0.711
NSW	0.7376	0.6905	0.8578	1	0.8265
QLD	0.6082	0.5405	0.711	0.8265	1

Table 6.4. Demand and wind generation correlation coefficients between power systems for data of year 2014-2016

		Wind Generation			
Demand		*SA*	*TAS*	*VIC*	*NSW*
	SA	-0.0163	-0.0561	-0.0267	0.0021
	TAS	0.1073	0.0392	0.1461	0.1248
	VIC	0.0226	-0.0459	0.0306	0.0458
	NSW	0.026	-0.0771	0.0145	0.0445
	QLD	-0.0512	-0.1671	-0.0927	-0.0273

In addition, diversity exists between the energy demands of different power systems within NEM operation, as observed from the correlation coefficients between the demands of two power systems presented in Table 6.3. It is found that the energy demand in TAS has the lowest correlation coefficient with the energy demands of all other power systems. Hence the wind generation and the demand diversity along with the support from the interconnections between the power systems and the deregulated electricity market operation can be utilised in the generation planning strategy towards achieving the RET. The correlation coefficient values presented in Table 6.2 and Table 6.3 are estimated using the wind generation and demand data of year 2012-2014 from the National Transmission Network Development Plan 2012 (NTNDP 2012) Database [31]. In order to show that the trend of the correlation between the wind generation and the load demand holds up over time, the correlation coefficient values are estimated using the wind generation and demand data of year 2014-2016 from the same database. The correlation coefficient values estimated from data of year 2014-2016 are presented in Table 6.4 and it is found that the maximum difference between the corresponding correlation coefficients values is approximately 8%. It can also be observed that the relative differences between the correlation coefficients are similar to the relative differences between the correlation coefficients presented in Table 6.2. Hence, the trend in relative differences between the wind generation and the load demand correlation coefficients holds up for these values over time.

6.5.2 Trade-off Analysis

The trade-off analysis described in the previous Section is applied to the NEM network to allocate the share of installed wind generation capacity for achieving the RET of the different States. In this analysis, it is assumed that the wind energy penetration targets of SA, VIC, TAS, NSW and QLD are 40%, 20%, 15%, 20% and 10% of the total electric energy demand of the corresponding States, respectively. The wind energy penetration target for each state in Southeast Australia is chosen based on the Renewable Energy Target Review published by the Climate Change Authority (CCA) of Australian Government [33].

The share of the wind energy from each state to achieve the combined renewable energy target of the interconnected power systems is varied and a number of

combinations of the wind energy share are generated satisfying the constraint given by (6.9). Since SA has the highest wind resource potential, the minimum share of the wind energy from SA is set to be 30%. The shares of the wind energy from the other states are adjusted so that the constraint given in (6.9) is satisfied. For each share of wind energy, the optimum share of each wind farm in the additional installed wind generation capacity of each state is estimated and feasible options are generated. The objective functions (*f*1, *f*2, and *f*3) are estimated for each option. The trade-off plot for normalised objective functions *f*1, *f*2 and *f*3 is presented in Fig. 6.5. It can be observed from Fig. 6.5 that no single option is highly dominant over other options. Hence, a strict and significantly dominance criterion will have to apply on the options to select the better options.

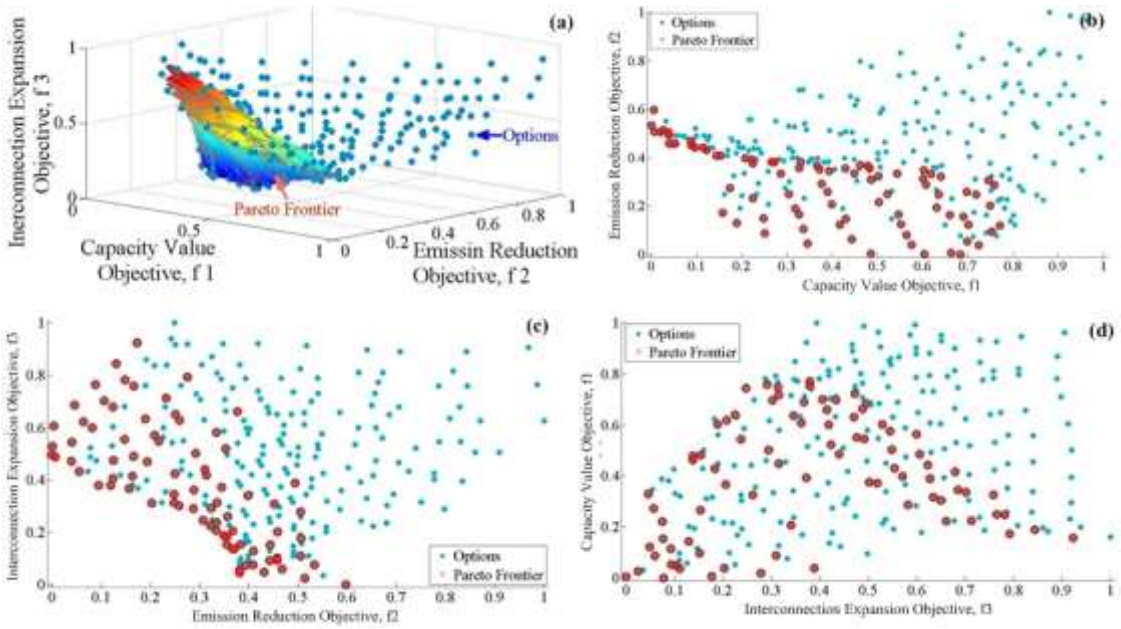

Fig. 6.5. Trade-off plot between normalised attributes: (a) *f1*, *f2* and *f3* objective space, (b) *f1* and *f2* objective space, (c) *f2* and *f3* objective space and (d) *f3* and *f1* objective space.

6.5.3 Results and Discussions

The strict dominance criterion is applied to the options and Pareto Frontier set of options is found. The Pareto Frontier set of options is indicated by the solid surface in Fig 6.5. The Pareto Frontier set provides 88 non-inferior options for wind resource sharing strategy which are not strictly dominated by any other option in the objective space. The smaller knee Set can be extracted by applying the significantly dominance

criterion. The significantly dominant options are determined by applying the “much worse” and “significantly better” indices to all the options. The numbers of options in the knee set for different values of “much worse” and “significantly better” indices are presented in Fig. 6.6. The values of “much worse” (Δmw) and “significantly better” (Δsb) indices for each attribute are presented as a percentage of the difference between the values of the worst and best alternatives of the attribute. It can be observed from Fig. 6.6 that for the greater value of Δsb and the smaller value of Δmw, the number of options in the knee set is less for the case of the wind resource share in the Southeast Australian power grid. The number of options in knee set increases as the value of Δmw is increased or the value of Δsb is decreased. Reduced options from outside of the Pareto Frontier are included in the knee set due to smaller values selection of the Δmw indices and reduced options from the Pareto Frontier are taken into the knee set due to the selection of greater values of the Δsb indices. Hence, the decision maker has a choice to pick the values of Δsb and Δmw for the expected size of the knee set.

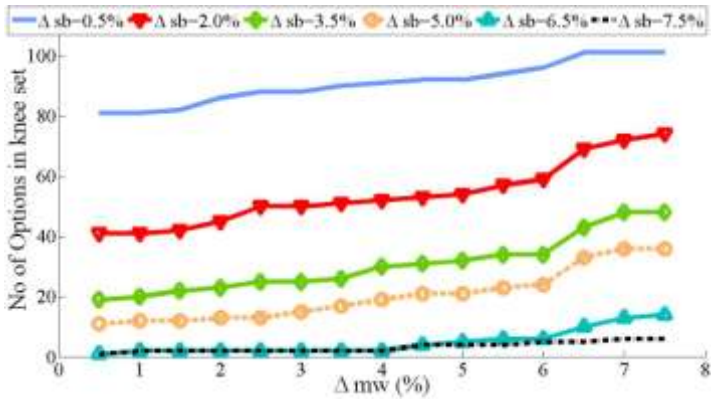

Fig. 6.6. Number of options in knee set for different values of Δsb and Δmw.

The knee set for the Southeast Australian power grid is extracted by applying both significance dominance indices Δsb and Δmw equals to 6.5%, and 10 significantly non-dominated options are found in the knee set. The shares of the additional wind generation installed in each power system as a percentage of the total wind generation installation in the whole interconnected power systems for the options in the knee set are shown in Table 6.5. It is found that the wind resources in all the states are used in the wind resource sharing strategy of option#2 in the knee set of Table 6.5. When the selection criterion for the knee set is stretched further by setting the significance dominance indices Δsb = 7.5% and Δmw = 5.0%, only option#10 in Table 6.5 is found

in the knee set. To illustrate the outcome of the wind resource sharing strategy, the share of each power system in the installed wind generation capacity in each state for option#2 and option#10 in the knee set are shown in Table 6.6 and Table 6.7, respectively. Table 6.6 shows that for option #2 of Table 6.5, the additional wind generation capacities required to be installed in SA, VIC, TAS and NSW to achieve the RET specified by the respective states from the wind resources are 2612 MW, 2177 MW, 435 MW and 3052 MW, respectively. The total interconnection capacity upgrade required to support the wind generation sharing strategy is 3975 MW. An additional 1775 MW capacity of the interconnection between SA and VIC needs to be upgraded to facilitate the transfer of the wind power from the 2375 MW installed wind generation capacity in SA to VIC, TAS, NSW and QLD. Additional 1855 MW and 345 MW capacities of interconnections between VIC and NSW and between NSW and QLD is to be upgraded to facilitate the wind resource sharing strategy, respectively.

Table 6.5. Shares of the wind generation installed in each power system as a percentage of the total wind generation installation for the options in the knee set.

Option #	**SA**	**VIC**	**TAS**	**NSW**
1	30	25	0	45
2	30	25	5	40
3	30	70	0	0
4	35	60	0	5
5	35	65	0	0
6	50	50	0	0
7	55	45	0	0
8	60	40	0	0
9	65	3	5	0
10	65	35	0	0

The distribution of the wind generation capacity share among the power systems follows the correlation between the wind generation output power and the system demand as shown in Table 6.2. For example, it can be observed from Table 6.6 that for NSW power system, the highest wind generation capacity is allocated from its own wind generation systems. This is because the correlation between the wind generation output power in NSW and the demand of NSW is the highest. The wind generation in SA has the second highest correlation with NSW demand as shown in Table 6.2 and

hence the second largest wind generation capacity share for NSW power system is allocated from the wind generation systems in SA. Similar trend is found for the QLD, VIC and SA power systems. However, the wind generation sharing for TAS power system is different from the other power systems in the energy pool. Despite the fact that system demand of TAS has the highest correlation with the wind generation output power in VIC, the power system in TAS and the wind generation systems in VIC is not sharing any wind generation capacity as shown in Table 6.5 for option#2. This is due to the wind generation capacity limit in VIC as shown in Table 6.5. Additionally NSW and QLD require higher wind generation capacity share to achieve their individual RET. For option#10, all the wind generation capacity is installed in SA and VIC as can be found from Table 6.5. The wind generation capacity is allocated for different power system depending on the additional wind generation requirement to achieve the individual RET and minimum tie-line capacity upgrade requirements. The feasibility analysis of option#2 and option#10 can be carried out using the objective function values of the options.

Table 6.6. Installed wind generation capacity distributions among the power systems for option #2 of Table 6.5

Target Systems	**Wind Generation**			
	SA	**VIC**	**TAS**	**NSW**
SA	237	0	0	35
VIC	458	965	0	547
TAS	111	0	0	188
NSW	1217	959	435	1599
QLD	589	253	0	683

Table 6.7. Installed wind generation capacity distributions among the power systems for option #10 of Table 6.5

Target Systems	**Wind Generation**			
	SA	**VIC**	**TAS**	**NSW**
SA	273	0	0	0
VIC	1007	980	0	0
TAS	306	0	0	0
NSW	2438	1730	0	0
QLD	1201	338	0	0

The values of the objective functions for the 10 options in the knee set with Δsb = Δmw = 6.5% are presented in Fig. 6.7. From Fig. 6.7, it can be observed that option#2 in knee set is inferior to that of option#10 with respect to emission reduction objective function, *f*2. However in terms of the capacity value objective function, *f1* and the interconnection capacity objective function, *f3*, option#2 is superior to option#10. The final decision making in choosing a single option from the knee set can be made either based on the relative preference of the decision maker on the objective functions or based on external preferences. For example, if the energy regulator is interested in utilising the available wind resources in all the states to achieve the individual RET, option#2 can be selected as the final option for the wind resource sharing among the Southeast Australian power systems. On the other hand, if the energy regulator is particularly interested in maximising the emission reduction from the utilisation of the wind generation sharing, option#6 can be preferred as the final option due to the minimum value of the emission reduction as given by objective function, *f2*. However, the emission reduction maximisation can be achieved by compromising the maximum capacity support from the wind generation systems and further utilisation of the wind resources in NSW and TAS is not possible in that case.

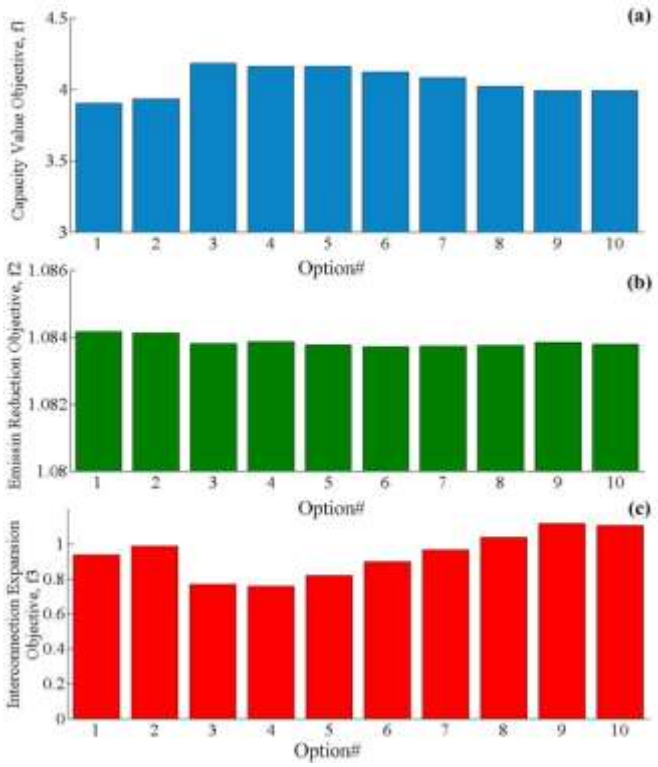

Fig 6.7. Values of objective functions for different options in Knee Set of Table 6.5.

6.6 Conclusion

This chapter presents a sharing strategy of spatial diversification of wind resources among interconnected power systems to achieve the national and international renewable energy target. The proposed wind resource sharing strategy facilitates the power systems with less wind resources to invest on the wind generation plants in power systems with high wind resources, and the dedicated share of the installed wind generation capacity can be realised through a supergrid or transmission interconnections. In this chapter, three different objective functions have been formulated as a part of the multi-objective decision making problem in order to obtain the share of each power system in the installed wind generation capacity. The objectives of the multi-objective decision making problem includes the maximisation of the generation adequacy and the GHG emission reduction with minimum interconnection capacity upgrade. A trade-off analysis has been used to select the best wind resource sharing plans with the consideration of conflicting attributes associated with network upgrades, wind generation adequacy and emission offset. The proposed wind resource sharing strategy has been tested on the interconnected power systems operated within the National Electricity Market framework of Southeast Australia to demonstrate its effectiveness. The result suggests that high wind potential states within the NEM framework plays important role in achieving the RET of individual power system through a wind resource sharing strategy. Additionally, it has been found that in order to utilise the wind resource of all the states in achieving the individual RET from wind generation systems, the maximum emission reduction objective has to be compromised by interconnected power systems in Southeast Australia.

References

[1] Katzenstein, W., Fertig, E., Apt, J.: 'The variability of interconnected wind plants', Energy Policy, 2010, 38, pp. 4400-4410

[2] Kempton, W., Pimenta, F.M., Veron, D.E. and Colle, B.A., "Electric power from offshore wind via synoptic-scale interconnection", Proceedings of the National Academy of Sciences, 2010, 107(16), pp. 7240-7245.

[3] Dvorak, M.J., Stoutenburg, E.D., Archer, C.L., Kempton, K., Jacobson, M.Z., "Where is the ideal location for a US East Coast offshore grid?." Geophysical Research Letters, 2012, 39,(6), pp. 1-6.

[4] Rau, N.S., Necsulescu, C., Schenk, K.F., Misra, R.B.: 'Reliability of interconnected power systems with correlated demands', IEEE Trans. on Power Apparatus and Systems, 1982, PAS-101,(9), pp. 3421-3430

[5] Schenk, K.F., Ahsan, Q., Vassos, S.: 'The segmentation method applied to the evaluation of loss of load probability of two interconnected systems', IEEE Transaction on Power Apparatus and Systems, 1984, PAS-103, (7), pp. 1537-1541

[6] Yin, C.K., and Mazumdar, M.: 'Reliability computations for interconnected generating systems via large devaiation approaximation', IEEE Transaction on Power Systems, 1989, 4, (1), pp. 1-8

[7] Gordon, S.: 'Supergrid to the rescue', Power Engineer, 2006, 20, (5), pp. 30-33

[8] Cole, S., Karoui, K., Vrana, T.K., Fosso, O.B., Curis, J.B., Denis, A.M., Liu, C.C.: 'A European supergrid: Present state and future challenges', Proc. Power Systems Computation Conference (PSCC), Stockholm, Sweden, 2011

[9] Zhang, X.P., Rehtanz, C., Song, Y.: 'A grid for tomorrow', Power Engineer, 2006, 20, (5), pp. 22-27

[10] Leite da Silva, A.M., Guilherme de Carvalho Costa, J., Lima, L.H.L.: 'A new methodology for cost allocation of transmission systems in interconnected energy markets', IEEE Transaction on Power Systems, 2013, 28, (2), pp. 740-748

[11] Singh, C., Gubbala, N.: 'Reliability evaluation of interconnected power systems including jointly owned generators', IEEE Transaction on Power Systems, 1994, 9, (1), pp. 404-412

[12] Scheidt, J.L., Schulte, R.P., Koehler, J.E., Kaake, E.J., Niman, S.R.: 'Problem associated with the operation of jointly-owned generators', IEEE Transaction on Power Apparatus and Systems, 1984, PAS-103, (7), pp. 1569-1575

[13] Ahsan, Q., Rahman, S.F.: 'Evaluation of the reliability and production cost of interconnected systems with jointly owned units', IEE Proceedings Generation, Transmission and Distribution, 1987, 134, (6), pp. 377-382

[14] Cobian, M.J.: "Optimal pumped storage operation with interconnected power systems", IEEE Transaction on Power Apparatus and Systems, 1971, PAS-90, (3), pp. 1391-1399

[15] Burke, W.J., Schweppe, F.C., Lovell, B.E.: 'Trade off methods in system planning', IEEE Transaction on Power Systems, 1988, 3, (3), pp. 1284-1290

[16] Gavanidou, E.S., and Bakirtzis, A.G.: 'Design of a stand alone system with renewable energy sources using trade off methods', IEEE Transaction on Energy Conversion, 1992, 7, (1), pp. 42-48

[17] Niimura, T., Nakashima, T.: 'Multiobjective tradeoff analysis of deregulated electricity trasactions', Electrical Power and Energy Systems, 2003, 25, (), pp. 179-185

[18] Carpinelli, G., Celli, G., Mocci, S., Pilo, F., Russo, A.: ' Optimisation of embedded generation sizing and siting by using a double trade-off method', IEE Proceedings Generation, Transmission and Distribution, 2005, 152, (4), pp. 503-513

[19] Agalgaonkar, A.P., Kulkarni, S.V., Khaparde, S.A.: 'Evaluation of configuration plans for DGs in developing countries using advanced planning techniques', IEEE Transaction on Power Systems, 2006, 21, (2), pp. 973-981

[20] Loutan, C., Hawkins, D.: 'Integration of Renewable Resources: Operational Requirements and Generation Fleet Capability at 20% RPS', California ISO report, November 2007.

http://www.caiso.com/Documents/Integration-RenewableResources-OperationalRequirementsandGenerationFleetCapabilityAt20PercRPS.pdf, accessed June 2013

[21] Australian Energy Market Operator, "Wind integration in electricity grids: International practice and experience", Wind Integration Investment Work Package 3. http://aemo.com.au/Electricity/Planning/Related-Information/~/media/Files/Other/planning/0400-0049%20pdf.ashx, accessed June 2013

[22] Maisonneuve, N., Gross, G.: 'A production simulation tool for systems with integrated wind energy resources', IEEE Transaction on Power Systems, 2011, 26, (4), pp. 2285-2292

[23] Wood, M.J., Russell, C.J., Davy, R.J., Coppin, P.A.: 'Simulation of wind power at several locations using a measured time-series of wind speed', IEEE Transaction on Power Systems, 2013, 28, (1), pp. 219-226

[24] Billinton, R., Gao, Y., Karki, R.: 'Composite system adequacy assessment incorporating large-scale wind energy conversion systems considering wind speed correlation', IEEE Transaction on Power Systems, 2009, 24, (3), pp. 1375-1382

[25] Xie, K., Billinton, R.: 'Determination of the optimum capacity and type of wind turbine generators in a power system considering reliability and cost',IEEE Transaction on Power Systems, 2011, 26, (1), pp. 227-234

[26] Milligan, M.R., Factor, T.: 'Optimizing the geographic distribution of wind plants in Iowa for maximum economic benefit and reliability', Wind Engineering, 2000, 24, (4), pp 271-290

[27] Australian Energy Market Operator, "Wind Integration in Electricity Grids Work Package 3: Simulation using Historical Wind Data", Wind Integration Investment Work Package 3. http://aemo.com.au/Electricity/Planning/Related-Information/~/media/Files/Other/planning/0400-0056%20pdf.ashx, accessed May 2013

[28] Li, Q., Choi, S.S., Yuan, Y., Yao, D.L., "On the Determination of Battery Energy Storage Capacity and Short-Term Power Dispatch of a Wind Farm," IEEE Trans. Sustainable Energy, 2011, vol.2, no.2, pp.148-158.

[29] Khodayar, M.E., Shahidehpour, M., Lei Wu, 'Enhancing the Dispatchability of Variable Wind Generation by Coordination With Pumped-Storage Hydro Units in Stochastic Power Systems', IEEE Transactions on Power Systems, 2013, 28, (3), pp.2808-2818.

[30] A.M. Leite da Silva, L.A.F. Manso, W.S. Sales, S.A. Flavio, G.J. Anders, and L.C. Resende. "Chronological Power Flow for Planning Transmission Systems Considering Intermittent Sources," IEEE Trans. on Power Systems, vol. 27, no. 4, pp 2314-2322, Nov. 2012.

[31] Australian Energy Market Operator, National Transmission Network Development Planning 2012. Online, Avaialable: http://aemo.com.au/Electricity/Planning/National-Transmission-Network-Development-Plan/Overview.

[32] Department of Resource, Energy and Tourism. "Energy white paper 2012: Australia's energy transformation", http://www.ret.gov.au/energy/facts/white_paper/Pages/energy_white_paper.aspx, accessed June 2013.

[33] Climate Change Authority, Australian Government, Renewable Energy Target Review 2012, Online, Available: http://climatechangeauthority.gov.au/ret.

Chapter 7

A Power Dispatch Control Strategy for Wind Farms Using Energy Storage Systems

ABSTRACT

The uncertainty in the availability of wind generation and the lack of coincidence between wind generation and system peak demand cause wind farms (WFs) to be non-dispatchable energy resources and impose limits on the potential penetration of wind generation in the generation mix. Battery energy storage systems (BESSs) integrated with WFs can reduce the variability of wind generation output allowing them to be dispatched for the network support, especially under peak load conditions. This chapter proposes an effective power dispatch control strategy of wind farms with the aid of BESSs to improve the supply reliability taking into account the uncertainties in wind generation output and load demand. A stochastic programming model is formulated considering uncertainty in wind generation and energy price to schedule WF dispatch. A novel ranked-based BESS dispatch control algorithm is developed to achieve the assured WF power output levels for dispatching. Also the application of the power dispatch control strategy is presented with simulation study. Simulation results suggest that the implementation of the proposed strategy will improve supply reliability and revenue stream of the WFs.

7.1 Introduction

Mitigation of uncertainty and intermittency in the availability of generation from wind farm (WF) is a challenging task for the WF designers and energy market operators. Battery energy storage system (BESS) is a promising option for mitigating the stochastic characteristics of wind generation availability and enabling the integrated WF and storage system that can be dispatched in the same manner as that of a conventional generating unit [1, 2]. Since BESS is an expensive and energy limited resource, an intelligent utilisation strategy should be devised to maximise the benefits offered by the BESS.

The BESS integrated WF has been proposed in the literature to reduce the variability of wind generation [3-9]. The concept of a BESS integrated WF, as shown in Fig. 7.1, is to store the generated wind energy during the high wind speed time intervals and supply the stored energy during the low wind speed time intervals. The control strategies of the BESS integrated WF are required to perform an effective and efficient operation.

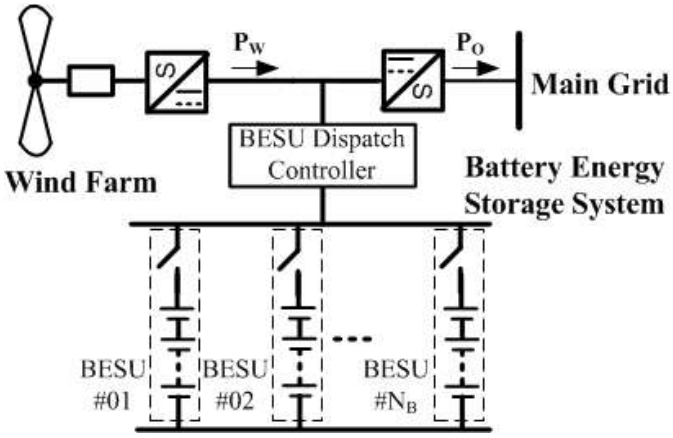

Fig. 7.1. BESS integrated WF schematic diagram.

A STATCOM based BESS control strategy has been developed in [3] using the average value of the next hour WF output to maintain a constant hourly WF dispatched output. The BESS control strategy proposed in [3] uses wind generation output and battery state of charge (SOC) feedback to secure a constant generation output during each dispatch interval. A first order low pass filter based BESS control strategy has been developed in [6] to smooth the WF generation. An energy price based BESS control strategy is proposed in [10] to mitigate the WF generation fluctuation within an

hour. However, these BESS control methods require exact wind speed forecasting and constant power output during each dispatch interval which cannot be guaranteed due to the uncertainty in the forecasted wind speed. In [4], a BESS control strategy is presented to achieve the firm dispatch levels during charging and discharging periods considering the uncertainty in wind generation output. According to this control strategy, maximum service life time of BESS is achieved through the completion of a fully charging cycle followed by a discharging cycle which allows the BESS to charge up to the maximum SOC level and to discharge up to the specified depth of discharge (DOD) level. However, in this strategy, the dispatch schedule needs to be revised based on the realised actual wind farm power output.

In this chapter, a stochastic programming model is proposed to schedule the BESS integrated WF dispatch level during each dispatch interval considering the uncertainty in the wind generation output and energy price forecasting. A ranked based dispatch algorithm has been developed for multiple battery energy storage units (BESUs) in a BESS, accounting the scheduled dispatch level submitted to the energy market operator in advance, and the realised WF generation output. The ranked BESU dispatch algorithm is developed to maintain an equal lifetime of each BESU and to restrain frequent switching between the charging and the discharging modes.

7.2 Problem Definition and Solution Approach

In decentralised market environment, all generating units need to submit their power generation schedules to the electricity market operator in advance. Due to uncertainty in forecasting and fluctuating nature of WF generation output, it is challenging for WF operator to maintain a constant output level during each dispatch interval and to dispatch maximum power during peak demand hours.

In practice, the wind speed at the hub height of the wind turbine fluctuates during each dispatch interval and the forecasting of wind speed involves uncertainty as shown in Fig. 7.2. The normalised maximum and minimum forecasted values are presented by the dotted lines and the solid lines, respectively. The actual realised WF generation during a time interval can be a value between the maximum and minimum forecasted

range of WF generation. Also, system demand and energy price forecasting have uncertainty as shown in Fig. 7.2.

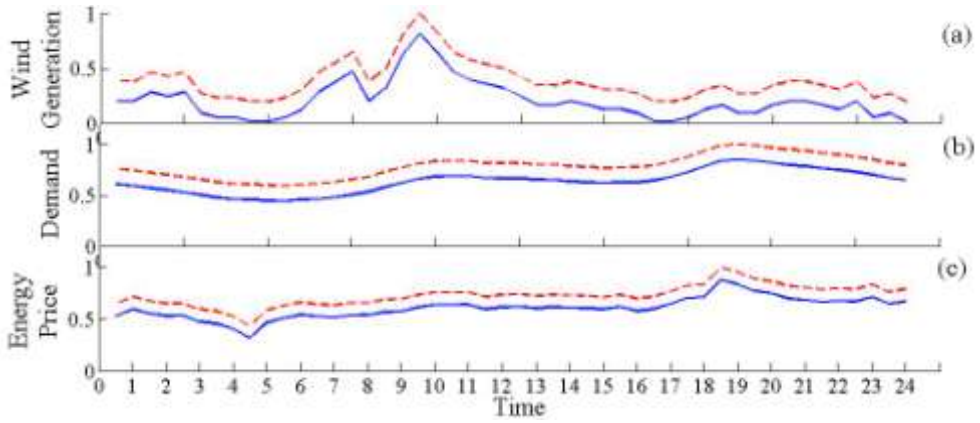

Fig. 7.2. Forecasted maximum and minimum values of normalised (a) WF generation, (b) system demand and (c) energy price.

An integrated BESS with WF demands for a control strategy that provide no or less variability in the power output and improved battery service lifetime, can maximise revenue from energy market and has the ability to adapt to wind speed and demand uncertainty. The strategy should ensure that the integrated WF and BESS is competitive with the conventional generating units.

The revenue maximisation and capacity support for the overall system from WF requires dispatching most of the WF generated energy during the peak energy price and the peak demand hours. Hence the BESS control strategy should be able to incorporate WF generation, energy price and system demand uncertainty while mitigating generation fluctuation.

The cost-effective (or economic) operation of the BESS integrated WF is a challenge, as frequent switching between the charging and discharging mode of the BESS reduces the lifetime of the BESS [4, 6]. The traditional WF fluctuation mitigation operation of the BESS involves charging and discharging of the BESU for a short period of time which will deteriorate the lifetime of the BESS. The maximum service life time of BESS can be ensured by the completion of a fully charging cycle followed by a discharging cycle which allows the BESS to charge up to the maximum SOC level and discharged up to the specified DOD level. The BESS lifetime is generally

dependent on the maximum allowable DOD [6]. A maximum allowable DOD level must be chosen to extend the BESS lifetime [11].

Most of the BESS control strategies to mitigate WF generation fluctuation reported in the literature only considered the forecasted mean values of wind speed [3, 5, 6, 10]. Hence such BESS control strategies fail to address the uncertainty involved in practice as shown in Fig. 7.2 and therefore cannot estimate dispatch schedule in advance. The BESS control strategy reported in [4], can estimate the WF dispatch schedule taking into account the uncertainty associated with the wind generation forecasting and mitigate WF generation fluctuation. The WF dispatch schedule is prepared based on the maximum and the minimum WF generation forecasted values during discharging and charging periods, respectively. However, an alteration of the dispatch schedule is required based on the actual WF generation realisation and therefore the requirement to dispatch most of the energy during the peak demand period cannot be guaranteed.

There exists a positive correlation between energy price and system demand [12]. Hence, dispatching BESS integrated WF with maximum power when energy price is at the peak will ensure maximum revenue from energy selling and maximum capacity contribution to the generation system. The proposed revenue maximisation based control strategy of the BESS can ensure dispatching most of the WF generated energy during system peak demand period and maximising the capacity credit of the WF.

The proposed dispatch scheduling of the WF is formulated as a stochastic programing model incorporating WF generation and energy price uncertainty. The objective of the stochastic programing is to maximise the revenue from selling energy to the energy market which in turn ensures a maximum power support during system peak demand hours in addition to the WF generation fluctuation mitigation. In contrast to the proposed method in [4], an adjustment of WF dispatch schedule can be avoided by applying proposed method.

The optimal dispatch schedule of the BESS integrated WF requires frequent switching between charging and discharging based on the actual WF generation realisation. Failing to allow the frequent switching between charging and discharging mode of BESS will not assure the fluctuation mitigation of WF generation. In order to encounter this issue, the paper proposes the BESS to be separated into a group of

parallel BESUs which are dispatched based on the assigned charging and discharging rank of each BESU.

7.3 Proposed Wind Farm and BESS dispatch strategy

The objectives of the proposed WF and BESS dispatch strategy are to maximise the revenue from selling energy to the energy market, to mitigate the WF generation fluctuation while maximising the BESU life, and to consider the uncertainty in the wind generation availability and the energy price. Since the availability of generation from WF and the energy price include uncertainty, a scenario based stochastic programming is proposed to estimate the power dispatch levels of the combined WF and BESS for the following day.

7.3.1 The Stochastic Programming Model Formulation

Let us consider a WF of W_{cap} installed capacity and the associated BESS with a storage capacity of B_{cap}. The generation unit dispatch interval in the energy market is denoted by $h = 1, 2,\ldots, H$ and H is the duration of time (e.g. 24 hours) for which a generation unit has to submit the dispatch schedule in advance. The power output from the generation unit cannot be altered during each interval, h (e.g. 30 min, 1 hour). The available wind generation time interval index in a dispatch interval is denoted by $t = 1, 2,\ldots, T$ and within each t (e.g. 5 min) the available wind generation output is assumed to be constant. The total revenue from selling the energy in the energy market can be estimated as follows.

$$F_H(C_h, P_{O,h}) = \sum_h C_h \times P_{O,h} \times \Delta h \tag{7.1}$$

where, C_h is the energy unit price and $P_{O,h}$ is the dispatched output from the combined WF and BESS during h^{th} dispatch interval. Δh is the time in each dispatch interval expressed in hour. It is expected that the WF makes as much revenue as possible from selling the energy to the energy market and becomes financially competitive to the conventional generation plants. Hence, the objective is to maximise the total revenue, $F_H(C_h,P_{O,h})$ over H duration where $P_{O,h}$ is the decision variable and C_h is a parameter.

Therefore, the corresponding optimisation problem can be formulated as maximisation of (7.1) subject to following constraints.

$$P_{W,h,t} - \frac{P_{Ch,h,t}}{\eta_{Ch}} + \eta_{Dch} \times P_{Dch,h,t} = P_{O,h} \qquad \forall t,h \tag{7.2}$$

$$E_{B,h,t} = E_{B,h,t-1} + P_{Ch,h,t} \times \Delta t - P_{Dch,h,t} \times \Delta t \;\; \forall t,h \tag{7.3}$$

$$P_{Ch,h,t} \times P_{Dch,h,t} = 0 \qquad \forall t,h \tag{7.4}$$

$$0 \le P_{Ch,h,t}, P_{Dch,h,t} \le P_{B,\max} \qquad \forall t,h \tag{7.5}$$

$$(1 - DOD_{\max}) \times B_{cap} \le E_{B,h,t} \le B_{cap} \qquad \forall t,h \tag{7.6}$$

$$0 \le P_{O,t} \le W_{cap} + B_{cap} \qquad \forall t,h \tag{7.7}$$

The constraint in (7.2) ensures the power balance between the WF generation output $P_{W,h,t}$, the charging power $P_{Ch,h,t}$, the discharging power $P_{Dch,h,t}$ and the dispatched output $P_{O,h}$ during the t^{th} time interval of the h^{th} dispatch interval. The overall charging and discharging efficiencies of the BESS are denoted by η_{Ch} and η_{Dch} in (7.2), respectively. Δt is the time in each time interval expressed in hour. The state of charge (SOC) of the BESS, $E_{B,h,t}$ is balanced by the constraints in (7.3). The mutual exclusive property of BESS charging and discharging during each time interval is ensured using the constraints in (7.4). The charging/discharging rate, SOC of BESS and dispatched output in each dispatch interval h are bounded by the constraints in equations (7.5) to (7.7). The maximum charging/discharging rate and the allowable DOD of BESS are indicated by $P_{B,max}$ and DOD_{max} in (7.5) and (7.6), respectively. Hence, the fluctuation in the generated power from WF $P_{W,h,t}$ is mitigated with the aid of BESS and the dispatch output $P_{O,h}$ is kept constant during each dispatch interval, h.

In the classical deterministic optimisation problem formulation given by (7.1) to (7.7), it is assumed that the parameters like, the energy price, C_h and the wind generation, $P_{W,h,t}$, can be predicted accurately. However, in the real case, the predicted values of these parameters include some degree of uncertainty and the actual quantities can be different from the predicted values. Hence it is realistic to represent these quantities using random variables and formulate the combined WF and BESS output dispatch problem using a stochastic programming model. The dispatch output levels for H dispatch intervals is to be submitted to the energy market operator in advance (e.g. in

some utilities the generation unit operators have to submit the following day dispatch schedule to the energy market operators). Hence, the WF operators have to make a decision on the WF dispatch levels prior to the realisation of the actual wind speeds and energy prices during the dispatch intervals in the following day. This decision is referred to as the *first stage* in the stochastic programming. Based on the decision in the *first stage*, and the realisations of the wind speed and the energy price, the BESS charging/discharging rate has to be controlled which is referred to as the *second stage* in the stochastic programming. Hence the WF dispatch strategy is to be modeled as a two-stage problem [12].

The two stage problem of the WF dispatch scheduling is formulated using the scenario based stochastic programming. It is assumed that the probability distributions of the random variables are known in each time interval. Additionally, it is assumed that the maximum power ratings of the WF and BESS are small enough to influence the energy price of the market and there is poor or no correlation between the energy price and the wind speed at the WF location. The stochastic optimisation model of WF dispatch scheduling is modeled to maximise the expected revenue from selling the energy in the energy market for different possible future scenarios of energy price and WF generation output, as follows.

maximise

$$E[F_H(C_{h,s}, P_{O,h})] = \sum_{s \in Sp} p_s \times (\sum_h C_{h,s} \times P_{O,h} \times \Delta h) \tag{7.8}$$

subject to:

$$P_{W,h,t,s} - \frac{P_{Ch,h,t,s}}{\eta_{Ch}} + \eta_{Dch} \times P_{Dch,h,t,s} = P_{O,h} \tag{7.9}$$

$$E_{B,h,t,s} = E_{B,h,t-1,s} + P_{Ch,h,t,s} - P_{Dch,h,t,s} \tag{7.10}$$

$$P_{Ch,h,t,s} \times P_{Dch,h,t,s} = 0 \tag{7.11}$$

$$0 \le P_{Ch,h,t,s}, P_{Dch,h,t,s} \le P_{B,\max} \tag{7.12}$$

$$(1 - DOD_{\max}) \times B_{cap} \le E_{B,h,t,s} \le B_{cap} \tag{7.13}$$

$$0 \le P_{O,h} \le W_{cap} + B_{cap} \tag{7.14}$$

where, $\forall t, h \quad and \quad s \in Sw$

In the objective function of the formulated stochastic programming given by (7.8), $E[.]$ indicates the expected or mean value function of the argument. The probability of

each price scenario is represented by p_s and Sp is the set of price scenario. The constraints in (7.9) to (7.13) are to be satisfied for each time interval, dispatch interval and wind speed scenario. The wind power output scenario is represented by the set Sw.

7.3.2 Scenario Generation for Stochastic Programming

There are a few different approaches to forecast the time series of wind speed such as, the time series method, the numerical weather prediction (NWP) and the combination of time series and NWP approach [13]. With the application of advanced computation methodologies and technologies, the forecasted wind speed is usually obtained within a close proximity of the actual wind speed and the error between actual and forecasted time series is bounded within a range. The uncertainty in wind speed forecast for every time interval can be modeled using a probability distribution. In this study it is assumed the probability distribution of uncertainty in wind speed forecasting during each time interval is known.

The wind speed time series for the time H ahead is generated using time series forecasting approach and this time series wind speed is considered as the mean forecasted wind speed, μ_{W0}. Hence a $N_{HT}\times N_{HT}$ covariance matrix, Σ_{W0}, for the time series wind speed data is estimated from the historical data of wind speed. N_{HT} is the number of time intervals during the dispatch schedule time H. For example: for 5 min time interval of wind speed data, the 24 hours dispatch schedule time N_{HT} would be 288. The covariance matrix, Σ_{W0} contains the covariance coefficients between the wind speeds of two time intervals. Hence multivariate normal random numbers of $N_{dW0}\times N_{HT}$ order are generated using the parameters $N(\mu_{W0}, \Sigma_{W0})$ of the multivariate normal distribution. N_{dW0} is the number of initial desired scenario for time series wind speed. The inverse transformation method of sampling [14] is applied to the multivariate normal random numbers in order to generate multivariate random numbers of the desired probability distribution, i.e. the probability distribution of the wind speed forecasting uncertainty.

The time series of the WF power output is generated from the time series wind speed using the energy conversion model of the wind turbine. Fast backward/forward scenario reduction method as discussed in [14-16] is then applied to reduce the number of time

series of the WF power output scenarios to N_{Sw}, which is the number of wind generation output scenarios used in the stochastic optimisation.

The historical time series of the energy price data is used to forecast time series energy price for the H time ahead. Since the energy price can differ every year, the historical time series of the energy price for each day of the year are normalised with respect to the peak energy price. The desired number of scenario, N_{Sp} for normalised energy price is then generated using the method previously described for the wind generation scenario output. The normalised time series of energy price scenario are multiplied by the forecasted peak energy price of the day to estimate the actual forecasted time series energy price.

7.4 BESS Unit Scheduling Strategy

The lifetime of BESS is limited by a finite number of charge-discharge cycles and frequent charging and discharging cycles will reduce the operational lifetime of the BESS [4, 6]. However, in order to mitigate the fluctuation in the WF generation output, the integrated BESS needs to be switched between charging and discharging modes frequently. The operational lifetime of BESS is adversely affected by this frequent mode switching operation. Hence, strategies are to be developed for the BESS dispatch to increase the operational lifetime of BESS for use in the WF generation fluctuation mitigation.

7.4.1 BESS Units Configuration

BESS consists of battery banks connected in parallel to provide the required energy storage capacity for the WF fluctuation mitigation operation. In the WF power dispatch control and fluctuation mitigation study, BESS is considered as a single unit [3-5, 7]. In the parallel battery banks with a single DC/AC conversion unit system, all the parallel batteries share the total BESS charging and discharging energy equally. Since in the WF generation fluctuation mitigation operation, BESS undergoes frequent charging/discharging mode switching, all the parallel battery units encounter shortened operational lifetime.

A dual-battery energy storage configuration is proposed in [8] to prevent frequent charging/discharging mode switching in the WF generation fluctuation mitigation operation. The parallel battery bank is divided into two groups. One group of battery charges while other group of battery is dedicated for discharging. The dual-battery configuration encounters challenges when the charging energy is larger than the storage capacity of each battery group. During this situation, the battery group allocated for discharging mode will have to switch to charging before completing discharging operation. Hence, it is challenging to keep the synchronisation in the charging/discharging cycle between the two battery groups particularly when considering the uncertainty factors associated with the forecasted wind speed.

In [6, 9] the BESS is modeled as a combination of parallel battery banks for smoothing WF generation fluctuation. This type of battery configuration will be used for the purpose of this study. Since the total energy storage capacity is distributed among a larger number of separately controllable battery units connected in parallel, the frequent charging/discharging mode switching can be avoided even when the uncertain wind speed scenario is taken into account. Hence, the BESS is configured as the parallel combinations of the separately controllable battery energy storage units (BESUs) as shown in Fig. 7.1. The dispatch control algorithm for each BESU is illustrated in the following subsection where the BESS is modeled as N_B numbers of identical BESUs connected in parallel.

7.4.2 BESU Dispatch Algorithm

The dispatched power from the combined WF and BESS for every time interval is evaluated using the stochastic programming for different energy price and wind speed scenario as described in Section 7.3.1. The total power output from the BESS can be estimated from the actual WF generation realised during the system actual operation and the scheduled dispatch power for every time interval. A control algorithm is developed in this section to dispatch the BESUs of BESS which will maintain the resultant BESS output power after realising the actual WF generation output during every time interval. A novel charging/discharging ranking based BESU dispatch algorithm is proposed to serve this.

The prime objective of the proposed BESU dispatch algorithm is to maintain an equal number of charging/discharging cycles of individual BESU. An equal number of charging/discharging cycles of each BESU will retain similar operational lifetime of the battery bank in each BESU. By means of conserving similar operational lifetime of each BESU, the battery replacement cost can be minimised since the sum of the individual replacement cost of BESU is greater than the overall BESS replacement cost.

The BESUs are numbered as Unit#*1*, Unit#*2*,...,Unit#N_B. Additionally each BESU is assigned with two ranks namely: charging rank and discharging rank. Each BESU is assigned with a unique charging rank number and a unique discharging number. The BESU with lowest charging rank number (i.e. charging rank = 1) will have the highest priority for charging and will store energy until fully charged (i.e. normalised SOC of this BESU becomes equal to 1). After being fully charged, the BESU with the lowest charging rank will be assigned with the highest charging rank number (charging rank N_B) and the charging ranks of all other BESUs are reduced by 1 at the same time as shown in Fig. 7.3. Similarly, the BESU with lowest discharging rank (discharging rank 1) will be given the highest priority for discharging the stored energy. The lowest discharging ranked BESU will continue discharging until the the SOC of the BESU reaches the allowed minimum SOC level (SOC_{min}). Once the SOC of the lowest discharging ranked BESU reaches SOC_{min}, the discharging ranks of all the BESUs are reduced by 1 and the last discharging BESU is assigned the highest discharging rank (discharging rank N_B).

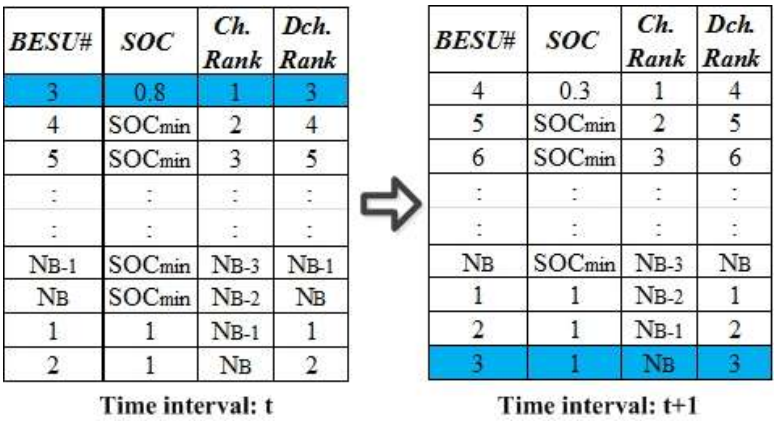

Fig. 7.3. Transition in charging rank of BESU during charging time interval.

At the beginning of the BESS operation when the normalised SOC level of all the BESUs are at SOC_{min} (or at 0), both the charging and the discharging ranks of the BESUs are set equal to their unit number. With the course of time, the charging and discharging rank will be updated based on the rules illustrated above. The overall flow chart of the proposed BESU dispatch algorithm is presented in Fig. 7.4. The SOC, charging and discharging ranks of each BESU are updated after each time interval.

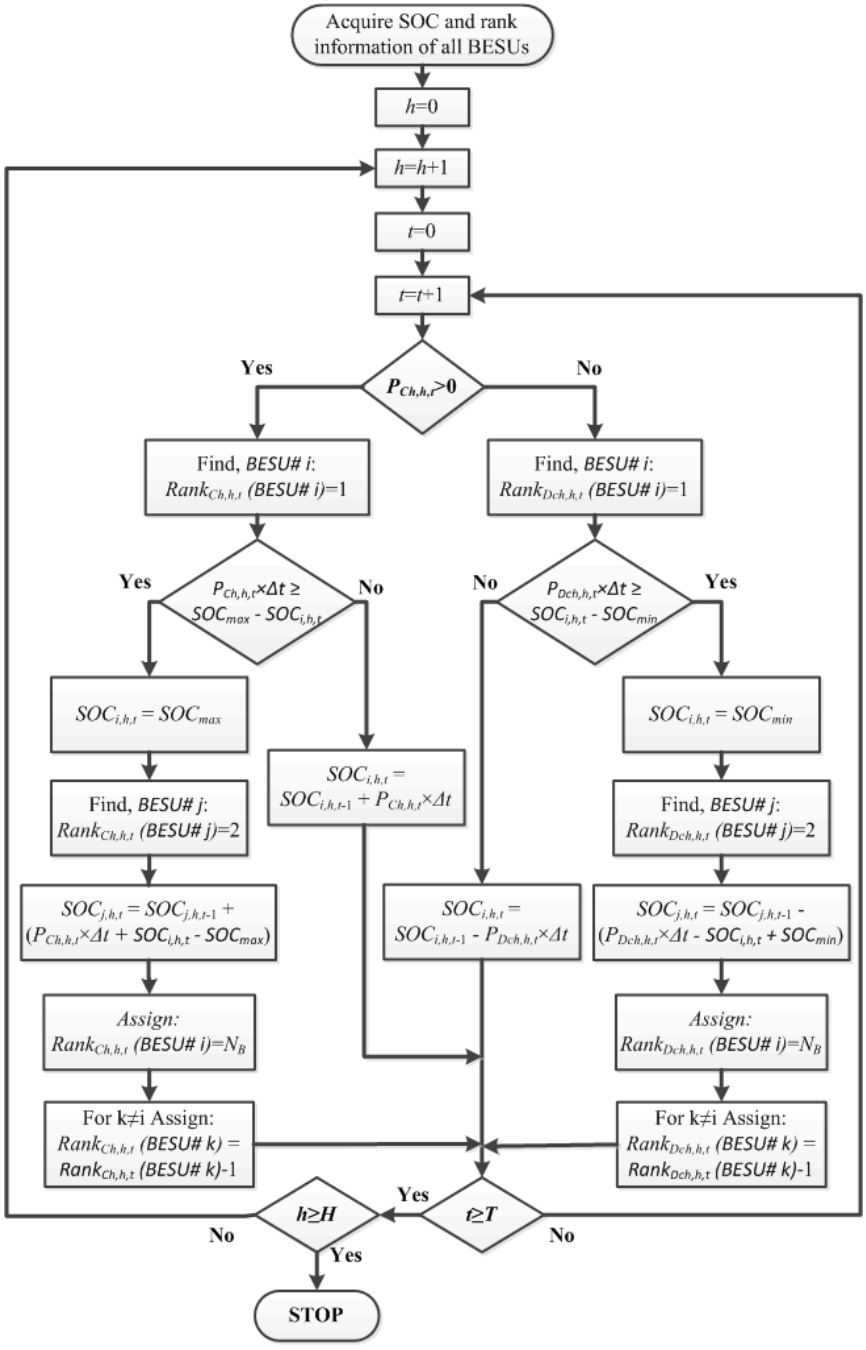

Fig. 7.4. BESU dispatch control algorithm.

The charging and discharging operation of BESUs follows the hierarchical charging and discharging rank, respectively. Hence the individual BESU goes through one complete charging and discharging cycle before the next charging operation starts. After the charging is complete, a BESU is assigned to a rank with lowest charging priority. The BESU will have to wait for all other BESUs to be charged although the BESU can be discharged in the meantime. This hierarchical rank based dispatch scheduling of BESUs will ensure an equal number of charging/discharging cycles and hence a similar lifetime of every BESU is maintained.

During the continuing operation of WF and BESS, the charging unit with ranked 1 and the discharging unit with ranked 1 can be different BESUs as observed from Fig. 7.3. During a dispatch interval, if the WF generation output is greater than the committed dispatch level for most of the time intervals, the BESS will be charging for most of the time interval. However, if the WF generation output goes lower than the committed dispatch level for a few time intervals, the BESS is immediately switched to discharging mode for those time intervals. The BESU with charging rank 1 will stop charging and BESU with discharging rank 1 will start to discharge. After the time intervals when the WF generation output is greater than the committed dispatch level, the BESU with charging rank 1 will continue charging keeping BESU with discharging rank 1 in a rest mode. As a result, the frequent charging/discharging mode switching of the same BESU is mitigated through the proposed rank based BESU dispatch scheduling algorithm.

The total amount of energy to be charged and discharged during each time interval is estimated from the actual WF generation output realisation and the committed dispatch schedule. Unlike the deterministic BESU dispatch scheduling algorithms proposed in [6-7, 9], the proposed algorithm can mitigate WF generation output fluctuation without the information of fixed WF generation output power for each time interval. Hence the proposed BESU dispatch scheduling algorithm is applicable even for the case when uncertainty is involved with the wind speed forecasting.

7.5 Simulation Results

The proposed WF and BESS dispatch strategy is tested using the observed historical wind speed data at the weather station near Capital Wind Farm, New South Wales, Australia [17]. The rated capacity of the Capital WF is 140 MW. The wind speed data of the two typical winter days are used for testing the proposed algorithm. The wind speed data of 5 min time interval and the hourly dispatch interval of the energy market is considered for this study and each generation unit must submit its 24 hour dispatch schedule for the following day to the energy market operator. The maximum and minimum values (up to 99.74% probability of forecasting error from the mean value) of the forecasted WF generation and the energy price for each time interval used for this study are shown in Fig. 7.5. The developed BESS dispatch strategy to mitigate the WF generation fluctuation is implemented using MATLAB and LINGO software.

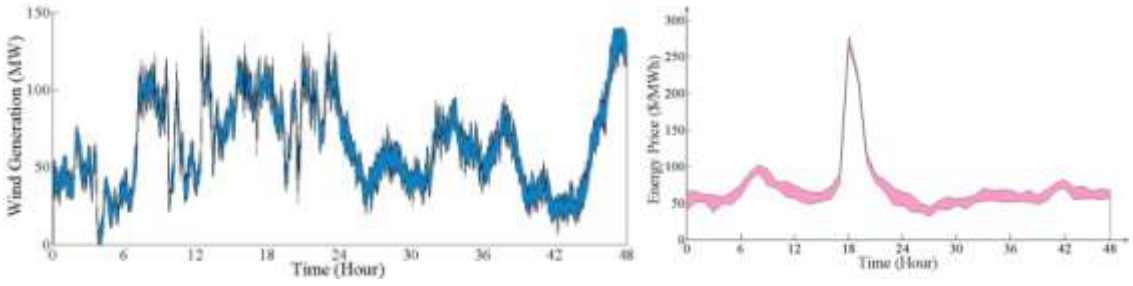

(a) **(b)**

Fig. 7.5. (a) Wind Farm generation output and (b) Energy price forecast.

A BESS of 400 MWh energy storage capacity along with the considered WF is used to investigate the performance of the developed algorithm to mitigate the WF generation fluctuation. The energy storage capacity of BESS is selected to provide support for around 3 hours during no or low WF generation output. The total energy storage capacity is distributed among 16 parallel BESUs. The charging and the discharging efficiency of each BESU are considered to be 80% for this study. The maximum DOD used for this study is considered to be 80% and hence each BESU can be discharged up to 20% of the maximum SOC. The scheduled and realised dispatched output power of

the combined WF and BESS are simulated using a deterministic optimisation model and the proposed stochastic programming model and the results are presented in Fig. 7.6.

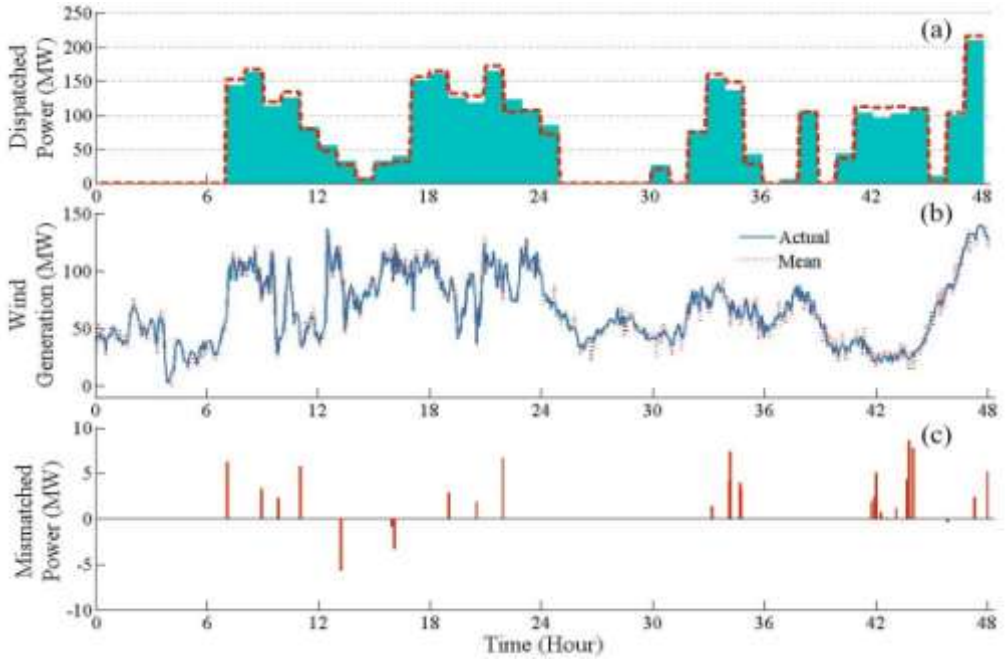

Fig. 7.6. (a) Dispatched output power of combined WF and BESS [dotted: deterministic, bars: stochastic], (b) mean and actual WF generation, (c) Power mismatch between scheduled and actual output.

In Fig. 7.6(a) the dotted line and the solid bars represent the scheduled dispatch output power of the BESS integrated WF estimated using the deterministic and the stochastic programming, respectively. It can be observed from Fig. 7.6(a) that there are differences in the scheduled dispatch output power estimated using two different methods. The differences are due to the fact that the deterministic programming model obtains dispatch schedule maintaining the constraints for only one scenario of the random variables. The WF generation and energy price scenario with the highest probability is considered as the realised WF generation and energy price in the following analysis. For the deterministic optimisation program, the mean values of the WF generation and the energy price are considered. The mean values of the realised WF generation output during different time intervals are presented in Fig. 7.6(b). It can be noticed that the actual realisation of WF generation is different from the mean values. Due to the differences between the mean forecast and the realised values of the WF generation, the actual dispatched output of the combined WF and BESS cannot maintain the scheduled dispatch power level estimated using the deterministic optimisation

model. The power mismatch between the scheduled and the actual dispatched output power is shown in Fig. 7.6(c). On the other hand, the scheduled dispatched output estimated using the developed stochastic programming can be maintained with 100% accuracy for the realised WF generation scenario. Hence the proposed stochastic programming approach is effective for high accuracy WF generation fluctuation mitigation.

The impact of the energy price on the dispatched power estimated using the deterministic optimisation and the stochastic programming can be observed from Fig. 7.6(a). The dispatch output power during the low energy price hours between midnight to early morning (6 a.m.) is zero. The BESS stores energy during these hours and uses the stored energy to discharge during high energy price hours (late morning and evening hours).

The power output and SOC of the BESS for the WF generation realisation have been presented in Fig. 7.7(a) and 7.7(b), respectively. The positive values in Fig. 7.7(a) indicate the BESS charging and the negative values represent the discharging of BESS. From Fig. 7.7(b), it is observed that most of the time the BESS is completing charging and discharging operation cyclically. However, between hours 33 to hour 40, the BESS switches from charging to discharging and then discharging to charging mode again. This is due to the uncertainty involved with WF generation and could potentially reduce the lifetime of the BESS. However, the proposed multiple parallel BESU based BESS design and dispatch algorithm can mitigate the frequent charging and discharging operation as illustrated using Fig. 7.7(c) to 7.7(e) and hence improve the BESS lifetime.

Three BESUs (BESU#06, BESU#13 and BESU#14) are chosen from the parallel configuration and the SOC of these BESUs are shown in Fig. 7.7(c) to 7.7(e), respectively. The charging/discharging rates of the BESUs vary depending on the actual WF generation fluctuation. The BESU#06 is charged up to SOC_{max} and then discharged up to SOC_{min} in a cyclic order, 4 cycles in two days. The similar charging/discharging operation is observed for BESU#13 and BESU#14 with 3 cycles per two days. The reason behind the difference in the charging/discharging cycles between the different BESUs within these two day timeframe is the switching between charging and discharging mode of the BESS operation for a short period of time during 33^{th} to 40^{th} hour as shown in Fig. 7.7(b). In order to response against this certain change in WF

generation, the BESU#13 and BESU#14 with discharging rank 1 and 2 respectively, are discharged between 33th and 40th hour to maintain the scheduled dispatch level.

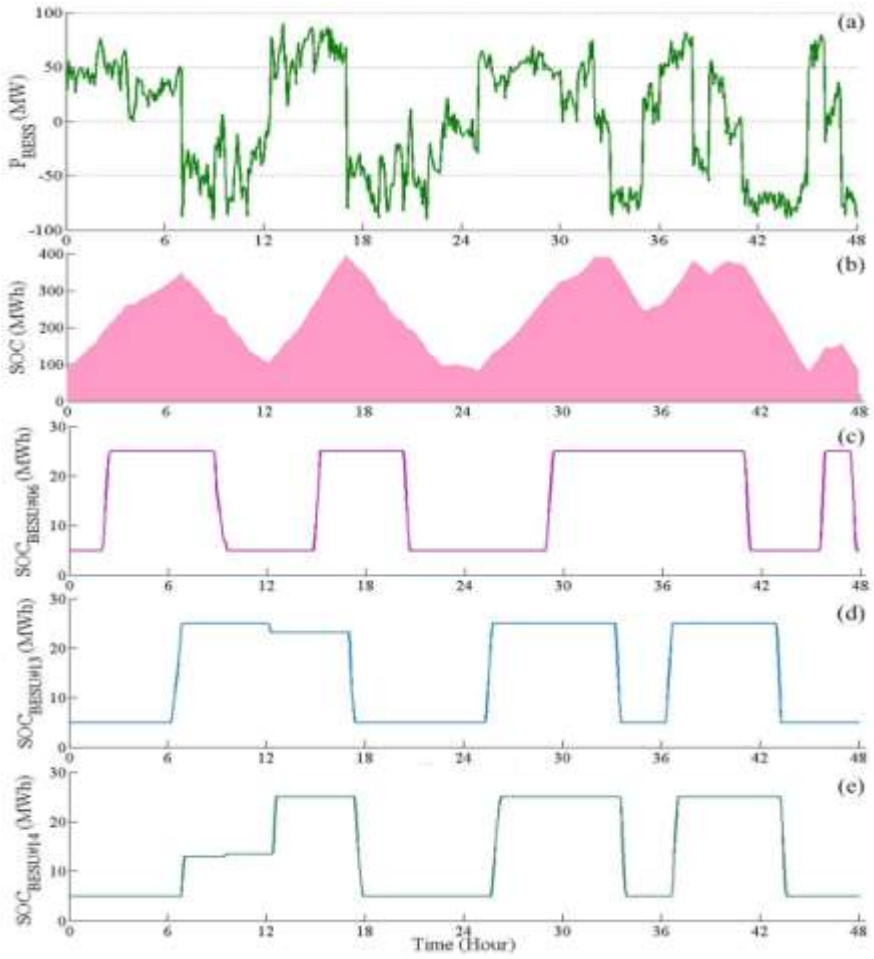

Fig. 7.7. (a) BESS output power, (b) SOC of the BESS, (c) SOC of BESU#6, (d) SOC of BESU#13, (e) SOC of BESU#14.

The benefits of the developed BESU dispatch algorithm can be observed from the SOC of BESU#13 and BESU#14 at Fig. 7.7(d) and 7.7(e), respectively. BESU#13 is fully charged at 6th hour and then BESU#14 starts charging. Before the BESU#14 is fully charged up to SOC_{max}, the unit is required to start discharging to maintain the scheduled dispatch level. As a result BESU#14 is kept in resting mode with ranked 1 for charging. In the meantime, the BESU#06 has to be discharged between 7th and 12th hour. All the fully charged BESUs are discharged during this time period and at 12th hour BESU#13 discharges slightly. After 12th hour the BESS returns to charging mode again and then BESU#13 goes to resting mode with ranked 1 for discharging. The BESU#14 is at the highest priority for charging at the beginning of 13th hour and

resumes charging until fully charged. This operation of BESUs demonstrates the effectiveness of the proposed algorithm for maximising BESS lifetime by avoiding the frequent switching between charging and discharging mode.

The impact of the proposed BESS dispatch control strategy on the power generation system reliability is investigated using the IEEE reliability test system (RTS). The WF is added to the IEEE RTS generation system and demand of two winter days are considered for Loss of Load Probability (LOLP) estimation. The system demand, combined WF and BESS dispatched output for the realised WF generation and LOLP of the system are presented in Figs. 7.8(a)-(c). It is observed from Figs. 7.8(a) and 7.8(b) that with the application of proposed dispatch control strategy the combined WF and BESS are scheduled to dispatch maximum power during the peak demand hours. As a result the system LOLP is reduced significantly compared to the case when WF has no BESS support.

The performance of the proposed combined WF and BESS dispatch control strategy has been compared with the dispatch control strategy based on the maximum and minimum forecasted values (MMFV) as reported in [4]. The comparative results are presented in Fig. 7.9. The energy storage capacity of the BESS in this case is considered to be 150 MWh so that the BESS can store the rated WF generation for 1 hour. The charging, discharging efficiency and the maximum DOD of the BESS are considered to be same as in the previous case.

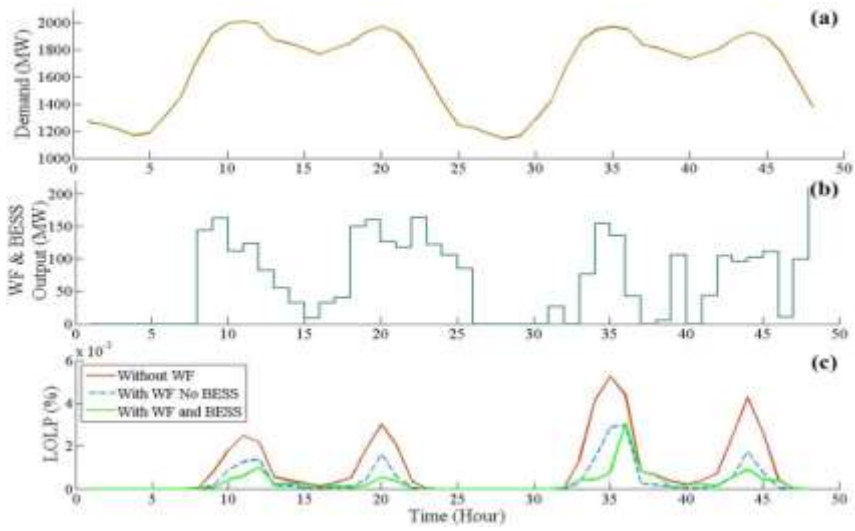

Fig. 7.8. (a) System demand (b) WF dispatched output power (c) System LOLP.

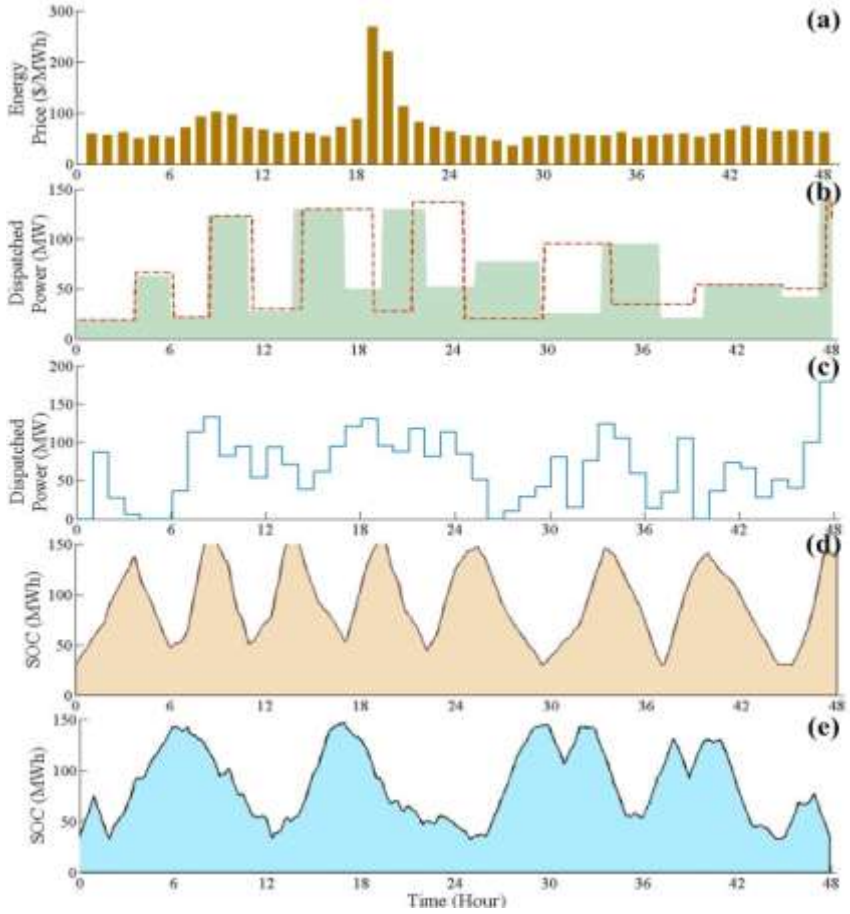

Fig. 7.9. (a) Realised energy price (b) Scheduled and actual dispatched output power using MMFV method, (c) Scheduled dispatched output power using proposed method (d) SOC of the BESS for MMFV method, (e) SOC of the BESS for proposed method.

The realised energy price is shown in Fig. 7.9(a). The scheduled dispatch level and the actual dispatched output power based on the WF generation output realisation are shown in Fig. 7.9(b). The dotted line indicates the scheduled dispatch level whereas the solid bars represent the actual dispatch levels. It is observed that the actual dispatch output cannot follow the scheduled dispatch level because the actual WF generation output is different from the maximum and the minimum forecasted values. Additionally the scheduled dispatch fails to dispatch maximum power during the higher price hours. The scheduled dispatched output estimated using the proposed strategy is shown in Fig. 7.9(c). The actual dispatched output power is maintaining the scheduled level estimated using the proposed strategy. Hence, Fig. 7.9(c) presents the actual dispatched output power of the combined WF and BESS. It is to be noted that the scheduled dispatch level estimated using the proposed strategy ensures a maximum possible power dispatch during higher energy price hours. The SOC of the BESS using MMFV and the proposed

method are shown in Fig. 7.9(d) and 9(e), respectively. From the SOC level shown in the figure, it can be found that the number of complete charging and discharging cycles in the MMFV and proposed method are 7 and 5, respectively. Hence the proposed method reduces the number of charging and discharging cycles for the operation time of same duration.

Table 7.1. Revenue from different methods and BESS storage capacities.

Method	BESS Capacity (MWh)	Revenue ($/48h)
No BESS	0	236588.25
Deterministic	400	279819.30
Stochastic	400	276538.50
MMFV	150	223037.00
Stochastic	150	254817.80

The revenues earned by the WF for the presented 48 hour time period following the different dispatch control strategies and for the different energy storage capacity of BESS are presented in Table 7.1. It is observed that the BESS with higher energy storage capacity makes the higher revenue if the proposed dispatch control strategy is used. Moreover, it is to be noted that installation of BESS along with WF and using the proposed dispatch control strategy increases the WF revenue in addition to the WF generation fluctuation mitigation as compared to the case without BESS. However, the dispatch control strategy based on the deterministic optimisation model results in $3,280.80 higher revenue than the stochastic programming based strategy. This excess revenue is called the ‘Expected Value of Perfect Information (EVPI)’ [12]. Due to the limitation of having perfect wind speed forecasting, the WF along with the BESS misses the EVPI. From the comparison of the revenues obtained from the MMFV and the proposed method, it is revealed that the proposed method aids the WF to receive higher revenue than the MMFV method.

7.6 Conclusion

A power dispatch control strategy has been proposed in this chapter to improve the generation schedulability of a battery energy storage system (BESS) integrated wind farm (WF) considering the uncertainty in the wind generation and the energy price. The contribution of this chapter is the development of a novel scheduling algorithm using stochastic programming model and a novel ranked based BESS dispatch control strategy that enables the BESS integrated WF to schedule firm dispatch levels. The results from the simulation studies emphasises that the proposed method can schedule BESS integrated WF dispatch and maintain the scheduled dispatch level for the forecasted wind generation output power with uncertainty. Hence adjustment of the WF dispatch schedule can be avoided. In addition to that the proposed ranked based BESS dispatch strategy can enhance the lifetime of BESS by avoiding frequent charging and discharging operation of the BESS. Hence the proposed solution methodology for WF dispatch scheduling can support the growth of wind resources in the electricity generation system and aid to be competitive against the conventional generation systems.

References

[1] M. Black, G. Strbac, “Value of bulk energy storage for managing wind power fluctuations”, *IEEE Transactions on Power Systems*, vol. 22, no. 1, pp. 197-205, Mar. 2007.

[2] J. P. Barton, D. G. Infield, “Energy storage and its use with intermittent renewable energy”, IEEE Transactions on Energy Conversion, vol. 19, no. 2, pp. 441-448, June. 2004.

[3] S. Teleke, M. E. Baran, A. Q. Huang, S. Bhattacharya, L. Anderson, "Control Strategies for Battery Energy Storage for Wind Farm Dispatching", *IEEE Trans. Energy Conversion*, vol. 24, no. 3, pp. 725-732, Sept. 2009.

[4] Q. Li, S. S. Choi, Y. Yuan, D. L. Yao, "On the Determination of Battery Energy Storage Capacity and Short-Term Power Dispatch of a Wind Farm", *IEEE Trans. Sustainable Energy*, vol. 2, no. 2, pp. 148-158, 2011.

[5] M. A. Abdullah, K. M. Muttaqi, A. P. Agalgaonkar, D. Sutanto, " Estimating the capacity value of energy storage integrated with wind power generation", *Proc. Of IEEE Power and Energy Society General Meeting*, July 2013, Vancouver, Canada.

[6] Q. Jiang, Y. Gong, H. Wang, "A Battery Energy Storage System Dual-Layer Control Strategy for Mitigating Wind Farm Fluctuations", *IEEE Transactions on Power Systems*, vol. 28, no. 3, pp. 3263-3273, Aug. 2013.

[7] A. Gabash, P. Li, "Flexible Optimal Operation of Battery Storage Systems for Energy Supply Networks", *IEEE Transactions on Power Systems*, vol. 28, no. 3, pp. 2788-2797, Aug. 2013.

[8] D. L. Yao, S. S. Choi, K. J. Tseng, T. T. Lie, "Determination of Short-Term Power Dispatch Schedule for a Wind Farm Incorporated With Dual-Battery Energy Storage Scheme", *IEEE Transactions on Sustainable Energy*, vol. 3, no. 1, pp. 74-84, Jan. 2012.

[9] X. Li, D. Hui, X. Lai, "Battery Energy Storage Station (BESS)-Based Smoothing Control of Photovoltaic (PV) and Wind Power Generation Fluctuations", *IEEE Transactions on Sustainable Energy*, vol. 4, no. 2, pp. 464-473, April 2013.

[10] M. Dicorato, G. Forte, M. Pisani, M. Trovato, “Planning and operating combined wind storage system in electricity market”, *IEEE Transactions on Sustainable Energy*, vol. 3, no. 2, pp. 209-217, Apr. 2012.

[11] J. McDowall, "Battery life considerations in energy storage applications and their effect on life cycle costing," *Power Engineering Society Summer Meeting 2001*, vol. 1, pp. 452-455, 2001.

[12] J. R. Birge, F. Louveaux, *Introduction to Stochastic Programming*, Springer-Verlag New York, Inc. 1997.

[13] G. Giebel, R. Brownsword, G. Kariniotakis, M. Denhard, C. Draxl, *The State-Of-The-Art in Short-Term Prediction of Wind Power: A Literature Overview*, 2nd edition, ANEMOS.plus, 2011. 109 p.

[14] X. Y. Ma, Y. Z. Sun, H. L. Fang, "Scenario Generation of Wind Power Based on Statistical Uncertainty and Variability", *IEEE Transaction on Sustainable Energy*, vol. 4, no. 4, pp. 894-904, Oct. 2013.

[15] N. Growe-Kuska, H. Heitsch, and W. Romisch, “Scenario reduction and scenario tree construction for power management problems”, *Proc. IEEE Power Tech Conference 2003*, Bologna, 2003.

[16] J. Dupačová, N. Gröwe-Kuska, W. Römisch, “Scenario reduction in stochastic programming”, *Mathematical Programming*, vol. 95, no. 3, pp. 493-511, March 2003.

[17] Bureau of Meteorology (BoM), Australia. Online. Available: www.bom.gov.au.

Chapter 8

Estimating Load Carrying Capability of Generating Units in a Renewable Rich Electricity Infrastructure

ABSTRACT

It is important to estimate the contribution of the renewable generation units in the evaluation of system generation adequacy for power generation planning taking into account the demand and renewable generation correlation and uncertainty. The effective load carrying capability (ELCC) is usually used for this purpose. In this chapter, a non-iterative analytical method is proposed for estimating the peak load carrying capability (PLCC) and ELCC of conventional and renewable generation units. The proposed method is verified using the IEEE RTS and an electricity network in New South Wales, Australia, and the results are compared with other estimation methods. The results show that the correlation between demand and renewable generation influences the ELCC of a renewable generation unit– the higher the correlation, the higher the ELCC and vice versa. The main contribution of this chapter is the development of an analytical non-iterative and computationally efficient technique, which accounts for the correlation between demand and available renewable generation.

8.1 Introduction

The power output from the renewable generation systems and the load demand are uncertain variables due to their inherently fluctuating nature. With growing penetration of renewable generation in the electricity generation system, the generation adequacy estimation methodology needs to be modified to include the variability and uncertainty associated with the renewable generation and load demand and the correlation between the two.

A number of indices to estimate the capacity contribution of the intermittent generation systems, such as effective load carrying capability (ELCC), demand time matching (DTIM), equivalent conventional power (ECP), and equivalent firm power (EFP) has been proposed in the literature [1-4].

Different entities including system operators, power utilities and academics have reached a consensus to use the ELCC index as the capacity value for intermittent renewable generation systems. The ELCC index is an indicator of the contribution of an additional generator (or a group of generators) in the generation adequacy to meet the peak load demand of the system [1-13]. Authors of [9] define ELCC as the amount of increase in the peak demand that can be added to a system while maintaining a specific risk level such as the loss of load expectation (LOLE) after an additional generator (or a group of generators) is added.

The ELCC index has been used for power generation planning of (i) concentrating solar power plants in Southwest United States [1], (ii) tidal wave [7], (iii) solar photovoltaic power plants [2, 4], and (iv) wind generation systems [3, 9, 11, 13, 14].

A graphical method is proposed in [10] to estimate the ELCC of an additional generating unit into the generation system. This is further modified in [11] to include the addition of wind generation unit using multi-state representation of the availability of the wind turbine outputs. The graphical method to estimate LOLE using an exponential function can lead to significant errors [15] as discussed in Section 8.2.

The Z-statistic method, proposed in [12], is a non-iterative method for ELCC estimation, which presumes that the probability distribution of the generation surplus during the peak demand period is a Gaussian distribution. The ELCC of the system is

estimated using the changes in the generation surplus probability distribution during peak demand periods of the system due to the additional generation unit. It keeps the Z-statistic value constant which is equivalent to maintaining a constant loss of load probability (LOLP) and therefore can be considered as an approximate method for ELCC calculation during the peak demand period. The main advantage of this method is a significant reduction in computation time compared to the more onerous iterative method using chronological demand and renewable energy system data. However the correlation between the demand and renewable generation has not been taken into account in this method. Further, the Z-statistic method assumes that the addition of a wind plant does not change the probability distribution shape of the generation surplus. Hence it is especially accurate for the addition of small wind generation unit and less accurate for the addition of large unit on a power system.

In [13], a Genetic-Algorithm-based LOLE estimation method is proposed for a power system with wind generation plant using the chronological data of demand and wind generation. An iterative method for estimating the ELCCs of the wind generation units is used in [13, 14] using the data of demand and wind generations for several years. The iterative method along with the time series data can account for both the seasonal and diurnal variation of wind generation, and the correlation between demand and wind generation. However, the iterative method is computationally intensive due to the large time series data set requiring several iterations and is not suitable for generation planning involving optimization of a large system lasting for several years.

In this chapter, instead of using chronological data and the commonly used iterative method to account for seasonal and diurnal variation and the correlation between demand and available renewable generations, a non-iterative analytical technique using joint probability distribution of the demand and the renewable generations is proposed to estimate the LOLE and peak load carrying capability (PLCC) of the system, and ELCC of the renewable generation plant. The ELCC of the renewable generation plant is estimated from the PLCC values of the system before and after adding the renewable generation plant in the generation system. Since the proposed method of ELCC estimation for the renewable generation plant is non-iterative, it is less computationally intensive and can provide greater insight into the influencing attributes associated with the ELCC of the renewable generation plant as compared to the iterative method.

8.2 Motivation for the Research Work

8.2.1 Errors in the Graphical Methods for ELCC Estimation

In the non-iterative probabilistic graphical methods [10, 11], the LOLE of the system is approximated by the exponential function of the system peak demand using curve fitting technique. For a small system from reference [15], this approximation using curve fitting will produce large error, particularly for higher peak demand as shown in Fig. 8.1. For a large system, such as the IEEE reliability test system (RTS) [16], the error reduces as shown in Fig. 8.2. Despite the closeness of the fitted curve to the actual curve, a large relative error in the estimation of LOLE can be introduced as shown in the zoomed portion inside Fig. 8.2.

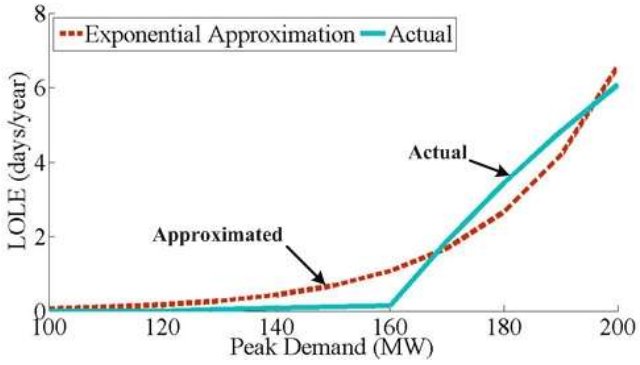

Fig. 8.1. LOLE vs peak demand curve for a system presented in [15].

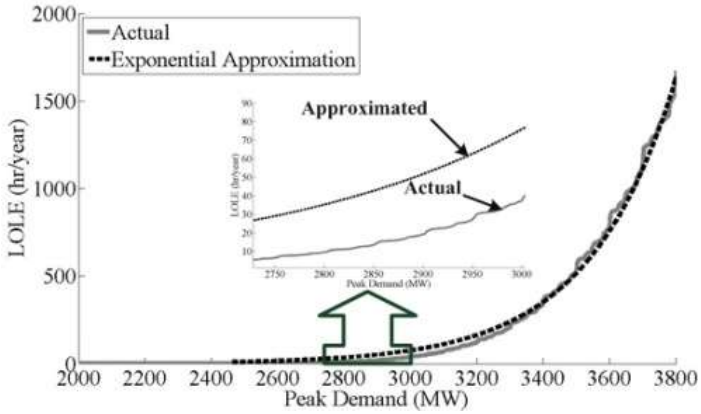

Fig. 8.2. LOLE vs peak demand curve for a IEEE RTS.

This is particularly acute when the system has a small value of LOLE as the effect of erroneous approximation gets further amplified in such case. The error in LOLE will

lead to error in the estimation in ELCC. An improved methodology needs to be developed to reduce this error.

8.2.2 Errors in Assuming that the Wind and Load Demand is not Correlated

The multi-state non-iterative method [11] does not incorporate the correlation between demand and the renewable generation, which can lead to errors in the estimation of ELCC.

Fig. 8.3 shows the total wind generation from all the wind farms in the state of California, USA during a heat wave from 17-26 July, 2006, when excessive usage of air conditioning equipment resulted into the peak demand in the state [17]. In Fig. 8.3, the red dots indicate the wind generation level during that period.

Fig. 8.3 shows that there is a clear negative correlation between peak demand and the wind energy generation. On July 17, the wind energy generation at peak load was 4% of the wind generator nameplate. This suggests that the ELCC of the wind generator for peak load in this case should be very low and other types of generation will be needed to guarantee the reliability of supply for the system in peak hours [17].

This correlation is, however, a complex function of both location and weather. Fig. 8.4 shows a similar graph to Fig. 8.3 for the wind generation in summer season (1-10 December, 2010) for the state of New South Wales (NSW), Australia. Fig. 8.4 shows that there are days when the peak load is correlated with significant wind generator output.

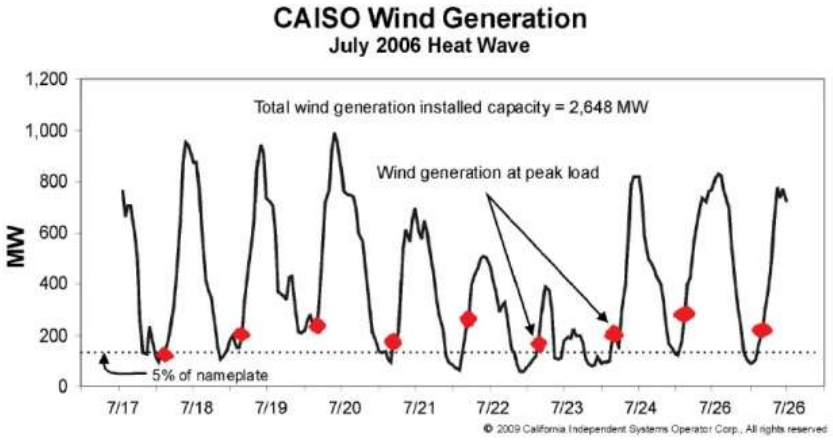

Fig. 8.3. California heat wave in July 2006 [17].

Figs. 8.3 – 8.4 show that there is a correlation between demand and renewable generation and it needs to be considered in the estimation of ELCC to avoid significant calculation errors. Errors that can arise in the estimation of ELCC by ignoring the correlation between the renewable generation and the load are demonstrated in Section 8.4.4.

Therefore, it is important to develop a method that can include the correlation between the renewable generation and the load demand, while avoiding the use of the exponential curve fitting. Moreover, shorter computation time needs to be ensured compared to the iterative method which relies on the chronological data of load and renewable generation.

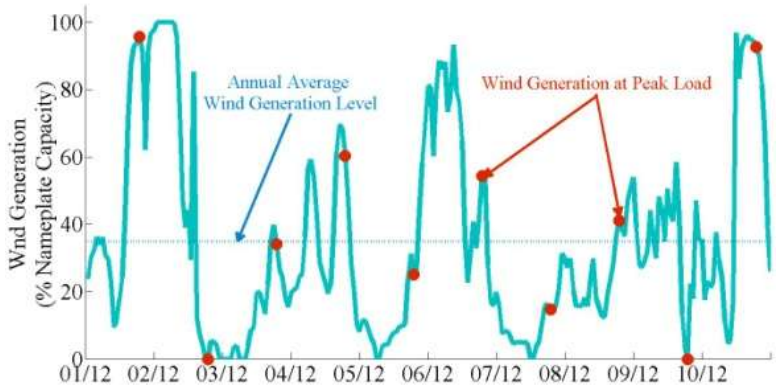

Fig. 8.4. NSW summer wind generation and peak demand coincidences.

In the following sections, a non-iterative method to estimate LOLE for a system using the availability capacity probability table (ACPT) is proposed only for conventional i.e. non-renewable generating units. The proposed method is validated using the IEEE RTS and the results are compared with the traditional iterative method. The addition of renewable generating units to the above system, with peak demand-renewable generation correlation, will then be considered using the joint-probability distribution between demand and renewable generation.

8.3 Proposed Non-Iterative ELCC Estimation Technique for Conventional Generating Units

8.3.1 Available Capacity Probability Table

For a generation system composed of N conventional units with M failed units, the available generating capacity, AGC_i and its corresponding state probability, $P\{AGC_i\}$ for state i can be determined by (8.1) and (8.2), from which the ACPT can be obtained:

$$AGC_i = \sum_{j=M+1}^{N} G_j \tag{8.1}$$

$$P\{AGC_i\} = \prod_{j=M+1}^{N} A_j * \prod_{j=1}^{M} FOR_j \tag{8.2}$$

where A_j, FOR_j and G_j are the availability, forced outage rate (FOR) and the available generating capacity of unit j respectively.

Consider a sample system consisting of three 25 MW generating units, with a forced outage rate of 0.02 for each unit. Table 8.1 shows the ACPT for the sample system.

Table 8.1. Available Capacity Probability Table

Units Out #	Capacity Out	Capacity In (C_A)	Probability $P[C=C_A]$	Cumulative Probability
None	0 MW	75 MW	(0.98×0.98×0.98)=0.9412	1
1, or 2, or 3	25 MW	50 MW	3×(0.02×0.98×0.98)=0.0576	0.0588
1,2 or 1,3 or 2,3	50 MW	25 MW	3×(0.02×0.02×0.98)=0.0012	0.0012
1,2,3	75 MW	0 MW	(0.02×0.02×0.02)=0.0000	0.0000

8.3.2 LOLE Estimation

The generation reserve margin, $R_{C,k}$ of the system for the load level, L_j due to the available generation capacity level, AGC_i can be defined as the excess available

generation capacity after serving the demand, L_j as shown in (8.3). It is assumed that the outage of the conventional generating units is purely random and independent of the demand levels as used in [15]. Therefore, the individual probability of the generation reserve margin level, $P\{R_{C,k}\}$ will be equal to the product of the probability of system demand level, $P\{L_j\}$ and the probability of available system generation level, $P\{ AGC_i\}$ as given in (8.4).

$$R_{C,k} = AGC_i - L_j \tag{8.3}$$

$$P\{R_{C,k}\} = P_i\{AGC_i\} \times P\{L_j\} \tag{8.4}$$

Consider the system whose ACPT is given in Table 8.1. The system has a simplified load duration curve where a peak load of 70MW is present for 40% of the time (3500h) and the off peak load of 40MW is present for the rest of the year as shown in Fig. 8.5. For the system, the generation reserve margin, $R_{C,k}$, and the associated probability are given in Table 8.2. In Table 8.2, Column 5 shows the generation reserve margin while the associated probability of the generation reserve margin level is given in column 6.

The LOLE is the amount of time when the available generated power is less than the total demand of the system during the period of study [15].

Therefore, a loss of load will take place if the generation reserve margin is negative, and the LOLE of the system with N_{Rcg} number of the negative generation reserve levels can be estimated using (8.5).

$$LOLE = \sum_{k=1}^{N_{Rcg}} P\{R_{C,k} < 0\} \times T \tag{8.5}$$

where, T is the number of hours considered for LOLE estimation.

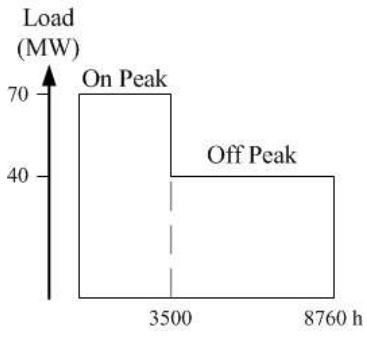

Fig. 8.5. Simplified load duration curve.

Table 8.2. Generation Reserve Margin, $R_{C,G,k}$ and associated probabilities for the Example System

Cap. In AGC_i (MW)	Probability $P\{G_{C,i}\}$	Demand L_j (MW)	Probability $P\{L_j\}$	Generation reserve margin, $R_{C,k}$ (MW)	Probability $P\{R_{C,k}\}$
75	0.9412	70	0.3995	5	0.3760
75	0.9412	40	0.6005	35	0.5652
50	0.0576	70	0.3995	-20	0.0231
50	0.0576	40	0.6005	10	0.0346
25	0.0012	70	0.3995	-45	0.0005
25	0.0012	40	0.6005	-15	0.0007
0	0.0000	70	0.3995	-70	0.0000
0	0.0000	40	0.6005	-40	0.0000

The LOLE of the system with generation reserve margin shown in Table 8.2 can be calculated as:

LOLE = (0.0231+0.0005+0.0007+0.0000+0.0000)*8760

= 212.868 h/yr (with a probability of 0.0243).

Table 8.3 shows the sorted generation reserve margins and their probability referred to as the generation reserve margin probability table (GRMPT) from the most negative to the most positive reserve margin.

Table 8.3. Generation Reserve Margin Probability Table (GRMPT) of the Example System

Generation reserve margin, $R_{C,k}$	Probability $P[R_C=R_{C,k}]$	Cumulative Probability $P[R_C \leq R_{C,k}]$	$P[R_C \leq R_{C,k}] \times T$
-70 MW	0.0000	0.0000	0.0000
-45 MW	0.0005	0.0005	4.38
-40 MW	0.0000	0.0005	4.38
-20 MW	0.0231	0.0236	202.356
-15 MW	0.0007	0.0243	212.868
5 MW	0.3760	0.4003	3506.628
10 MW	0.0346	0.4349	3809.724
35 MW	0.5652	1.0000	8760

In table 8.3, the third column of the GRMPT is the cumulative probability of the generation reserve margin levels and the fourth column shows the cumulative probability values multiplied by *T*, from which the LOLE can be estimated. The LOLE is the value that corresponds to the least negative value of the generation reserve margin

levels in column one, which is -15MW. Hence, the value of LOLE in this case is 0.0243 pu or 212.868 h/yr.

8.3.3 Proposed Non-Iterative ELCC Estimation

Traditionally, for estimating the ELCC of a conventional generating unit, the iterative method is used to estimate the PLCCs of the generation system before and after the addition of a new generating unit into the system. The PLCC of a system is defined as the peak demand of the system that can be supplied by the committed generating units while maintaining a specific level of LOLE.

In the iterative method for estimating PLCC, the demand of a system is adjusted iteratively by either increasing or decreasing certain amount of load demand until the LOLE of the system has reached to a specified level. Subsequently, the increased or decreased demand is added or subtracted, respectively, from the actual peak demand of the system to estimate the PLCC of the system.

In this chapter, a non-iterative method is proposed to estimate the PLCC of a generation system. Consider the same sample system whose GRMPT is given in Table 8.3 with an assumption that the requisite LOLE level is 0.01 pu or 87.6 h/yr. Since the original LOLE of the system is 0.0243 pu or 212.868 h/yr, 20 MW demand should be deducted from the system (i.e. -20 MW generation reserve margin corresponds to the probability of 0.0236 in the GRMPT and reducing it further will lead to the probability of 0.005 which is below the required LOLE of 0.01 as shown by the window in Table 8.3). The system peak demand that is to be supplied by the committed generating units while ensuring an LOLE of 0.01 pu or 87.6 h/yr is (70 - 20) = 50 MW. Hence, the PLCC of the system before the addition of a new unit is 50 MW. Table 8.4 shows the GRMPT of the system after adding an additional 30 MW of conventional generating unit having forced outage rate (FOR) of 0.02.

The LOLE of the system with the generation reserve margin shown in Table 8.4 is 0.000952 pu or 8.367 h/yr. If the specific LOLE level required is 0.01 pu or 87.6 h/yr, then 10 MW demand should be added to the system (resulting into the LOLE that will be higher than 0.0085 pu and less than 0.032 pu). The PLCC to have an LOLE of 0.01 pu or 87.6 h/yr after the addition of a new generating unit is (70+10) = 80 MW. The

ELCC of the new unit in the system with LOLE of 0.01 pu or 87.6 h/yr can be estimated as the difference between PLCCs of the system before and after the addition of the new unit in the system and is found to be (80 - 50) = 30 MW.

Any unit with a reliability value less than 100% should have a capacity value less than its installed capacity. The mismatch between the result and that from practical experience is due to the simplistic nature of the example. In the example system, the load duration curve contains only two load levels and the generation system consists of three generation units each with a force outage rate of 0.02. As a result, the difference between two consecutive generation reserve margin values is large in the GRMPT and the generation reserve margin levels jump from 5 MW and 10 MW as shown in Table 8.4. This results in the capacity value of a 30 MW generation unit equal to 30 MW. However, for a practical system with many generation units and a load duration curve with many demand levels, the difference between two consecutive generation reserve margin levels will be very small and the appropriate number can be found from GRMPT. A validation of this for the IEEE RTS system is given in Section 8.3.5.

Table 8.4. GRMPT of the Example System with 30 MW Generation unit

Generation reserve margin, $R_{C,k}$ (MW)	Probability $P[R_C = R_{C,k}]$	Cumulative Probability $P[R_C \leq R_{C,k}]$	$P[R_C \leq R_{C,k}] \times T$
-70	0	0	0
-45	9.60E-06	9.60E-06	0.084096
-40	0	9.60E-06	0.084096
-20	0.0004608	0.0004704	4.120704
-15	0.0004848	0.0009552	8.367552
-10	0	0.0009552	8.367552
5	0.0075296	0.0084848	74.326848
10	0.0232704	0.0317552	278.175552
15	0.0007056	0.0324608	284.356608
35	0.3802448	0.4127056	3615.301056
40	0.0338688	0.4465744	3911.991744
65	0.5534256	1	8760

In order to justify the validity of the proposed method for the small systems, the load duration curve of the example system presented in Section 8.3.2 is modified. The load of the system increases by 1 MW step from the minimum load level of 40 MW to the peak load of 70 MW as shown in Fig. 8.6. The probability of each load level is assumed to be equal. The cumulative probability of the GRMPTs for the system with and without the 30 MW additional generation unit is presented in Fig. 8.7. The PLCC of the system

without the 30 MW generation unit is found to be 54 MW corresponding to the LOLE level of 0.01 pu. The PLCC of the system with 30 MW generation plant is estimated 81 MW maintaining the system LOLE level of 0.01 pu. Hence the ELCC of the 30 MW generation unit is found to be 27 MW using the proposed method.

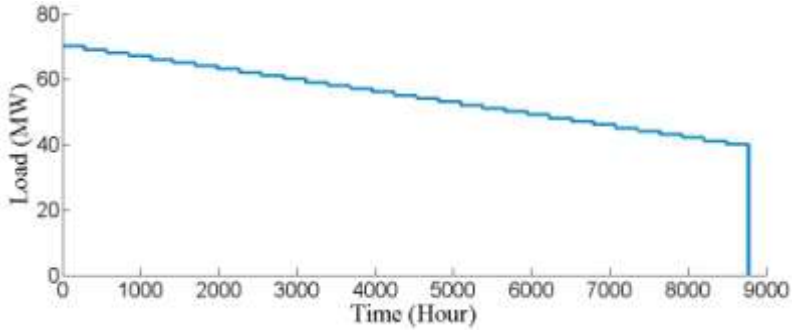

Fig. 8.6. Load Duration Curve.

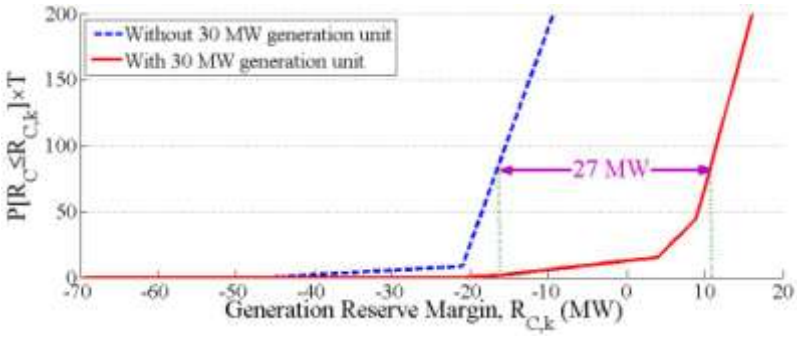

Fig. 8.7. Generation Reserve Margin.

8.3.4 Computational Procedures

The sequential computational procedures associated with the proposed non-iterative method of estimating the ELCC of an additional conventional generation unit are presented as follows.

a) Construct the ACPT with the aid of relevant information related to the conventional generation units of the system without additional generation unit, such as installed capacity, FOR, and availability rate using (8.1) and (8.2).

b) Construct the GRMPT using the data from ACPT and probability distribution of demand using (8.3) and (8.4).

c) Estimate the PLCC of the system without additional generation unit using the GRMPT and the specific LOLE for the system.

d) Obtain the availability model and FOR of the additional conventional generation unit.

e) Construct the new ACPT with the aid of the previously constructed ACPT and the availability model of the additional generation unit using (8.1) and (8.2).

f) Construct the new GRMPT using the data from the new ACPT and the probability distribution of demand using (8.3) and (8.4).

g) Estimate the new PLCC level of the system with the additional generation unit using the new GRMPT and the specific LOLE for the system.

h) Estimate the ELCC of the additional generation unit from the PLCC values of the system with and without the additional generation unit.

8.3.5 Validation using IEEE RTS

The IEEE RTS [16] is used to validate the proposed non-iterative method for estimating the ELCC of additional generating units. The generation and demand data of IEEE RTS can be found in [16]. One of the 100MW generating units is considered as an additional unit. The ELCC of the additional 100 MW generating unit is estimated using the proposed method and compared with the value estimated using the iterative method [6]. In this analysis, the number of load levels considered in the system load duration curve is 100. The system risk level for ELCC estimation of the additional 100 MW generating unit is considered to be an LOLE of 9.3452 hrs/yr which is the actual chosen LOLE for the IEEE RTS. The comparative results are presented in Table 8.5.

Table 8.5. ELCC of 100 MW unit in IEEE RTS.

	Proposed Method	**Iterative Method [3]**	**% Error**
$PLCC_{-100MW}$	2754.3 MW	2753.1 MW	0.04
PLCC	2850 MW	2850 MW	0
$ELCC_{100MW}$	95.7 MW	96.9 MW	1.24

The PLCC of the IEEE RTS is found to be 2754.3 MW and 2850 MW using the proposed method without and with the additional 100 MW generation unit, respectively. Hence, the ELCC of the 100 MW generating unit is found to be 95.7 MW and 96.9 MW using the proposed method and the iterative method, respectively, which corresponds to

the relative error less than 1.5% highlighting the acceptable level of accuracy for the proposed estimation method. This error is mainly due to the quantisation of the demand carried out during the probability distribution estimation.

8.4 Proposed Non-Iterative ELCC Estimation of a Non-Conventional Generating Unit Using Joint Probability Distribution

The load demand and available renewable generation profile usually contain both seasonal and diurnal variation. Usually, there is a correlation between the peak demand and the available renewable generation within the same time interval as demonstrated in Section 8.2.2.

The non-iterative method proposed in the previous section can be used to estimate the value of ELCC of an additional renewable generating unit if the generation availability of renewable generating unit is independent of the load demand. However, to take into account the correlation between peak demand and renewable generation due to seasonal and diurnal variation, a large dataset of historical values involving complex computation is required.

8.4.1 Joint Probability Distribution

To reduce the computational efforts, the joint probability distribution between demand and renewable generation is firstly obtained in this chapter from the chronological data of the available renewable generation during the different levels of demand. Once it is obtained, it can be used in the proposed non-iterative method described in Section 8.3.3, to estimate the ELCC of the renewable generating unit in terms of the difference between the PLCC of the system before and after the addition of the renewable generating unit.

The joint probability distribution is one of the established concepts in the technical literature. For example, the joint probability distribution of the wind speed and the wind generator location has been used in [18] to estimate the reliability indices of a generation system. The joint probability between demand and available renewable

distributed generation (DG) output has also been used in the optimization problem to estimate the DG hosting capacity of a distribution network [19]. However, it is to be noted that the joint probability distribution of load demand and renewable generation has not been used in the estimation of ELCC till date, which is one of the newly proposed subject matters of this chapter.

8.4.2 Joint Probability Distribution Considering Dependency

Let us consider two dependent random variables, D and G_R. The probability distribution that defines the probability of the simultaneous occurrence of $D = d$ and $G_R = g$ is referred to as the joint probability distribution [20], and can be estimated using (8.6):

$$P\{D=d, G_R=g\} = \frac{n_{d,g}}{\sum_{i=1}^{N_D}\sum_{j=1}^{N_{GR}} n_{i,j}} \tag{8.6}$$

where, $P\{D=d,\ G_R=g\}$ and $n_{d,g}$ are the joint probability density and number of occurrence of the simultaneous event ($D=d,\ G_R=g$) respectively, and $n_{i,j}$ is the number of occurrence of the event ($D=d_i,,\ G_R=g_j$). N_D and N_{GR} are the total numbers of the possible states of the random variables D and G_R, respectively. If the random variables are not dependent, the joint probability between them would be the product of the individual probability.

The joint probability distribution between the dependent demand and available renewable generation can be evaluated using (8.6) from the chronological time series data of demand and available renewable generation. The use of joint probability distribution in the ELCC estimation of renewable generation systems can reduce the computational effort when compared with the time-series based estimation methods. One important drawback of using joint probability distribution in ELCC estimation is that the accuracy of the results depends on the number of coincidental demand-generation levels used to evaluate the joint probability distribution. It is difficult to define the optimal number of the demand-generation levels in the joint probability distribution evaluation. However, similar difficulties can be found in the iterative method of ELCC estimation in terms of the selection of the optimal step value.

The red-dotted line in Fig. 8.8 shows that the available renewable generation is 0 MW during peak demand and 100% of the nameplate capacity (say 30MW) during off-peak period. In other words, the FOR of the wind generating unit is 0.4. The sample case for the state of California, USA, shown in Fig. 8.3, where there is a negative correlation between demand and the renewable generation output is simulated to test the concept. The first three columns of Table 8.6 show the joint probability distribution between the demand and available renewable generation calculated using (8.6).

Table 8.6. Joint Probability Distribution between Demand and Available Wind Generation (Negative and Positive Correlation)

Negative Correlation			Positive Correlation		
Demand	Wind Generation	Probability	Demand	Wind Generation	Probability (Considering Dependency)
70 MW	30 MW	0	70 MW	30 MW	0.114
70 MW	0 MW	0.4	70 MW	20 MW	0.285
40 MW	30 MW	0.6	70 MW	10 MW	0
40 MW	0 MW	0	40 MW	30 MW	0.172
			40 MW	20 MW	0
			40 MW	10 MW	0.429

The joint probability distribution between demand and available renewable generation in the last three columns of Table 8.6 is estimated considering the case where the available renewable generation during the peak demand is 30 MW for 1000 hours and 20 MW for 2500 hours and the available renewable generation during the off-peak demand time is 30 MW for 1500 hours and 10 MW for 3760 hours shown as blue-dotted line in Fig. 8.8. This case is derived from the state of NSW, Australia as shown in Fig. 8.4, where there is a positive correlation between demand and the renewable generation output.

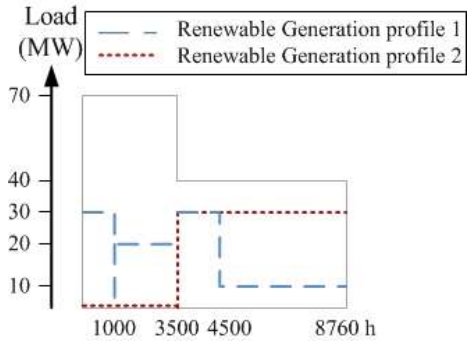

Fig. 8.8. Coincidental load duration and generation curve.

8.4.3 The Non-Iterative PLCC and ELCC Estimation Using Joint Probability Distribution

The generation reserve margin level and the associated probability distribution after the addition of the renewable generation unit can be estimated using (8.7) and (8.8), respectively.

$$R_{C+R,k} = AGC_i + G_{R,j} - L_j \tag{8.7}$$

$$P\{R_{C+R,k}\} = P_i\{AGC_i\} \times P\{L = L_j, G_R = G_{R,j}\} \tag{8.8}$$

where, $R_{C+R,k}$ is the k^{th} generation reserve margin due to i^{th} available conventional generation level and j^{th} demand and renewable generation level of the system. $G_{R,j}$ is the available renewable generation level occurring simultaneously with demand level of L_j. $P\{L=L_j,G_R=G_{R,j}\}$ is the joint probability distribution between demand level of L_j and renewable generation level of $G_{R,j}$.

For the red-dotted line in Fig. 8.8, the generation reserve margin levels and associated probability of the system with ACPT shown in Table 8.1, and joint probability distribution between demand and available renewable generation with negative correlation shown in Table 8.6 are calculated and presented in Table 8.7.

Table 8.7. Generation Reserve Margin taking into account the Joint probability Distribution

Cap In (MW)	Probability $P\{G_{C,i}\}$	Demand L_j (MW)	Wind Generation $G_{R,j}$ (MW)	Probability $P\{L_j, G_{R,j}\}$	Generation Reserve Margin, $R_{C,k}$	Probability $P\{R_{C,k}\}$
75	0.9412	70	30	0	35	0
75	0.9412	70	0	0.4	5	0.37648
75	0.9412	40	30	0.6	65	0.56472
75	0.9412	40	0	0	35	0
50	0.0576	70	30	0	10	0
50	0.0576	70	0	0.4	-20	0.02304
50	0.0576	40	30	0.6	40	0.03456
50	0.0576	40	0	0	10	0
25	0.0012	70	30	0	-15	0
25	0.0012	70	0	0.4	-45	0.00048
25	0.0012	40	30	0.6	15	0.00072
25	0.0012	40	0	0	-15	0
0	0	70	30	0	-40	0
0	0	70	0	0.4	-70	0
0	0	40	30	0.6	-10	0
0	0	40	0	0	-40	0

Table 8.8 shows the sorted generation reserve margins and their probabilities, referred as the GRMPT, from the most negative to the most positive reserve margin.

From Table 8.8, it can be seen that the LOLE of the system has been improved from 0.0243 pu (or 212.868 h/yr) as given in Table 8.3 to 0.02352 pu (or 206.035 h/yr) with the integration of the renewable generation unit. The PLCC after integrating the renewable generation unit for an LOLE of 0.01 pu (or 87.6 h/yr) is (70-15) = 55 MW. From Section 8.3.3, the PLCC before integrating the renewable generating plant is 50MW and therefore, the ELCC of the additional renewable generating unit for an LOLE of 0.01 pu (or 87.6 h/yr) is (55-50) = 5 MW. This suggests that the additional renewable generation unit, which has a negative correlation between its output and peak demand will result in little benefit to the system.

Table 8.8. GRMPT of Table 8.7

Generation Reserve Margin, $R_{C+R,k}$	Probability $P[R_{C+R}=R_{C+R,k}]$	Cumulative Probability $P[R_{C+R}\leq R_{C+R,k}]$	$P[R_{C+R}\leq R_{C+R,k}]\times T$
-70	0	0	0
-45	0.00048	0.00048	4.2048
-40	0	0.00048	4.2048
-20	0.02304	0.02352	206.0352
-15	0	0.02352	206.0352
5	0.37648	0.4	3504
10	0	0.4	3504
15	0.00072	0.40072	3510.3072
35	0	0.40072	3510.3072
40	0.03456	0.43528	3813.0528
65	0.56472	1	8760

The PLCC after integrating the renewable generating unit with the generation pattern given by the blue-dotted line in Fig. 8.8 can be similarly estimated, and the PLCC and ELCC of the additional renewable generating unit are found to be 70 MW and 20 MW, respectively.

The results show that the ELCC of the additional renewable generating unit depends on whether there is negative or positive correlation between the load demand and the available renewable generation output.

8.4.4 Impact of Demand-Generation Correlation on ELCC

To further investigate the impact of time varying renewable generation and the intermittent period of peak demand on the ELCC value, three cases are simulated for the system whose ACPT is given in Table 8.1 and the load demand is given in Fig. 8.5. In Case 1, the FOR of the additional renewable generation unit is varied from 1 to 0, independent to the demand level. In Case 2, at the beginning, no generation is available from additional renewable generating unit (i.e. FOR of the unit having a value of 1), and then with a small increment of generation available from the additional renewable generation is added, starting from the 8760th hour to the 1st hour causing the FOR to decrease from 1 to 0, as shown in Fig. 8.9(a). In Case 3, the increment is started from the 1st hour to the 8760th hour resulting in the FOR to decrease from 1 to 0 as shown in Fig. 8.9(b). Case 2 initially corresponds to the case when the additional renewable generation only available during off-peak hour, and Case 3 initially corresponds to the state when the additional generation is available mainly in the peak hour. The ELCC is estimated for an additional renewable generation rated at 30 MW.

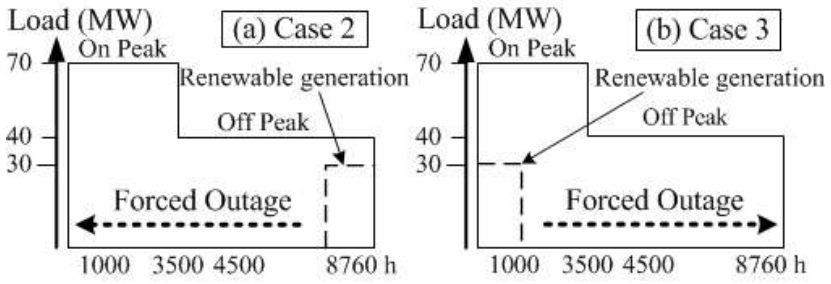

Fig. 8.9. Load duration curve along with the operation duration curve for a 30 MW renewable generation unit for (a) Case 2, and (b) Case 3.

Fig. 8.10 shows the variation in the values of ELCC as the FOR of the new generation unit is reduced in all the three cases. For Case 1, the ELCC values increase from 5 to 25 MW when the FOR reduces to 0.41 while the ELCC increases to 30 MW when the FOR reduces to 0.025. For Case 2, when the additional new generation unit is incremented starting from the off-peak period, the ELCC value increases from 5 MW to 25MW when the FOR reduces to 0.17 (i.e. 2052 hours of peak demands and 5260 hours of off-peak demand are reduced by the additional unit) and then increases to 30MW when the FOR is 0.01 (i.e. 3412 hours of peak demand and 5260 hours of off-peak

demand are reduced by the additional units). However in Case 3, when the new unit starts incrementing during the peak period, the ELCC value increases to 25MW even when the FOR is 0.77 (i.e. 2000 hours of peak demand are reduced by the additional unit), and rises to 30MW when the FOR is 0.6 (i.e. 3416 hours of peak demand are reduced by the additional unit).

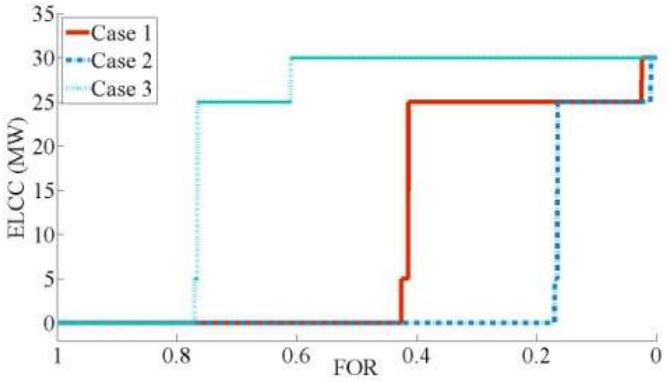

Fig. 8.10. Impact of FOR of a renewable generation unit on the ELCC.

Fig. 8.10 shows that the ELCC value of the additional generation unit could be different depending on the level of correlation between the available generation and the peak demand. For example, when there is no correlation between the generation and the peak load (Case 1), the ELCC of the additional generation unit with FOR of 0.3 is found to be equal to 25 MW. However, when the available generation is correlated with the off-peak demand (Case 2), the ELCC of the additional generation unit with the same FOR and installed capacity is found to be 0 MW. This corresponds to an error of 25 MW in the ELCC value of the generation unit because the demand-generation correlation is ignored. When the available generation is correlated with the peak demand (Case 3), the ELCC value of the additional generation unit with same FOR and installed capacity is found to be 30 MW. The corresponding error in ELCC value due to ignoring the demand-generation correlation is 5 MW. Hence, the correlation between the available generation and the demand is important and should be considered in order to avoid the error in the ELCC estimation of the intermittent generation units such as renewable generation units. Moreover, it is noted that the reduction of peak load due to the additional generation is more important than the reduction of the off-peak load.

8.4.5 Computational Procedures

The sequential computational procedures associated with the proposed non-iterative method of estimating the ELCC of an additional renewable generation unit, taking into account its correlation with the load demand, are presented as follows.

a) Estimate the joint probability density between the demand and available renewable generation based on the associated co-incidental time series data using (8.6).

b) Construct the ACPT with the aid of relevant information related to the conventional generation units, such as installed capacity, FOR, and availability rate using (8.1) and (8.2).

c) Construct the GRMPT using the data from ACPT and joint probability distribution between demand and available renewable generation using (8.7) and (8.8).

d) Estimate the PLCC of the system with and without renewable generation unit using the GRMPT and specific LOLE for the system.

e) Estimate the ELCC of the renewable generation unit from the PLCC values of the system with and without a renewable generation unit.

8.5 Case Study

The PLCC and ELCC of different renewable generation systems, such as wind and solar PV generation, currently under consideration for a large scale integration in the electricity network of NSW, Australia are estimated using the proposed methodology. The annual peak demand of the system is 11,810 MW in year 2010. The generation system for the state of NSW is composed of 19 conventional generation units with a total generation capacity of 16,392 MW [21]. Also, the NSW grid has tie-line interconnections with the two adjacent states with a total capacity of 2,378 MW. In this chapter, it is assumed that all the generation units are committed to supply load demand during the entire time period of the year. Individual generation units and the associated network interconnection are modeled using a two-state availability model. The data associated with the centrally dispatched generators of the NSW electricity system can be found in [21], from which the ACPT is set up based on the procedure explained in section 8.3.1. The load demand data for the years 2008-2011 is collected from the Australian energy market operator (AEMO) website [22].

Seven geographical areas within the state of NSW, known as wind bubbles [23], are identified as the potential sites for the wind generation units as shown in Fig. 8.11. The solar power generation site is located in Hunter Valley area as shown in Fig. 8.11. In this chapter, the wind and solar generation data are derived from the database of year 2010 of the national transmission network development plan (NTNDP 2010) [21] to estimate the ELCC of the respective wind and solar generation units.

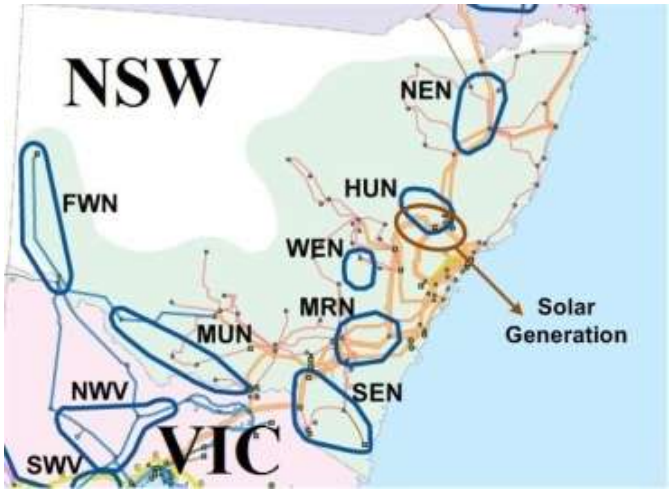

Fig. 8.11. Wind bubbles and solar generation in NSW, Australia [23].

The joint probability distributions of demand-generation for the HUN wind bubble and the demand-generation for the solar plant, as shown on the state map in Fig. 8.11 are calculated and shown in Fig. 8.12. The probabilities of the variable wind generation levels during peak demand periods are higher than those of the solar generation levels. The correlation coefficients between the monthly demand and the wind generation of HUN and MUN wind bubbles from 10 years data are presented in Fig. 8.13, which shows that the monthly demand and the wind generation of HUN and MUN wind bubbles are consistently correlated year to year. Similar consistent correlation coefficients between the monthly demand and the renewable generation are also observed for the other three wind bubbles and the solar power over the 10 years period. Hence, the correlation between the demand and renewable generation should be considered in the ELCC estimation of the renewable based generation plants.

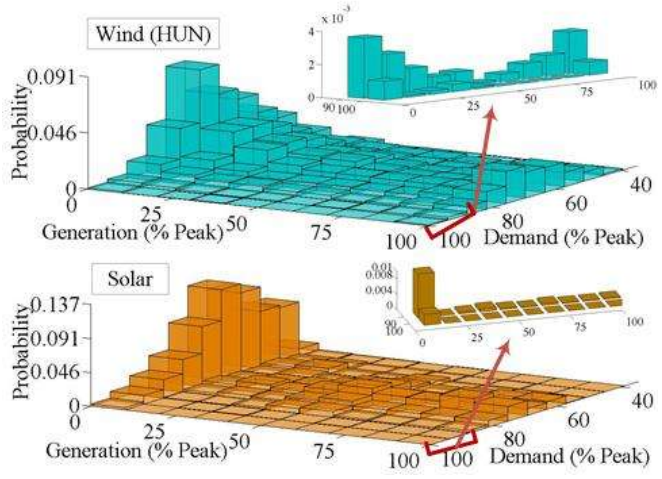

Fig. 8.12. Joint probability distribution for wind and solar generation during peak load.

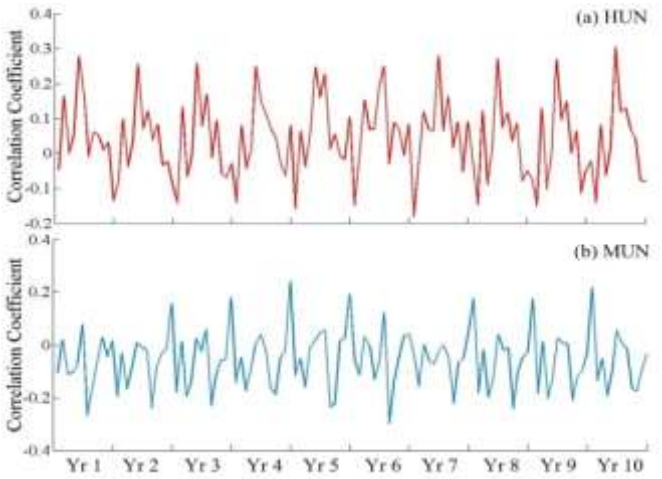

Fig. 8.13. Correlation coefficients between demand and wind generation of (a) HUN and (b) MUN wind bubble.

A computer program has been developed to implement the proposed non-iterative method of the ELCC estimation using MATLAB. The PLCC of the wind generation units of the five wind bubbles are estimated using the proposed and the iterative method [6]. To show the effect of increasing the number of demand-generation levels in the evaluation of the joint probability distribution of demand and wind generation, 250 and 800 demand-generation levels are used in the simulation studies.

The installed capacity of each type of wind generation unit is assumed to be the same as that of an existing wind farm in the state of NSW, which is 140 MW. The results of the PLCC estimations using the proposed and the iterative method using 250 and 800

demand-generation levels in the evaluation of the joint probability distribution are presented in Fig. 8.14. The relative errors between the PLCC values estimated using the proposed and the iterative method are shown by the numbers above the respective bars in Fig. 8.14. For example for the HUN wind bubble, the relative errors between the proposed and the iterative method using 250 and 800 demand-generation levels in the joint probability distribution are 0.1% and 0.04%, respectively.

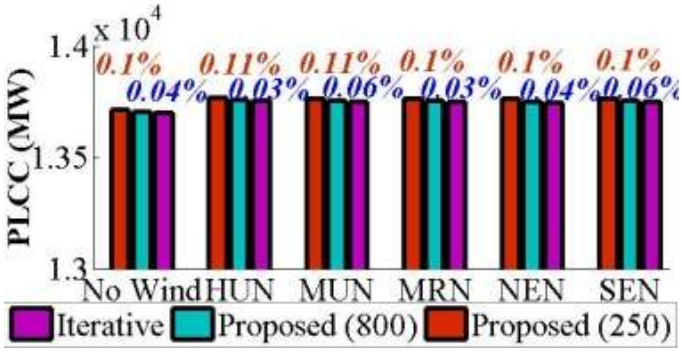

Fig. 8.14. PLCC of the NSW generation system.

Since, the multi-state graphical method [11] cannot estimate the PLCC of a system, the PLCC results cannot be compared for this method. It is found that the relative errors of the proposed method are within 0.1% of those from the iterative method, which implies that the proposed method can estimate the PLCC of the system with an acceptable accuracy. Fig. 8.14 shows that the results obtained using the proposed method with 800 levels in the joint probability distribution between demand and wind generation is closer to the results obtained using the iterative method compared to those with 250 levels. This is due to the quantisation of the demand and wind generation output value carried out during the joint probability distribution estimation. Joint probability distribution between demand and wind generation with 250 demand-generation levels has higher quantisation error than that with 800 demand-generation levels. This confirms that the relative error can be reduced by increasing the number of demand-generation levels used in the joint probability distribution calculation. However, increasing the number of levels in the joint probability distribution will also increase the computation time.

The ELCC of the additional wind generation units, each rated at 140 MW as indicated earlier, located at the five different wind bubbles in NSW are estimated using

the multi-state graphical method, the proposed method, and the iterative method (using 20 states) for each of the wind generation unit. The ELCC estimated using the three different methods are presented in Fig. 8.15.

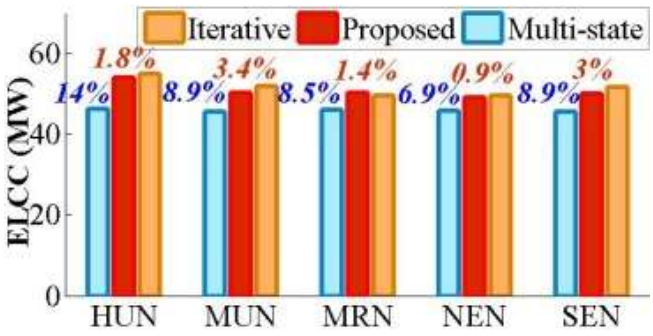

Fig. 8.15. ELCC and relative errors for the five wind bubbles in NSW.

The relative errors in ELCC estimation for the proposed method and the multi-state graphical method are compared with respect to the iterative method and the associated values are shown above the respective bar graphs in Fig 8.15. The five wind bubbles have different correlation coefficients with the load demand in NSW which signify the spatial diversity among the wind generations from different wind bubbles located at different geographical locations. Hence, the ELCCs of the different wind bubbles are different from each other. For example, a higher correlation exists between the demand and the wind generation of HUN wind bubble when compared to that with the MUN wind bubble as apparent from Fig. 8.13. As a result, the ELCC value of the wind generation from HUN wind bubble is higher when compared with that from the wind generation from MUN wind bubble as shown in Fig. 8.15.

The phenomena can be observed in Fig. 8.15 for the ELCC estimated using the proposed method and the iterative method. On the other hand, the multi-state graphical method cannot account for the correlation between the renewable generation units and the load demand, and hence produces the same ELCC values for the different wind generation units. As a result, the relative errors in the ELCC estimation using the multi-state graphical method vary between 7 - 14% for different wind generation units, which is quite high compared to the relative errors of 0.8 - 3% obtained using the proposed method.

The efficiency of the proposed non-iterative method for ELCC estimation is

compared with the iterative method in terms of computation time. For the iterative method, an accelerated iterative method [24] is used for fast convergence. The computational time to estimate the ELCC of the MUN wind bubble using the proposed non-iterative method (with 250 and 800 demand-generation levels in the evaluation of the joint probability distribution) and the conventional iterative method are presented in Table 8.9.

Table 8.9. Computation Time Comparison

	Iterative	***Non-iterative (250 levels)***	***Non-iterative (800 levels)***
Computation Time (Sec)	39.8006	5.6497	12.4844

From Table 8.9, it is observed that the number of demand-generation levels in evaluating joint probability distribution has an impact on the computation time. When the number of demand-generation levels is 250 and 800, the proposed non-iterative method takes 5.6497 sec and 12.4844 sec to estimate the ELCC of the wind generation system in the MUN wind bubble. Though the number of demand-generation levels is increased by 3.20 times, the computation time only increases by 2.56 times. Hence, the computation time does not change dramatically due to the increase in the number of the demand-generation levels in the joint probability distribution evaluation. Further, the proposed non-iterative method with 800 demand-generation levels in the evaluation of the joint probability distribution takes less than one third computation time when compared with the iterative method in the ELCC estimation of the wind generation system in the MUN wind bubble. This result emphasises the computational efficiency of the proposed non-iterative method in the ELCC estimation of renewable generation systems.

The ELCC of the wind generation unit in the HUN wind bubble region and the ELCC of the solar generation unit (shown in Fig. 8.9) for different installed capacities are estimated using the proposed method with and without considering the correlation between the demand and the available renewable generation, and the results are presented in Fig. 8.16.

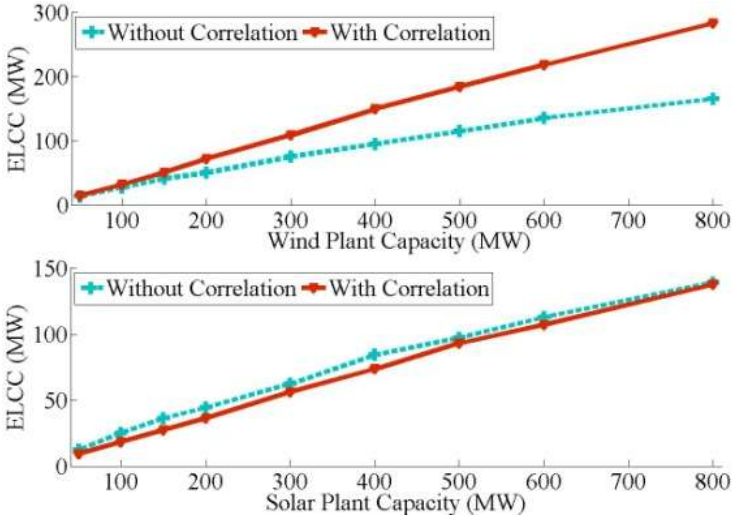

Fig. 8.16. ELCC of renewable generation plants in NSW.

Fig. 8.16 shows that the correlation between the load demand and the wind generation has a significant impact on the estimated ELCC values of the additional wind generation unit, particularly when its capacity is higher.

The correlation between the load demand and the solar generation has a small impact on the estimated values of ELCC. The reason for this phenomenon can be explained from the joint probability distribution for wind and solar generation plants during peak load as shown in Fig. 8.12. Since the marginal probabilities for different levels of wind generation during the period of system peak demand are higher than those of the solar generation, this implies that the availability of wind generation is more than the availability of the solar generation during system peak demand. This results in the ELCC of the wind generation unit to be higher than the ELCC of the solar generation unit of the same installed capacity. As a result, the wind generation unit in HUN wind bubble can contribute more to the generation adequacy of the NSW electricity generation system than the solar generation unit.

8.6 Conclusion

In this chapter, a non-iterative analytical method is proposed for estimating the ELCC of conventional and renewable generating units. A generation reserve margin probability table is generated using the available capacity probability table for the conventional generation units and the probability density of system demand. A procedure has been presented with examples to estimate the system risk level and the

ELCC of the conventional generating unit using the generation reserve margin probability table. One of the main advantages of the proposed non-iterative analytical approach is an efficient estimation of the ELCC. The proposed method is tested on a standard reliability test system and compared with the iterative method. The results are found to be very close. Procedures have also been demonstrated to estimate the system risk level and hence the ELCC of the renewable generation unit. The seasonal and diurnal variation in the renewable generation availability and the correlation between demand and available renewable generation are taken into consideration using the joint probability distribution between demand and available renewable generation. The proposed approach is then applied to estimate the ELCC of potential renewable generation units in a practical system and the results are compared with an iterative and a non-iterative method reported in the literature. The performance of the proposed method is found to be better than the existing non-iterative approach and comparable with the iterative approach. It is to be noted that the proposed method accounts for the correlation between the renewable generation and the load demand while avoiding the use of the exponential curve fitting techniques. Moreover, the proposed method is found to be computationally efficient than the iterative technique. Results demonstrate that the proposed analytical method can be used to accurately estimate the ELCC of future addition of renewable generation units to the existing electricity system.

References:

[1] S. H. Madaeni, R. Sioshansi, and P. Denholm, "Estimating the Capacity Value of Concentrating Solar Power Plants: A Case Study of the Southwestern United States," *IEEE Transaction on Power Systems*, vol. 27, no. 2, pp. 1116-1124, May. 2012.

[2] S. H. Madaeni, R. Sioshansi, and P. Denholm, "Comparing capacity value estimation techniques for photovoltaic solar power," *IEEE Journal on Photovoltaics*, vol. 3, no. 1, pp. 407-415, Jan. 2013.

[3] J. Haslett, M. Diesendorf, "The capacity credit of wind power: A theoretical analysis," *Solar Energy*, vol. 26, pp. 391-401, 1981.

[4] R. Perez, M. Taylor, T. Hoff, J. P. Ross, "Reaching consensus in the definition of photovoltaics capacity credit in the USA: A practical application of satellite-derived solar resource data," *IEEE Journal of Selected Topics in Applied Earth Observations and Remote Sensing*, vol. 1, no. 1, pp. 28-33, Mar, 2008.

[5] M. Amelin, "Comparison of Capacity Credit Calculation Methods for Conventional Power Plants and Wind Power," *IEEE Transaction on Power Systems*, vol. 24, no. 2, pp. 685-691, May. 2009.

[6] R. Billinton, H. Chen, "Assessment of risk-based capacity benefit factors associated with wind energy conversion systems," *IEEE Transaction on Power Systems*, pp. 1191 - 1196 vol. 13, no. 3, Aug. 1998.

[7] J. Radtke, C. J. Dent, S. J. Couch, "Capacity Value of Large Tidal Barrages," *IEEE Transaction on Power Systems*, vol. 26, no. 3, pp. 1697-1704, Aug. 2011.

[8] R. Billinton, G. Bai, "Generating capacity adequacy associated with wind energy," *IEEE Transaction on Energy Conversion*, vol. 19, no. 3, pp. 641- 646, Sept. 2004.

[9] W. Wangdee, R. Billinton, "Considering load-carrying capability and wind speed correlation of WECS in generation adequacy assessment," *IEEE Transaction on Energy Conversion*, vol. 21, no. 3, pp. 734-741, Sept. 2006.

[10] L. L. Garver, "Effective Load Carrying Capability of Generating Units," *IEEE Transaction on Power Apparatus and Systems*, vol. PAS-85, no. 8, pp. 910-919, Aug. 1966.

[11] C. D'Annunzio, S. Santoso, "Noniterative Method to Approximate the Effective Load Carrying Capability of a Wind Plant," *IEEE Transaction on Energy Conversion*, vol. 23, no. 2, pp. 544-550, Jun. 2008.

[12] K. Dragoon, V. Dvortsov, "Z-method for power system resource adequacy applications," *IEEE Transaction on Power Systems*, vol. 21, no. 2, pp. 982- 988, May. 2006.

[13] Lingfeng Wang; C. Singh, "An Alternative Method for Estimating Wind-Power Capacity Credit based on Reliability Evaluation Using Intelligent Search," in *Proceedings of the 10th International Conference on Probabilistic Methods Applied to Power Systems*, *PMAPS '08*, pp. 1-6, 25-29 May 2008

[14] A. Keane, M. Milligan, C. J. Dent, , B. Hasche, , C. D'Annunzio, K. Dragoon, H. Holttinen, N. Samaan, , L.Soder, and M.O'Malley, "Capacity Value of Wind Power," *IEEE Transaction on Power Systems*, pp. 564 - 572 vol. 26, no. 2, May 2011.

[15] Roy Billinton, Ronald N. Allan, *Reliability evaluation of power systems*, 2nd edition, Plenum press, New York, 1996.

[16] IEEE Subcommittee, P.M.; "IEEE Reliability Test System," *IEEE Transaction on Power Apparatus and Systems*, vol.PAS-98, no.6, pp.2047-2054, Nov. 1979

[17] C. Loutan, D. Hawkins, "Integration of Renewable Resources", California ISO report, Nov. 2007.

[18] N. Maisonneuve, G. Gross, "A Production Simulation Tool for Systems With Integrated Wind Energy Resources," *IEEE Transaction on Power Systems*, vol. 26, no. 4, pp. 2285-2292, Nov. 2011.

[19] L. F. Ochoa, C. J. Dent, G. P. Harrison, "Distribution Network Capacity Assessment: Variable DG and Active Networks," *IEEE Transaction on Power Systems*, vol. 25, no. 1, pp. 87-95, Feb. 2010.

[20] Robert V. Hogg, Allen Thornton Craig, Introduction to mathematical statistics, 4th edition, Macmillan Publishing Co. Inc. New York, 1978.

[21] National Transmission Network Development Plan 2010, Australian Energy Market Operation, 2010, [Online]. Available: http://aemo.com.au/Electricity/Planning/Archive-of-previous-Planning-reports/2010-NTNDP/2010-NTNDP-Data-and-Supporting-Information

[22] Australian Energy Market Operation (AEMO) demand data, access via internet on January 2012. [Online]. Available: http://aemo.com.au/Electricity/Data/Price-and-Demand/Aggregated-Price-and-Demand-Data-Files

[23] Australian Energy Market Operation, "Wind integration in electricity grids work package 5: Market simulation studies", 2012, [Online]. Available: http://www.aemo.com.au/Electricity/Planning/Related-Information/Wind-Integration-Investigation

[24] M. Watanabe, F. Jin, L. Pan, "Accelerated iterative method for solving steady problems of linearized atmospheric models," *Journal of the Atmospheric Sciences*, vol. 63, no. 12, pp. 3366-3382, Dec 2006.

Chapter 9

Conclusions and Recommendations for Future Work

This thesis has developed comprehensive and realistic planning approaches for transmission and distribution expansion, and proposed new strategies for climate change mitigation in electricity networks through increasing renewable energy penetration. General conclusions of the thesis and directions of future works are provided below.

9.1 Concluding Remarks

This thesis emphasises electricity network planning considering renewable based generation systems to contribute to the climate change mitigation from the perspective of the electricity generation, transmission and distribution facilities. The uncertainty and variability in the available generation from renewable resources are articulated to support the penetration of renewable based generation system in the electricity infrastructure. The environmental impacts from electricity generation, generation adequacy and techno-economic aspects of renewable resource integration are considered in the development of electricity network planning techniques. The work presented in this thesis can be summarised as follows:

1. In Chapter 2, the dependency between the time varying load demands of different consumer classes and the intermittent generation from different types of renewable resources are modelled by the cross moments and cumulants. A transformation matrix based load flow formulation is developed to solve the probabilistic load flow. Pearson distribution functions are used to estimate the probability distributions of the line flows from their cumulants. Consequently an analytical method has been developed for the probabilistic load flow solution of a distribution network with renewable distributed generation (DG) considering the coincidental variation of different consumer classes and intermittent generation

systems to reduce the computational time and effort. The developed probabilistic load flow solution can aid the distribution network planners to have better insight in the network operational impacts assessment due to renewable DG integration.

2. In Chapter 3, the joint probability distribution is used to model the coincidental variations between the load demand and the available generation from renewable resources. A new set of indices has been developed to estimate the energy supply and the continuity of services adequacy which are essential to evaluate the distribution network adequacy and reliability. Hence, an analytical method based on the joint probability distribution is formulated to assess the adequacy in terms of energy supply and the continuity of service in distribution networks embedded with DG systems. The results suggest that a significant capacity in distribution feeder can be released with the integration of renewable DG and the proposed adequacy assessment method can highlight the distribution capacity release.

3. In Chapter 4, a life cycle assessment (LCA) method has been applied to estimate the embodied emission and the life cycle cost of electricity (LCOE) of the renewable based hybrid energy system (HES). Method of moments is used to estimate the supply continuity, related to the uncertainty in renewable resources, from the renewable based HES. Therefore, a multi-objective optimisation technique considering life cycle embodied emissions, LCOE and supply continuity has been formulated to design a renewable based HES to achieve sustainability in power generation and distribution. Based on the results, it is found that energy storage system can potentially improve the emission reduction and the system reliability while implementing the HES.

4. The marginal emission of individual generation unit is modelled using a thermodynamic model of the unit in Chapter 5. The aggregated emission model for the energy supplied through the grid from a number of generation plants is developed based on the fuel mix of the grid. The change in the average demand, the variation in the peak and off-peak demand, the generation flexibility and the generation mix index are considered to evaluate the impact of the climate change mitigation strategies to facilitate the renewable generation growth in the electricity network. Hence, the impacts of the climate change mitigation technology on emission reduction by increasing the renewable generation penetration are

assessed for the electricity grid of New South Wales, Australia. The results suggest that the coordination between different climate change mitigation technologies are required to efficiently achieve the goal of emission reduction from renewable resources.

5. Computational models for emission reduction, capacity value and interconnection expansion are formulated in Chapter 6 for the wind generation capacity sharing strategy. Consequently, a multi-objective wind generation capacity sharing strategy is developed considering the objectives of maximising emission reduction and capacity value of the aggregated wind generation, and minimising the interconnection expansion. Based on the interconnected power systems in Southeast Australian power pool case study, the results suggest that wind generation capacity are allocated based on the correlation coefficient value between the system load and the wind generation power output.

6. To improve the schedulability of the battery energy storage system (BESS) integrated wind farm (WF) dispatch level during each dispatch interval, a stochastic programming model is developed considering the uncertainty in wind generation output and energy price forecasting in Chapter 7. Further, a ranked based dispatch algorithm is developed for BESS with multiple battery energy storage units (BESUs) to limit the frequent switching between the charging and the discharging modes which can reduce the lifetime of BESS. It has been found from the simulation results that the proposed scheduling and dispatch control strategy can improve the system reliability and the revenue stream of the wind farm in addition to wind generation fluctuation mitigation.

7. In order to estimate the effective load carrying capability (ELCC) of the renewable generation plant, a non-iterative analytical technique using the joint probability distribution of the demand and the renewable generations is proposed in Chapter 8. The seasonal and diurnal variation and the correlation between the load demand and the available renewable generations are modelled by the joint probability distribution of the demand and the renewable generations. The simulation results confirm that the proposed method reduces the computational time as compared to the existing ELCC estimation methods.

8. In Chapter 9, concluding remarks of the thesis have been presented by summarising the contents of the chapters 2 to 8. The recommendations for future to expand the presented works are included along with the concluding remarks of the thesis.

9.2 Recommendations for Future Work

The work presented in this thesis can be expanded by incorporating the following recommendations:

1. The methodology presented in this thesis for a probabilistic load flow solution of renewable enriched distribution network can be expanded for use in the transmission network with the application of renewable resources sharing among multi-area power systems. The correlation between the load of different power systems and the different renewable based generation units can be modelled using the proposed cross cumulants.

2. A set of indices are developed in this thesis to assess the distribution network adequacy. The results suggest that the integration of renewable DG can release the distribution feeder capacity. Hence using the developed indices and methodology of distribution network adequacy assessment, the capacity credit estimation methodology can be developed for renewable based DG. Advanced distribution network planning techniques can be developed to ensure the maximum utilisation of the distribution network infrastructure. Moreover, based on the findings of the thesis, the distribution network capacity released due to the distributed energy storage integration can be investigated in the future.

3. In this thesis the solar PV, wind turbine and battery energy storage systems are considered for the HES design. In future, studies can be conducted to assess the optimal combinations of advanced renewable based generation system technologies for the HES design. In this thesis, the HES design methodology only considers to meet the electricity demand. The HES design methodologies can be developed in the future, incorporating co-generation options to meet electricity and heat demand.

4. The impact of different climate change mitigation technologies on the emission reduction by renewable resource integration has been investigated in this PhD project. The work can be expanded by developing new techniques in the future to evaluate the optimum mix of different climate change technologies and renewable resource integration to achieve the target emission reduction level.

5. The methodology to share wind resource diversity among interconnected power systems is developed in this thesis. This can be expanded by incorporating economic analysis from market responses in adapting the wind resource sharing strategy. Moreover, the feasibility of sharing different types of renewable resources such as solar thermal, hydro and tidal wave can be conducted in future as an extension of the present work.

6. The control strategies developed in this thesis for BESS integrated wind farm scheduling have the potential to mitigate the wind generation fluctuation and facilitate the wind farm to be competitive against conventional generation systems. The BESS is configured as the parallel combinations of the separately controllable BESUs. The number of BESUs in the parallel may have impact on the BESS service lifetime. Hence, study can be carried out in future to select optimum number of parallel BESUs in the BESS configuration considering the long term operation of the wind generation system.

7. The joint probability distribution of the demand and the renewable generation is considered in this thesis for the development of a non-iterative method to estimate the ELCC of the renewable based generation systems. The number of demand-generation level used to estimate the joint probability distribution affects the accuracy of the results. Hence in future, techniques can be developed to estimate the optimal number of levels in demand-generation joint probability distribution which will be able to maintain reasonable compromise between the accuracy of the result and the total computational time.